MILLENNIAL-SCALE CLIMATIC AND OCEANOGRAPHIC VARIATIONS IN THE NORTH ATLANTIC ACROSS MARINE ISOTOPE STAGES 21 TO 11. INSIGHTS FROM IODP SITE U1385

Gloria María Martín García

Tesis doctoral

Salamanca, 2016

VNiVERSiDAD D SALAMANCA
CAMPUS DE EXCELENCIA INTERNACIONAL

Facultad de Ciencias

Departamento de Geología - Área de Paleontología

VARIACIONES CLIMÁTICAS Y OCEANOGRÁFICAS A ESCALA MILENARIA EN EL ATLÁNTICO NORTE DUERANTE LOS ESTADIOS ISOTÓPICOS MIS 21 AL 11. APORTACIONES DESDE EL SITIO IODP U1385

Memoria presentada por Gloria María Martín García para optar al Grado de Doctor en Geología por la Universidad de Salamanca con Mención "*Doctor Internacional*"

Trabajo realizado bajo la dirección de los Profesores

Dr. Francisco Javier Sierro Sánchez

Dr. José Abel Flores Villarejo

D. Francisco Javier Sierro Sánchez y **D. José Abel Flores Villarejo**, profesores del Área de Paleontología del Departamento de Geología de la Universidad de Salamanca

CERTIFICAN que:

Dña. Gloria María Martín García ha realizado en el Departamento de Geología de la Universidad de Salamanca y bajo nuestra supervisión el trabajo:

VARIACIONES CLIMÁTICAS Y OCEANOGRÁFICAS A ESCALA MILENARIA EN EL ATLÁNTICO NORTE DUERANTE LOS ESTADIOS ISOTÓPICOS MIS 21 AL 11. APORTACIONES DESDE EL SITIO IODP U1385

Y para que conste, firmamos el presente certificado en Salamanca, a diciembre de 2015

Los directores:

Dr. Francisco J. Sierro Sánchez Dr. José A. Flores Villarejo

El doctorando:

Gloria M. Martín García

To my father, amateur fossil hunter and my first teacher, who awakened in me the love for books and knowledge. He transmitted to me his passion for Fossils and History.

To my mother, who always saw fossils the first. Always supportive and always pushing forward, without her suggestion and help I would never have begun nor finished this Ph.

A mi padre, aficionado a los fósiles y mi primer maestro, quien me inculcó el amor por los libros y el conocimiento. Él me transmitió su pasión por los Fósiles y la Historia.

A mi madre, siempre la primera en encontrar fósiles. Siempre animando y apoyando; sin su ayuda yo nunca hubiera empezado ni terminado esta tesis.

"... Nada de lo vivido hasta ahora es comparable a la emoción de descubrir algo así. No sé si tendrá mucha importancia científica o será una mandíbula más en un catálogo interminable de fósiles olvidados, pero para mí su importancia es inmensa. Ella es la razón de que yo esté aquí, renunciando a mis vacaciones, soportando el tedio, el desaliento... La razón de que estudie, de que lea, de que me pase horas y horas encerrado en bibliotecas... Y, sobre todo, es mi recompensa. Y mi promesa. La promesa de que habrá más: mañana, pasado o dentro de diez años. Seguiré y conseguiré ser yo el que estudie las mandíbulas una vez extraídas, el que pase los inviernos en un laboratorio rodeado de huesos y los veranos visitando excavaciones por todo el mundo..."

El Antropólogo. Gloria María Martín García

ÍNDICE / *INDEX*

CAPÍTULO I

PRESENTACIÓN Y OBJETIVOS

CAPÍTULO I:
PRESENTACIÓN Y OBJETIVOS

El estudio de las variaciones climáticas y ambientales a lo largo de la historia geológica responde al interés por conocer el funcionamiento de los sistemas naturales y sus efectos. Una cuestión clave para su comprensión reside en el conocimiento de la forma concreta en que cada sistema terrestre responde a los cambios ambientales y la escala temporal a la que lo hace. En el caso del océano, la respuesta dinámica a las influencias climáticas tiene como consecuencia la reorganización de la circulación superficial global y el reajuste de la circulación termohalina ("*conveyor belt model*"). Como consecuencia, el registro de las variaciones climáticas pasadas y los procesos paleoceanográficos asociados a ellas ha venido centrando el interés de la comunidad científica en los últimos años. La comprensión de los mecanismos y procesos que han actuado a lo largo de la historia geológica reciente permitirá interpretar los procesos ambientales que están ocurriendo en la actualidad, así como predecir el comportamiento y evolución del sistema climático en un futuro próximo.

Para resolver tales cuestiones es clave la utilización de registros sedimentarios marinos cuya localización geográfica y alta resolución temporal permitan estudiar los distintos procesos que integran el sistema climático terrestre. El margen occidental de la península Ibérica es una de estas áreas estratégicas. Se ha demostrado que su registro sedimentario puede compararse directamente con los registros de hielo antártico y de Groenlandia, ofreciendo datos fiables para el estudio de variaciones climáticas a escala milenaria tanto del hemisferio norte como del sur. Esto es especialmente interesante para reconstruir el sistema climático de épocas para las que no se dispone de registros de hielo.

El margen occidental ibérico está en el área de influencia del giro subtropical del Atlántico Norte y recibe aguas tanto de la corriente de las Azores, como de la corriente de Portugal, rama descendente de la Corriente del Atlántico Norte. Esta especial

localización, en el límite entre distintas masas de agua, hace de esta un área muy sensible a cambios de intensidad en el flujo de dichas corrientes y, por lo tanto, clave para el estudio de variaciones paleoceanográficas en el Atlántico Norte. De hecho, diversos estudios han relacionado las variaciones climáticas milenarias registradas en esta región durante el Cuaternario con cambios en los frentes oceánicos y en la distribución de las corrientes.

Sin embargo ningún estudio realizado en el margen ibérico alcanzaba más allá de los 580 ka, puesto que no existían registros sedimentarios anteriores. La campaña de IODP 339, con su sondeo U1385, ha permitido extender el registro sedimentario disponible hasta el millón de años. Para la elaboración de esta tesis doctoral he estudiado las asociaciones de foraminíferos planctónicos y los datos isotópicos obtenidos de los sedimentos de este sondeo para reconstruir la historia climática y oceanográfica de esta región a escala milenaria entre los estadios isotópicos MIS 21 y MIS 11, así como su correlación con eventos oceanográficos en el Atlántico Norte y climáticos a escala global.

Los principales objetivos de esta tesis podrían resumirse en:

- Elaboración de un registro de las variaciones en las asociaciones de foraminíferos planctónicos durante el período estudiado
- Reconstrucción de paleotemperaturas mediante distintas funciones de transferencia, basadas en asociaciones de foraminíferos planctónicos
- Reconstrucción de la paleoproductividad exportada mediante funciones de transferencia, basadas en asociaciones de foraminíferos planctónicos
- Estudiar las oscilaciones climáticas a escala milenaria durante los estadios isotópicos 21 al 11
- Identificar las causas de dichas variaciones climáticas y el agente responsable (orbital, oceanográfico…)
- Estudiar el comportamiento de las corrientes oceánicas superficiales del Atlántico Norte que afectan al área de estudio durante los estadios glaciales del MIS 20 al MIS 14

- Estudiar variaciones ambientales tanto superficiales como profundas, que afectan a la distribución de comunidades bentónicas durante los estadios isotópicos MIS 13 al MIS 11
- Comparar los registros obtenidos con datos publicados procedentes de otras regiones para poder establecer variaciones ambientales a nivel global

El presente trabajo opta al grado de "Doctor Internacional", por lo que está escrita mayoritariamente en inglés. No obstante, se adjuntan sendos capítulos "Resumen" y "Conclusiones", en español.

CAPÍTULO II

RESUMEN / ABSTRACT

CAPÍTULO II:
RESUMEN / ABSTRACT

RESUMEN

En esta tesis se reconstruyen las condiciones paleoceanográficas superficiales en el margen occidental ibérico mediante el análisis de las asociaciones de foraminíferos planctónicos de sedimentos procedentes del testigo IODP-U1385 (37º34.285´N, 10º7.562´W; 2585 m de profundidad). Los datos proporcionan un registro climático continuo y de alta resolución para los estadios isotópicos marinos (MIS) 21 a 11, ampliando el registro existente del margen ibérico hasta el noveno ciclo climático (867 ka).

Se identifican oscilaciones en la temperatura del agua superficial a escala milenaria tanto durante los períodos interglaciales como los glaciales, pero las oscilaciones de mayor amplitud (>5 º C) suceden en los inicios y terminaciones glaciales. En todas las desglaciaciones del Pleistoceno medio se registraron eventos de extremando enfriamiento marcados por máximos en el porcentaje de *Neogloboquadrina pachyderma* sinistral, con valores altos de $\delta^{18}O$ medido en foraminíferos planctónicos y mínimos en la relación Ca/Ti. Estos eventos de prominente enfriamiento de las aguas superficiales a lo largo del margen ibérico son el resultado de importantes reorganizaciones de la circulación en el Atlántico Norte, tanto a nivel de superficie como de aguas profundas, que tuvieron lugar como consecuencia del aporte de grandes cantidades de agua dulce al Atlántico Norte al inicio de las deglaciaciones. De hecho, la mayor parte de estos eventos fríos ocurrieron cuando la insolación de verano del hemisferio norte estaba próxima a sus valores máximos. La disminución de la formación de agua profunda en el Atlántico Norte redujo el aporte de aguas cálidas hacia el norte, que tiene lugar mediante el giro

subtropical del Atlántico Norte. Esta disminución de aporte cálido fue registrada en el margen ibérico por el incremento en el aporte de aguas subpolares frías. Después de cada episodio de enfriamiento profundo asociado a las deglaciaciones, el agua superficial experimentó un rápido calentamiento que marcaba el inicio del óptimo climático durante la fase temprana de los interglaciales. Los calentamientos bruscos quedaron registrados por un aumento repentino de la asociación subtropical, lo que indica incremento en el transporte del calor hacia latitudes altas a través de la corriente del Atlántico Norte. En el inicio de las glaciaciones, la temperatura de superficie en el margen portugués se mantuvo relativamente cálida, mientras que las aguas superficiales del Atlántico Norte se enfriaban, generando un alto gradiente latitudinal de temperatura superficial oceánica.

Se ha demostrado que el margen Ibérico suroeste es muy sensible a cambios en la distribución de corrientes oceánicas y masas de agua superficiales del Atlántico norte, así como a variaciones en la posición de los frentes ártico y subtropical. Durante los estadios glaciales del final del Calabriense y el Pleistoceno medio, tuvo lugar una importante reorganización en la circulación del Atlántico Norte que afectó a la distribución superficial de las distintas masas de agua y el trazado de las corrientes oceánicas. Este cambio tuvo lugar principalmente durante el estadio isotópico MIS 16, asociado al cambio de posición del frente ártico y a la intensificación en la formación de agua profunda Nord-atlántica, fenómenos ambos que tuvieron lugar durante este estadio glacial y el interglacial previo. Durante los períodos glaciales anteriores al MIS 16 el frente ártico estaba localizado en latitudes medias, lo que unido a los continuos flujos de hielo que al fundirse producían grandes cantidades de agua de muy baja salinidad, y por tanto muy baja densidad, dificultaba en gran medida la formación de aguas profundas Nord-atlánticas. La drástica reducción de la circulación profunda debilitó la circulación superficial, afectando a la corriente Nord-atlántica y facilitando la dispersión de aguas polares por latitudes medias del Atlántico Norte. La corriente del Atlántico Norte quedaba desviada al sur, adquiriendo una trayectoria casi oeste-este, y las aguas cálidas subtropicales llegaban al margen de Portugal circulando superficialmente sobre las aguas polares que llegaban desde el norte. Desde el MIS 16 el frente ártico adquiere una posición más al norte, lo que unido al incremento en la

formación de aguas profundas reactivó la NAC y facilitó el aporte de aguas templadas altas latitudes. La corriente de Portugal incrementó su intensidad a lo largo del margen oeste ibérico, impidiendo que las aguas subtropicales aportadas por la corriente de las Azores llegaran cerca de la costa, como quedó registrado en el sondeo U1385 por la reducida abundancia relativa de la asociación cálida superficial.

Parte del trabajo de esta tesis consiste en el estudio integrado de las condiciones oceánicas superficiales y las profundas durante los estadios isotópicos 13 al 11. Este estudio revela el predominio de aguas bien oxigenadas en el fondo, así como abundancia de disponibilidad de alimento para las comunidades bentónicas. La concentración de foraminíferos bentónicos en los sedimentos y las variaciones de las asociaciones de foraminíferos planctónicos sugieren cambios significativos en la productividad superficial y el aporte de nutrientes hacia el fondo marino desde el final del MIS 13 hasta el final del MIS 11. Hacia el final del MIS 13 la productividad exportada fue muy baja. Este hecho, junto a la presencia de sedimentos claros indica bajo aporte de carbono orgánico al fondo y altos niveles de oxigenación. Posteriormente, el aporte de materia orgánica se incrementó considerablemente y mantuvo altos valores hasta la Terminación V, permitiendo condiciones eutróficas, indicadas por valores altos de la tasa de acumulación de foraminíferos bentónicos. Durante el MIS 11 se registraron valores más bajos en la tasa de acumulación de foraminíferos bentónicos, lo que sugiere condiciones oligotróficas en el fondo y menor aporte de carbono orgánico. Esta variación de las condiciones ambientales bentónicas responde a cambios importantes en la ventilación del agua, probablemente ligados a variaciones en la circulación termohalina profunda del Atlántico Norte que, en último término determina el contenido de oxígeno y la disponibilidad de alimento en los sedimentos.

ABSTRACT

In this work I reconstruct past sea surface water conditions on the SW Iberian Margin by analysing planktonic foraminifer assemblages from IODP Site U1385 (37º34.285´N, 10º7.562´W; 2585 m depth). The data provide a continuous climate record from Marine Isotope Stages (MIS) 21 to 13, extending the existing paleoclimate record of the Iberian Margin back to the ninth climatic cycle (867 ka).

Millennial-scale variability in Sea Surface Temperature (SST) occurred during interglacial and glacial periods, but with wider amplitude (> 5 ºC) at glacial onsets and terminations. Pronounced stadial events were recorded at all deglaciations, during the middle Pleistocene. These events are recorded by large amplitude peaks in the percentage of *Neogloboquadrina pachyderma* sinistral coincident with heavy values of planktonic $\delta^{18}O$ and low Ca/Ti ratios. This prominent cooling of surface waters along the Portuguese margin is the result of major reorganizations of North Atlantic surface and deep-water circulation in response to freshwater release to the North Atlantic when ice sheets collapse at the onset of deglaciations. In fact, most of these cooling events occurred at times of maximum or increasing northern Hemisphere summer insolation. The slowdown of deep North Atlantic deep-water formation reduced the northward flow of the warm subtropical North Atlantic Drift, which was recorded on the Iberian margin by enhanced advection of northern cold subpolar waters. Following each episode of severe cooling at the onset of deglaciations, surface water experienced abrupt warming that initiated the climatic optimum during the early phase of interglacials. Abrupt warming was recorded by a sudden increase of the subtropical assemblage that indicates enhanced northward transport of heat through the North Atlantic Drift. At the onset of glaciations, SST along the Portuguese margin remained relatively warm while the surface waters of the North Atlantic experienced cooling, generating a large latitudinal SST gradient.

The Southwest Iberian margin is highly sensitive to changes in the distribution of North Atlantic currents and water masses, as well as to changes in the position of the Arctic and subtropical fronts. Variations in abundance of microfaunal assemblages indicate a change in the general North Atlantic circulation during MIS 16, associated

with the shift in the Arctic Front (AF) position and intensification of North Atlantic Deep Water (NADW) formation that happened at the time. During glacials previous to MIS 16 the southern position of the AF and the surges of icebergs and associated production of meltwater severely reduced the NADW formation, which resulted in a weakened North Atlantic Current and the dispersal of polar water over the North Atlantic. The NAC followed an almost pure west to east drift, and off the SW Iberian margin warm subtropical water overflowed (probably northward) the colder polar and subpolar water masses advected southward. Since MIS 16, the northern position of the Arctic Front and increased production of NADW reactivated the North Atlantic Current, which advected warmer water to higher latitudes. Off the Iberian margin, the Portugal Current became stronger and diverted warmer water offshore, reducing the relative abundance of warm surface-dwelling species in Site U1385.

Integrative research including deep and surface analysis has been conducted to evaluate the incidence that surface changes had on deep-sea environment from MIS 13 to MIS 11. Results reveal the predominance of well-oxygenated bottom and pore-waters, as well as abundance of food in the sediment for benthic communities. Benthic foraminifer concentration in the sediments and variations of the planktonic foraminifer assemblages suggest significant changes in surface productivity and food supply to the sea floor since the ending of MIS 13 to the end of MIS 11. At the end of MIS 13 values of Annual Export Productivity were very low, what together with the presence of light-color sediments reveals lower organic carbon flux to the bottom and high oxygen conditions. Afterwards the organic matter supply increased rapidly and remained very high until Termination V, determining an eutrophic environment, expressed by high benthic foraminifer accumulation rates, and reduced availability of oxygen. Lower benthic foraminifer accumulation rates during MIS 11 suggest oligotrophic conditions at the bottom consistent with lower inputs of organic carbon, associated to high oxygen content of bottom waters that agrees with the lighter color of the sediments. The evolution of the macrobenthic tracemaker community during MIS 13 and 11 responds to major changes in bottom water ventilation probably linked to variations in deep water (North Atlantic) thermohaline circulation, determining variations in oxygen and food availability.

CHAPTER III

INTRODUCTION

CHAPTER III

INTRODUCTION

1. CLIMATE DURING THE PLEISTOCENE

1.1. Glacial cycles

During the Quaternary period global climate has been characterised by periodic oscillations of advance/retreat of the ice sheets that partly covered the Earth´s continents (e.g., Lisiecki and Raymo, 2007). Each climatic cycle begins with a very warm interval known as interglacial climatic optimum, when ice volume reaches a minimum value. Models suggest that some of these ice volume minima, like during MIS 11, were even lower than present day values (Raynaud et al., 2003). The climatic optimum is followed by progressive cooling and increase of ice volume, marked by cool-warm oscillations of lesser amplitude and higher frequency (21 ky) than glacial-interglacial ones, which culminates with the highest extension of ice sheets during the cycle, known as glacial maximum.

During the last million of years these climatic cycles have followed an approximate periodicity of 100 ky with superimposed climatic oscillations of ~41 ky and ~21 ky (e.g., Imbrie et al., 1992; Ruddiman, 2006; Huybers, 2007), all of which can be correlated with the orbital cycles described by Milankovitch (1941). Nevertheless, at a lower time scale, discrepancies exist between climatic records and orbital parameters, which suggest the influence of other factors in modulating the global climatic system. Some of these factors are thought to be the atmospheric concentration of greenhouse gases (Shackleton and Pisias, 1985; Kennett et al., 2000; Ruddiman, 2003, 2006; Toggweiler et al., 2006), oceanic circulation (Broecker, 1989; Raymo et al., 1997; McManus et al., 2004; Pisias et al., 2010), ice sheets size, and albedo effect (Imbrie et al., 1993; Denton el al., 2010).

1.2. Suborbital climate variations: Heinrich Events and Daansgard-Oeschger oscillations

During middle and late Pleistocene several millennial-scale iceberg surges into the North Atlantic occurred that altered the ocean´s heat conveyor and caused fundamental reorganisations of the ocean-climate system, producing extreme cooling (Heinrich, 1988; Broecker, 1994, Cortijo et al., 1995; Hodell et al., 2008; Channel et al.,

2012). These episodes, known as "Heinrich events" (Broecker et al., 1992), had a duration of a few hundred to a thousand years and a recurrence of ~7-10 ky (e.g. Bond and Lotti, 1995). Superimposed on this variability, a series of large shifts in air temperature, up to 15 ºC (Huber et al., 2006), in a few decades (Stuiver and Grootes, 2000), termed Dansgaard–Oeschger (D–O) oscillations have been registered in the Greenland ice-core records (e.g., Dansgaard et al., 1993; Grootes et al., 1993); the final event coincided with the Younger Dryas (e.g. Bond et al., 1992). These stadial-interstadial oscillations appear to be grouped in sequences of progressively cooler events, the end of each sequence marked by the deepest cooling; such sequences are known as "Bond cycles" (e.g., Broecker et al., 1990) and are thought to be linked to changes in the mode of overturning circulation in the Atlantic ocean (Broecker et al., 1985).

Most of Heinrich events happened at the end of the colder phase of a Bond cycle and were followed by warming to almost interglacial temperatures (e.g. Bond et al., 1992; Wright and Flower, 2002).

1.3. Climate in the subtropical and middle latitude North Atlantic

The climate regime over middle latitude North Atlantic and Western Europe is mainly governed by the position and intensity of the Azores high-pressure area (AzH) and its latitudinal motion and intensification through the annual seasonal cycle. During spring/summer the AzH migrates northward, which results in strong northerly winds, while during fall/winter months the AzH is significantly weaker (Maze et al., 1997; Coelho et al., 2002). In consequence, this region is under the influence of the North Atlantic Oscillation (NAO) anomaly (Hurrell, 1995). This anomaly is measured by the NAO index, that records the difference in atmospheric pressure between the Iceland low and the AzH. The anomaly is positive (NAO^+) when the Az high is reinforced and the difference with the Iceland low is greater. In this scenario, westerly winds become stronger and the Gulf Stream migrates northward, which results in anomalously mild and wet winters for northern Europe, while southern Europe becomes anomalously cold and dry (Fig. III-1). The NAO also affects the sea ice coverage in the North Atlantic (Deser et al., 2000) and, indirectly, the thermohaline circulation (Dickson et al., 1996).

Off Portugal, NAO^+ phases are associated with reinforcement of the upwelling via strengthening of NE trade winds. In NAO^- conditions the westerlies are weaker, the Gulf Stream is located southward, climate in NW Europe is dry while in the south is wet and off Iberia the Azores Current prevails, inducing warm conditions and the reduction of the upwelling (Dickson et al., 1996).

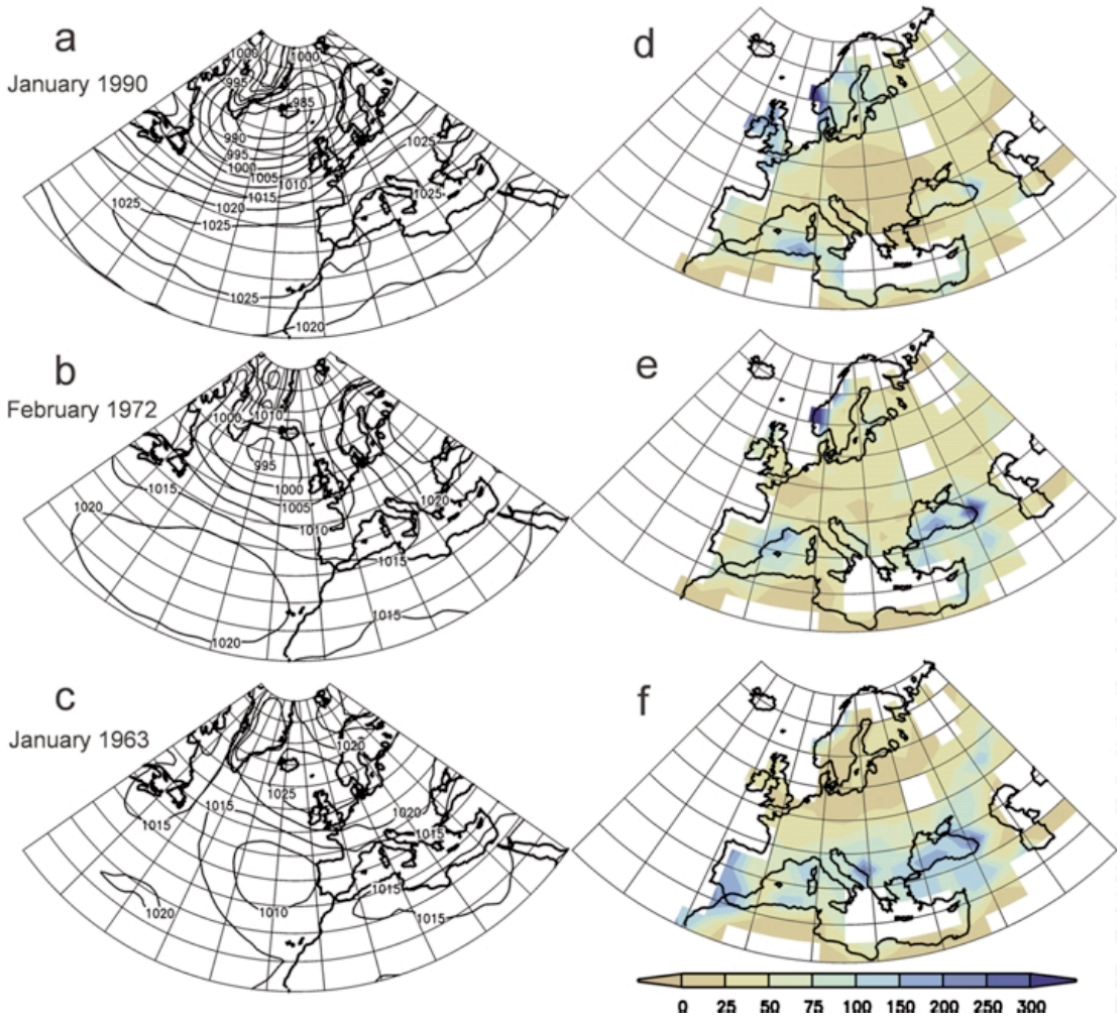

Figure III-1. Sea level pressure (a-c, hPa) and precipitation (d-f, mm) for months with positive (a,d), negative (b,e) and extremely negative (c,f) NAO index (from Wanner et al., 2001).

In tropical regions, climatic conditions are mainly governed by the alternation of rainy (warm) and dry (colder) seasons that trace the seasonal motion of the ITCZ. The

southward migration of the ITCZ appears to be linked to cooling on the North Atlantic over various time- scales (Black et al., 1999; Peterson et al., 2000; Schmidt et al., 2004) through weakening of the Atlantic Meridional Overturning Circulation (Schiller et al., 1997).

The climate of southern Europe, specifically the Iberian Peninsula, is also connected with the ENSO through more complex mechanisms. For example, both ENSO and NAO phenomena influence rainfall in Iberia (Rodo et al., 1997; Trigo et al., 2002). ENSO oscillation signals have been observed in the rainfall records of the past century in Iberia. There is clear evidence that the western part of the peninsula is more generally under the influence of NAO in winter while the eastern part is under the influence of ENSO in spring and autumn.

2. PLANKTONIC FORAMINIFERA AS OCEANOGRAPHIC PROXIES

2.1. Main species in the region

Some key species or groups of species can be used as paleoceanographic and paleoclimate tracers. This work focuses on these ones.

The polar species ***Neogloboquadrina pachyderma*** **sinistral** (Nps), with a temperature tolerance range between –1 and 8 ºC and an optimum of 2 ºC (Tolderlund and Bé, 1971), has been extensively used within the North Atlantic as a proxy for climate cooling (Ruddiman et al., 1986; Bond et al., 1993) and to monitor southward penetrations of very cold water masses of polar origin, usually associated to iceberg discharges and/or migrations of the polar front (eg., Bond et al., 1992; Cayre et al., 1999; de Abreu et al., 2003; Eynaud et al., 2009). At present, this species is absent from plankton tows (Ottens, 1991) and surface sediments (Pflaumann et al., 2003) (Simmax database) collected in the study area (Fig. III-2).

Turborotalita quinqueloba (Tq) has a temperature tolerance range of 4.6ºC – 10.8ºC (Tolderlund and Bé, 1971), with an optimum of 12ºC (Stangeew, 2001) and is usually associated to high phytoplankton productivity (Bé, 1977; Johannessen et al., 1994). High percentages of this species are found south of Iceland (Pujol, 1980), and its

maximal abundance has been recognized as associated with the arctic front (Johannessen et al., 1994; Cayre et al., 1999; Wright and Flower, 2002).

Globigerina bulloides (Gb) lives in the upper 50-60 m of the water column, with a tolerance range between 2 and 16 ºC (Tolderlund and Bé, 1971; Bé, 1977; Schiebel et al., 1997; King and Howard, 2005). This species is abundant in areas of high phytoplankton productivity and deep mixing layer, as well as in subpolar waters (north of 48 ºN), which are rich in nutrients (Reynolds and Thunell, 1985; Schiebel et al., 2001) (Fig. III-2). It is traditionally considered a proxy for upwelling (Prell, 1984), particularly in the northeastern subtropical Atlantic (Chapman et al., 1996) and at the Iberian margin (de Abreu et al., 2005; Salgueiro et al., 2008).

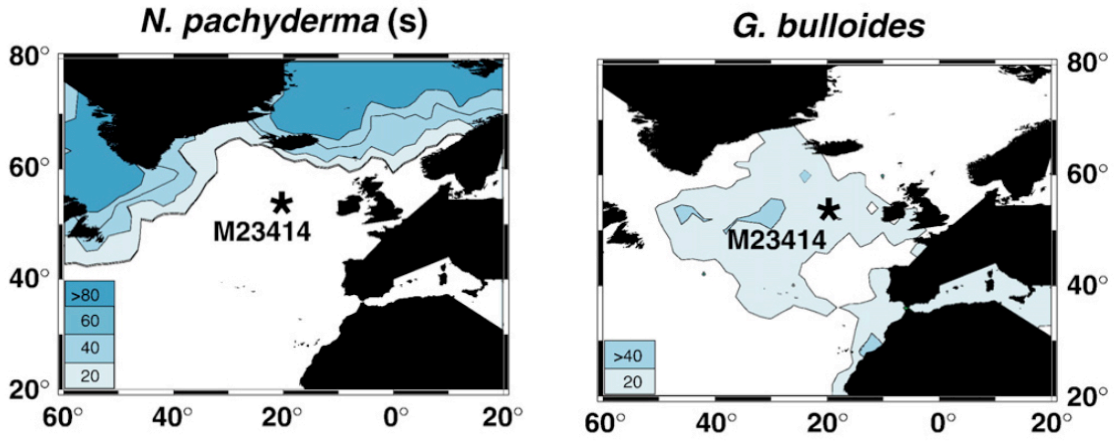

Figure III-2. Distribution of *Neogloboquadrina pachyderma* sinistral and *Globigerina bulloides* in the North Atlantic (from Kandiano and Bauch, 2007; data set: Pflaumann et al., 2003).

Neogloboquadrina pachyderma **dextral** (Npd) has a temperature optimum between 10-18 ºC and the limit with Nps is associated to the April isotherm of 7.2 ºC (Ericson, 1959). It lives at ~100 m water depth, near the thermocline and the chlorophyll deep maximum (Reynolds and Thunell, 1989). In the region, this species is typical of the stratified, low productivity waters produced toward the end of upwelling season (Rogerson et al., 2004) and has been used as a proxy for the Portugal Current (Salgueiro et al., 2008).

Globorotalia inflata represents the transitional North Atlantic water (Ottens, 1992) and can tolerate a wide temperature range, with higher percentages occurring between 10.4 – 19.9ºC (Bé and Tolderlund, 1971). It is a deep dweller (100-250 m) and thrives below the chlorophyll deep maximum (Fairbanks et al., 1980; Mortyn and Charles, 2003; King and Howard, 2005). High percentages of this species (>15%) occur at the present day western boundary of the upwelling front in the region, coinciding with oligotrophic waters (Salgueiro et al., 2008).

Globigerinita glutinata is a non-spiny species that feed on diatoms (Hemleben et al., 1989). The study of the living planktonic fauna in the eastern Atlantic has confirmed that this opportunistic species prefers productive environments (Ottens, 1992) and high percentages of it are observed in relation to surface current eddies that help to increase the nutrient input to the mixed layer (Schmuker and Schiebel, 2002; Olson and Smart, 2004). This early bloom species (Schiebel, 2000) has been used as a tracer for changing paleoproductivity (Mohtadi and Hebbeln, 2004; Vautravers and Shackleton, 2006).

Globigerinoides ruber is a surface dweller of subtropical waters (Ottens, 1991) (Fig. III-3) and can tolerate a wide range of salinity (Bijma et al., 1990). It is present today in the area during non-upwelling months (Salgueiro et al., 2008).

Globigerina falconensis is a tropically adapted symbiont-bearing form of *G. bulloides* (Hemleben et al., 1989) and its presence may suggest warm conditions. However, in the Arabian Sea it has been found related to conditions of enhanced productivity and mixing of water (Schulz et al., 2002).

Globorotalia scitula is a deep-dwelling cosmopolitan species, most frequent in temperate waters (Bé, 1977; Hemleben et al., 1989). In the surface sediments of the North Atlantic, this species reaches its maximum abundance in the Azores region to the north of the Azores Front (Prell et al., 1999). In consequence, changes in abundance of this species can be used as an indicator of the Azores Front position (Schiebel et al., 2002).

Globorotalia truncatulinoides (Got) (250-300 m) has been used to detect possible changes in the structure of the deep thermocline (e.g., Hemleben et al., 1989; Abrantes et al., 2001; Matzumoto and Lynch-Stieglitz, 2003; de Abreu et al., 2005). The

left coiling variety of this species preferentially lives in cold waters (Fig. III-3) and is considered an index for the influence of oligotrophic intermediate water masses (e.g., ***Globorotalia hirsuta*** is another deep dweller that, similarly to Got, needs good mixing of water in order to develop (e.g., Hemleben et al., 1989).Peeters et al., 2002; Matzumoto and Lynch-Stieglitz, 2003; de Abreu et al., 2005).

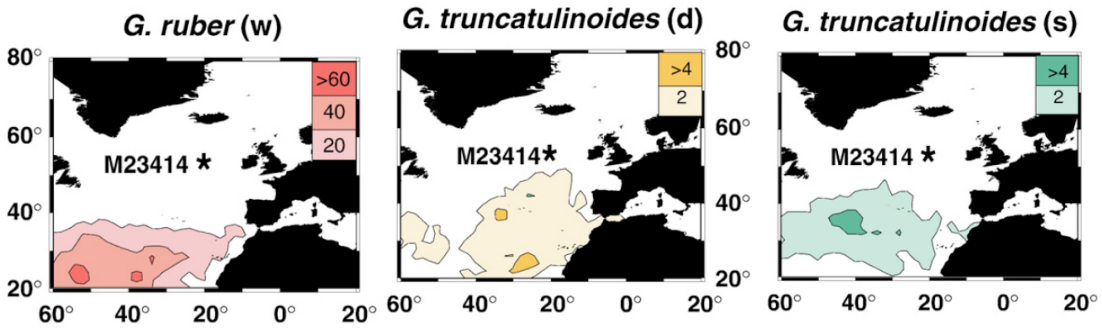

Figure III-3. Distribution of *Globigerinoides ruber* white and of *Globorotalia truncatulinoides* dextral and sinistral in the North Atlantic (from Kandiano and Bauch, 2007; data set: Pflaumann et al., 2003).

2.2. Planktonic foraminifer assemblages

Works on surface water masses and surface sediments have identified several distinct assemblages of planktonic foraminifer fauna for the North Atlantic (e.g., Kipp, 1976; Ottens, 1991; Cayre et al., 1999; Chaisson et al., 2002; Schiebel et al., 2002; Vautravers et al., 2004; de Abreu et al., 2005; Salgueiro et al., 2008). These assemblages (Appendix IV) have been used to characterize the different water masses in the region.

3. OCEAN SEDIMET CORES - RECORDING THE PAST

The bottom of the ocean constitute depositional environments which register not only events and conditions of the bottom, but also those happening at the surface of the ocean, in the continents and even in ice sheets like central Greenland (e.g., Ruddiman and Bowles, 1977; Heinrich, 1988; Shackleton et al., 2000; Sánchez Goñi et al., 2002). As deposition prevails over erosion throughout most of the ocean, the oceanic sedimentary record provides useful data along prolonged time series, which allows faithful reconstruction of past climate and oceanographic characteristics.

Several oceanic drilling actions have been conducted to retrieve sediment cores from the different seas and oceans. After the Deep Sea Drilling Project, 1985 saw the start of the Ocean Drilling Program (ODP), which was an international cooperative effort to explore and study the composition and structure of the Earth's sub-seafloors. The Integrated Ocean Drilling Program (IODP 2003-2013), built upon the international partnerships and scientific success of previous joint-campaigns, was financed by the contributions from 26 participating nations and conducted 52 expeditions.

Figure III-4. *JOIDES Resolution* at Lisbon, during Expedition 339 (Expedition 339 Scientists, 2012).

4. EXPEDITION IODP-339

Integrated Ocean Drilling Program (IODP) Expedition 339 combined IODP Proposal 644-Full2 and ancillary proposal letter (APL)-763. The expedition focused mainly in the significance of Mediterranean Outflow Water (MOW) on North Atlantic Ocean circulation and climate (Stow et al., 2012). This expedition provided the opportunity to understand the global link between paleoceanography, climate variations and sea level changes from Messinian to recent time and focussed on the

importance of ocean gateways in regional and global ocean circulation and climate variations. Nevertheless, a second objective was addressed, to produce a continuous marine reference section of Pleistocene climate variability and changes in surface and deep-water circulation along western Iberian margin (Expedition 339 Scientists, 2012).

Seven sites were cored during the campaign (Fig. III-5, III-6). Six Sites, located in the Gulf of Cádiz and on the West Iberian margin, addressed the study of the sedimentary and paleoceanographic implications of the MOW and the evolution of its influence since the Messinian. Site U1385 was cored further offshore to serve the second objective of Expedition 339 (APL)-763.

IODP core U1385 was retrieved using the APC and nonmagnetic core barrels on board the scientific drillship, D/V *JOIDES Resolution*. A total of 622 m of hemipelagic sediments were recovered, covering a continuous sedimentary succession extending back to 1.4 Ma (Fig. III-6). Five holes (A, B, C, D and E) were cored to produce a primary splice and two secondary ones, the later using intervals from only two holes each.

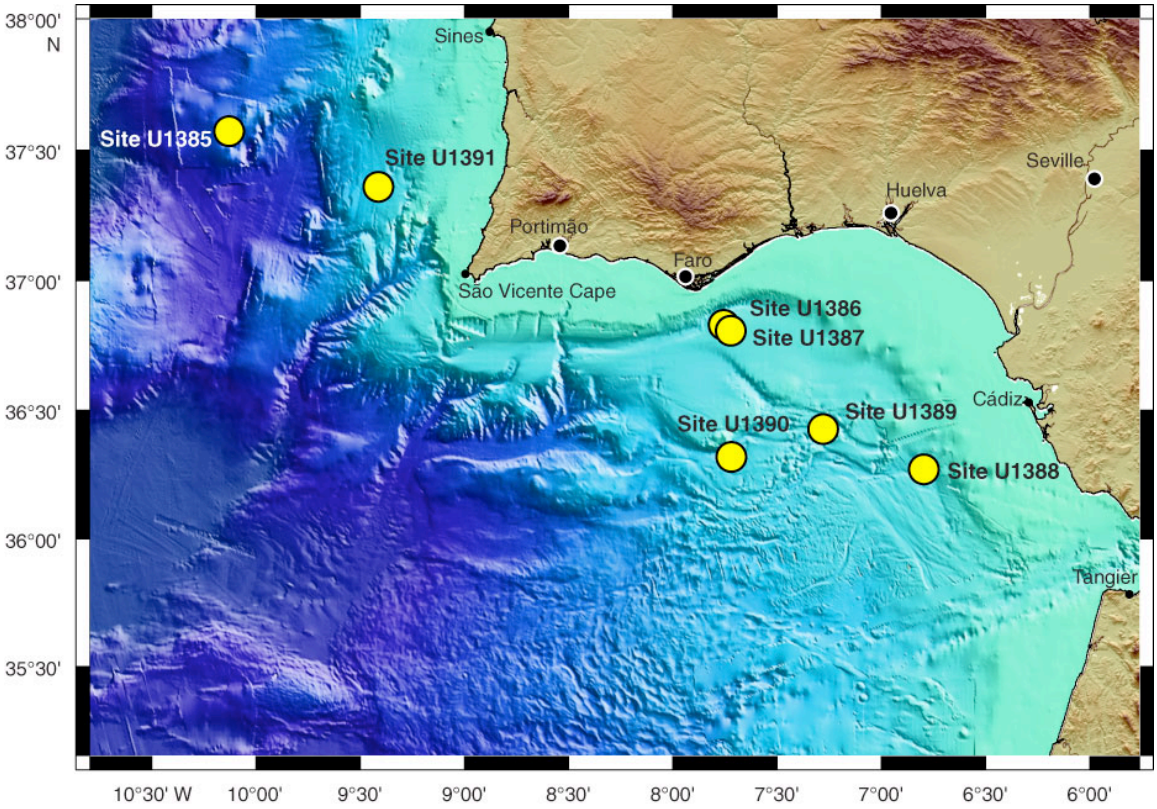

Figure III-5. Expedition 339 sites in the Gulf of Cádiz and West Iberian margin (Expedition 339 Scientists, 2012).

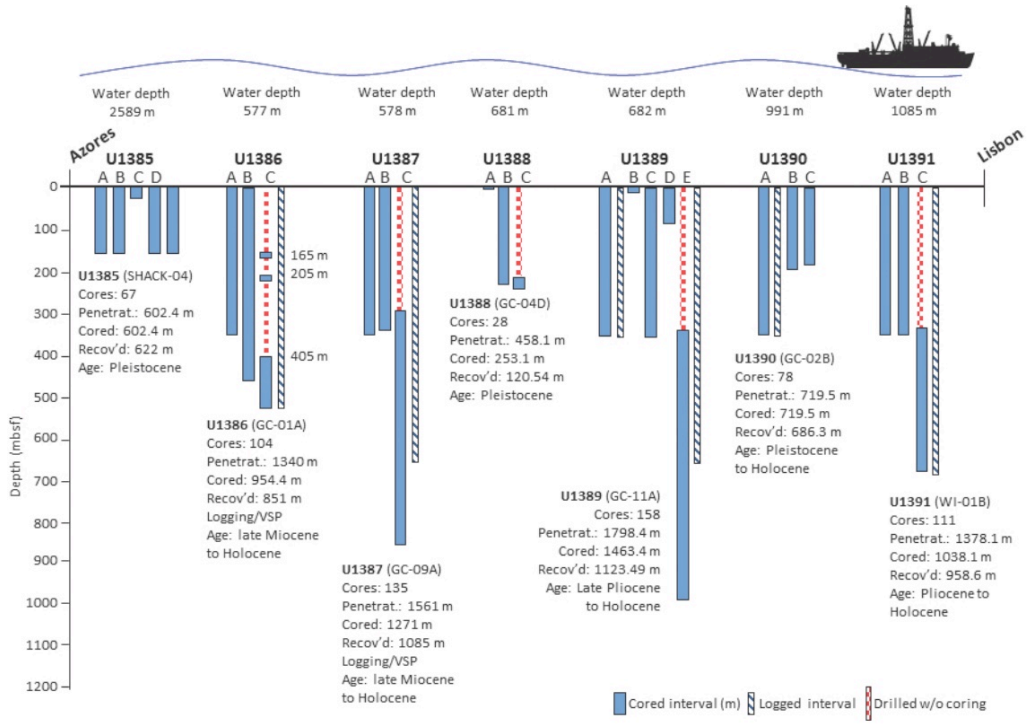

Figure III-6. Expedition 339 sites´ coring information (Hernández-Molina et al., 2013).

CHAPTER IV

SITE SETTING

CHAPTER IV

SITE SETTING

1. SITE IODP-U1385

1.1. Importance of the Shackleton Site

The Southwestern Iberian margin is a focal location for comprehensive evaluation of climatic variability in both hemispheres over long time periods. A number of studies have been conducted on sediment cores obtained in this margin to characterize the late Pleistocene (Shackleton et al., 2000, 2004; de Abreu et al., 2003; Roucoux et al., 2005; Martrat el al., 2007; Rodrigues et al., 2011; Hodell et al., 2013a). Nick Shackleton was the first in highlighting the global importance of a specific area of this margin (Shackleton et al., 2000) that has ever since been known as the Shackleton site. Sediments in this area preserve a high-fidelity record of millennial-scale climate variability for the last glacial cycle that can be correlated precisely to polar ice cores in both hemispheres (Fig. IV-1). Moreover, the narrow continental shelf off Portugal results in rapid delivery of terrestrial material (e.g., pollen) to the deep-sea environment, thereby permitting correlation of marine and ice-core records to European terrestrial sequences (e.g., Shackleton et al., 2000, 2004; Sánchez Goñi et al., 2002; Margari et al., 2010). The continuity, high sedimentation rate and fidelity of the record in the area make this Site a key location for paleoclimate and oceanographic researches (Hodell el al., 2013b).

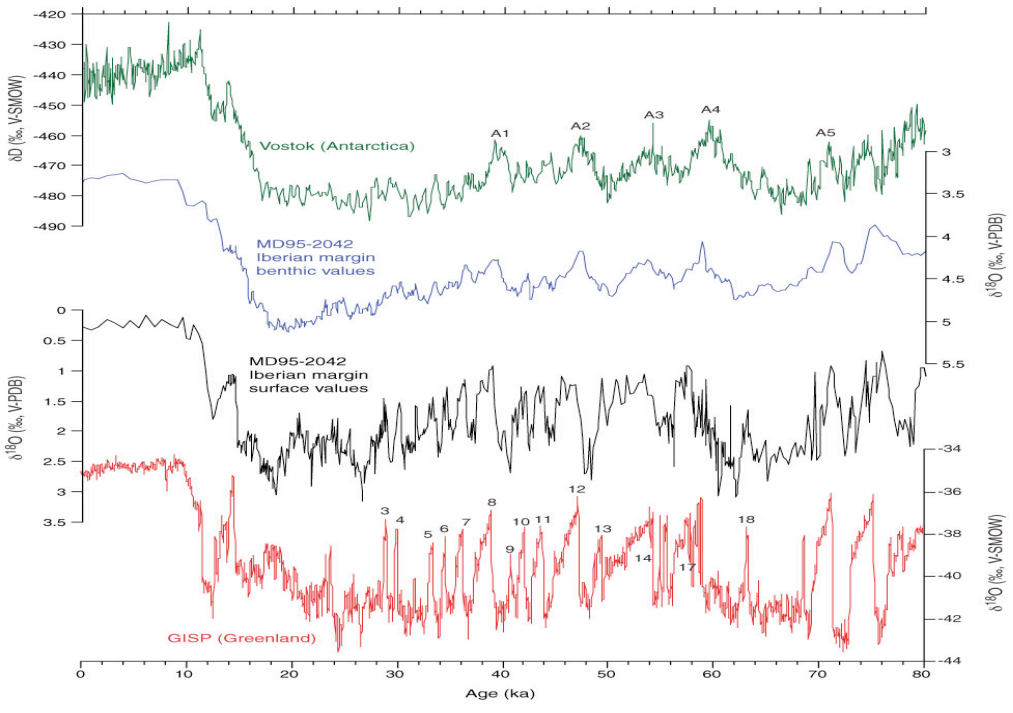

(Previous page) **Figure IV – 1.** Correlation of $\delta^{18}O$ record of GISP ice core (red line; 1–18 = marine isotope stages) to $\delta^{18}O$ of Planktonic foraminifer *Globigerina bulloides* (black line) in Core MD95-2042. Resulting correlation of Vostok δD (green line; A1–A5 = oscillation events) and benthic $\delta^{18}O$ of Core MD95-2042 (blue line) based on methane synchronization. V-PDB = Vienna Peedee belemnite, V-SMOW = Vienna standard mean ocean water. Age is from Shackleton et al. (2004). (Expedition 339 Scientists, 2012)

1.2. Site description

Site IODP-U1385 was drilled at the same location of piston Core MD01-2444, off the western Iberian margin (37º34.284´N, 10º7.562´W) at 2589 metres water depth, on a spur on the upper slope that is elevated above the abyssal plain on the continental rise, far from submarine canyons and out of the direct influence of the Tagus river (Fig. IV-2). Pelagic sedimentation prevails during interglacials, while terrigenous input is enhanced during glacials due to a lowered sea level. Both during glacial and interglacial periods, a high sedimentation rate (~ 10 cm/ky) prevails (Stow et al., 2012).

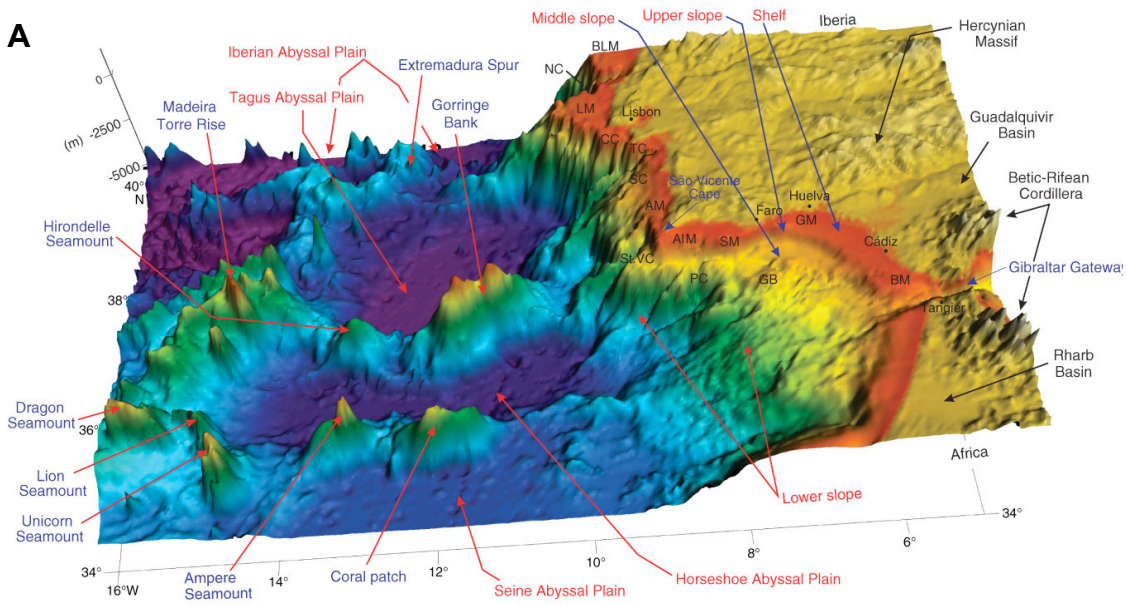

Figure IV - 2a. Three-dimensional regional bathymetric map of the southwestern Iberian margin (Expedition 339 Scientists, 2012). *BLM* = Beira litoral margin, *NC* = Nazaré Canyon, *LM* = Lisbon margin, *CC* = Cascais Canyon, *TC* = Tagus Canyon, *SC* = Setúbal Canyon, St. *VC* = São Vicente Canyon, *AlM* = Algarve margin, *SM* = Sudiberic margin, *PC* = Portimao Canyon, *GB* = Guadalquivir Bank, *GM* = Guadalquivir margin, *BM* = Betic domain margin.

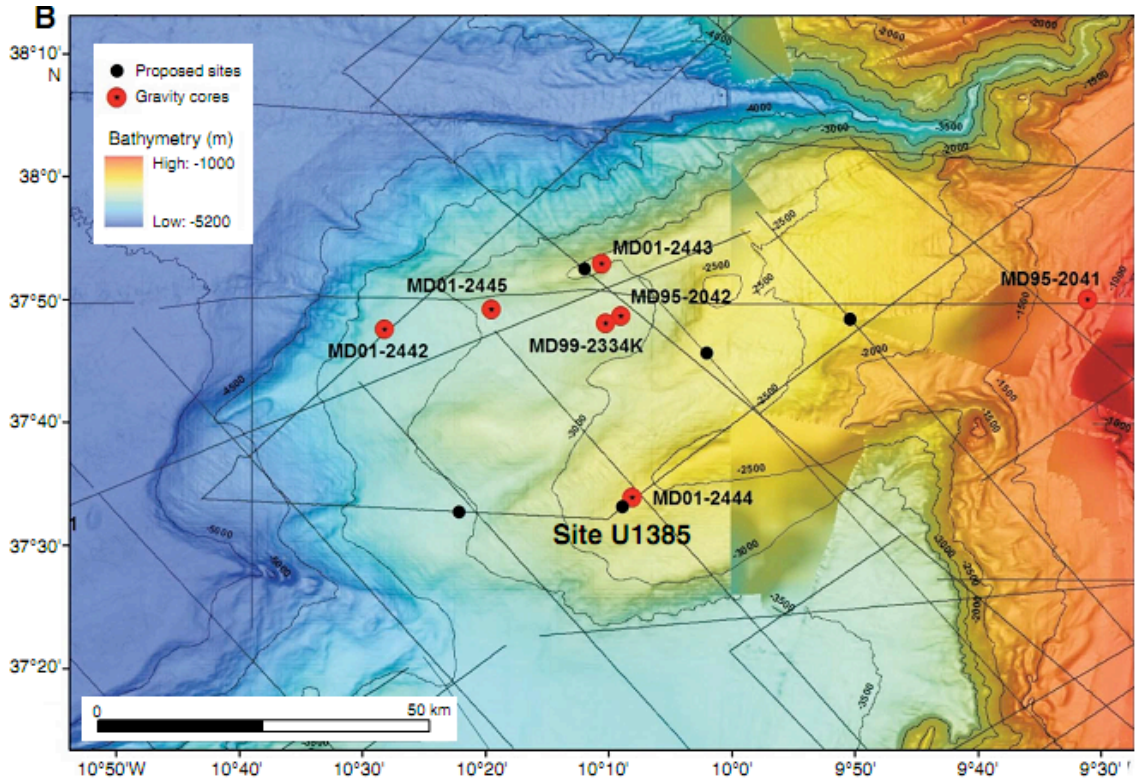

Figure IV - 2b. Detailed bathymetric map of the Shackleton Site showing the position of Site U1385 and nearby *Marion Dufresne* piston Cores (after Stow et al., 2013).

2. GEOLOGICAL SETTING

The southwestern margin of the Iberian Peninsula, at the eastern segment of the Azores–Gibraltar fracture zone, is the location of the diffuse plate boundary between Eurasia (Iberia) and Africa (Nubia). The present plate convergence rate between the African and Eurasia plates in the Gulf of Cadiz area is ~4 mmyr^{-1} (e.g., Stich et al., 2006) with a WNW–ESE direction. A series of thrusts (Fig. IV-3) and dextral strike- slip faults (Zitellini et al., 2009) can be identified. The tectonic structure of this area, related with the rifting of the central and North Atlantic basins, was mainly set up from the Late Triassic to the Early Cretaceous (Maldonado et al., 1999) and later modified during the Cainozoic, especially in the Miocene (Zitellini et al., 2009; Duarte et al., 2011).

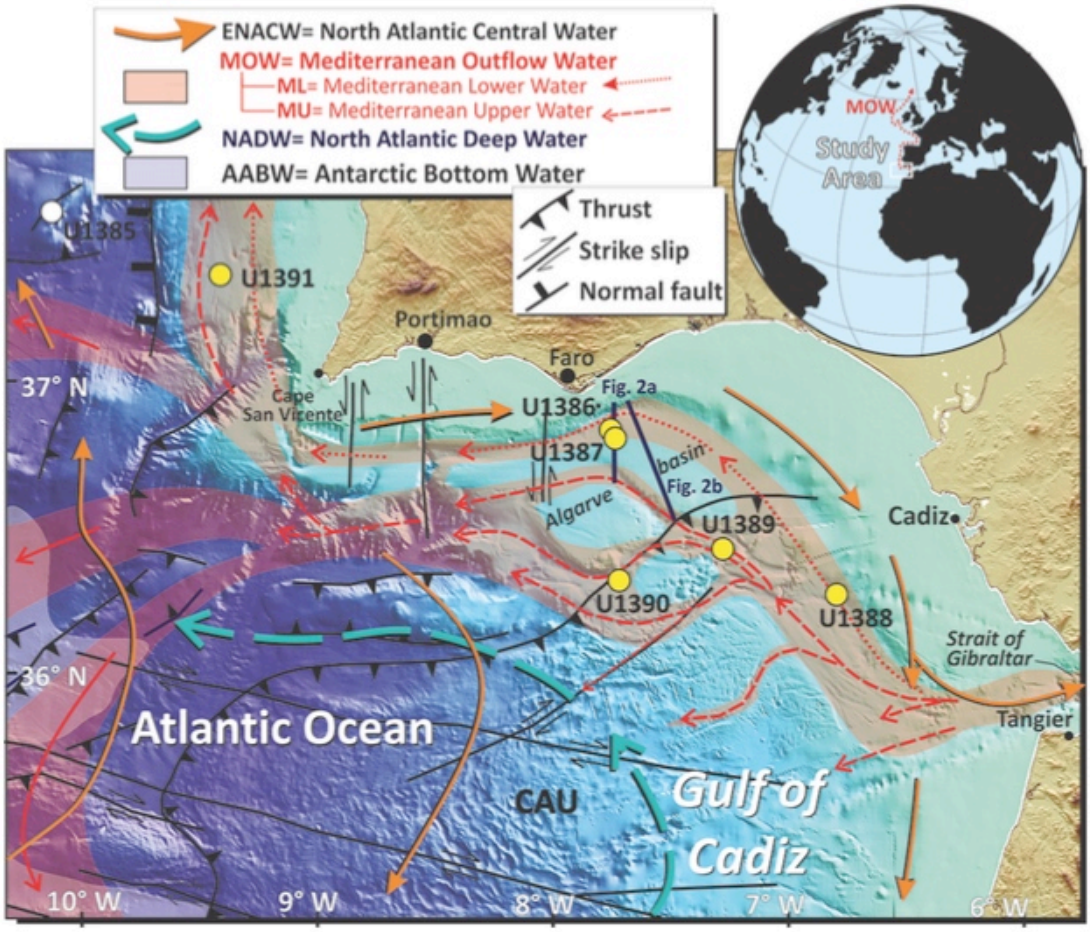

Figure IV - 3. Tectonic setting of the Gulf of Cadiz and location of Expedition 339 sites (yellow solid circles) (Hernández-Molina et al., 2013).

3. OCEANOGRAPHYC SETTING

The western Iberian margin lies under the influence of several distinct water masses clearly identified and characterized (e.g. Fiúza et al., 1998; Hernández-Molina et al., 2011). These are, from top to bottom: the *North Atlantic Central Water* (NACW), reaching around 500-600 m depth and characterized by a complex circulation pattern; the *Mediterranean Outflow Water*, warm and very saline, flowing to the north and west along the middle slope between the NACW and 1,500m; the *Labrador Sea Water* (LSW), flowing towards the southwest across the Northeast Atlantic, can reach 2,200 m depth, depending on the thermohaline equilibrium with the *North Atlantic Deep Water* (NADW), which flows below or at the same depth than the LSW down to 4,000 m depth; and, across the lower slope and abyssal plains, the *Lower Deep Water*,

composed mainly of Antarctic Bottom Water and carbonate corrosive. The studied site is under the influence of NACW in the surface and the NADW in the bottom (Fig. IV-4).

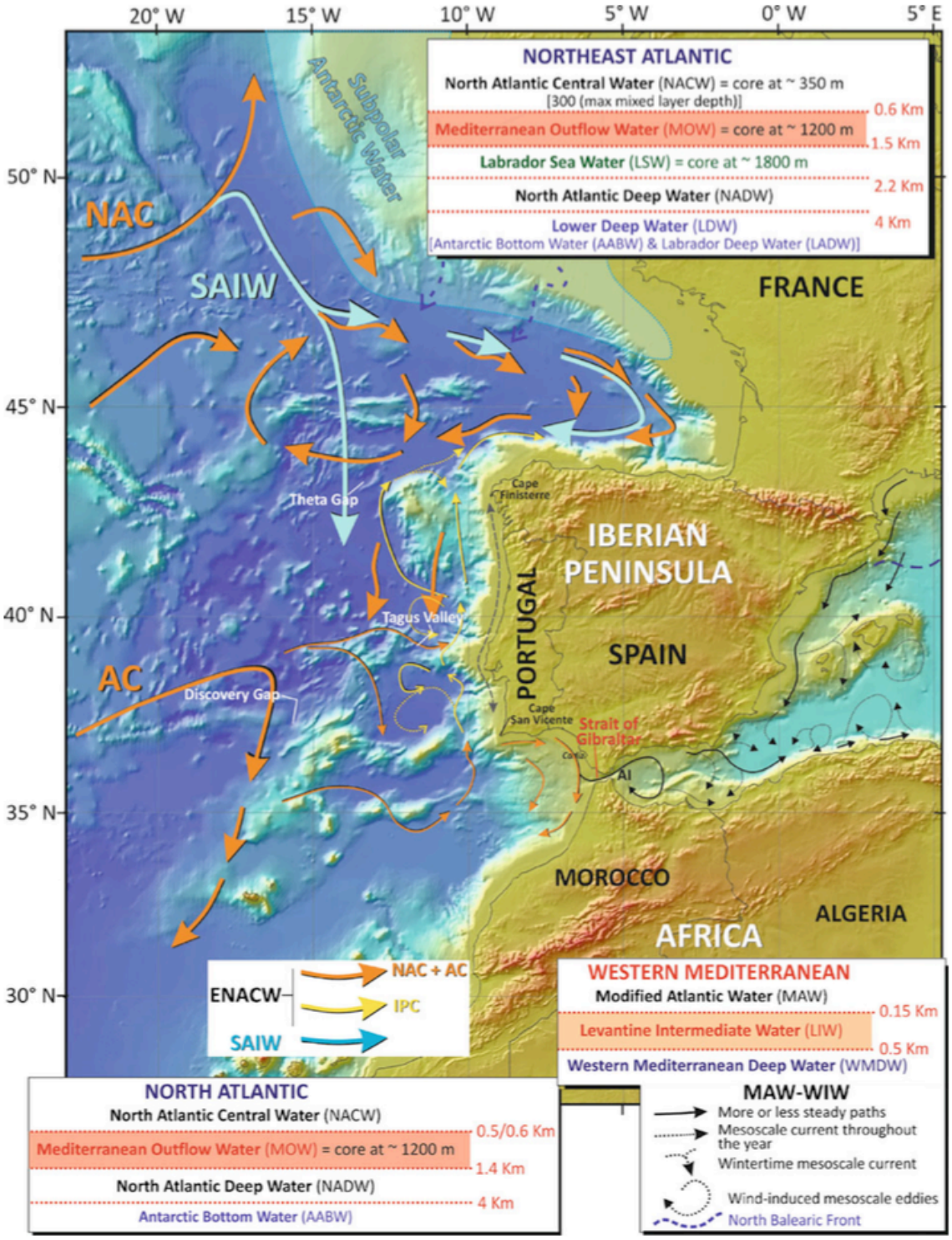

Figure IV - 4a. Superficial water circulation in the area. *AC* Atlantic Current, *ENACW* East North Atlantic Current Water, *IPC* Iberian Polar Current, *NAC* North Atlantic Current, *SAIW* Subarctic Intermediate Water (from Hernández-Molina et al., 2011).

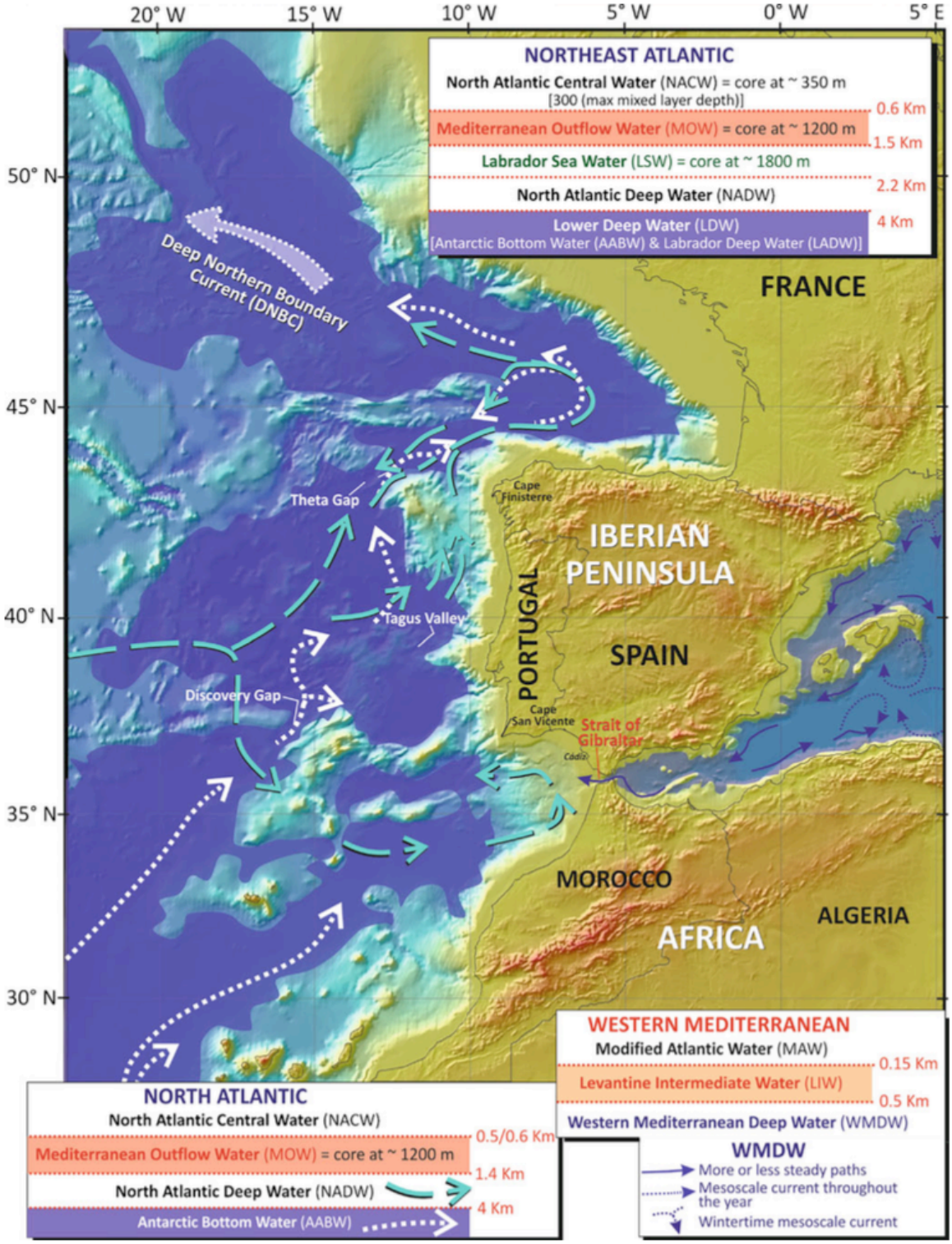

Figure IV - 4b. Deep-water circulation in the area (from Hernández-Molina et al., 2011).

Surface water circulation in the region (Fig. IV-5) is determined by the eastern gyre of the North Atlantic (Eastern North Atlantic Central Water or ENACW) which consists of two branches with different origin and distinct thermohaline characteristics. The North Atlantic Current in the north, of sub polar origin (ENACWsp), is formed in the eastern Atlantic north of 46º (McCartney and Talley, 1982; Branbilla and Talley, 2008) and the Azores Current in the south, of subtropical origin and formed along the Azores Front at about 35–37º N (Rios et al., 1992). The subtropical branch (ENACWst) is saltier (S = 35.8 – 36.75), warmer (13.13ºC - 18.50ºC) and less dense than the subpolar branch (S = 35.4 – 35-66; T = 10ºC – 12.2ºC) and overflows it with a decreasing lower limit from south to north until around 42.7ºN, where a transition zone limiting the two different masses of water in surface has been identified (the "Galicia Front", Fiúza el al., 1998), but the actual transition between both water masses depends on the variability of their thermohaline characteristics. The general circulation in the upper layers of the Central Water in the eastern North Atlantic is an eastward flow, due to the Azores Current, that bifurcates while approaching the Iberian coast in the north and the African one in the south; the northern branch of the ENACWst takes the designation of Portugal Coastal Countercurrent and advects warm waters northwards (Peliz et al., 2005).

This general distribution of water masses is influenced by the seasonal migration of the Azores anticyclonic cell and its associated large-scale wind pattern. During most of the year coastal convergence conditions prevail, favouring convection of surface waters that can reach depths between 700 m, in the north of the Iberian margin, and less than 200 m towards the south (Fiúza el al., 1998). In summer, the weakening of the Iceland Low Pressure area allows the strengthened Azores high-pressure cell to migrate northwards; the strong northerlies produced along west Iberia induce the southward Portugal Coastal Current, responsible for the onset of a coastal upwelling of cold, less salty and nutrient-rich waters of the deeper layers of Eastern North Atlantic Central Water (ENACW). Upwelled waters form an averaged 50 km wide band along the coast, with extensions and filaments that can penetrate more than 200 km offshore (Sousa and Bricaud, 1992). Site U1385 is located inside this band.

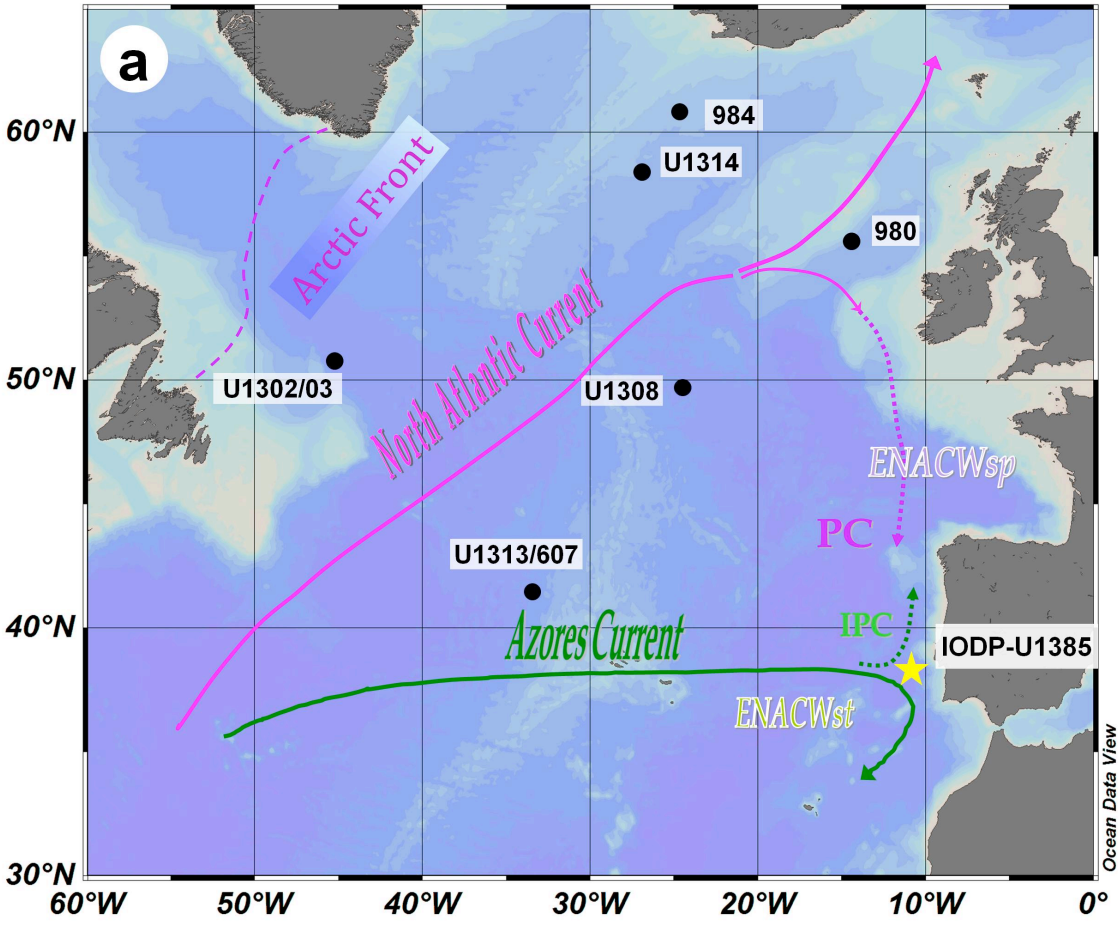

Figure IV - 5. Map showing the location of Site IODP-U1385 in the Iberian margin and its oceanographic setting (Position of the Arctic Front, from: Swift, 1986 and Pflaumann et al., 2003). *PC* Portugal Current, *IPC* Iberian Poleward Current, *ENACWsp* Eastern North Atlantic Central Water of subpolar origin, *ENACWst* Eastern North Atlantic Central Water of subtropical origin. Sites mentioned in this work are also depicted. Geographical data of these core sites are listed in Table IV-1.

Site	Latitude	Longitude	Water depth
ODP-984	61º25´N	24º04´W	1650 m
IODP-U1314	58.4º N	27.9º W	2820 m
ODP-980	55º29.09´N	14º42.13´W	2168 m
IODP-U1302/03	50º10´N	45º38.3´W	3520 m
IODP-U1308	49º52.67´N	24º14.3´W	3427 m
DSDP 94-607 // IODP-U1313	41º00.07´N	32º57.40´W	3412 m
MD01-2446	39º03.35´N	12º37.44´W	3570 m
MD03-2699	39º02.20´N	10º39.63´W	1865 m
IODP-U1385	37º34.284´N	10º7.562´W	2589 m

Table IV- 1: Location of core sites mentioned in this work.

4. THE NORTH ATLANTIC OCEANIC CIRCULATION ALONG THE PLEISTOCENE

Present-day North Atlantic is characterized (Fig. IV-6) by a continuous flow of warm and salty surface water originated in the tropical region and transported northwards by the Gulf Stream, which continues as the NAC. The NAC forms the transition zone between the cold and productive waters located at the North of the Arctic Front (AF) (eg., Johannessen et al., 1994), and the warm and oligotrophic waters from the subtropical gyre in the South. During Pleistocene glacial periods, the AF and associated productivity maximum moved southward into mid-latitude North Atlantic (Stein et al., 2009; Villanueva et al., 2001), cold polar waters expanded to lower latitudes and the NAC did not reach as far North as during interglacials (Pflaumann et al., 2003; Alonso-Carcia et al., 2011). After MIS 21 a northwest shift in the position of the AF began, both during interglacials (Hernandez-Almeida et al., 2013) and glacials (Alonso-Garcia et al., 2011b), which culminated after MIS 16 in similar positions as it occupies today (Wright and Flower, 2002), and allowed increased influence of the NAC in higher latitudes during glacials.

Various studies have shown that surface water characteristics in the mid-latitude North Atlantic depend on the strength and position of the NAC and the associated oceanic fronts (e.g., Calvo et al., 2001; Naafs et al., 2010; Voelker et al., 2010). Over the last glacial cycle, the northern Iberian margin recorded peak displacement events of the AF (Eynaud et al., 2009) and was, in general, more affected by the subpolar water masses than the southern part, which was more influenced by the subtropical water masses from the Azores Current (Rodrigues et al., 2011). Core IODP-U1385 lies near the present day boundary (Fiúza et al., 1998) between both areas of different water masses predominance, which makes it privileged to study in detail the variations of the distribution of North Atlantic currents and the fluctuations in the position of subtropical and subpolar fronts, along the Pleistocene.

CHAPTER V

MATERIALS AND METHODS

CHAPTER V

MATERIALS AND METHODS

1. LITHOLOGY

Site U1385 cores consist of hemipelagic sediments, very uniform in lithology throughout the whole Pleistocene-Holocene section and with an average sedimentation rate of ~10 cm/ky. The sedimentary succession is dominated by bioturbated calcareous muds and calcareous clays, with the occasional occurrence of ice rafted debris (IRD). Carbonate material is mainly of biogenic origin and varies from 23% to 39%, this difference being reflected in color variation (lighter - more calcareous, darker - more terrigenous) (Fig. V-1). Towards the upper part of the sequence the lithology becomes more terrigenous; nevertheless the variation is not enough to define additional lithological units (Fig. V-2). No primary sedimentary structures are observed and the most obvious secondary one is bioturbation, which ranges from sparse to moderate. Other features, such as small-scale, subvertical microfaults and contoured beds, have been identified at several intervals, but they are local and of minor importance and do not seriously disrupt the continuity of the stratigraphic section (Expedition 339 Scientists, 2012).

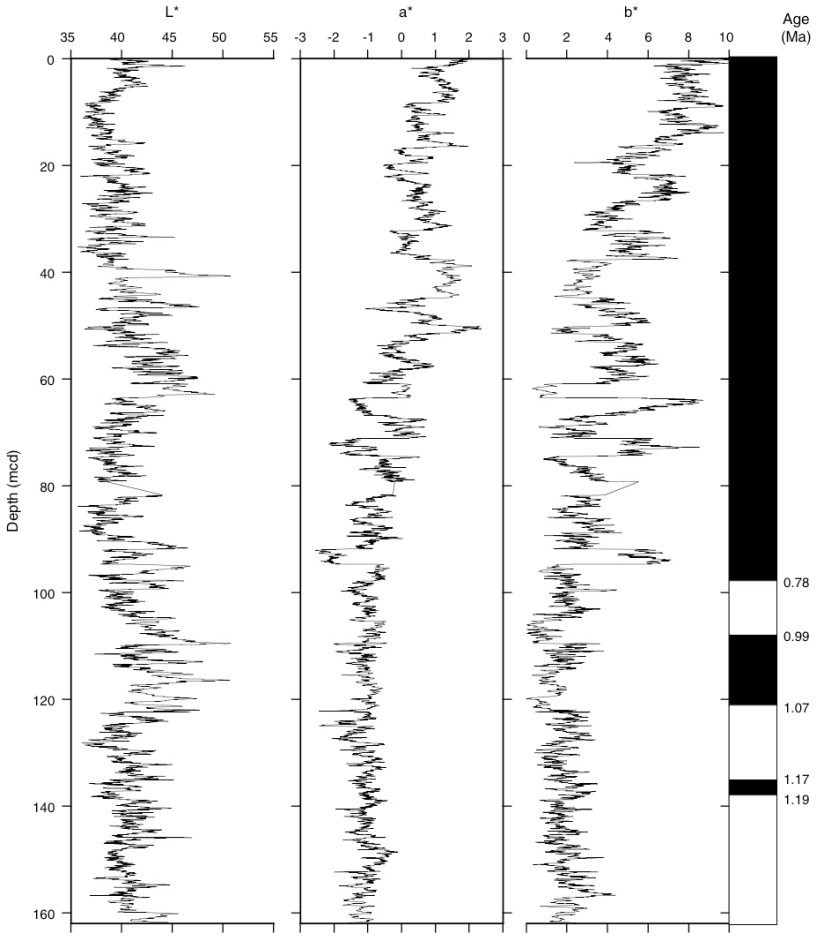

Figure V-1. Spliced colour reflectance records and polarity reversal stratigraphy for Site U1385 (Expedition 339 Scientists, 2012).

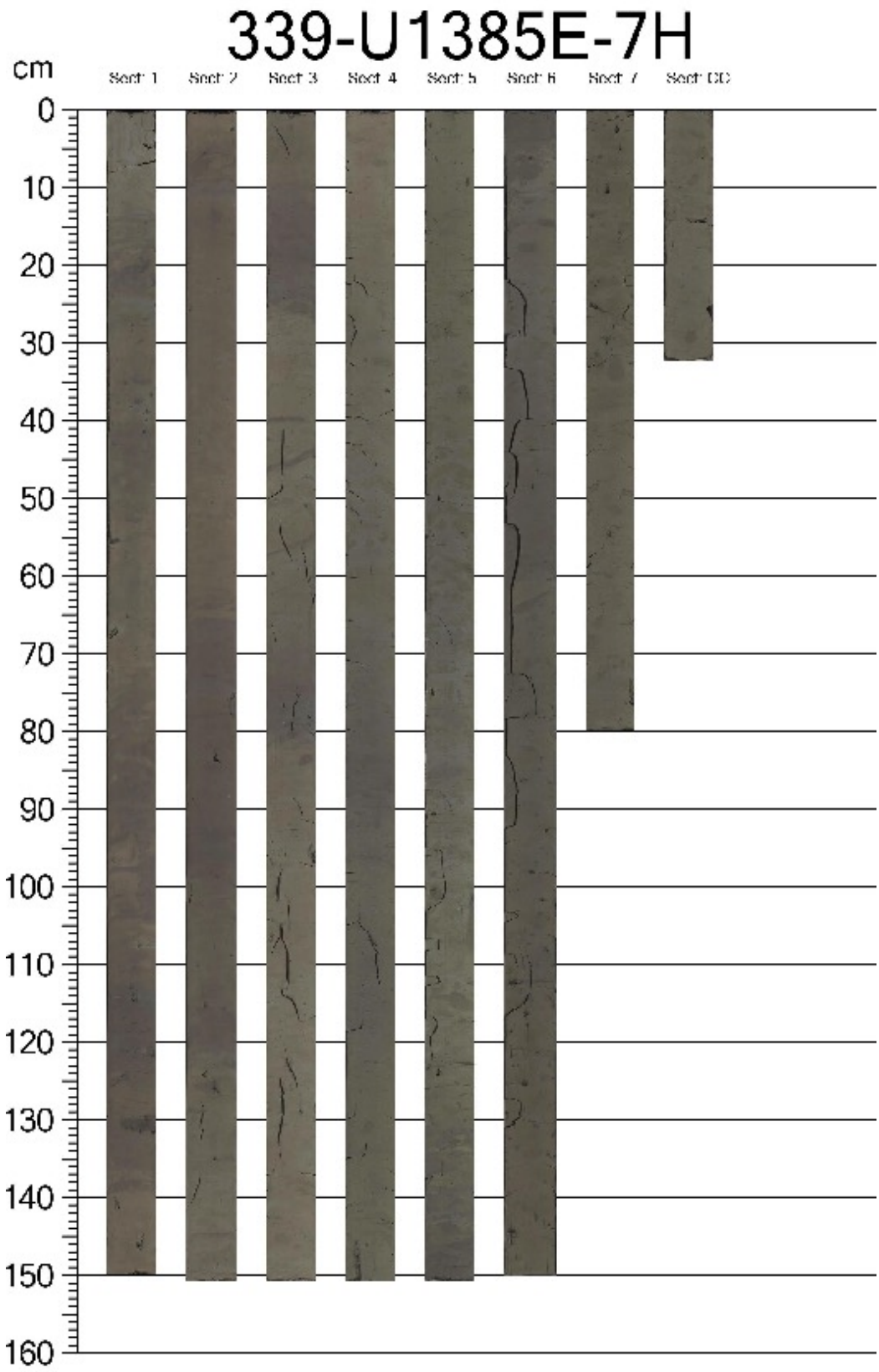

Figure V-2. Uniform lithology of sediments in site U1385 (http://web.iodp.tamu.edu).

Cyclic variations in physical properties (Fig. V-3) and color (fig. V-1) reflect cyclic changes in the proportion of biogenic carbonate and detrital material delivered to the site (Hodell el al., 2013).

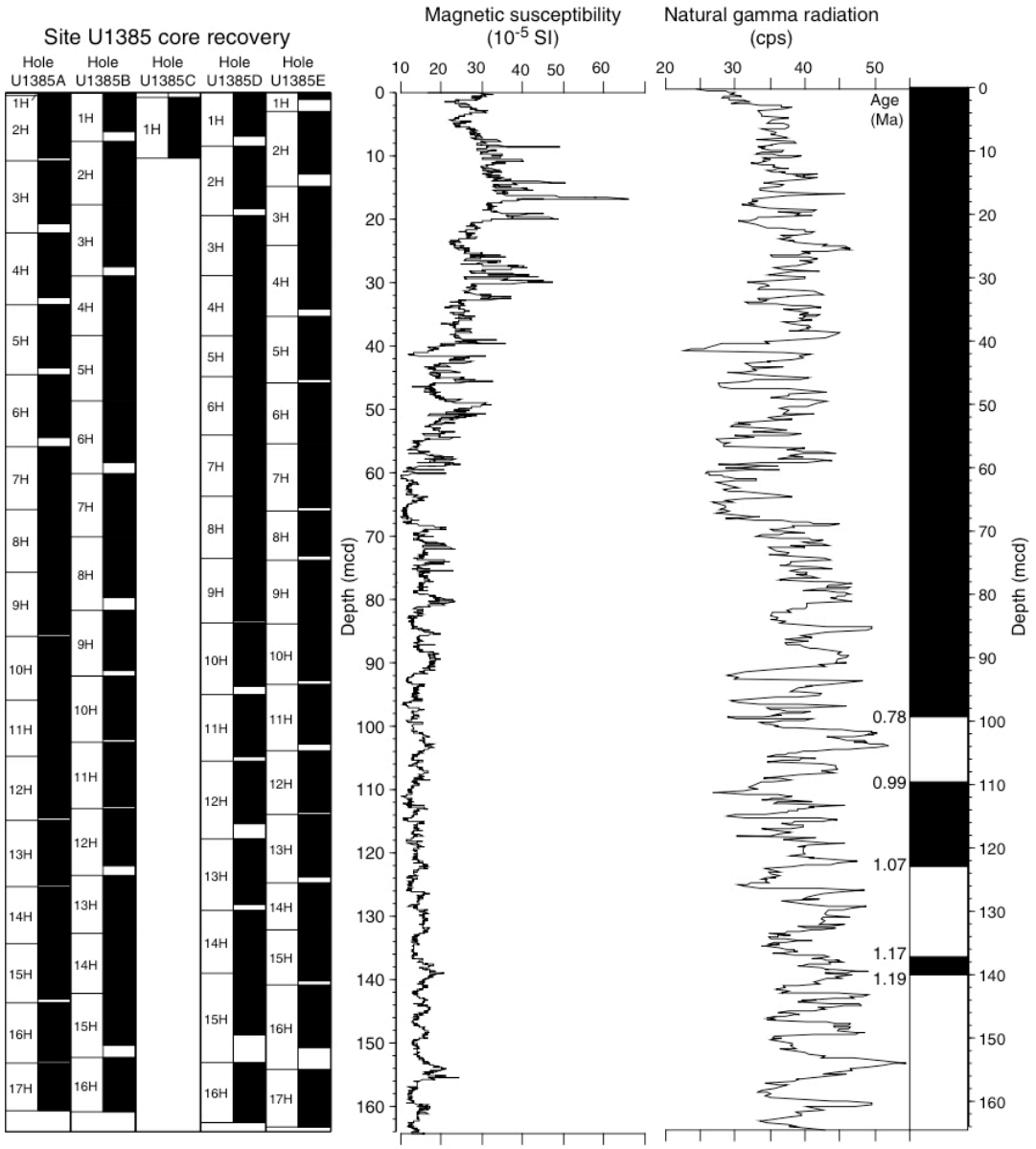

Figure V-3. Core recovery, magnetic susceptibility, natural gamma radiation and polarity reversal boundaries for the spliced composite section (Expedition 339 Scientists, 2012).

This work covers a section from the secondary splice U1385D/E (Hodell et al., 2013a) between 54.60 and 99.33 crmcd (corrected revised meters composite depth).

2. SAMPLING AND FORAMINIFERAL STUDY

2.1. Sample preparation

Samples were taken every 20 cm for the intervals 54.60–55.14 crmcd and 60.65–99.33, providing an average estimated 1.76-ky resolution record. For the interval in between samples were taken at an average 4.4 cm separation, with an estimated average 0.74 ky resolution. A total of 336 samples 1 cm thick were dried, weighed and washed over a 63 μm mesh sieve. The >63 μm residue was dried, weighed and sieved again to separate and weigh the >150 μm fraction.

Counts of detrital grains were conducted in the >150 μm fraction for samples between 54.60 and 65.75 crmcd and its quantitative abundance in number per gram of dry sediment, calculated.

2.2. Foraminifer identification

Census counts of planktonic foraminifera taxa and of planktonic foraminifer fragments were conducted on the sediment fraction larger than 150 μm, using a stereomicroscope. Each sample was successively split until a minimum of 300 specimens was obtained. The identification of the planktonic foraminifer species is based on the work of Kennett and Srinivasan (1983). A total of twenty-eight different species and ten morphotypes of planktonic foraminifers have been identified (Appendix I) all belonging to the living fauna in the area (Duprat, 1983; Levy et al., 1995; Martins and Gomes, 2004).

Relative abundance of each different species and morphotypes of planktonic foraminifer were calculated, as well as the number of specimens per gram of dry sediment. To monitor carbonate dissolution, planktonic foraminifer fragmentation index was calculated as percentage of test fragments related to the total amount of fragments plus specimens (Thunell, 1976).

Counts of total benthic foraminifer tests were conducted on the same sediment fraction and the aliquot used for planktonic counting.

3. AGE MODEL

The age model of this work (Fig. V-4) is based on the correlation of the benthic oxygen isotope record with the global benthic LR04 isotope stack (Lisiecki and Raymo, 2005) using *Analyseries* software (Paillard et al., 1996). The age control points are from Hodell et al. (2015).

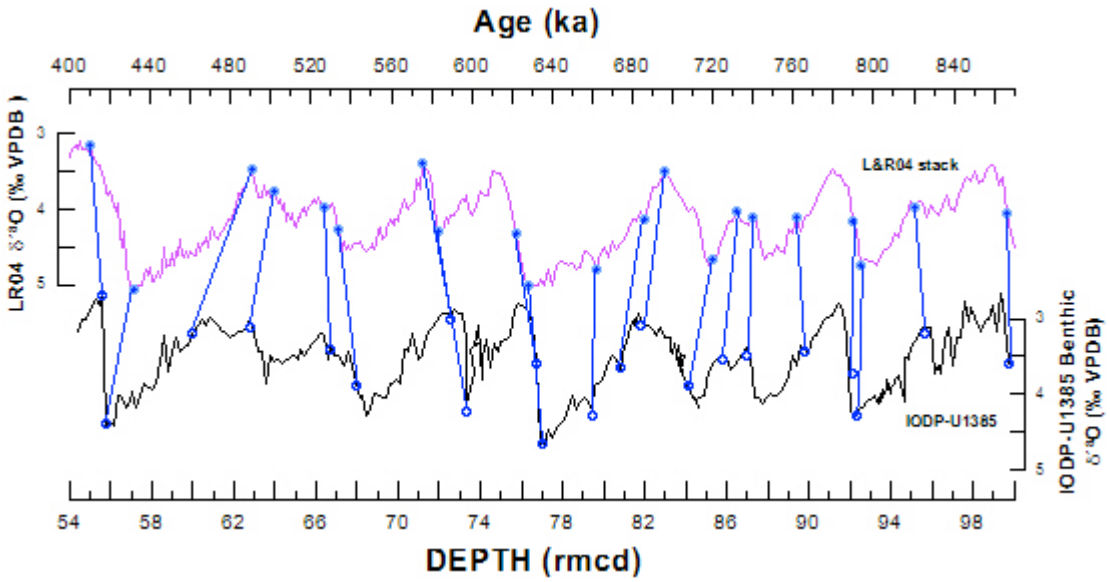

Figure V-4. Age model construction for site U1385. Blue dots represent the age control points defined for this site (Hodell et al., 2015).

4. RECONSTRUCTION OF SEA SURFACE TEMPERATURE

According to the Charles Lyell´s uniformitarian principle, the present-day relationship between physic-chemical conditions and faunal distribution can be used to reconstruct the palaeoenvironments corresponding to sediments whose fossil assemblage is known. Furthermore, if this relationship could be expressed by a mathematical formula the palaeoenvironmental reconstruction could be quantified and expressed in units. In this context, the transfer function approach, involving mathematical analysis of census counts of microfossil assemblages, is the most commonly used physical paleoproxy. This approach was firstly used in 1971, to reconstruct the paleotemperature of the surface ocean by Imbrie and Kipp, and later improved and brought to prominence by the CLIMAP group by reconstructing surface

ocean paleothermometry for the last glacial maximum (CLIMAP Project Members, 1976, 1981). Since then new, high-quality data sets have been produced and several approaches been developed, all of them based on the comparison of fossil assemblages with modern calibration data sets.

For constructing a modern geographically constrained calibration data set, data of faunal assemblages (e.g., count of planktonic foraminifer taxa) in recent ocean sediments are needed, as well as values of modern oceanographic parameters (e.g., sea surface temperature) instrumentally recorded at the same locations of the measured assemblages. The most important property of a calibration data set is its coverage, both in terms of geographical area and the range of the environmental variable or parameter. A good calibration data set has to include samples representing the entire range of the environmental variable as observed today (Kucera et al., 2005). With this objective, the MARGO project compiled a database with different partitions for the different oceans (Fig. V–5).

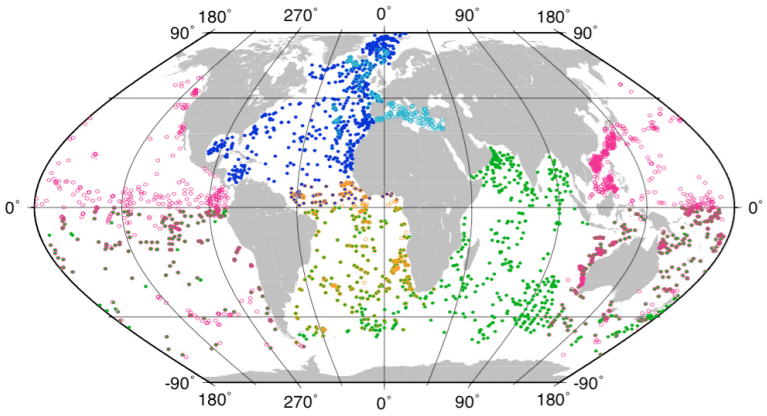

Figure V–5. Location of coretop samples with planktonic foraminifer counts used for regional SST calibration in MARGO database. North Atlantic coretops are represented as solid blue circles. (From Kucera et al., 2005)

In this work two different methods have been used to reconstruct past sea surface temperature (SST), the *Modern Analogue Technique* and the *Artificial Neural Network*. In both reconstructions fossil assemblages from IODP site U1385 are compared with the North Atlantic partition of the MARGO database.

4.1. Modern Analogue Technique (MAT)

Developed by Hutson (1980), this method searches the database of modern fauna for samples with assemblages that most resemble the fossil one. The

paleotemperature estimated for the fossil sample is then reconstructed from the SST recorded in the best modern analog samples. To improve the reconstruction, a subset of 10 best analogs from the database is used to obtain 10 SST values for each sample and then, estimate the average. The prediction error of this method for the North Atlantic dataset of MAGO ranges between 1.26-1.42 ºC (Kucera et al., 2005).

Although conceptually in line with Lyell´s unifomitarianism, MAT can only provide the most similar modern situations to the fossil one, but it cannot extrapolate; in consequence it performs poorly at the extremes of the range of the estimated environmental parameter (Kucera et al., 2005). This technique is completely dependent on the size and coverage of the calibration data set (Kucera and Darling, 2002) and its power to generalise may be limited (Kucera et al., 2005).

4.2. Artificial Neural Network (ANN)

Malmgren and Nordlund (1997) first proved this approach efficient in reconstructing paleoceanographic conditions. The method relies on the assumption that there is a relationship between the distribution of fauna and the physical properties (SST) of the environment and can overcome problems of non-linear relationships between sets of input (faunal assemblages) and output (e.g., SST) variables. Generally a set of 10 neural networks are used, which provides 10 different SST reconstructions for each component (winter, summer, annual and seasonality). The average value of these ten estimations is used as the final SST reconstruction. The prediction error of this method for the North Atlantic dataset of MAGO ranges between 0.96-1.14 ºC (Kucera et al., 2005). This method allows extrapolation, is very good at generalizing and it is not dependent on the size of the calibration data set as MAT (Kucera et al., 2005).

To compare IODP-U1385 planktonic foraminifer assemblages with the MARGO North Atlantic database, I used the commercial software NeuroGenetic Optimiser v2.6 (Biocomp).

When trained on the same database ANN performed slightly better than MAT, but when applied to an independent validation data set and fossil data set, the ANN approach proved much better than the other method (Malmgren et al., 2001). This

difference can be observed in the different SST reconstructions obtained for site U1385 (Fig. V-6). In consequence, the method favoured for SST reconstructions in this work was ANN.

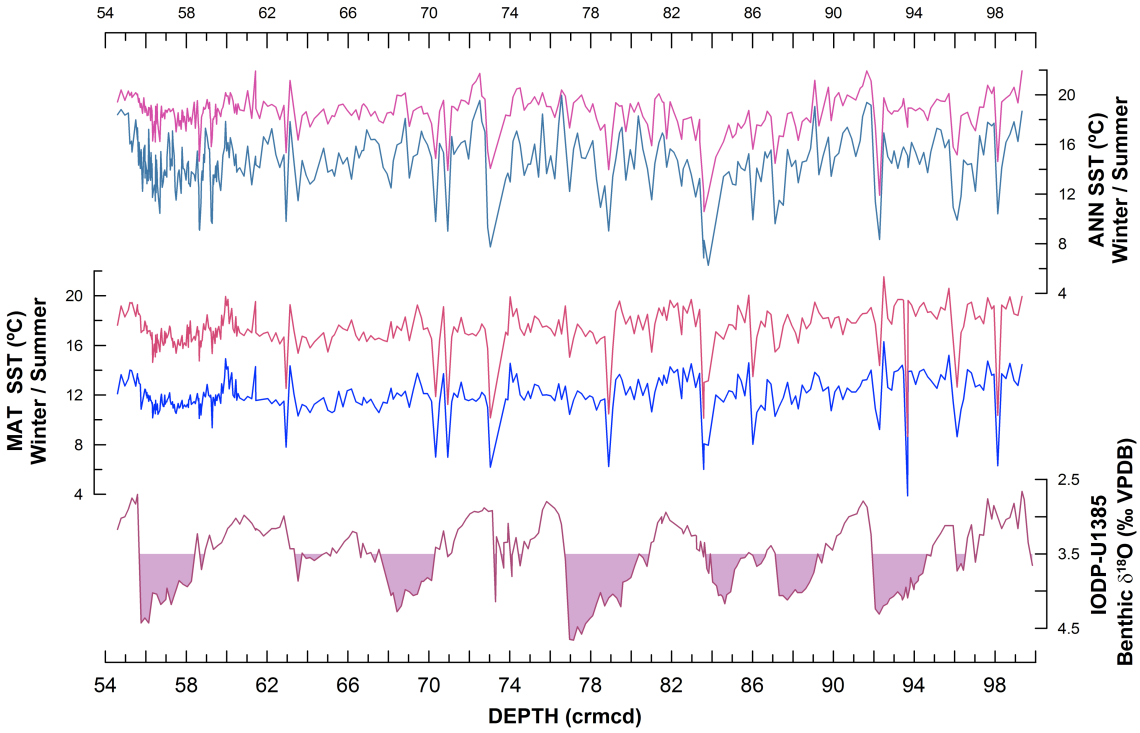

Figure V-6. Sea surface temperature reconstructions for Site U1385 by both MAT and ANN methods. Benthic δ ^{18}O is from Hodell et al. (2015); filling enhances the ice volume threshold separating glacial and interglacial conditions for the North Atlantic (McManus et al., 1999).

5. RECONSTRUCTION OF EXPORT PRODUCTIVITY

Export productivity was reconstructed with the modern analogue technique (MAT) (Hutson, 1980), as described by Salgueiro et al., (2008), comparing IODP-U1385 planktonic fossil assemblage with the modern analog database compiled by Salgueiro et al (2010).

CHAPTER VI

SEVERE COOLING EPISODES AT THE ONSET OF DEGLACIATIONS FROM MARINE ISOTOPE STAGE 21 TO 13

CHAPTER VI

SEVERE COOLING EPISODES AT THE ONSET OF DEGLACIATIONS FROM MARINE ISOTOPE STAGE 21 TO 13 (*)

* This Chapter is based on: **Martin-Garcia, G.M.**, Alonso-Garcia, M., Sierro, F.J., Hodell, D.A., Flores, J.A. (2015) Severe cooling episodes at the onset of deglaciations on the Southwestern Iberian margin from MIS 21 to 13 (IODP site U1385). *Global and Planetary Change*, doi:10.1016/j.gloplacha.2015.11.001 (Appendix VII)

ABSTRACT

Here we reconstruct past sea surface water conditions on the SW Iberian Margin by analysing planktonic foraminifer assemblages from IODP Site U1385 sediments (37º34.285´N, 10º7.562´W; 2585 m depth). The data provide a continuous climate record from Marine Isotope Stages (MIS) 21 to 13, extending the existing paleoclimate record of the Iberian Margin back to the ninth climatic cycle (867 ka). Millennial-scale variability in Sea Surface Temperature (SST) occurred during interglacial and glacial periods, but with wider amplitude (> 5 ºC) at glacial onsets and terminations. Pronounced stadial events were recorded at all deglaciations, during the middle Pleistocene. These events are recorded by large amplitude peaks in the percentage of Neogloboquadrina pachyderma sinistral coincident with heavy values of planktonic δ18O and low Ca/Ti ratios. This prominent cooling of surface waters along the Portuguese margin is the result of major reorganizations of North Atlantic surface and deep-water circulation in response to freshwater release to the North Atlantic when ice sheets collapse at the onset of deglaciations. In fact, most of these cooling events occurred at times of maximum or increasing northern Hemisphere summer insolation. The slowdown of deep North Atlantic deep-water formation reduced the northward flow of the warm subtropical North Atlantic Drift, which was recorded on the Iberian margin by enhanced advection of northern cold subpolar waters. Following each episode of severe cooling at the onset of deglaciations, surface water experienced abrupt warming that initiated the climatic optimum during the early phase of interglacials. Abrupt warming was recorded by a sudden increase of the subtropical assemblage that indicates enhanced northward transport of heat through the North Atlantic Drift. At the onset of glaciations, SST along the Portuguese margin remained relatively warm while the surface waters of the North Atlantic experienced cooling, generating a large latitudinal SST gradient.

1. INTRODUCTION

The western Iberian margin has proven to be a crucial location for the comprehensive evaluation of millennial climate variability between hemispheres over the late Pleistocene, offering a direct comparison with Antarctic and Greenland ice core records (e.g. Shackleton et al., 2000; Martrat et al., 2007). A large number of studies have been conducted using piston cores from this area to partially characterize the last six climatic cycles (Cayre et al., 1999; Bard et al., 2000; de Abreu et al., 2003; Roucoux et al., 2005; Vautravers and Shackleton 2006; Martrat el al., 2007; Rodrigues et al., 2011).

The western part of the Iberian Peninsula is very sensitive to variations in the North Atlantic surface circulation dynamics. The Iberian margin is located in a key region characterized by the interplay of subpolar waters brought by the Portugal Current, which constitutes the descending branch of the North Atlantic Drift, and subtropical waters brought by the Azores Current. Changes in the intensity of the northward flow of the North Atlantic Drift drive a deep impact on the north Atlantic subpolar and subtropical gyres, as well as on the position of the Polar, Arctic and subtropical fronts. For the last climatic cycles various studies have illustrated the relationship between ice sheets instabilities in the northern Hemisphere and the southward migrations of the Arctic Front (AF) as far south as the Iberian margin (Bard et al., 2000) via the recirculation of cold water through the subtropical gyre eastern current. Millennial-scale oscillations of Sea Surface Temperature (SST) at the Portuguese margin have been related to changes in North Atlantic surface circulation driven by freshwater perturbations at high latitudes (eg., Lebreiro et al., 1996,1997; Zahn et al., 1997; Cayre et al., 1999; de Abreu et al., 2005; Vautravers and Shackleton, 2006; Martrat et al. 2007; Eynaud et al., 2009; Rodrigues et al., 2011). These oscillations also affected the continental climate across southern Europe via atmosphere-ocean coupling (Allen et al., 1999; Roucoux et al., 2005; Sanchez-Goñi et al., 2008; 2013).

During the last glacial cycle a series of layers with high abundances of the polar species Neogloboquadrina pachyderma sinistral (Nps) were recorded along the Portuguese margin during Heinrich events (e.g., Lebreiro et al., 1997; de Abreu et al.,

2003). In certain sites those layers also contained important amounts of Ice rafted debris (IRD) although the presence or absence of IRD rich layers off the Iberian margin during these events depends on the proximity to the shore. Sites located further offshore usually record IRD layers (Lebreiro et al., 1996; Bard et al., 2000) whereas sites nearshore rarely register them (Zahn et al., 1997).

At the same time, the Portuguese margin provides an excellent location to monitor past changes in deep water circulation and heat and salt exchange between Hemispheres (Hodell et al., 2013a). Millennial-scale oscillations in surface circulation recorded along the Portuguese margin were linked to significant changes in deep water circulation. Shutdown or reduced deep water formation in the North Atlantic in response to freshwater perturbations is registered in the SW Iberian margin by reduced flux of the North Atlantic Deep Water (NADW) and a rapid replacement by the northward flux of the Antarctic Bottom Water (AABW) (Shackleton et al. 2000; Skinner et al. 2003)

Before Integrated Ocean Drilling Program (IODP) Expedition 339 the existing sediment cores in the western Iberian margin only provided climatic and oceanographic reconstructions back to late Marine Isotope Stage 15 (e.g. Bard et al., 2000; Rodrigues et al., 2011). The sediment cores from Site U1385 (Shackleton Site), retrieved during Expedition 339, allow us to extend the record back to 870 ka and investigate the response of the mid-latitude eastern North Atlantic to climatic changes during the interval between 870 and 490 ka. In this work we studied planktonic foraminifer assemblages and combined them with the oxygen isotopes records from IODP Site U1385 to reconstruct the history of sea surface temperature on the southwest Iberian Margin from MIS 21 to MIS 13, thereby extending the existing record in the area back to the ninth climatic cycle.

Given that previous works suggested the Iberian Margin can play a pivotal role in understanding the millennial-scale climate variability during the last glacial cycle (Shackleton et al., 2000, Vautravers and Shackleton, 2006), in this work we aim to study the suborbital climate variability at this location during the last part of the middle Pleistocene transition (MPT, ~1250-700 ka; Clark et al., 2006) and state the

influence that subpolar North Atlantic climatic oscillations and meridional SST gradients had on climatic events during and since the emergence of the 100-ky cycles.

2. MATERIAL AND METHODS

Sediments at Site U1385 define a single lithological unit dominated by calcareous muds and calcareous clays, with varying proportions of biogenic carbonate (23% - 39%) and terrigenous sediment. Pelagic sedimentation prevails during interglacials, while terrigenous input is enhanced during glacials; however, sedimentation rates remain high (~ 10 cm/ky) for glacial and interglacial periods (Stow et al., 2012). Occasional occurrence of ice rafted debris (IRD) is also recorded. Cyclic variations in physical properties and color reflect cyclic changes in the proportion of biogenic carbonate and detrital material delivered to the site (Hodell el al., 2013b).

This study covers a section from the secondary splice U1385D/E (Hodell et al., 2013a) between 59.95 and 99.84 crmcd (corrected revised meters composite depth) (MIS 21 - MIS 13). Samples for the microfaunal analysis were taken every 20 cm, providing an average estimated 1.76-ky resolution record. A total of 210 samples 1 cm thick were dried, weighed and washed over a 63 µm mesh sieve. The >63 µm residue was dried, weighed and sieved again to separate and weigh the >150 µm fraction. Census counts of planktonic foraminifera taxa and of planktonic foraminifer fragments were conducted on the sediment fraction larger than 150 µm, using a stereomicroscope. Each sample was successively split until a minimum of 300 specimens was obtained. A total of twenty-eight species and ten morphotypes (Kennett and Srinivasan, 1983) of planktonic foraminifers have been identified (Appendix A) and their relative abundances, calculated, as well as the number of specimens per gram of dry sediment. To monitor carbonate dissolution, planktonic foraminifer fragmentation index was calculated as percentage of test fragments related to the total amount of fragments plus specimens (Thunell, 1976).

Sea surface temperature (SST) values (annual, winter, summer and seasonality - difference between winter and summer parameters) were reconstructed according to the Artificial Neural Network (ANN) method, using a back propagation neural network

system (Malmgren et al., 2001) to compare our fossil planktonic foraminifera assemblages with MARGO North Atlantic database. We used the commercial software NeuroGenetic Optimiser v2.6 (Biocomp), as described in Kucera et al. (2005), who calculated an error of prediction of 1.02 ºC. The same set of 10 neural networks as in Kucera et al. (2005) was used in this study, providing 10 different SST reconstructions for each component (winter, summer, annual and seasonality). The average value of these ten estimations was used as the final SST reconstruction. Additionally, in order to calculate a similarity index and corroborate the ANN results, we applied a Modern Analog Technique (Prell, 1985) on the fossil data using the same MARGO modern dataset as was used for the training of the ANN (Kucera et al., 2005). The same methodology has been followed to reconstruct winter SST of Site U1314, using the same planktonic foraminifer assemblages as in Alonso-Garcia et al. (2011b). Site U1314 (~1 ky resolution) has been included in this work to better compare with the subpolar North Atlantic.

The age model of the studied section is based on the correlation of the benthic oxygen isotope record to the global benthic LR04 isotope stack (Lisiecki and Raymo, 2005) (see Hodell et al., 2015, this issue).

3. RESULTS

Preservation in the studied interval is analysed considering the planktonic foraminifer fragmentation index. This index remains generally lower than 20% (Fig. VI-1g), which informs of a very good preservation in the samples, except for some short intervals of increased dissolution. Nevertheless, the fragmentation index did not surpass the 40% threshold above which planktonic foraminifer assemblages begin to suffer modifications due to dissolution (Miao et al., 1994). Therefore, we can assume that the assemblages used for this work are not modified by dissolution and they are suitable to infer water mass properties.

Planktonic foraminifer accumulation rate ranges between 500 and 49,800 specimens per gram of dry sediment and ky, lowest values corresponding to levels of high bioturbation, where metallic deposits conform most of the coarse fraction of the sediment.

Figure VI - 1. Down-core results for marine isotope stages 13 to 21 from IODP-1385 and comparison with global LR04 benthic stack. (a) Age control points used to correlate both stacks (marked with crosses). (b) Benthic $\delta^{18}O$ profiles from LR-04 stack (Lisiecki and Raymo, 2005) and from U1385; filling enhances the ice volume threshold separating stable and unstable climatic regimes, which has been identified for the North Atlantic in $\delta^{18}O$ value of 3.5 ‰ (McManus et al., 1999). This threshold has been used to locate in the core the limits between glacial and interglacial conditions and determine the duration of climatic cycles. Substages are named according to Railsback et al. (2015). U1385 benthic $\delta^{18}O$ record shows a much higher variability and around 0.5 ‰ VPDB lower values than the global stack. (c) Winter ANN-reconstructed sea surface temperature. (d) Summer ANN-reconstructed sea surface temperature. Both winter and summer records are compared with present day temperatures on the site (horizontal dashed lines) from Locarnini et al. (2010). (e) ANN-reconstructed seasonality compared with present-day seasonality on the site (dashed line). (f) MAT-reconstructed similarity index (Prell, 1985) between fossil planktonic foraminifer assemblage in Site U1385 and MARGO dataset (Kucera et al., 2005). (g) Planktonic foraminifer fragmentation index (number of test fragments related to the total amount of fragments plus specimens) (Thunell, 1976) and averaged with a 3-point running mean.

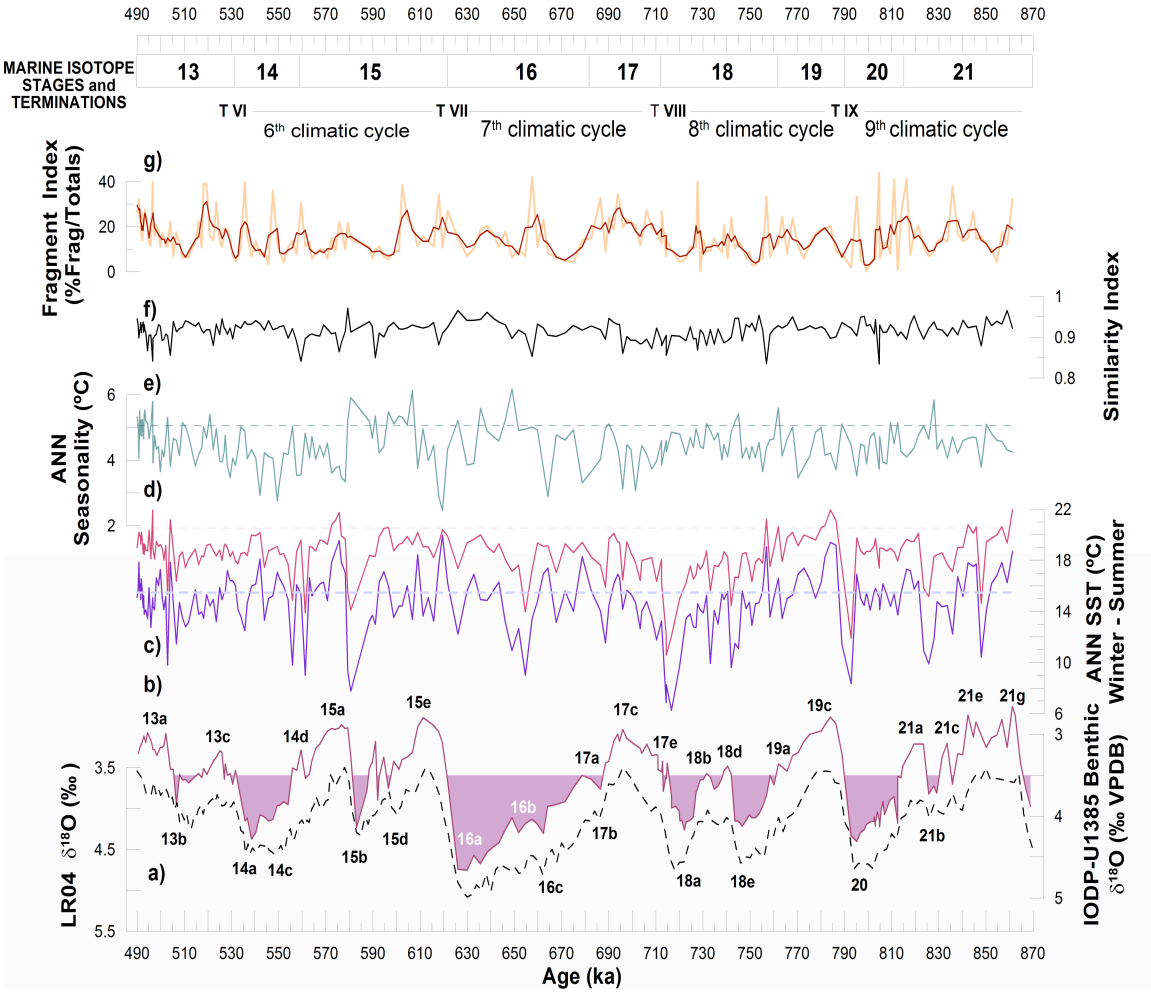

3.1. Planktonic foraminifer results

The microfaunal analysis focuses on species and assemblages that can be directly used to monitor any change in climatic or oceanographic conditions in North Atlantic surface water.

The species Neogloboquadrina pachyderma sinistral (Nps), with a temperature tolerance range between –1 and 8 ºC and an optimum of 2ºC (Bé and Tolderlund, 1971; Tolderlund and Bé, 1971; Bauch et al., 1997; Pflaumann et al., 2003), is particularly abundant in the Arctic water (Johannessen et al., 1994). This species has been used to monitor southward penetrations of polar water masses, usually associated with iceberg discharges in mid-latitude North Atlantic (eg., Bond et al., 1992) as well as in the Portuguese margin (Cayre et al., 1999; de Abreu et al., 2003; Vautravers and Shackleton, 2006; Eynaud et al., 2009). This species ranges from 0 % to a maximum of almost 50 % during MIS 18. The species is more abundant before MIS 16 where high values occurred during interglacials, except for MIS 19, as well as glacials (Fig. VI-2e).

The subtropical assemblage (Ottens, 1991) consists mainly of species of Globigerinoides genus and it is usually linked to the subtropical branch of ENACW, transported to the Northeast Atlantic by the Azores Current, which flows northward over the site during non-upwelling months (Peliz et al., 2005). Variations in the abundance of the subtropical assemblage (Fig. VI-2f) are consistent with climatic cycles. Variations in the subtropical assemblage resemble the planktonic $\delta^{18}O$ record, during both glacial and interglacial periods (Fig. VI-2).

3.2. Sea Surface Temperature variations

The similarity index of MAT (Fig. VI-1f) ranges between 0.9 and 1 for almost all the interval, suggesting that the studied samples are well represented in the modern dataset and that SST reconstructions (Fig. VI-1) are not affected by no-analog artefacts (Kucera et al., 2005).

Figure VI – 2. Comparison between IODP-U1385 record and orbital parameters. (a) Benthic $\delta^{18}O$ profile: LR-04 stack (Lisiecki and Raymo, 2005) in dashed line, and record from U1385 (Hodell et al., 2015); filling enhances the ice volume threshold separating stable and unstable climatic regimes (McManus et al., 1999). Substages are named according to Railsback et al. (2015) (b) Planktonic foraminifer Globigerina bulloides $\delta^{18}O$ record from U1385 (Hodell et al.,

2015). (c) Log Ca/Ti record from U1385 (Hodell et al., 2015) (d) Winter SST for Site U1385 (values above average are shaded). (e) Relative abundance of the planktonic foraminifer polar species Neogloboquadrina pachyderma sinistral in U1385. (f) Relative abundance of the subtropical assemblage (Ottens, 1991) in U1385. (g) Orbital parameters: obliquity (Laskar et al., 2004) (black) and 65 ºN 21st June Insolation values (W/m^2) (blue) (Huybers, 2006) and integrated summer energy at 65 ºN (>275 W/m2) (red) (Huybers, 2006). Vertical bands mark pronounced cooling coinciding with deglaciations; grey bands mark events close to obliquity maxima and green bands mark the exceptions (no obliquity maxima or no deglaciation). Blue lines mark other pronounced cooling not linked to either deglaciations or obliquity maxima.

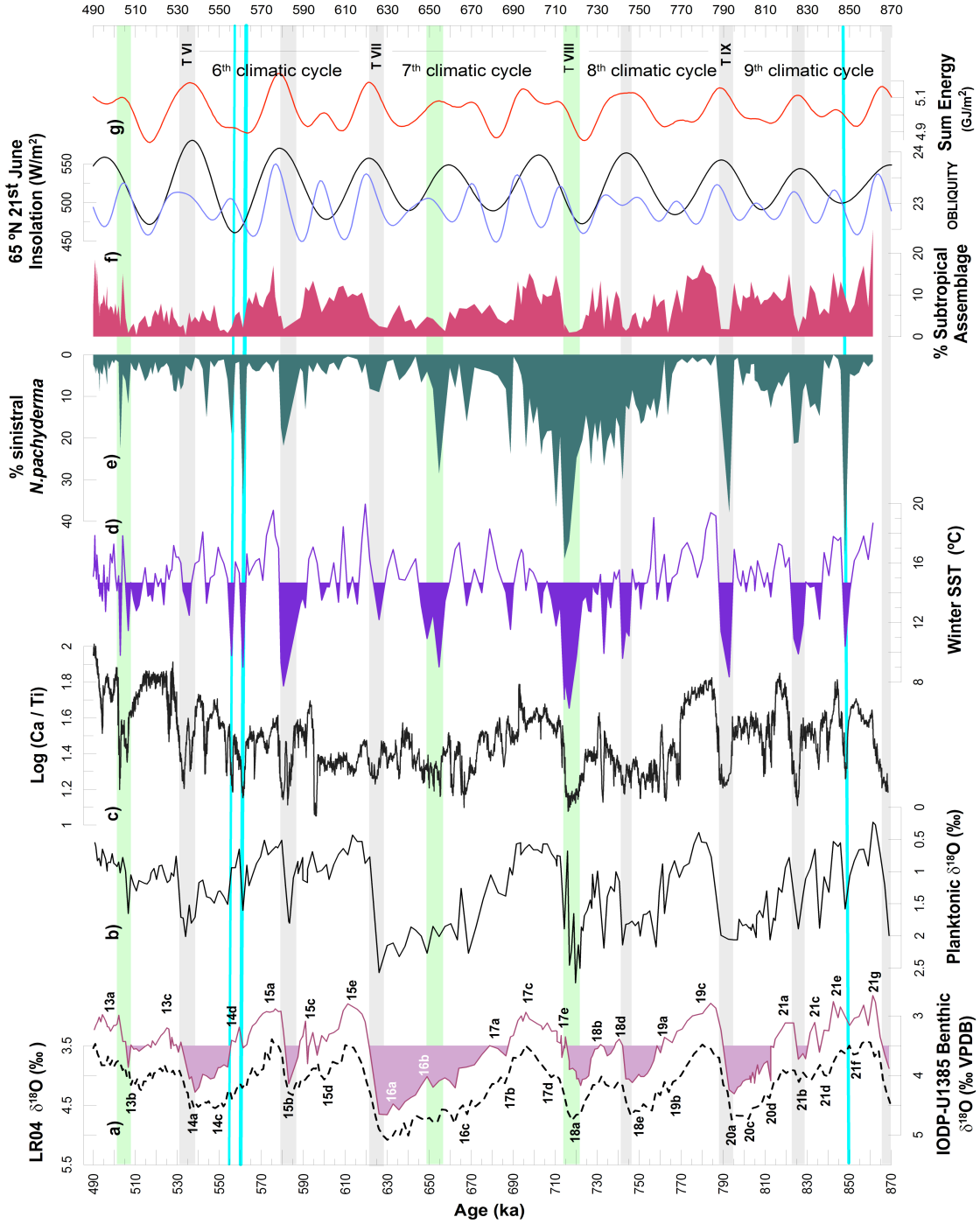

In general, winter SST off the southwestern Iberian Margin resemble the planktonic oxygen isotope variations (Fig. VI-2, b and d). Minimum temperature occurred during Terminations or during glacial inceptions. SST in the area was generally colder during the studied interval (mean annual value, 16.6 ºC) than at present (18 ºC) (Locarnini et al., 2010), even during interglacials. During interglacial periods, summer SST (Fig. VI-1d) were on average 1 to 2 ºC colder than at present and, during glacials, they were 2 to 4ºC colder. Nevertheless, during cooling episodes, summer SST dropped 6 ºC below Holocene levels (18 ºC, Bard et al., 2000) and those of previous interglacial, MIS 3, (17-18 ºC, de Abreu et al., 2003; Vautravers and Shackleton, 2006). Winter SST (Fig. VI-1c) remained, on average, less than 1 ºC lower than at present during all interglacials and during glacials MIS 20 and MIS 14, and were higher than today during most of MIS 19, in the warmest periods of MIS 21 and 15, and even in some very short spells during glacial stages MIS 18, MIS 16 and MIS 14. Only during MIS 18 winter SST were considerably lower (2.5 ºC in average) than at present. The warmest period of the studied interval was MIS 19 and the coldest one was MIS 18. Isotope stages 17 and 13 were the coldest interglacial periods, with summer SST between 1 and 2 °C colder than at present and closer to the values recorded during glacial periods, and winter SST generally below modern values.

SST oscillations were, in general, less frequent and less pronounced during interglacials (less than 7 ºC drop or rise) than during glacials (up to 11 ºC oscillation), except for MIS 21f, that shows one of the steepest sea surface temperature oscillations (7.3 ºC) of the whole studied interval.

ANN-reconstructed seasonality (Fig. VI-1e) during middle Pleistocene is lower than today and, in general, it shows small amplitude variability along the whole interval. Most of the deep oscillations in seasonality correspond to outstanding SST fluctuations in SST. Increases in seasonality coincide with drops in winter SST and vice-versa. The highest seasonality values occurred in MIS 16b (6.2 ºC), MIS 15e (6 ºC) and 15b (5.9 ºC). Since MIS 15a seasonality values were lower and show a slow increasing trend until the end of MIS 13, encompassing the cooling trend recorded by SST. During isotope stages 16 and 15 the amplitude of seasonality oscillations was between 1 and 2 ºC higher than during the rest of the interval.

4. DISCUSSION

4.1. Sea surface cooling on the Portuguese margin at deglaciations during middle Pleistocene

The planktonic foraminifer assemblages, SST and oxygen isotope data studied at Site U1385 indicate that during this period, and superimposed on the glacial-interglacial variations, suborbital millennial-scale climatic variability off Iberia reflects the influence of millennial changes in surface circulation in the NE Atlantic.

In order to identify millennial-scale climate events that may not be resolved with the resolution of our SST record we compare our data with the Ca/Ti record (Hodell et al., 2015), which provides an estimated resolution of 0.1 ky. Previous studies along the Portuguese margin reported that Ca/Ti reflects millennial-scale climate changes as well as sea level variations (Hodell et al., 2013a). Higher Ca/Ti ratios are linked to higher productivity of calcareous plankton during warmer periods and lower siliciclastic input from the continent (Hodell et al., 2013a).

Summer SST at the Portuguese margin remained relatively warm from MIS 21 to MIS 13, although lower than present-day summer SST, oscillating between 15 and 18 ºC irrespective of the glacial or interglacial periods (Fig. VI-1d). This relatively warm temperature was, however, punctuated by abrupt SST cooling events, recorded throughout the record by pronounced peaks in abundance of Nps and sharp increases of G. bulloides $\delta^{18}O$ values, as well as very low values of the Ca/Ti ratio (Fig. VI-1, 2).

A close comparison of SST with the benthic $\delta^{18}O$ record for U1385 and the global benthic oxygen isotope stack (LR04) shows that all these cooling events were coetaneous with drops in the benthic $\delta^{18}O$. Longer and more pronounced cooling episodes in the Portuguese margin occurred at Terminations (Fig. VI-1a-c), particularly during Termination IX and VIII, but also at the transitions from glacial-interglacial substages MIS 21b to 21a, MIS 18e to 18d, and, especially, MIS 15b to 15a.

4.1.1. MIS 21-20

During the ninth climatic cycle (MIS 21 - MIS 20) four main cooling events (6 to 8 ºC drop) were recorded, all of them at transitions from higher to lower $\delta^{18}O$ values in the benthic oxygen isotope record. The amplitude and duration of these cooling episodes are related to the amplitude of the benthic isotope change (Fig. VI-1a-c). The

most pronounced cooling occurred at Termination IX corresponding with a high amplitude change in the isotopes undoubtedly related to a major sea level rise and deglaciation. Another major cooling (6.4 ºC) occurred at the transition MIS21b/a, also related to an important deglaciation and sea level rise. The first two cooling events recorded in this period also occurred at glacial/interglacial transitions, MIS 21f/e and MIS 21d/c. All these events of cool surface temperatures are also registered by heavier planktonic $\delta 1^{8}O$ and lower Ca/Ti values (Fig. VI-2b-d).

Based on the benthic $\delta^{18}O$ record climatic cycle MIS 21-20 encompasses two glacial, obliquity-driven cycles, the two more pronounced cooling events reflecting the culmination of these two glacial cycles. These cooling events were followed by remarkably warm intervals, showing the characteristic millennial-scale, stadial-interstadial climate oscillations (Fig. VI-2a,d,g). In particular, the four cool-warm oscillations recorded in MIS 21 have also been recorded in various sites of the North Atlantic (Flower et al., 2000; Kleiven et al., 2003; Hodell et al., 2008; Ferretti et al., 2010; Hernandez-Almeida et al, 2012) during the stage of progressive extension of the northern Hemisphere ice sheets during MIS 21. The cooling events off Iberia were marked by high percentages of the polar species Nps (Fig. VI-2e) but they were not linked to high IRD as has been reported for the same events at sites 984, 980 (Wright and Flower, 2002; hereafter, W&F02) and U1314 (Hernandez-Almeida et al, 2013) in the North Atlantic.

4.1.2 MIS 19-18

During this cycle, sea surface waters along the Portuguese margin experienced a pronounced cooling during three episodes (Fig. VI-2d), being the greatest in amplitude (7.2 ºC) and the coldest (6.2 ºC, winter SST), the one recorded at Termination VIII. The other two cooling events were also linked to global drops in benthic $\delta^{18}O$ at the transitions MIS 18e/d and MIS 18b/c (Fig. VI-2a,d). Like in the previous climate cycle the amplitude of the cooling events is related to the amplitude of the deglaciations, being the cooling event associated to MIS 18b/c of lesser amplitude. Low Ca/Ti ratios, high planktonic $\delta^{18}O$ and high percentages of Nps also registered these cooling events that, with the exception of Termination VIII when SST increased gradually, were followed by abrupt warming (Fig. VI-2b-e).

Similar cooling episodes have been recorded in the subpolar North Atlantic at sites 980 (W&F02), U1314 (Alonso-Garcia et al., 2011a) (Fig. VI-3b) and U1302 (Channell et al., 2012), as well as at site U1308 (Hodell et al., 2008), but in that region they were associated to ice-rafting events (Fig.VI-3c).

4.1.3. MIS 17 – 16

Based on the global benthic Stack (LR04) MIS 16 was the longest and the most prominent glacial of the middle Pleistocene. Ice sheets grew continuously from 695 to 630 ka, with a lower rate of growth or retreat between 660 and 650 ka. It is at this time when surface waters in the Portuguese margin experienced a prominent drop (8 ºC) in temperature (Fig. VI-2d). The beginning of this prominent cooling (659 ka) was synchronous with a low-amplitude warming phase recorded in Antarctic ice cores (Fig. VI-3b,d) and occurred nearly in phase with maximum obliquity of Earth´s axis (Fig. VI-2d,g).

Unlike other Terminations, a weak cooling event (12.2 ºC winter SST) was recorded at Termination VII, although this is one of the largest amplitude deglaciations. An also low amplitude drop in Ca/Ti reflects the small magnitude of this event (Fig. VI-2c). Nevertheless, it coincided with IRD accumulation in site 980 (Fig. VI-3c) and was contemporaneous with Heinrich event 16.1 recorded at sites U1308 and U1302/03 (Hodell et al., 2008; Channell et al., 2012).

4.1.4. MIS 15 – 13

In the upper part of our record, again SST experienced prominent cooling events at deglaciation between MIS 15b/a (7.7 ºC winter SST) and at transition MIS 13b/a (11.4 winter SST). Two more short cooling events (9 and 9.7 ºC winter SST) occurred at 561.35 and 555.87 ka, similar to those recorded in the subpolar cores 980 and U1314 (Fig. VI-3b).

A less pronounced cooling (5ºC drop) occurred at Termination VI that is also marked by a decrease in Ca/Ti (Fig. VI-2c-d).

(Next page) **Figure VI – 3.** Comparison between SST record from site IODP-U1385 (this work) and other climatic records from ninth to fifth climatic cycles. (a) Benthic $\delta^{13}C$ profile from U1385 (pink) and ODP-980 (W&F02) (brown). (b) Winter SST records from 58º N site U1314 (this work, grey), from 55ºN site 980 (W&F02) (blue) and from site U1385 (green). SST above average for the interval are shaded in all the plots. (c) IRD content (in number of particles

per gram of sediment) from site 980 (W&F02). The age model for site 980 has been recalculated according to LR04. (d) Antarctic Dome C δD record (purple) and reconstructed temperature (black dashed line) (Jouzel et al., 2007) (e) Content of greenhouse gases CH_4 (green) and CO_2 (red) in the Antarctic ice (Loulergue et al., 2008 and Lüthi et al., 2008, respectively).

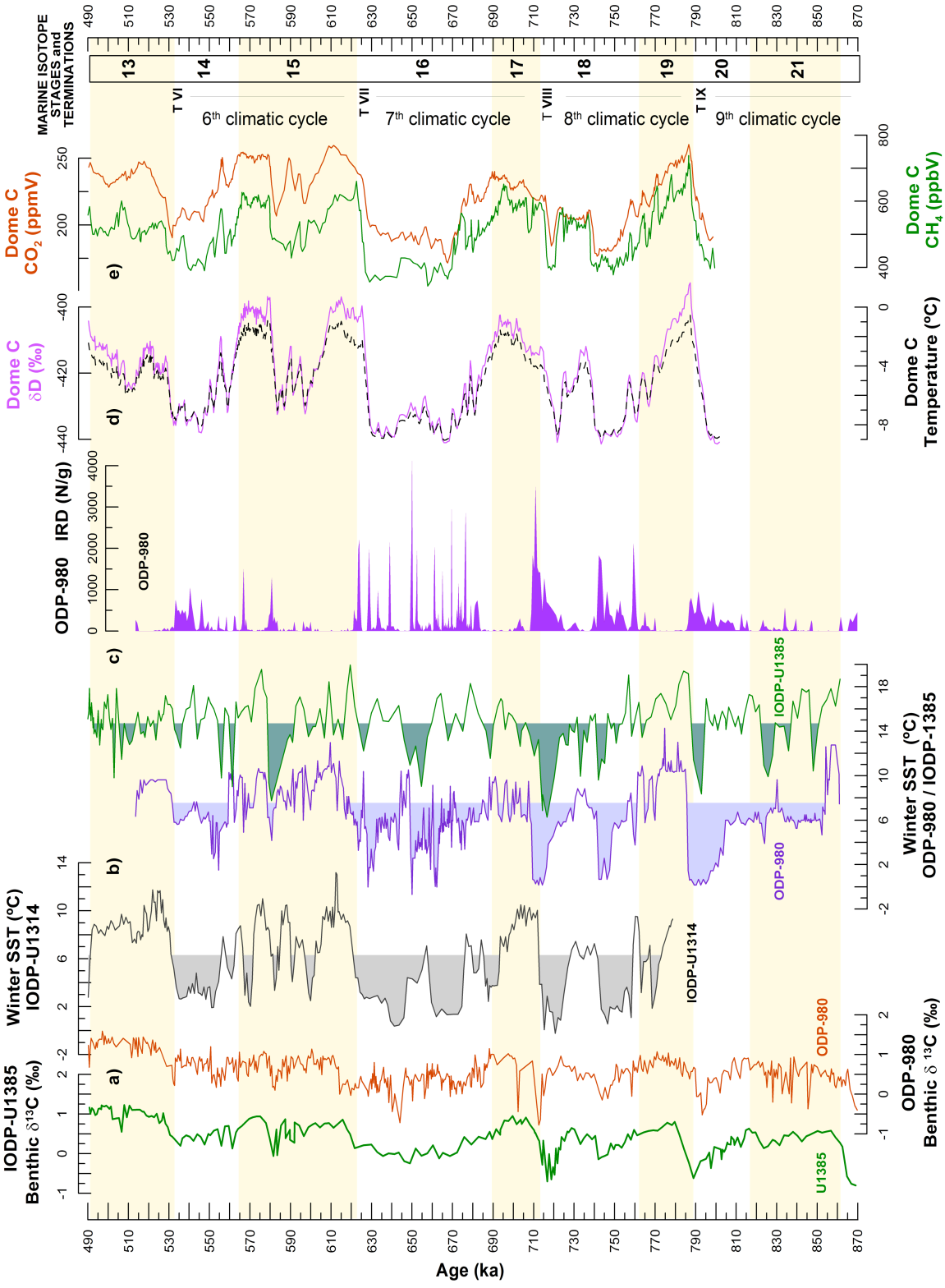

4.2. Important reorganizations of North Atlantic circulation at the onset of northern Hemisphere ice sheet retreats

While in other North Atlantic sites, especially those that are at higher latitude, SST remained relatively low during glacial times, the Portuguese margin was under the influence of relatively warm temperate waters during most glacial periods (Fig. VI-3b). The occurrence of temperate-warm surface waters at site U1385 during long time periods reflects the persistent influence of the North Atlantic Current (NAC) and its continuous advection of temperate-warm waters to the eastern margin of the subtropical North Atlantic gyre. The stadial-interstadial oscillations observed in this study were the result of enhanced/reduced advection of heat to the Southern Iberian Margin through the NAC. However, during most deglaciations a major reorganization of surface circulation in the North Atlantic reduced the northward flow of the NAC, promoting the southward expansion of cold subpolar waters along the western European margin.

The severe cooling episodes associated to most deglaciations were followed by a prominent warming event that marks the onset of a climate optimum interstadial event usually present in the first stage of interglacial periods. This climate optimum event was the warmest interstadial of each interglacial. Good examples of these high amplitude changes in temperature can be seen at Termination IX, when SST rose from 8.3 to 19 ºC, and at transitions MIS 21f/e, MIS 21b/a, MIS 15b/a, etc (Fig. VI-1c-d, VI-2d).

In parallel to the pronounced surface cooling events, the record of the Portuguese margin shows that deep-water circulation was also severely affected. A remarkable decrease in the benthic $\delta^{13}C$ is observed at deglaciations (Fig. VI-3a), especially in Terminations IX and VIII, but also at other glacial-interglacial transitions. These drops in benthic $\delta^{13}C$ have been recognized in other sites from the North Atlantic (W&F02; Hodell et al., 2008; Alonso-Garcia et al., 2011b; Ferretti et al., 2015). Drops in the benthic $\delta^{13}C$ have traditionally been attributed to slowdown of NADW formation triggered by lower sea surface salinities in the north Atlantic. In more recent climate cycles lower benthic $\delta^{13}C$ have been observed during Heinrich events that were triggered by freshwater discharge at times of ice sheet collapse (Shackleton et al. 2000;

Skinner et al. 2006, 2007; Martrat et al. 2007). Pulses of repeated freshwater release to the North Atlantic originate the millennial-scale, stadial-interstadial oscillations of late Pleistocene caused by reduced/enhanced Atlantic meridional overturning circulation (AMOC) alternations. Events of reduced AMOC led to lower rates of heat transfer to the North Atlantic that resulted in decreased SST (e.g: Broecker, 1989; Stocker, 1999; McManus et al., 2004; Pisias et al., 2010). Although these millennial-scale climate oscillations are recorded at site U1385, the highest amplitude cooling/warming oscillations on the Portuguese margin coincided with deglaciations, both Terminations and the transitions from glacial to interglacial substages, and were marked by significant changes in the planktonic foraminifer assemblage from high percentages of Nps to increased relative abundance of subtropical species (Fig.VI-2e-f).

We interpret that the pronounced cooling events observed along the Iberian margin were triggered by freshwater released to the Atlantic at the onset of northern Hemisphere ice sheet retreats. The mechanism is similar to what happened during Heinrich stadials recorded at the end of the last two glacial periods (e.g. Rühlemann et al., 1999; Böhm et al., 2014), when the extension of the polar water and icebergs have been reported to reach the latitude of Southern Iberia (e.g., Skinner et al., 2003; Skinner and Shackleton, 2006). Although IRD were not recorded at site U1385 the advection of polar waters to the Portuguese margin only at deglaciations suggests that only freshwater perturbations of a certain magnitude, such as those related to ice-sheet retreats, had a profound effect on the SW Iberian margin.

The remarkable warming episodes that immediately followed deglaciations (Fig. VI-1a-c, VI-1a,d) were triggered by the resumption of NADW formation after the end of freshwater perturbations originated during ice sheet collapse. An increase in the strength of the AMOC led to invigoration of the NAC and the transport of warm surface waters to the Portuguese margin, which is recorded by a significant increase in the subtropical species in the planktonic foraminifer assemblage (Fig. VI-2f).

Ice sheets during Middle Pleistocene tended to collapse at times of high northern Hemisphere summer insolation that resulted from the combination of high obliquity and minimum precession (Imbrie et al. 1993; Huybers and Wunsch, 2003; Huybers 2011). While obliquity mainly governed the time between deglaciations, precession

determined the precise timing of deglaciations (Huybers 2011) and ice discharge to the Ocean. This, in turn, triggered the major reorganizations of surface circulation in the North Atlantic and the advection of polar water to the Iberian margin. The coincidence in timing between these pronounced cooling events in Portugal with increasing northern Hemisphere summer insolation (Fig. VI-2d,g), strongly suggests a causal effect with ice sheet collapse events and deglaciations. Most of these events occurred at times of obliquity maxima when obliquity governs insolation at high latitudes. However there are two notable exceptions, the cooling episodes recorded at 650 and 710 ka when obliquity was relatively low or decreasing (Fig. VI-2g). Instead, these two cooling events occurred at times of increasing summer insolation driven by precession when the perihelion was aligned with northern Hemisphere summer solstice.

Recently it has been proposed that the energy received during summer (called integrated summer insolation, with summer defined as the period when insolation intensity exceeds the ~275 W/m^2 threshold) is the parameter that better reflects the amount of ice sheet melting (Huybers, 2006). The summer energy at 65°N (using the 275 W/m^2 threshold) shows high values during all terminations and transitions from glacial to interglacial substages (Fig. VI-2g), and may be advocated as the trigger for the major reorganizations in North Atlantic circulation observed in our Iberian margin record, in response to deglaciations.

4.3. North Atlantic SST gradient during ice sheet growth

One of the most characteristic features of the SST record in the Portuguese margin is that both the early phase of ice sheet growth, as recorded by the rapid increase in the benthic and planktonic $\delta^{18}O$, and glacial maxima, were coeval with warm SST at Site U1385 (Fig. VI-1a-c, VI-2a,b,d). In fact, off the Iberian margin none of the ice volume maxima corresponded to the lowest SST. When comparing SST records of this study with those from northern sites 980 and U1314 (Fig. VI-3b) an increasing N-S latitudinal SST gradient can be observed. After the pronounced warming recorded at the beginning of interglacials, millennial-scale climate changes are recorded both at high and at middle latitudes, but southern waters remained relatively warm, while the northern ones cooled as a result of the progressive extension of the northern

Hemisphere ice sheets and associated southward advance of the AF (WF02; Alonso-Garcia et al., 2011a). This pattern is particularly noticeable at transitions MIS 19/18, MIS17/16 and MIS15/14. During the early phase of glacials, areas at latitudes of 37ºN were influenced by the warm subtropical waters of the Azores current, as indicated by the presence of the subtropical assemblage in our Site (Fig. VI-2f). SST were similar during glacials, especially MIS 20, and interglacials, especially during MIS 20. A similar situation was observed in site U1313 during MIS 16, when warm and stratified surface waters coexisted with the presence of IRD layers produced by Heinrich-like Events (Naafs et al., 2011).

This lack of correspondence between SST and ice volume maxima was also recorded in the mid-latitude North Atlantic in more recent isotope stages, like MIS 6 (Martrat et al., 2007) and the Last Glacial Maximum, when surface water temperature was almost as high as today, according to SST reconstructions from the Portuguese margin (Cayre et al., 1999; de Abreu et al., 2003) and the North Atlantic at the same latitude (Chapman and Shackleton, 1998).

This mismatch between increasing global ice volume, cool SST in the northern latitudes and warm surface waters off Iberia supports the instrumental role that warm surface waters of mid-latitude North Atlantic had in building northern hemisphere ice sheets, providing an important source of water vapor to promote ice growth (Ruddiman and McIntyre, 1981; Sanchez-Goñi et al. 2013).

6. CONCLUSIONS

Our study of the variation of planktonic foraminifers assemblages and SST, from the Shackleton site during the middle Pleistocene, as well as the comparison of our results with both benthic and planktonic $\delta^{18}O$ records and Ca/Ti data from the same Site (Hodell et al., 2015), allows the characterization of climatic conditions in the North Atlantic back to the ninth climatic cycle (867 ka). SST was generally colder during the middle Pleistocene than today off the southwestern Iberian margin, especially summer temperature, which was higher than today only during very short periods in some interglacials. During this period and superimposed on the glacial-interglacial variations, millennial-scale climatic variability was recorded.

All deglaciations on the Portuguese margin, both Terminations (particularly T IX and VIII) and the transitions from glacial to interglacial substages (MIS 21b/a, MIS 18e/d and especially MIS 15b/a), show a prominent (up to 10ºC in amplitude) cold-warm climate oscillation. This high amplitude variation in temperature during deglaciations is recorded by a remarkable change in the planktonic foraminifer assemblages from high relative abundance of the polar species Nps to high relative abundance of the subtropical association (Fig. VI-2e-f).

These high amplitude oscillations in temperature were the result of major reorganizations of Sea surface and deep water circulation in the North Atlantic triggered by freshwater releases to the Ocean when Ice sheets in the northern Hemisphere started to retreat. Reduced salinities at surface shutdown NADW formation and reduced the northward advection of heat and the transport of warm waters to the eastern margin of the subtropical gyre, causing the advection of subpolar waters to the SW Iberian margin. This scenario rapidly changed when the freshwater perturbation stopped. The re-initiation of NADW formation enhanced the strength of the AMOC leading to an intensification of the NAC and the flux of warm waters to the Iberian margin.

The comparison with SST records from higher latitudes of the North Atlantic reveals the development of a steeper latitudinal SST gradient between the sub-tropical and the sub-polar North Atlantic as ice sheets were growing in the northern Hemisphere, providing a source of water vapour that could promote the growth of ice sheets.

CHAPTER VII

VARIATION IN NORTH ATLANTIC CIRCULATION DURING GLACIAL MARINE ISOTOPE STAGES 20, 18, 16 AND 14

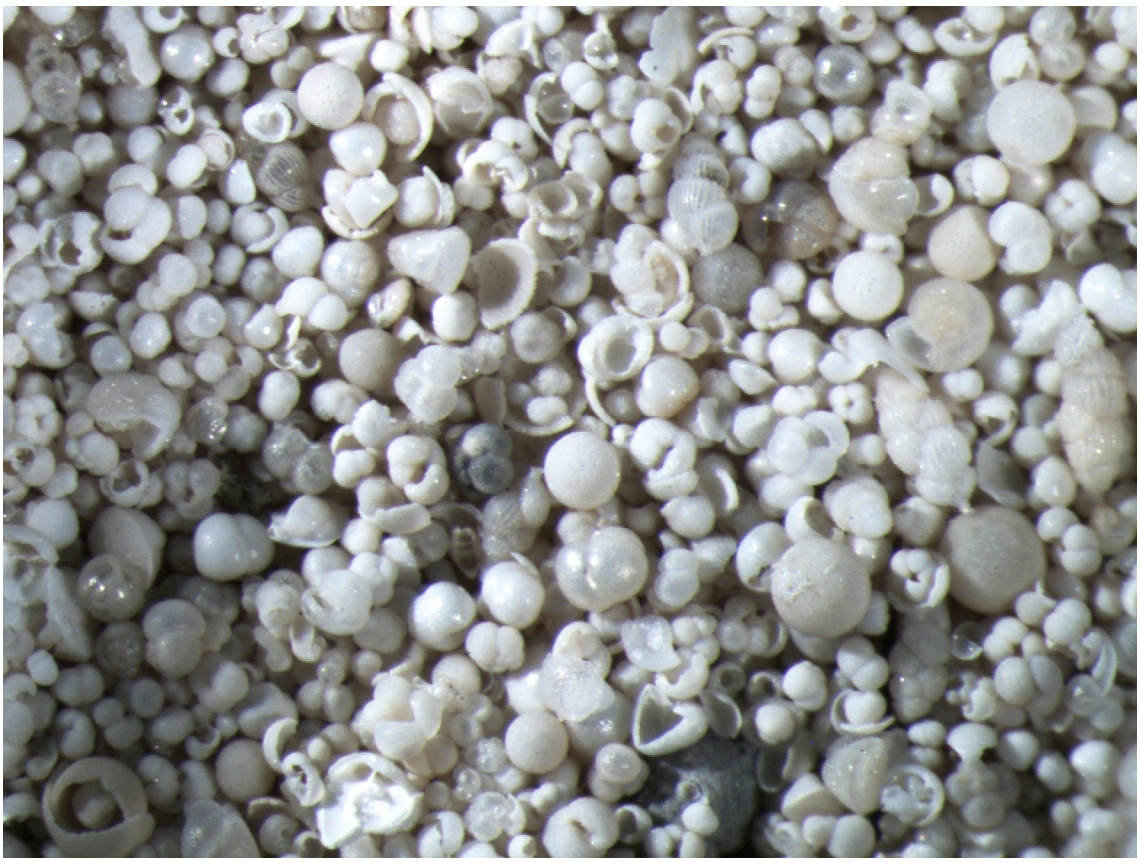

CHAPTER VII

VARIATION IN NORTH ATLANTIC CIRCULATION DURING GLACIAL MARINE ISOTOPE STAGES 20, 18, 16 AND 14 (*)

*This Chapter is based on: **Martin-Garcia, G.M.**, Sierro, F.J., Flores, J.A., Variations in North Atlantic circulation during glacials MIS 20, 18, 16 and 14. Insights from planktonic foraminiferal fauna. *Marine Microplaleontology*. (in preparation)

ABSTRACT

The Southwest Iberian margin is highly sensitive to changes in the distribution of North Atlantic currents and water masses, as well as to changes in the position of the Arctic and subtropical fronts. In this work we reconstruct the evolution of oceanographic parameters during glacial stages from 814 ka (MIS 20) to 530 ka (MIS 14), based on planktonic foraminifers analysis of core IODP-U1385 (37º34.285´N, 10º7.562´W; 2585 mbsl). By comparing our findings with records from other North Atlantic core sites located between 39 and 58.4 ºN, we are able to trace palaeoceanographic conditions across the North Atlantic for the interval. Variations in abundance of microfaunal assemblages indicate a change in the general North Atlantic circulation during MIS 16, associated with the shift in the Arctic Front (AF) position and intensification of North Atlantic Deep Water (NADW) formation that happened at the time. During glacials previous to MIS 16 the southern position of the AF and the surges of icebergs and associated production of meltwater severely reduced the NADW formation, which resulted in a weakened North Atlantic Current and the dispersal of polar water over the North Atlantic. The NAC followed an almost pure west to east drift, and off the SW Iberian margin warm subtropical water overflowed (probably northward) the colder polar and subpolar water masses advected southward. Since MIS 16, the northern position of the Arctic Front and increased production of NADW reactivated the North Atlantic Current, which advected warmer water to higher latitudes. Off the Iberian margin, the Portugal Current became stronger and diverted warmer water offshore, reducing the relative abundance of warm surface-dwelling species in Site U1385.

1. INTRODUCTION

The North Atlantic is characterized by a continuous flow of warm and salty surface water originated in the tropical region and transported northwards by the Gulf Stream, which continues as the North Atlantic Current (NAC). This mass of water returns, cooler, southward along the western European continental margin. The NAC forms the transition zone between the cold and productive waters located at the North of the Arctic Front (AF) (eg., Johannessen et al., 1994), and the warm and oligotrophic waters from the subtropical gyre in the South. Linked to the different water masses the planktonic foraminiferal fauna can be grouped into different assemblages, such as polar, subpolar, transitional, North Atlantic Current, Azores Current and tropicical (eg., Bé, 1977; Ottens, 1992; Johannessen et al., 1994; Cayre et al., 1999; Salgueiro et al., 2008). During glacials, the AF and associated productivity maximum moved southward into mid-latitude North Atlantic (Stein et al., 2009; Villanueva et al., 2001), cold polar waters expanded to lower latitudes and the NAC did not reach as far North as during interglacials (Pflaumann et al., 2003). After MIS 21 a northwest shift in the position of the AF began, both during interglacials (Hernandez-Almeida et al., 2013) and glacials (Alonso-Garcia et al., 2011b), which culminated after MIS 16 in similar positions as it occupies today (Wright and Flower, 2002) (Fig. VII-1), and allowed increased influence of the NAC in higher latitudes during glacials.

Various studies have shown that surface water characteristics in the mid-latitude North Atlantic depend on the strength and position of the NAC and the associated oceanic fronts (e.g., Calvo et al., 2001; Naafs et al., 2010; Voelker et al., 2010). Over the last glacial cycle, the northern Iberian margin recorded peak displacement events of the AF (Eynaud et al., 2009) and was, in general, more affected by the subpolar water masses than the southern part, which was more influenced by the subtropical water masses from the Azores Current (Rodrigues et al., 2011). As a consequence, a latitudinal temperature gradient was produced along the western Iberian margin which can be observed in SST reconstructions based both in alkenone (eg., Martrat et al., 2007) and in planktonic foraminifera data (Salgueiro et al., 2010). Nevertheless, there is evidence that polar to tropical planktonic foraminifers assemblages co-occurred in a latitudinal band around 35º –40ºN during the Last Glacial Maximum,

which suggests the absence of the North Atlantic Drift but the presence of a strong subpolar gyre (McIntyre et al., 1976). Core IODP-U1385 is located near the present day boundary (Fiúza et al., 1998) between different water masses and we expect it to have been close to the Arctic Front during some of the extreme cold events that punctuated the period between MIS 21 to 14, but also to have stayed under the influence of the tropical climate through surface current connections for a significant portion of this time interval. We think that faunal data from Site U1385 can provide valuable insight into the variations of the distribution of North Atlantic currents and the fluctuations in the position of subtropical and arctic fronts along the Pleistocene.

Previous studies (e.g., Cayre et al., 1999; Bard et al., 2000; de Abreu et al., 2003; Roucoux et al., 2005; Vautravers and Shackleton 2006; Martrat el al., 2007; Rodrigues et al., 2011) of oceanographic conditions off Iberia and reconstruction of surface circulation in the North Atlantic reach back to isotope stage MIS 15. As a contribution toward the improvement of palaeoceanographic reconstructions along the Pleistocene, this paper aims to describe the evolution of the sea surface circulation in the North Atlantic during glacial marine isotope stages (MIS) 20, 18, 16 and 14, based on planktonic foraminifer analysis of sediments from the IODP core U1385. To fit our finding into a larger context, we discuss surface water conditions across the North Atlantic by comparing our results with previous works conducted on cores from different locations in the North Atlantic.

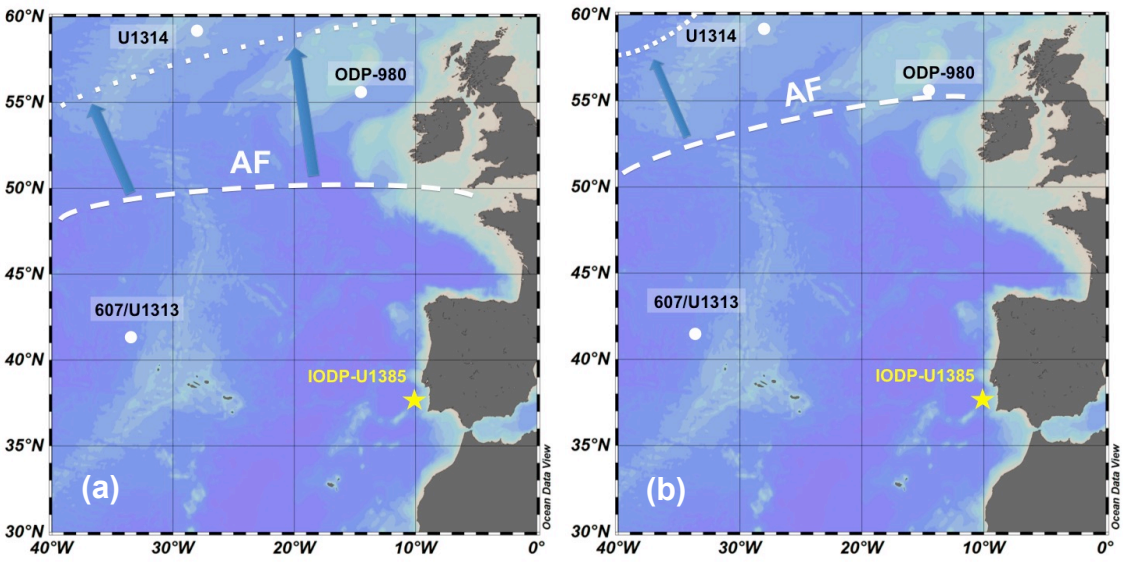

(previous page) **Figure VII - 1.** Position of the Arctic Front (AF) during glacials (dashed line) and interglacials (dotted line) before (a) and after (b) MIS 16 (from Wright and Flower, 2002). Site U1385 and other sites mentioned in this chapter are shown in the map.

2. MATERIAL AND METHODS

Sediments at Site U1385 define a single lithological unit, very uniform and dominated by calcareous muds and calcareous clays, with varying proportions of biogenic carbonate (23% - 39%) and terrigenous sediment and the occasional occurrence of ice rafted debris (IRD). Cyclic variations in physical properties and color reflect cyclic changes in the proportion of biogenic carbonate and detrital material delivered to the site (Hodell el al., 2013b).

This study covers four sections from the secondary splice U1385D/E comprised between 57.70–58.62, 60.18–62.94, 66.77–74.02 and 76.3–80.4 crmcd (MIS 14, 16, 18 and 20). Sampling was performed every 20 cm (1 cm for isotopic analysis), providing estimated resolution records of 1.4, 2.8, 1.5 and 1.4 ky for each of the four intervals. A total of 92 samples 1 cm thick were dried, weighed and washed over a 63 mm mesh sieve. The >63 mm residue was dried, weighed and sieved again to separate and weigh the >150 mm fraction. Census counts of planktonic foraminifera taxa were conducted on the sediment fraction larger than150 mm, which was successively split until a minimum of 300 specimens was obtained. A total of twenty-eight species and ten morphotypes (Kennett and Srinivasan, 1983) of planktonic foraminifers have been identified (Appendix I) and their relative abundances, calculated.

The age model of the studied section is based on the correlation of the benthic oxygen isotope record to the global benthic LR04 isotope stack (Lisiecki and Raymo, 2005) (see Hodell et al., 2015)

Sea surface temperature (Martin-Garcia et al., 2015) was reconstructed from planktonic foraminifer census counts according to the Artificial Neural Network method and comparing with MARGO North Atlantic database, as described in Kucera et al. (2005).

For sites U1314, 980 and 607(U1313), percentages of planktonic foraminifer assemblages have been estimated using original published data (Alonso-Garcia et al., 2011a; Wright and Flower, 2002 and Ruddiman et al., 1989, respectively). The age

model for these sites has been recalculated referred to the U1385 Age model, using *Analyseries* software (Paillard et al., 1996).

3. RESULTS: *Micropaleontological analysis*

Microfaunal analysis focuses on species and assemblages (Appendix IV) that can be directly used to monitor changes in North Atlantic water masses and currents.

The polar species *Neogloboquadrina pachyderma* sinistral (Nps) has a temperature tolerance range between –1 and 8 ºC and an optimum of 2 ºC (Tolderlund and Bé, 1971). In site U1385 this species presented generally higher relative abundance before MIS 16 than afterwards (Fig. VII-2c). The highest percentages of Nps occurred during deglaciations, both Terminations and partial reduction of ice sheets volume, and coincided with decrease of benthic $\delta^{13}C$, especially so during MIS 20 and 18. This suggests that the reduction of the North Atlantic Deep Water (NADW) formation and reduction of the Atlantic Meridional Overturning Circulation (AMOC) resulted in the increase of very cold water of polar origin advected southward.

Turborotalita quinqueloba (Tq) has a temperature tolerance range of 4.6ºC – 10.8ºC (Tolderlund and Bé, 1971), with an optimum of 12ºC (Stangeew, 2001). High percentages of this species are found south of Iceland (Pujol, 1980), and its maximal abundance has been recognized as associated with the AF (Johannessen et al., 1994; Cayre et al., 1999; Wright and Flower, 2002). In site U1385 this species became more abundant at 655 ka, in MIS 16b, and since then it kept higher percentages than before (Fig. VII-2d).

The North Atlantic Current (NAC) assemblage (Ottens, 1991) was more abundant during MIS 16 and 14 than before, the increase in its relative abundance happened ~655 ka, coinciding with the decrease of Nps (Fig. VII-2). During MIS 18 the relative abundance of this assemblage decreased progressively towards the end of the isotope stage.

Dextral *Neogloboquadrina pachyderma* (Npd) has a temperature optimum between 10-18 ºC and the limit with Nps is the April isotherm of 7.2 ºC (Ericson, 1959). This species is considered a proxy for the present-day Portugal Current (Salgueiro et al., 2008) and a component of the NAC assemblage (Ottens, 1991). Its record in site

U1385 is similar to the NAC assemblage one and during MIS 14 Npd becomes the species with highest percentage in this assemblage (Fig. VII-2e).

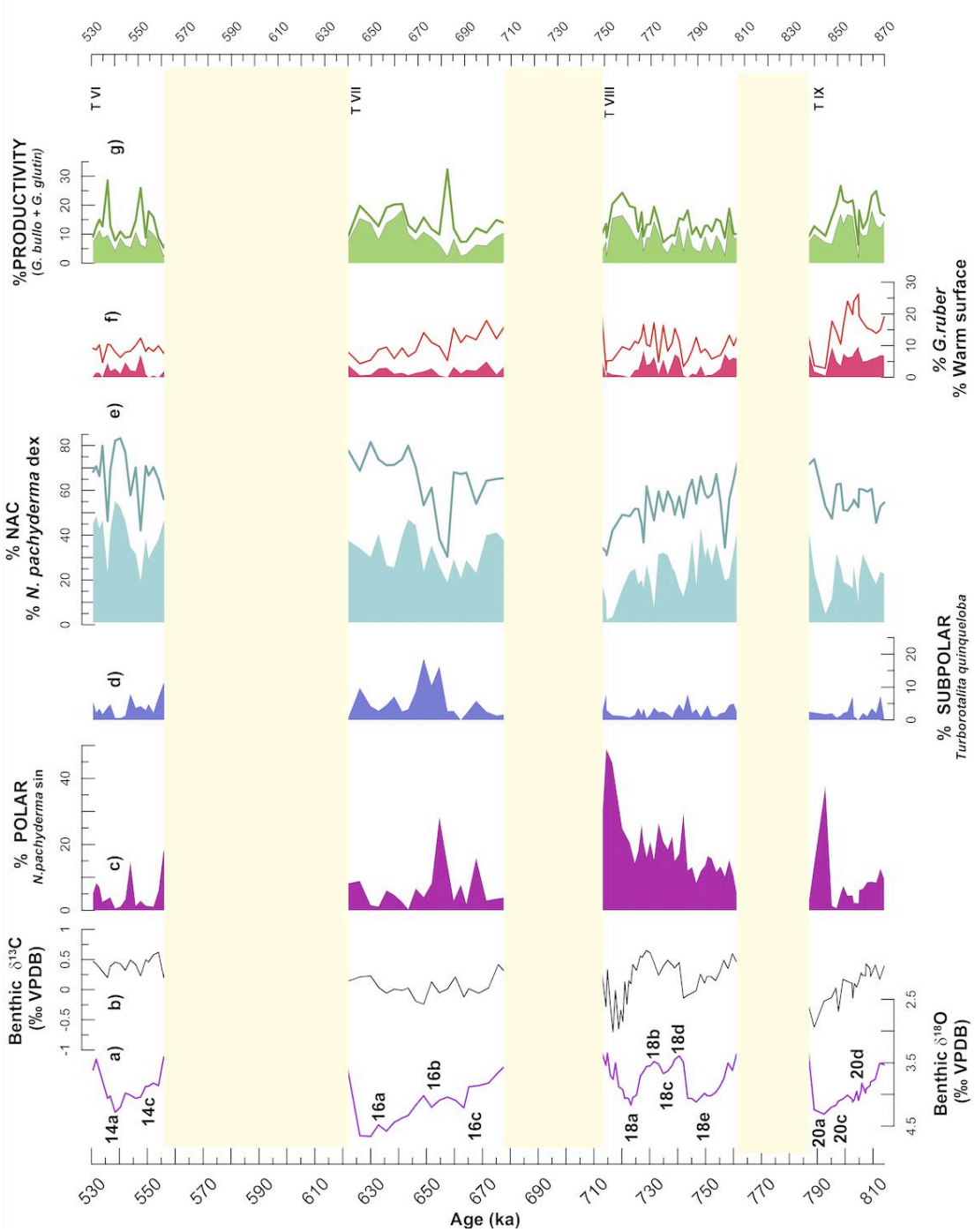

Figure VII - 2. Relative abundance of planktonic foraminifer species and assemblages in Site U1385. Benthic foraminifer $\delta^{18}O$ (a), and $\delta^{13}C$ (b) (Hodell et al., 2015). Relative abundances of (c) *Neogloboquadrina pachyderma* (sinistral); (d) *Turborotalita quinqueloba*; (e) North Atlantic Current assemblage (as defined by Ottens, 1991) and (filled) the percentage of *Neogloboquadrina pachyderma* (dextral); (f) Warm surface assemblage (as defined by

Vautravers et al., 2004) and (filled) *Globigerinoides ruber* (white); (g) Productivity assemblage (*Globigerina bulloides* + *Globigerinita glutinata*) and (filled) *Globigerina bulloides*. Marine isotope substages are named according to Railsback et al. (2015).

The surface-dweller subtropical species *Globigerinoides ruber* (Ottens, 1991) can tolerate a wide range of salinity (Bijma et al., 1990) and is a component of the warm surface assemblage (Vautravers et al., 2004). This assemblage is recorded in U1385 during all studied glacials (Fig. 2), even coinciding with high values of polar and subpolar species, which suggests the presence of subtropical surface water overflowing colder water of subpolar or polar origin, either during the whole year or seasonally. Since glacial maximum MIS 16a generally lower values of this assemblage occur, coinciding with generally high percentages of the North Atlantic Current assemblage and increasing abundance of the Portugal Current proxy (Fig. VII-2e-f).

The Azores Current assemblage (*Globigerinoides ruber* and *Globorotalia inflata*) is typical of the present-day subtropical branch of ENACW, transported to the Northeast Atlantic by the AzC and northward in Site U1385 during non-upwelling months (Salgueiro, 2008).

Globigerina bulloides is abundant in areas of high phytoplankton productivity and deep mixing layer, as well as in subpolar waters (north of 48 ºN), which are rich in nutrients (Reynolds and Thunell, 1985; Schiebel et al., 2001). It is traditionally considered a proxy for upwelling (Prell, 1984), particularly in the northeastern subtropical Atlantic (Chapman et al., 1996) and at the Iberian margin (de Abreu et al., 2005; Salgueiro et al., 2008). *Globigerinita glutinata* is an opportunistic species that prefers productive environments (Ottens, 1992) and high percentages of it are observed in relation to surface current eddies that help to increase the nutrient input to the mixed layer (Schmuker and Schiebel, 2002; Olson and Smart, 2004). Both species are grouped into a productivity assemblage (Fig. VII-2g) that keeps similar values during all glacials. Higher percentages of it coincide indistinctly with either warm, polar or NAC waters. This suggests an active upwelling throughout the study interval, with different source of upwelled waters.

4. DISCUSSION: changes in the distribution of currents in the North Atlantic

Variations in surface water characteristics at Site U1385 are interpreted to reflect changes in the influence of the different oceanic water masses present in the North Atlantic. To include our findings in the general oceanic context, we compare our results with data from other North Atlantic locations.

4.1. Marine Isotope Stage 20

The polar species Nps has been used to monitor southward penetrations of polar-sub polar waters in North Atlantic mid-latitudes that reached the Iberian margin (eg., Bond et al., 1992; Cayre et al., 1999; de Abreu et al., 2003; Eynaud et al., 2009; Martin-Garcia et al., 2015). The percentage of this species in Site U1385 remained relatively low until MIS 20b. Increase of the NAC assemblage is also recorded at the time (Fig. VII-3b-c).

Microfaunal data from site ODP-980 inform that the AF advanced rapidly southward towards its ~50ºN position during MIS 20d (Wright and Flower, 2002; hence for, W&F02). As the AF migrated southward, the area of NADW formation was affected and the AMOC weakened, assuming a close correlation between the rate of thermohaline circulation and benthic $\delta^{13}C$ levels (Zahn et al, 1997) (Fig. VII-3a-b). The progressive reduction of the AMOC during MIS 20d-b was punctuated by episodes of sharp decrease of NADW formation, probably related with sudden coverage of the area of sinking by the AF; after each one of these episodes the locus of deep water formation shifted to a southeastern position and allowed the recovery of the AMOC, as informed by rapid increase of $\delta^{13}C$. This progressive reduction of the AMOC resulted in the spread of polar waters into mid-latitude central ocean, which was recorded in site 607 as high percentage of the polar Nps and deep and prolonged cooling (Fig. VII-3b,e) (Ruddiman et al., 1989). The southward migration of the AF should have deflected the NAC eastward, similarly to what happened during the Last Glacial Maximum (Pflaumann et al., 2003) or the most severe cold glacials of early Pleistocene (Naafs et al., 2010), when the NAC acquired an almost pure west to east flow.

Contrary to what happened in the middle ocean, Site U1385 recorded warm SST during most of MIS 20 (Fig. VII-3e), and only the drastic reduction of the AMOC during MIS 20a produced substantial decrease of SST (Martin-Garcia et al., 2015) by the

advection of polar water via the Portugal Current (PC). The west-east surface temperature gradient that developed in the mid-latitude North Atlantic suggests that the subtropical gyre was deflected eastwards, at least during some episodes of southward advance of the AF in the western ocean, and warm surface water reached the Iberian margin but not site 607 in the central North Atlantic (Fig. VII-3d).

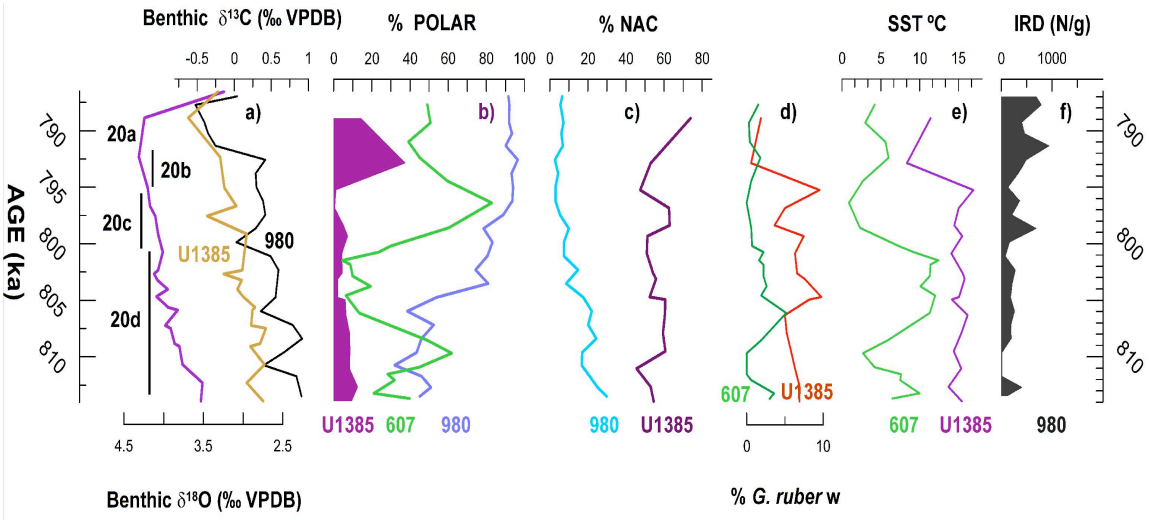

Figure VII - 3. Comparison between mid-latitude and subpolar North Atlantic during MIS 20. (a) Benthic $\delta^{18}O$ profile from U1385 (purple); benthic $\delta^{13}C$ record from U1385 (golden) and subpolar site ODP-980 (black). (b) Relative abundance of *N. pachyderma* (sinistral) from sites U1385 (filled purple) 607 (green) and 980 (blue). (c) Relative abundance of the NAC assemblage (as defined by Ottens, 1991) from sites 980 (blue) and U1385 (dark purple). (d) Relative abundance of *G. ruber* white from sites 607 (green) and U1385 (red). (e) SST data for sites 607 (green) and U1385 (purple). (f) IRD concentration in site 980. Data from site 980 are from W&F02; and data from site 607 are from Ruddiman et al. (1989).

4.2. Marine Isotope Stage 18

During MIS 18e, as ice sheets grew continuous iceberg discharges happened – recorded as thick IRD layers in subpolar North Atlantic (W&F02; Alonso-Garcia et al., 2011b) (Fig. VII-4f), with associated meltwater surges and the advection of fresh water, which gradually reduced the NADW formation. Mid-latitude site U1385 registered more ^{13}C-depleted bottom water than northern site 980 (Fig. VII-4a), which suggests that the formation of NADW was very weak at the time. The reduction of the AMOC resulted in the southward advance of the AF and the deflection of the NAC, which is

recorded by the progressive decrease of percentage of the NAC assemblage, mirroring the increase of the polar Nps, in site 980 (Fig. VII-4b-c). Site U1385 did not register substantial decrease of the NAC assemblage prior to the deglaciation of MIS 18e and associated drastic reduction of AMOC, which suggests that during MIS 18e the NAC progressively acquired a west - eastward flow and remained active in mid-latitude ocean. Towards deglaciation site 607 recorded higher percentages of the polar species Nps than U1385, which suggests that the in the western North Atlantic the AF would have acquired a more southern position than in the eastern, which would have diverted the NAC eastwards of site 607.

The NAC reached the subpolar North Atlantic during MIS 18d-b, when the ice sheets size was similar to interglacial conditions, the AF retreated northward and the AMOC was vigorous, as similar $\delta^{13}C$ from site 980 and site U1385 suggests (Fig. VII-4a,c). This allowed the northward advection of warm water, registered in mid-latitude North Atlantic by increased percentages of *G. ruber* and increased SST (Fig. VII-4d-e).

Since the glacial inception of MIS 18b, the continued southward migration of the AF produced a rapid weakening of the AMOC that resulted in drastic reduction of the surface circulation and the rapid spread of polar water across mid-latitude North Atlantic (Fig. VII-4b). Although during most of MIS 18a values of $\delta^{13}C$ from site 980 (W&F02) suggest NADW formation at the site, abyssal water in site U1385 was ^{13}C-depleted AABW (Fig. VII-4a), which indicates that the overturning was very shallow and not enough to maintain a vigorous surface circulation. Since the glacial maximum of MIS 18a, increasing frequency of IRD in high latitudes (W&F02) (Fig. VII-4f) informs of continuous massive surges and melting of iceberg that culminated in Termination VIII and drastically weakened the export of NADW, similarly to what happened during deglaciations in Terminations I and II (McManus et al., 2004). During T VIII the AMOC descended to its minimum value in the whole mid-Pleistocene, as minima in $\delta^{13}C$ from site U1385 suggest (Fig. VII-2b), and produced even further weakening of the NAC and southward advection of polar water. This is recorded by lowered percentages of the NAC assemblage both in subpolar and in middle latitudes as well as by lowered SST in site 607 (Ruddiman et al., 1989) and U1385 (Martin-Garcia et al., 2015) (Fig. VII-4c,e).

The presence of the warm surface water assemblage in site U1385 coinciding with high percentages of the polar Nps (Fig. VII-2) suggests that a warm subtropical water mass overflowed colder water of polar origin that was being advected southward in increasing quantity during MIS 18. This interpretation is consistent with warm surface alkenone-based SST data from the mid-latitude open ocean (Naafs et al., 2011b).

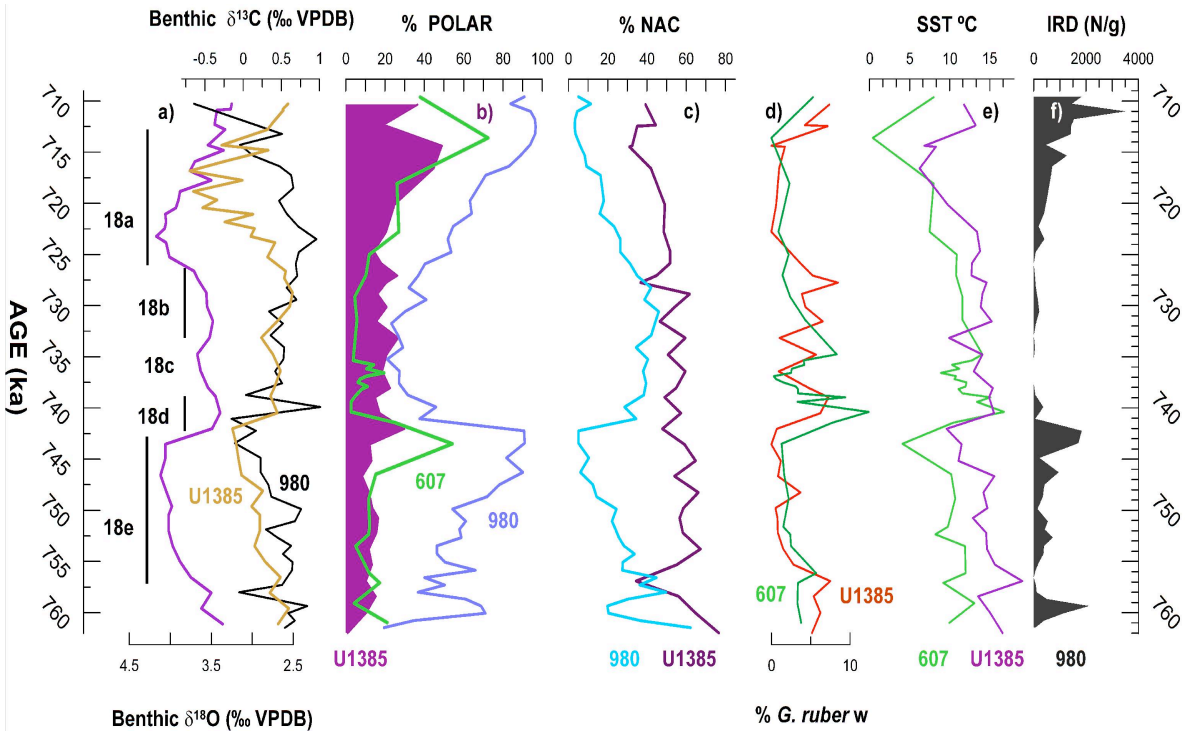

Figure VII - 4. Comparison between mid-latitude and subpolar North Atlantic during MIS 18. (a) Benthic $\delta^{18}O$ profile from U1385 (purple); benthic $\delta^{13}C$ record from U1385 (golden) and subpolar site ODP-980 (black). (b) Relative abundance of *N. pachyderma* (sinistral) from sites U1385 (filled purple) 607 (green) and 980 (blue). (c) Relative abundance of the NAC assemblage (as defined by Ottens, 1991) from sites 980 (blue) and U1385 (dark purple). (d) Relative abundance of *G. ruber* white from sites 607 (green) and U1385 (red). (e) SST data for sites 607 (green) and U1385 (purple). (f) IRD concentration in site 980. Data from site 980 are from W&F02, and data from site 607 are from Ruddiman et al. (1989).

4.3. Marine Isotope Stage 16

During MIS 16, sea surface waters remained warm and stratified across the whole mid-latitude North Atlantic, due to the northward position of the AF (Naafs et al., 2011), similarly to what happened in MIS 6, when the AF occupied a more northward position than that occupied during the Last Glacial Maximum (Calvo et al., 2001). This

position of the AF at the time combined with an increased production of NADW, as benthic $\delta^{13}C$ record in the subtropical North Atlantic documents (Poirier and Billups, 2014), allowed the arrival of warmer, mid-latitudes North Atlantic water to higher latitudes, providing more humidity to the area and, thus, enhancing the growth of ice sheets, as indicated by $\delta^{18}O$ records. Internal instabilities in the ice sheets or the calving effect of the continuously advected warm water masses, produced the intermittent collapse of the ice cap and the subsequent icebergs surges, which interfered with thermohaline overturn, without completely stopping it. Despite this apparent contradiction with the established deep circulation mode (Rahmstorf et al., 2002) for ice rafting episodes, recent studies for the last glacial cycle (Böhm et al., 2014) prove that shutdowns of NADW formation only occurred during Heinrich stadials close to glacial maxima with increased ice coverage. This interpretation is consistent with an important, yet highly oscillating, abundance of NAC assemblage in high latitude North Atlantic coetaneous with IRD layers and low $\delta^{13}C$ values in the region (W&F02) (Fig. VII-5a,c,f). In this sense, the outstanding episode that occurred ~645 ka, with the second lowest $\delta^{13}C$ value for the whole mid-Pleistocene in coincidence with very high abundance of the NAC assemblage in site 980 (W&F02) (Fig. VII-5a,c), points to an exceptionally vigorous but shallow NA overturning cell, underlain by significant volumes of southern-sourced water, similarly to the situation at the end of Termination II (Böhm et al., 2014). In the subtropical eastern North Atlantic, the sub polar species *Tq* gained importance along this stage, and since mid-MIS 16 it became more abundant than *Nps* (Fig. VII-2). As the maximum abundance of *Tq* is linked to the limit between the Artic and the NAC water masses (Johannessen et al., 1994), the foretold substitution of species can be interpreted as a change in the water mass that reached the Iberian margin during cold periods before – polar water – and after – NA water of sub-polar origin (ENAWsp) – mid-MIS 16, due to the retreat of the AF to a more northern position. Between 660 and 645 ka the southwester Iberian margin recorded a severe and prolonged cooling that was not recorded in the open ocean, probably because of the persistent influence of the Gulf Stream that blocked polar waters from the central North Atlantic and re-directed them eastwards, similarly to what happened during the glacial inception of MIS 11.32 (Stein et al., 2009).

For the whole MIS 16 the NAC maintained a Northeast direction, recirculating relatively warm waters to the sub-polar regions and southward again along the Iberian margin. As the ice sheets grew, and as a consequence of the more northern position occupied by the AF respect to previous glacials, the NAC was only slightly diverted southward and was still able to block almost completely the flooding of cold northern water masses into the subtropical ocean. Paradoxically, this blockage increased as the glacial advanced, as the low abundance of polar – subpolar species and the increasing importance of NAC assemblage from U1385 sediments suggest.

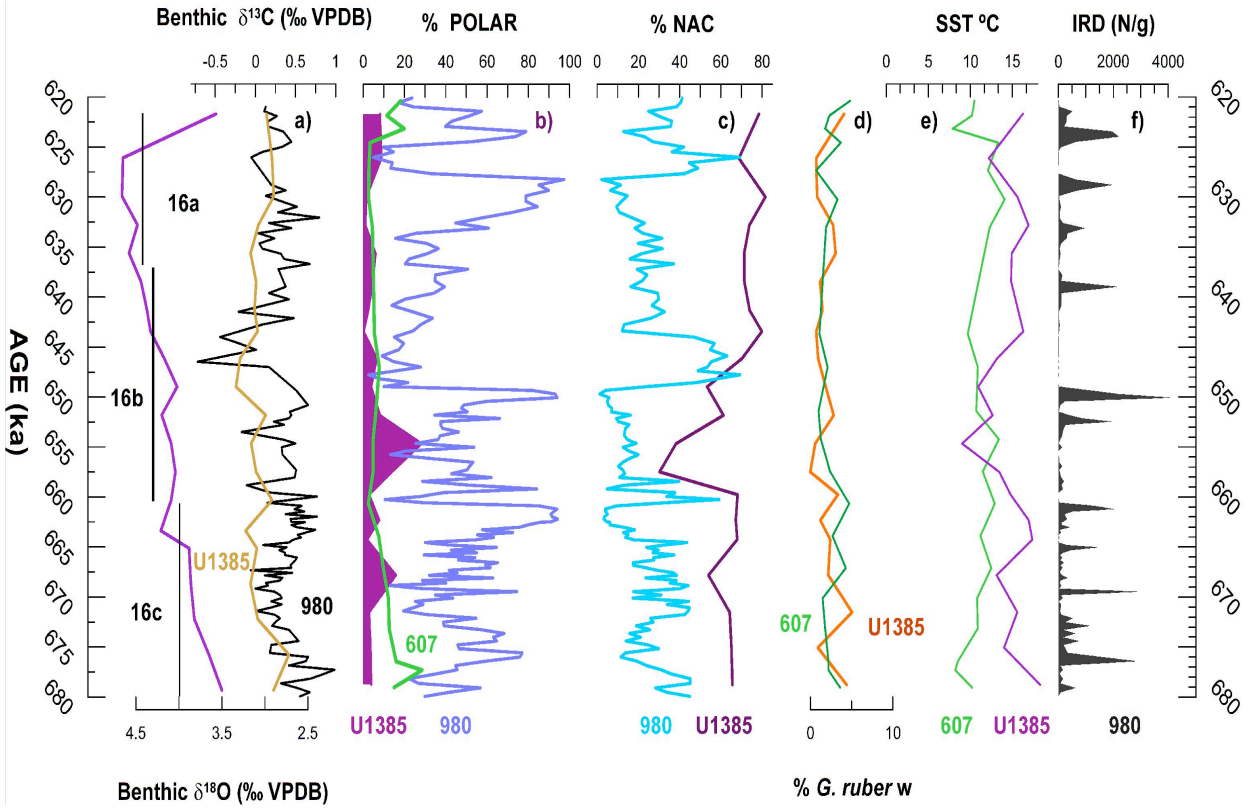

Figure VII - 5. Comparison between mid-latitude and subpolar North Atlantic during MIS 16. (a) Benthic $\delta^{18}O$ profile from U1385 (purple); benthic $\delta^{13}C$ record from U1385 (golden) and subpolar site ODP-980 (black). (b) Relative abundance of *N. pachyderma* (sinistral) from sites U1385 (filled purple) 607 (green) and 980 (blue). (c) Relative abundance of the NAC assemblage (as defined by Ottens, 1991) from sites 980 (blue) and U1385 (dark purple). (d) Relative abundance of *G. ruber* white from sites 607 (green) and U1385 (red). (e) SST data for sites 607 (green) and U1385 (purple). (f) IRD concentration in site 980. Data from site 980 are from W&F02, and data from site 607 are from Ruddiman et al. (1989).

4.4. Marine Isotope Stage 14

Off Iberia, Npd was the most abundant species during this interval and, contrary to previous glacials, during MIS 14 the NAC assemblage was almost exclusively composed of Npd (Fig. VII-2). Today this species is linked to the presence of ENACWsp, brought southward into the region via the PC, the descending branch of the NAC eastern drift (Salgueiro et al., 2008) and its continued and high abundance during this interval suggests an almost permanent, very vigorous southern drift of the ENAC and thus, a very active NAC. Nevertheless, the Npd percentage shows deep and sharp oscillations that happened in synchronicity with peaks in either polar – subpolar species (Nps and Tq) or warm subtropical ones (warm surface assemblage and *G.ruber*), which means that the general influence of the NAC over the whole North Atlantic was interrupted by episodes of southward flows of subpolar waters and others of northward migration of the subtropical gyre as far northward as to induce the advection of very warm waters along the Iberian margin. These cold episodes happened at the glacial inception of MIS 14d, and were probably caused by the combined action of a fast southward migration of the AF with iceberg discharges (W&F02; Alonso-Garcia et al., 2011b) that produced important surges of fresh waters in the source of the overturning, which temporarily reduced the NADW formation, weakened the NAC drift and subsequently favoured the spread of very cold waters across the North Atlantic (Fig. VII-6a-c). The afore mentioned warmest episodes happened always in association with sharp increases in benthic $\delta^{13}C$ (Fig. VII-6a,d), which suggests that sudden and sharp recovery of the AMOC, with the subsequent reactivation of the NAC, might have produced the northward migration of the ITCZ and the arrival of subtropical waters (ENACWst) to the southwester Iberian margin.

Other records from different latitudes in the North Atlantic support this interpretation. Site ODP-980 records fast and deep oscillations of the NAC assemblage that are consistent with data off Iberia in this way: increases of the NAC assemblage in Site 980 correlate with peaks of warm fauna in U1385, and sharp decreases of NAC assemblage in the northern Atlantic correlate with high values of polar – subpolar species off Iberia (Fig. VII-6). The different faunal distribution, as well as and increased SST gradient between middle and high latitudes (Martin-Garcia et al., 2015), suggest

and almost purely west to east flow direction of the NAC and a southern position of the AF, similarly to reconstructions for the Last Glacial Maximum (Pflauman et al., 2003). Icebergs and meltwater surges that produced episodes of sharp reduction of NADW formation were recorded in high latitudes by deep decreases in benthic $\delta^{13}C$, IRD layers and peaks in the polar Nps record (Wright and Flower, 2002) and in middle latitudes, by pronounced decreases of SSTs especially the most superficial water layer, according to alkenone-based reconstructions for U1313 (Naafs et al., 2011b) and for MD03-2699 in the Iberian margin (Rodrigues et al., 2011). Some of these cold episodes, like the one that occurred at the glacial inception of MIS 14, recorded the presence of IRD also in the mid-latitude ocean and were interpreted as Heinrich-like events (Stein et al., 2009; Rodrigues et al., 2011). Warmest episodes were recorded at high latitude by sharp increases of the NAC assemblage (Wright and Flower, 2002) and at middle latitude by sharp increases of temperature of the more superficial water layer (Naafs et al., 2011b).

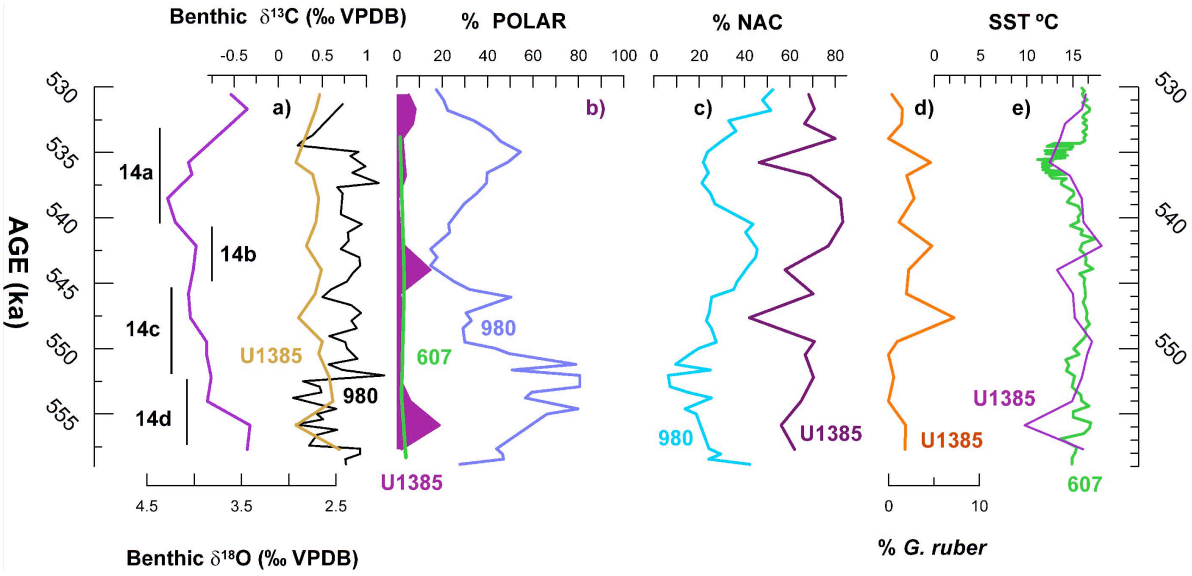

Figure VII - 6. Comparison between mid-latitude and subpolar North Atlantic during MIS 14. (a) Benthic $\delta^{18}O$ profile from U1385 (purple); benthic $\delta^{13}C$ record from U1385 (golden) and subpolar site ODP-980 (black). (b) Relative abundance of *N. pachyderma* (sinistral) from sites U1385 (filled purple) 607 (green) and 980 (blue). (c) Relative abundance of the NAC assemblage (as defined by Ottens, 1991) from sites 980 (blue) and U1385 (dark purple). (d) Relative abundance of *G. ruber* white from site U1385. (e) SST data from sites U1313 (green) and U1385 (purple). Data from site 980 are from W&F02, and data from site U1313 are from Naafs et al. (2011b).

5. CONCLUSIONS

Study of variations of planktonic microfaunal assemblages from the subtropical North-East Atlantic (IODP-U1385), and the comparison of our findings with records from other core sites of the North Atlantic, allow to trace paleoceanographic conditions across the North Atlantic during glacials MIS 20, 18, 16 and 14, and draw the following main conclusions.

The southwester Iberian margin is highly sensitive to changes in the distribution of North Atlantic currents and water masses, as well as to changes in the position of arctic and subtropical fronts.

Variations in abundance of microfaunal assemblages associated to different water masses indicate a change in the general North Atlantic circulation during MIS 16.

Previous to MIS 16, when the arctic front (AF) was located at a more southerly position during both glacials and interglacials, the North Atlantic circulation was determined by its southward migration as glacial conditions progressed. During peak glacial conditions of MIS 20 and MIS 18, coinciding with the southernmost position of the AF, the North Atlantic Current (NAC) was diverted southward and followed and almost pure west to east drift, transporting less heat to high latitudes. During these two glacials, especially during MIS 20, the Azores current (AzC) transported warm subtropical waters along the Iberian margin superficially over waters of polar origin.

Off Iberia, the shift in the AF position was recorded at ~655 ka by the decrease of relative abundance of the polar species *Neogloboquadrina pachyderma* (sinistral) and the increase of the subpolar one, *Turborotalita quinqueloba*.

Since MIS 16, the general circulation across the North Atlantic was lesser influenced by the different positions of the AF than before. The NAC reached high latitudes more frequently during MIS 16 than during previous glacials, and during MIS 14 the NAC became more important in the subpolar North Atlantic as glacial conditions progressed. In the subtropical eastern boundary the faunal assemblage associated with the NAC became the most abundant since MIS 16, which indicates that the PC became stronger along the Iberian margin and diverted warmer water offshore, reducing the relative abundance of warm surface-dwelling species in site U1385.

CHAPTER VIII

RESPONSE OF MACROBENTHIC AND FORAMINIFER COMMUNITIES TO CHANGES IN DEEP SEA ENVIRONMENTAL CONDITIONS FROM MARINE ISOTOPE STAGE 13 TO 11

CHAPTER VIII

RESPONSE OF MACROBENTHIC AND FORAMINIFER COMMUNITIES TO CHANGES IN DEEP SEA ENVIRONMENTAL CONDITIONS FROM MARINE ISOTOPE STAGE 13 TO 11 (*)

* This Chapter is based on: Rodríguez-Tovar, F.J., Dorador, J., **Martin-Garcia, G.M.**, Sierro, F.J., Flores, J.A., Hodell, D.A., 2015. Response of macrobenthic and foraminifer communities to changes in deep-sea environmental conditions from Marine Isotope Stage (MIS) 12 to 11 at the "Shackleton Site". *Global and Planetary Change*, doi: 10.1016/j.gloplacha.2015.08.012 (Appendix VII)

ABSTRACT

Integrative research including facies characterization, ichnological composition and foraminifers analysis has been conducted on cores from Site U1385 of the IODP Expedition 339 to evaluate the incidence of Marine Isotope Stage (MIS) 12 and 11 on deep-sea environmental changes. Four color facies groups have been differentiated, showing variable transitions between them (bioturbated, gradual and sharp contacts). Trace fossil assemblage, assigned to the *Zoophycos* ichnofacies, consists of light and dark filled structures, with *Alcyonidiopsys*, *Chondrites*, *Nereites*, *Planolites*, *Spirophyton*, *Thalassinoides*, *Thalassinoides*-like structures, and *Zoophycos*. A deep-sea multi-tiered trace fossil community is interpreted, revealing predominance of well-oxygenated bottom and pore-waters, as well as abundance of food in the sediment for macrobenthic tracemaker community. Changes in environmental parameters are interpreted associated to significant variations in trace fossil distribution according to the differentiated intervals (A to M). Benthic foraminifer concentration in the sediments and variations of the planktonic foraminifer assemblages suggest significant changes in surface productivity and food supply to the sea floor since the ending of MIS 13 to the end of MIS 11 that could be correlated with the registered changes in facies and trace fossil assemblages. At the end of MIS 13 values of Annual Export Productivity were very low, that together with the presence of light-color sediments and the continuous presence of light *Planolites* and *Thalassinoides*, reveals lower organic carbon flux to the bottom and high oxygen conditions (interval A). Afterwards the organic matter supply increased rapidly and remained very high until Termination V, determining an eutrophic environment, expressed by high benthic foraminifer accumulation rates, and reduced availability of oxygen, that correlate with the record of *Spirophyton* and *Zoophycos*, and the presence of *Chondrites*, observed in the intervals B and D. Lower benthic foraminifer accumulation rates during MIS 11 suggest an oligotrophic environment at the bottom consistent with lower inputs of organic carbon, associated to high oxygen content of bottom waters that agrees with the lighter color of the sediments as well as by the continuous presence of light *Planolites* and *Thalassinoides* in the differentiated interval M. The evolution of the macrobenthic tracemaker community during MIS 12 and 11 responds to major changes in bottom

water ventilation probably linked to variations in deep water (North Atlantic) thermohaline circulation, determining variations in oxygen and food availability.

1. INTRODUCTION

Glacial/interglacial climatic cycles occurring during the Quaternary have been extensively studied due to their incidence on variations in the atmosphere/ocean dynamics and on the involved biota, including hominids. From the several glacial/interglacial episodes, some of them are of special interest, as occurs with those corresponding with the Marine Isotope Stage (MIS) 12 and 11 (MIS 12 and MIS 11). The time interval involving the MIS 12 and 11 is considered one of the most extreme glacial and interglacial periods of the middle Pleistocene. The glacial MIS 12 is characterized by strong cold conditions, and the interglacial MIS 11 is one exceptionally long interglacial warm period. The Mid-Brunhes Event (MBE), close to the MIS 12/11 transition, at around 450 ka BP, a climatic transition between MIS 13 and MIS 11, separates 2 significantly different climatic modes, with interglacials characterized by only moderate warmth previous to this event (early Middle Pleistocene interglacials; 780-450 ka), and interglacial characterized by greater warmth after this event (Middle and Late Pleistocene interglacials; after 450 ka) (i.e., Candy et al., 2010). The transition MIS 12/11, corresponding with Termination V, is the longest glacial Termination of the past 450 ka, having major incidence for the biogeography and human occupation (Candy et al., 2014).

MIS 11 is considered as one of the appropriate climate analogue for the Holocene, being of special interest even for the analysis of future climate variations, which is reflected by the amount of information obtained on this episode (see two consecutive reviews by Droxler et al., 2003 and Candy et al., 2014). All this information allows a detailed characterization of MIS 11, the warm climatic features, and the induced changes in the atmosphere/ocean dynamics. Thus, according to the last revision by Candy et al. (2014), and references therein, several features of MIS 11 are the following: a) the warm episode MIS 11 consists of an interglacial (MIS 11c) and several interstadial and stadial events (i.e., MIS 11a and MIS 11b), with differences in the number and magnitude according to the studied records, b) the MIS 11c is a long warm

climate period that lasted for about 25-30 ky, c) temperature data reveals that MIS 11 was an interglacial of relatively moderate warmth, similar to, or slightly cooler than the Holocene, and d) most of the evidences suggest that MIS 11c is characterized by sea levels significantly above those from the Holocene, even turnover in fauna are consistent with prolonged period of lower sea levels at the beginning and middle part of MIS 11c.

Detailed analyses of MIS 11 and MIS 12 have been conducted in a number of studies on marine, ice core, lacustrine and terrestrial sequences, involving numerous biotic (i.e., pollen and foraminiferal assemblages) and abiotic (i.e., stable isotope and elemental chemistry) proxies, allowing interpretation of environmental parameters such as the global ice volume, or sea surface temperatures. In this sense, as pointed out by Candy et al. (2014) for the identification of MIS 11 in British terrestrial record, terrestrial deposits contain numerous proxies allowing interpretation of different environmental parameters, whereas ice and marine core records contain, frequently, a single proxy. In marine sediment cores the usually applied biotic proxies are foraminiferal (benthic and planktonic) assemblages. In this sense, little attention has been focused on the ichnological record, being very scarce or near absent, the approaches based on the study of the trace fossil assemblage (see Löwemark et al., 2006 and 2012, on trace fossil assemblages studies including MIS 11 in the eastern Mediterranean Sea and Artic Ocean, respectively). Here we present a detailed ichnological analysis of MIS 11 and MIS 12 on cores from IODP Expedition 339 Site U1385, in order to interpret changes in deep-sea environmental conditions, affecting the macrobenthic environment. Integration with information from benthic and planktonic foraminifers, allows integrative interpretations. Moreover, paleoceanographic implications will be assessed.

2. MATERIAL AND METHODS

The research has been conducted on Cores 7H-4 to 7H-1 from Hole U1385D ("Shackleton Site"). Facies characterization has been integrated with the analysis of trace fossils and benthic/planktonic foraminifers.

Facies analysis is based on the study of lithological composition, type of contacts and primary sedimentary structures, with special attention to stratigraphic variations. Digital image treatment allows recognition of variations in color, difficult to recognize based, exclusively, on visual observations (Dorador and Rodríguez-Tovar, 2014a). Ichnological analysis focused on trace fossil assemblages, including trace fossil composition, infilling material, cross-cutting relationships, tiering structure, and relative abundances. Ichnotaxonomical classification was conducted at the ichnogenus level, as usual for core analysis. Ichnological analysis was conducted on detailed observations of half-cut sections of the core in the IODP core repository at Bremen (Germany), together with the study of high-resolution images. Several techniques of digital image treatment to improve the trace fossil visibility were applied for ichnological characterization (Dorador and Rodríguez-Tovar, 2014; Dorador et al., 2014a, b; Rodríguez-Tovar and Dorador, 2014, in press).

Sampling for Export productivity (Pexp) reconstruction and isotope studies was performed every 20 cm providing an estimated average 2 ky resolution record, and for counts on both benthic and planktonic foraminifers sampling was performed at an average 4.6 cm separation, providing an estimated average 0.79 ky resolution. Samples (1 cm thick) were freeze-dried, weighed and washed over a 63 μm mesh sieve. The >63 μm residue was dried, weighed and sieved again to separate and weigh the >150 μm fraction. Counts on planktonic and benthic foraminifers taxa were conducted on this sediment fraction, which was successively split until a minimum of 300 specimens were obtained. Planktonic species (Appendix III) were used to reconstruct Pexp with the modern analogue technique (MAT) (Hutson, 1980) and the modern analog data-base compiled by Salgueiro et al (2010). Stable isotopes were measured on the planktonic foraminifer *Globigerina bulloides* picked from the 250 to 355 μm size fraction and the benthic foraminifer *Cibicidoides wuellerstorfi* from the >212 μm fraction (see Hodell et al., 2015). Isotopic measurements were performed at the Godwin Laboratory (University of Cambridge, Cambridge, United Kingdom) on a VG SIRA mass spectrometer with automatic carbonate preparation system and calibrated to the Vienna Peedee Belemnite (VPB) standard, allowing an analytical precision better than 0.08‰.

The age model of the studied section is based on the correlation of the benthic oxygen isotope record to the global benthic LR04 isotope stack (Lisiecki and Raymo, 2005; see Hodell et al., 2015).

3. RESULTS

3.1. Facies characterization

As in general for the entire Site U1385, the studied interval consists of bioturbated calcareous muds and calcareous clays (Expedition 339 Scientists, 2013a, b). Primary sedimentary structures (i.e., lamination) are near absent; occasionally horizontal lamination into the darker/black intervals is observed. Moreover, no significant changes in grain size are observed. In this general, homogenized, pattern, clear differentiations can be recognized, mainly related to variations in color, probably associated to the organic matter content, usually linked to changes in the trace fossil assemblage (see below). These variations in color can be observed directly on cores, but are even more evident when digital image treatment is applied (Dorador and Rodríguez-Tovar, 2015). Thus, mainly according to variations in color, upper and lower contact, and ichnological composition, several intervals have been differentiated (A to M); see Table 1 and Fig. VIII-1 for a detailed characterization of the intervals. These intervals can be grouped into four colors groups, from light tone grey/greenish, middle dark tone grey/greenish, very dark tone grey/greenish and dark/black, showing variable transitions between them (bioturbated, gradual and sharp contacts). From here we will refer to grey tone in substitution to grey/greenish.

As a general picture, light tone grey sediments are dominant, mainly registered and thicker in the lower/middle part of Core U1385D-7H-4 (interval A), and in the upper part of U1385D-7H-2 and the entire U1385D-7H-1 (interval M). Another thinner light interval is registered at the base of Core U1385D-7H-3 (interval E). In general these intervals show a relatively scarce trace fossils filled with light material.

At the opposite, dark/black intervals are scarce and thin, being located exclusively in the middle and upper parts of Core U1385D-7H-4 (intervals B and D). These intervals are characterized by dark trace fossils, which occasionally are also observed downward into the upper parts of the lighter intervals below (intervals A and C).

Middle and dark grey tone intervals are dominant in Cores U1385D-7H-2 and 3 (intervals F, G, H, I, J, K, and L), and are also registered in the upper part of Core U1385D-7H-4 (interval C). Middle grey tone intervals (intervals C, G, I, and lower K) mainly consist of a well developed light trace fossils assemblage on a mottled background. In the very dark tone grey intervals (intervals F, H, J and upper K) light and dark trace fossils are observed on a light/dark mottled background. Two intervals (intervals J and L) into the dark grey intervals show slightly differences in color, with the presence of greyish/blue/pink sediments.

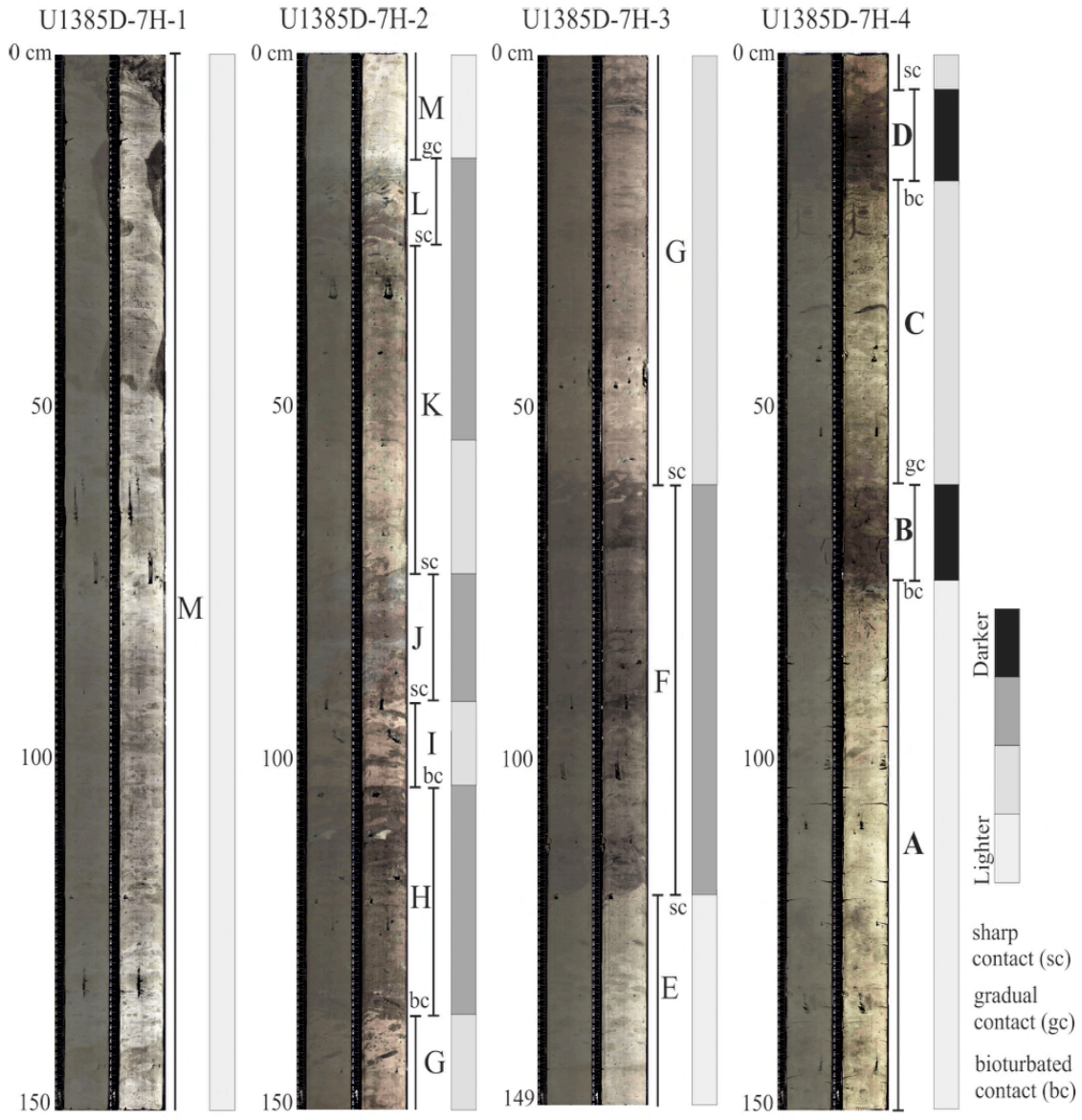

(Caption of the figure: next page)

(Previous page) **Figure VIII - 1.** Studied cores from 1385D-7H-1 to 1385D-7H-4, showing the recognized intervals A to M, as well as contacts and colour differentiation. Photographs before (left side) and after (right side) digital image treatment are represented for each core.

3.2. Ichnological analysis

Digital image treatment allows a clear differentiation between biodeformational structures and trace fossils (Dorador and Rodríguez-Tovar, 2014; Dorador et al., 2014a, b; Rodríguez-Tovar and Dorador, 2014, in press). Biodeformational structures, showing undifferentiated outlines and the absence of a defined geometry, which impede an ichnotaxonomical classification (see Uchman and Wetzel, 2011; Wetzel and Uchman, 2012), are registered as a mottled background, with color mixture and predominance of lighter or darker sediments related to the recognized intervals. Trace fossils show a variable degree of diffusiveness, from diffuse to discrete structures, as well as variable infilling material, from light to dark, being clearly distinguished from the host sediment based on their characteristic shape, although, sometimes, this differentiation is difficult.

3.2.1. Trace fossil assemblage

In general, a relatively diverse trace fossil assemblage was recognized, including structures filled with light and dark sediments (light and dark filled structures), consisting of *Alcyonidiopsys*, *Chondrites*, *Nereites*, *Planolites*, *Spirophyton*, *Thalassinoides*, *Thalassinoides*-like structures, and *Zoophycos* (Fig. VIII-2, VIII-3). Moreover, undifferentiated sinuous traces have been observed in interval L. Light infilling traces refer to those light traces slightly darker than the light host sediment. Light infilling *Planolites* and *Thalassinoides* are the dominant, near exclusive, ichnotaxa, whereas light *Nereites* are locally observed (Fig. VIII-2). Dark infilling traces can be produced into the middle and very dark tone grey intervals or into the dark/black sediments. In the dark trace fossil assemblage *Zoophycos* is dominant, *Planolites* and *Thalassinoides* are frequent, while *Alcyonidiopsis*, *Chondrites*, *Spirophyton*, and *Thalassinoides*-like structures are rare (Fig. VIII-3).

Figure VIII - 2. Light trace fossils and local dark *Zoophycos* from grey (light, middle and dark tone) intervals. (A) Diffuse dark *Zooophycos* (d*Zo*) from dark tone grey Interval K (U1385D-7H-2) on a well-developed mottled background. (B) Light *Thalassinoides* (l*Th*) and *Planolites*

(l*Pl*) from light tone grey Interval E (U1385D-7H-3). (C) Light *Thalassinoides* (l*Th*) and *Planolites* (l*Pl*), and dark *Zoophycos* (d*Zo*) from middle tone grey Interval C (U1385D-7H-4). (D) Light *Thalassinoides* (l*Th*) and *Planolites* (l*Pl*), and *Nereites* (*Ne*) from light tone grey Interval E (U1385D-7H-1).

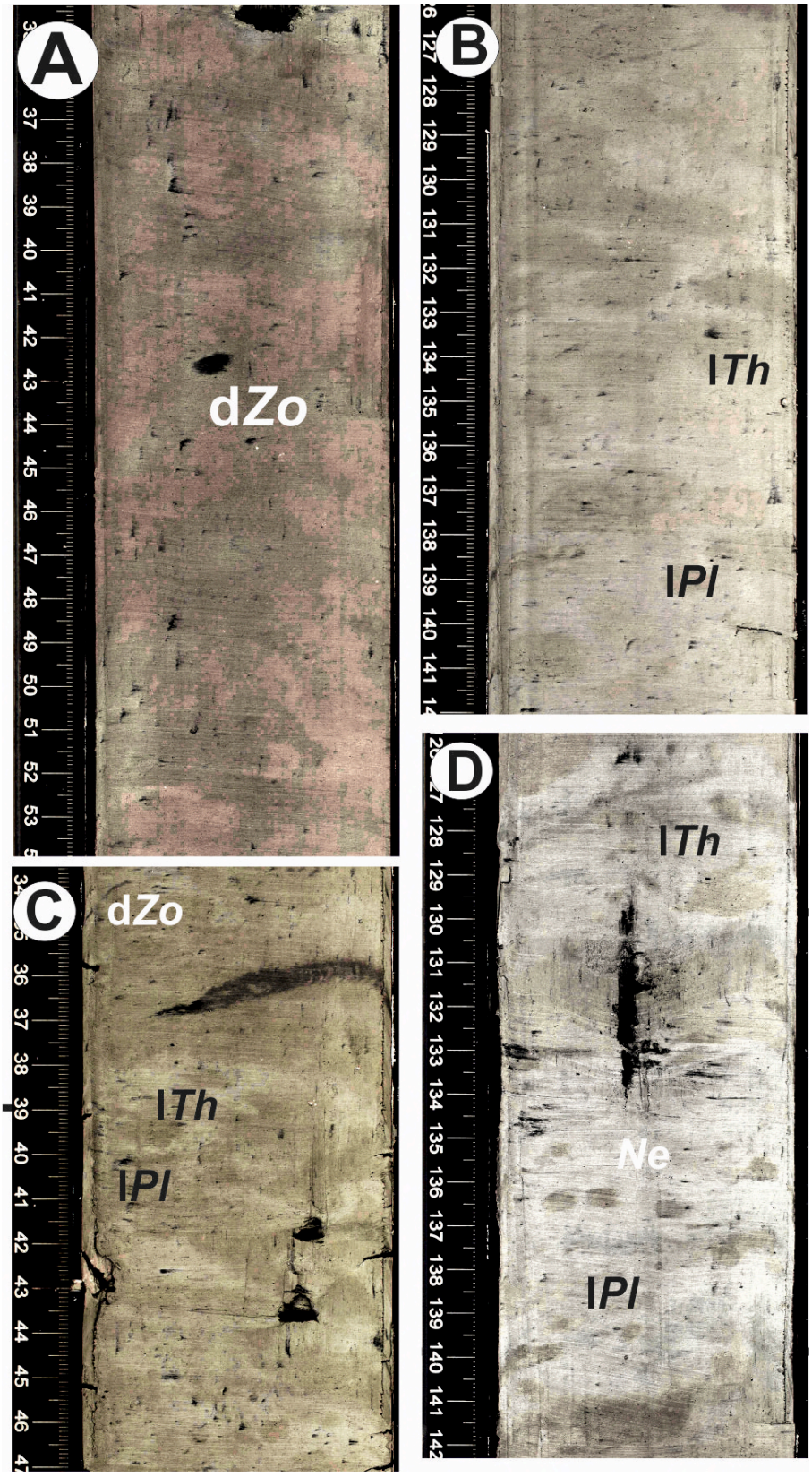

The trace fossil assemblage can be assigned to the *Zoophycos* ichnofacies, typical for deep-sea environments, as was previously proposed for Site U1385 (Rodríguez-Tovar and Dorador, 2014). As a general rule, dark trace fossils are registered as cross-cutting light ones. Into the dark trace fossil assemblage, usually *Chondrites* and *Zoophycos* are observed cross-cutting the rest of traces, such as *Planolites*, *Spirophyton* and *Thalassinoides*. A brief description of the differentiated ichnotaxa is as follow:

Alcyonidiopsis corresponds to a single elongate cylinder, slightly oblique, dark filled, 30 mm long and 6 mm wide, showing a pelloidal-like outline (see Uchman, 1999; Rodríguez-Tovar and Uchman, 2010 for interpretation).

Chondrites is generally observed as dense clusters of circular to elliptical spots, and short tubes, filled with dark sediment; occasionally branching. Mainly small forms (< 1.5 mm wide) are observed that could correspond to *C. intricatus* (Brogniart, 1823).

Nereites consists of small-medium size (2-5 mm diameter) circular to elliptical forms, with a dark-filled internal zone surrounded by a light filled envelope, observed as closed (paired) structures in horizontal planes.

Planolites occurs as unlined, unbranched, and mainly as circular to subcircular cylindrical tubular forms (4-7 mm in diameter, 5-2.5 mm in length). It is largely registered as horizontal or slightly oblique, filled with light or dark sediment, with a variable grade of diffusiveness. Fill is structureless, with different lithology from the host rock.

Spirophyton is registered as a single trace consisting of a central, axial, J-shaped shaft (around 8 cm high), with alternating horizontal structures (around 2-3 mm wide and 20 mm long) extending from the axial shaft. Spreite has not been observed. Similar to *Zoophycos*, it differs by the small size and shape of horizontal structures.

(Next page) **Figure VIII - 3.** Dark trace fossils from grey (middle and dark tone) and dark/black intervals. (A) Dark *Zoophycos* (d*Zo*) from the dark/black Interval D (U1385-7H-4). (B) Dark *Chondrites* (d*Ch*), *Planolites* (d*Pl*), *Spirophyton* (d*Sp*) and *Thalassinoides* (*dTh*) from the upper part of the middle grey tone Interval C transition to dark/black Interval D (U1385-7H-4). (C) Dark *Thalassinoides* (*dTh*) and dark *Zoophycos* (d*Zo*) from the upper part of dark grey tone Interval H to middle grey tone Interval I (U1385-7H-2) (D) Dark *Alcyonidiopsis* (d*Al*), *Chondrites* (d*Ch*), *Planolites* (d*Pl*), *Thalassinoides* (*dTh*) and *Zoophycos* (d*Zo*) from the upper part of the middle grey tone Interval G transition to dark grey tone Interval H (U1385-7H-2).

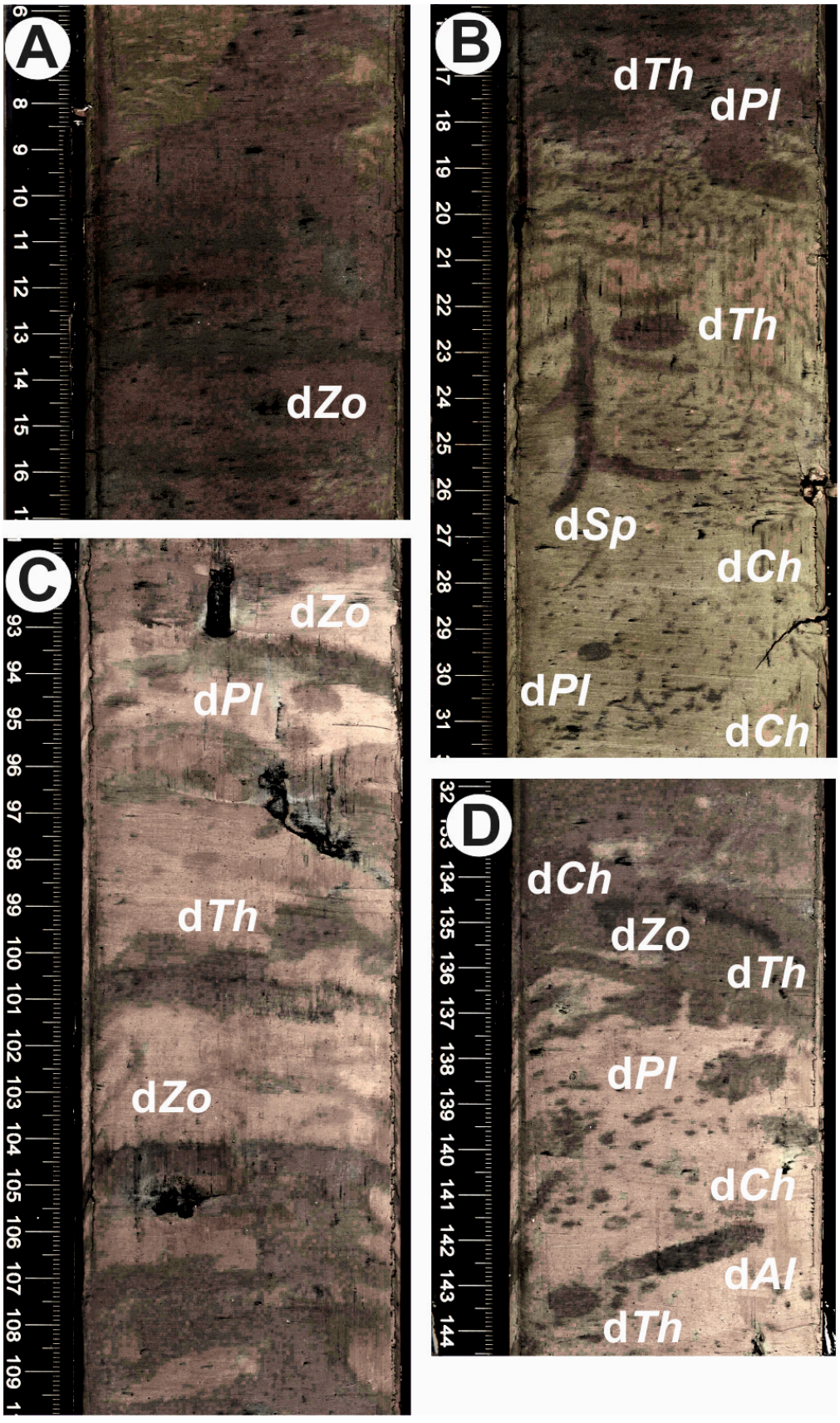
A
dZo
B
dTh
dPl
dTh
dSp
dCh
dPl
dCh
C
dZo
dPl
dTh
dZo
D
dCh
dZo
dTh
dPl
dCh
dAl
dTh

Thalassinoides is observed as large, oval spots, circular to subcircular (6-12 mm wide), together with straight or slightly winding, horizontal to oblique smooth cylinders (20-43 mm long), showing a variable grade of diffusiveness. Structures are filled with light or dark sediment. Occasionally, mainly light filled *Thalassinoides*, are observed in clusters of circular to elliptical spots, corresponding to variable cross-sections of branching burrow systems.

Thalassinoides-like structures occur locally as circular to subcircular sections, 6-12 mm wide, filled with dark sediment. Shape is similar to *Thalassinoides*, but showing a variably developed irregular wall, resembling *Ophiomorpha*.

Zoophycos is registered as repeated, more or less horizontal, spread structures (2-8 mm wide), consisting of alternating dark and light material. Variable degree of diffusiveness is observed, determining a more or less clear differentiation of the lamellae into the lamina. Frequently several horizontal traces (up to 6), probably belonging to a unique structure, are observed, evidencing a depth of penetration at least of 16 cm.

3.2.2. Distribution

The trace fossil assemblage shows clear variations along the differentiated intervals that can be related to the features (color) of the host sediment (Fig. VIII-4). Light trace fossils assemblage, consisting of *Planolites* and dominant *Thalassinoides*, is registered in most of the intervals, except, in the dark/black interval D, being dominant by light and middle grey tone intervals (A, C, E, G, I and M). However, in the light tone intervals (A and M), this light trace fossil assemblage is comparatively scarce, and the mottled background is less developed. The light trace fossil assemblage represents the bioturbation of tracemakers during deposition of the lighter host sediment. The dark trace fossil assemblage consist of frequent *Planolites* and *Thalassinoides*, associated to middle and very dark grey tone intervals, reflecting the mixture of phases of sedimentation corresponding to different color; bioturbation by shallowest and shallow tier organisms produce the observed mixture of colored sediment.

Figure VIII - 4. Distribution of light and dark trace fossils in the studied cores from Hole 1385D-7H-4 (bottom) to U1385D-7H-1 (top), according to the differentiated intervals A to M.

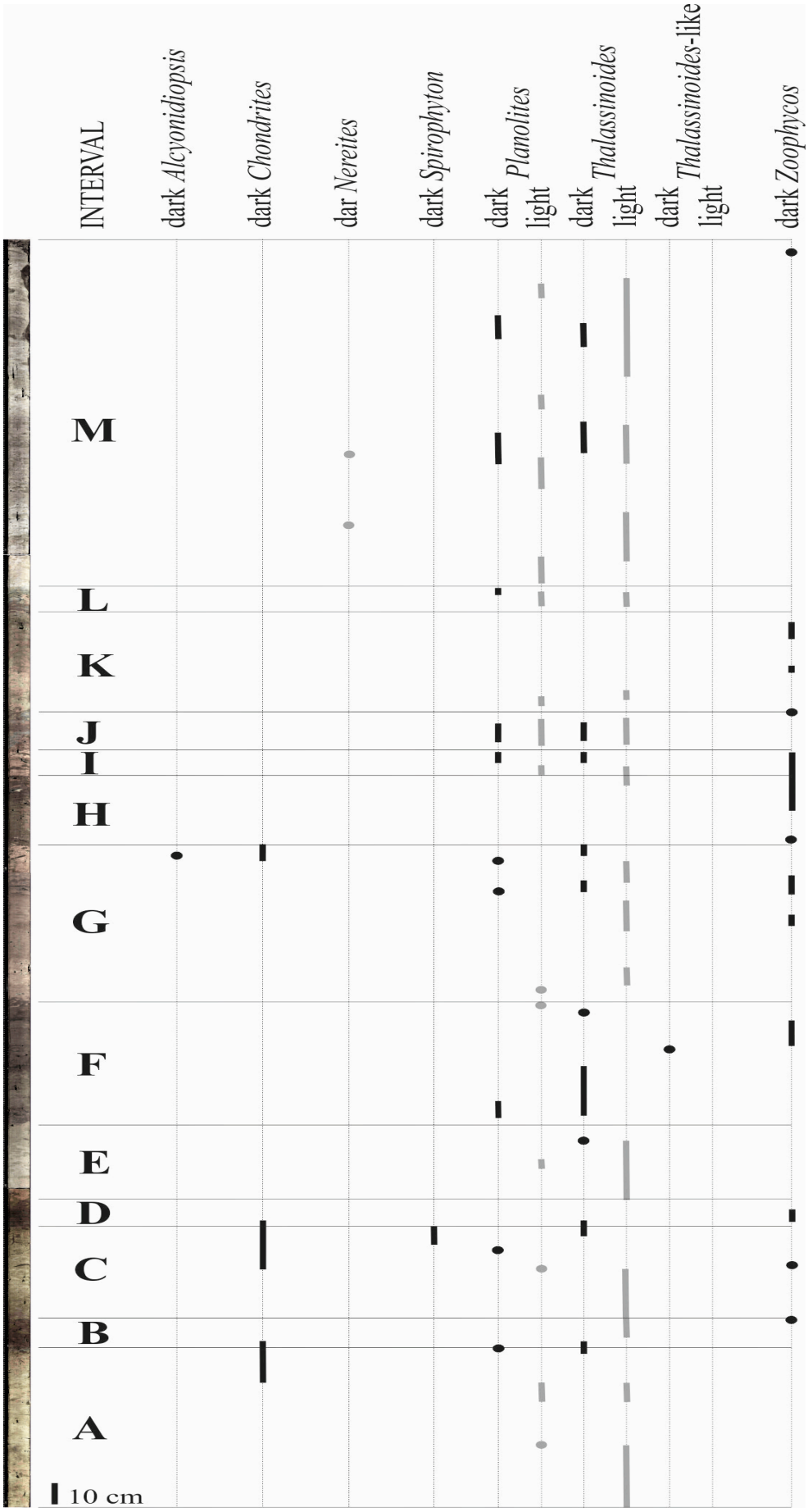
INTERVAL
dark Alcyonidiopsis
dark Chondrites
dar Nereites
dark Spirophyton
dark Planolites
light
dark Thalassinoides
light
dark Thalassinoides-like
light
dark Zoophycos
M
L
K
J
I
H
G
F
E
D
C
B
A
10 cm

These trace dark *Planolites* and *Thalassinoides* are also observed in intervals showing a more or less developed alternation, not mixture, of colored sediments, such as in interval M. Occasionally, this assemblage is also registered at the base of black/dark color sediment (intervals B and D), probably reflecting a progressive, gradual, change. *Zoophycos* is the dominant dark trace fossil, observed in middle and very dark grey intervals, as well as in the black/dark ones. This trace originated during deposition of darker sediments, probably revealing latter phases of bioturbation by the dark trace fossil community, after *Planolites* and *Thalassinoides* producer. *Chondrites* and *Spirophyton* are mainly related to the dark/black intervals (B and D), even are located downward in the lighter intervals below, and associated to the particular environmental conditions of these dark/black sediments.

3.3. Micropaleontological analysis

Benthic oxygen-isotopes values have been used to identify MIS 13 to 11 in the sediment cores. Based on the benthic oxygen isotope record glacial Termination V was recorded in IODP Site U1385 at around 55.70 crmcd. The previously described intervals A to M correspond to the final stage of MIS 13 (Intervals A, B and half of the C), MIS 12 (half of intervalC intervals D-L and the first 20 cm of interval M), and early MIS 11 (the rest of interval M) (Fig. VIII-5).

Analysis of the planktonic-benthic foraminifer ratio (Fig. VIII -5) reveals that planktonic microfauna is more abundant, in general, during interglacial conditions. However, during early glacial substage MIS 12b (and coinciding with interval G) elevated percentages of planktonic foraminifers were also recorded. These high planktonic/benthic values are mainly due to low benthic production, expressed both by concentration (Fig. VIII -5e) and accumulation rate (Fig. VIII -5f). Benthic accumulation rate (measured in number of tests per cm^2 and ky) is higher during the glacial stage, especially at the beginning and end of the stage. The extraordinarily high number of benthic foraminifers per mass of sediment (Fig. VIII -5e) during the glacial maximum MIS 12a, is probably due to low accumulation of other sedimentary components at this time (Fig. VIII -5). Export productivity (Pexp) is low during MIS 11 and much higher in MIS 12, especially in the early part of this stage, as well as during

the last part of MIS 13. In consequence, during the interglacial periods MIS 11 and 13 low Pexp at surface corresponds to low concentration of benthic foraminifers at the sea floor (Fig. VIII-5e,h). By contrast, high Pexp in MIS 12 is linked, in general, to higher benthic foraminifer production.

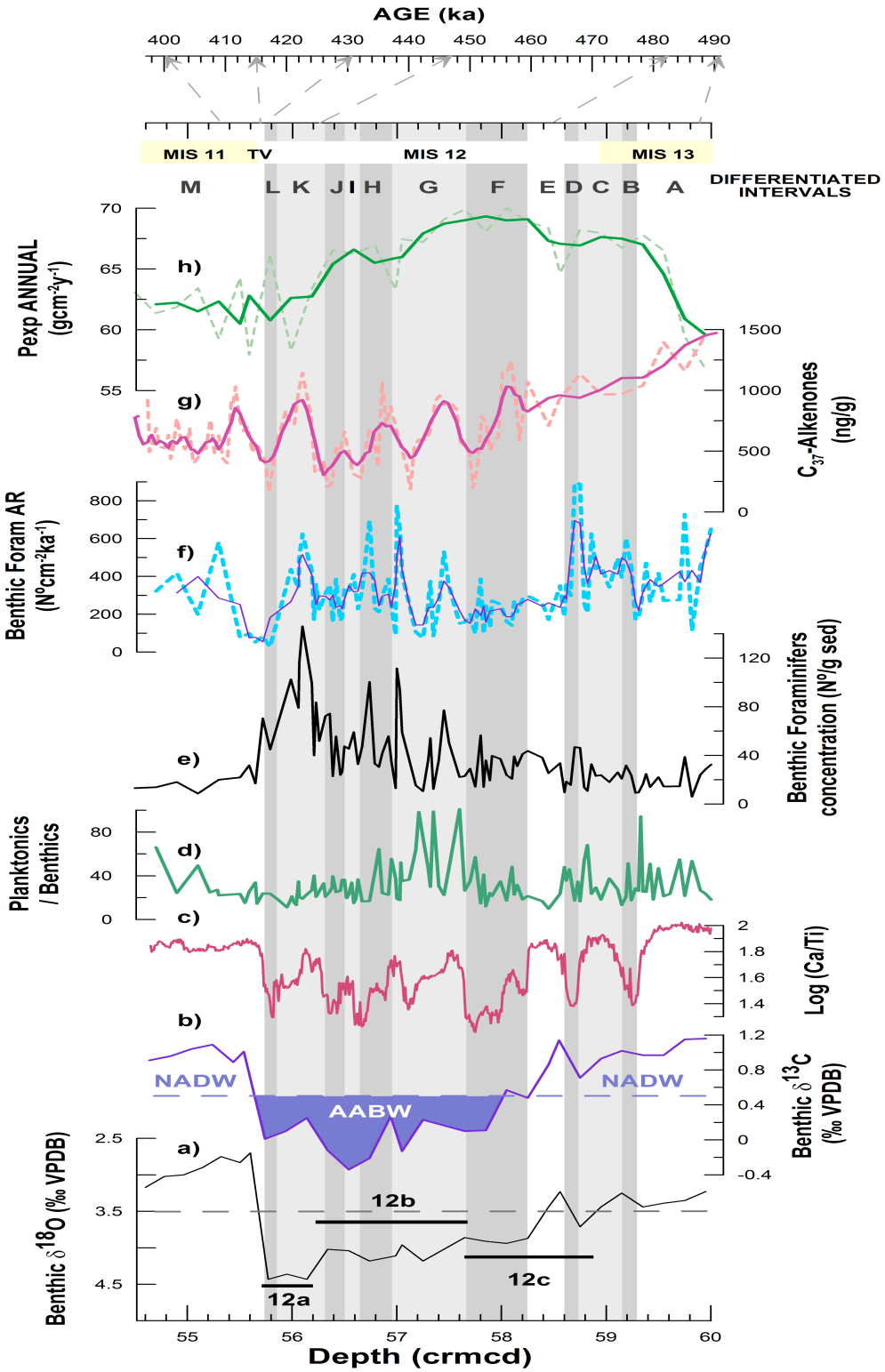

(Previous page) **Figure VIII - 5.** Stratigraphic and temporal distribution of the intervals A to M, differentiated according to color and trace fossil assemblage, and comparison with foraminifers records and other data from IODP-U1385. a) Benthic $\delta^{18}O$ (‰ VPDB) (Hodell et al., this issue); substages are named according to Railsback et al. (2015); horizontal dashed line shows the ice volume threshold separating stable and unstable climatic conditions (McManus et al., 1999). b) Benthic $\delta^{13}C$ record (‰ VPDB); filling indicates typical values for Antarctic Botom Water (AABW) according to Adkins et al. (2005) c) Log Ca/Ti record (Hodell et al., this issue). d) Planktonic / benthic foraminifers ratio. e) Benthic foraminifers concentration in number of tests per gram of dry sediment. f) Benthic foraminifers accumulation rate in number of tests per cm^2 and ky (dashed line) and 3-point running mean (solid). g) Total alkenone concentration (ng/g) of 37 carbon atoms (Maiorano et al., this issue; courtesy of T. Rodrigues) reflects the coccolithophore productivity (dashed line) and 5-point running mean (solid). h) Export productivity (dashed line) and 3-point running mean (solid). Glacial and interglacial stages are highlighted by horizontal bands. Vertical bands correspond to the differentiated intervals with lithological and ichnological features, with its facies color highlighted: light grey (in white) – middle dark grey – very dark/black. Control points linking depth (crmcd) to LR04-reconstructed age (Hodell et al., 2015) are represented by arrows.

4. INTERPRETATION AND DISCUSSION

4.1. Facies distribution and trace fossil composition

Major factors determining ichnological features (i.e., abundance, composition and diversity of trace fossil assemblages) in a deep-sea setting are food availability, bottom and pore-water oxygenation, substrate consistency, and rate of sedimentation (Wetzel, 1991; Uchman et al., 2008, 2013a, b; Rodríguez-Tovar et al., 2009a, b; Rodríguez-Tovar and Uchman, 2010; Uchman and Wetzel, 2011; Wetzel and Uchman, 2012; Rodríguez-Tovar and Reolid, 2013; Rodríguez-Tovar and Dorador, 2014). In the case study, the generalized mottled background, together with the observed trace fossil assemblage, reveals a deep-sea multi-tiered trace fossil community, interpreted as revealing predominance of well-oxygenated bottom and pore-waters, as well as abundance of food in the sediment for macrobenthic tracemaker community, as previously interpreted for Site U1385 (Rodríguez-Tovar and Dorador, 2014). In the generalized context of relatively good environmental conditions for the macrobenthic habitat, several changes can be interpreted, determining variations in facies and ichnological features.

Lighter sediments, as those represented by intervals A, E and M, are characterized by a relatively poorly developed mottled background together with light

Thalassinoides and *Planolites*. *Thalassinoides* and *Planolites*, as facies-crossing forms, are found in a great variety of marine environments, usually associated with oxygenated sediments. *Thalassinoides* is related to soft but cohesive sediments (see Fürsich, 1973; Ekdale et al., 1984; Ekdale, 1992; Schlirf, 2000), and *Planolites*, an actively filled burrow, is interpreted as a pascichnion in shallow tiers (see Pemberton and Frey, 1982; Keighley and Pickerill, 1995 for discussion). Thus, good environmental conditions (bottom and pore-water oxygenation, and food availability) can be interpreted, at least in the upper centimeters of the substrate, where shallowest and shallow tiers communities are developed. Variations in the relative abundance of light *Planolites* and *Thalassinoides*, as well as in the diffusiveness can correspond with the rate of deposition and the firmness. Presence of dark *Planolites* and *Thalassinoides*, together with the local record of *Nereites* at interval M could reveal fluctuations in the organic matter content probably associated with variations in the detrital input and in the surface export productivity as revealed by planktonic foraminifer-reconstructed Pexp (Fig. VIII-5h); the latter is interpreted as a shallow tier, pascichnia structure, in deep-marine, low energetic, oxygenated, environments (Uchman, 1995; Mángano et al., 2002; Wetzel, 2002; Löwemark et al., 2012), associated with increase food flux, feeding on microbes that occurs in high concentrations (Wetzel, 2002; Löwemark et al., 2012).

Dark/black sediments, as represented by intervals B and D, reveal significant changes in the environmental conditions. Presence of dark *Planolites* and *Thalassinoides* at the base of the intervals, and then *Zoophycos* and dominant *Chondrites* could be interpreted as a gradual deterioration of the environmental conditions, probably related to increase in the organic matter content and decreasing oxygenation more favorable for *Zoophycos* and *Chondrites* tracemakers. Both, *Zoophycos* and *Chondrites* are deep tier feeding structures. As general, *Zoophycos* producer has been related to variations in energy, sedimentation rate, food content, or bottom-water oxygenation; its relative independence of substrate features would allow for colonization of sediments with comparative low oxygenation, or even to collect food particles from the sea floor (e.g., Löwemark and Schäfer, 2003; Rodríguez-Tovar and Uchman, 2006, 2008). Several ethological models have been proposed of

Zoophycos tracemaker (see Löwemark and Werner, 2001; Leuschner et al. 2002; Bromley and Hanken, 2003, Löwemark and Schäfer, 2003; Löwemark and Grootes, 2004; Löwemark et al., 2004; Löwemark, 2015). *Chondrites* tracemaker is associated to poorly oxygenated bottom or pore waters, able to live in dysaerobic conditions, at the aerobic-anoxic interface, as a chemosymbiotic organism (Seilacher, 1990; Fu, 1991). Upwards in the dark/black intervals, a progressive return improvement can be envisaged by the presence of light structures (i.e., light *Thalassinoides*) in the upper part. The presence in the interval D of a well-developed dark trace fossil assemblage consisting of discrete structures, could be associated to a decrease in the sedimentation rate, increase in firmness and higher time of bioturbation, together with local concentration of food. This agrees with the record of delicate, complex, structures of *Spirophyton* and *Zoophycos*. *Spirophyton* has been interpreted, mainly for marine-margin deposits, as revealing an opportunistic strategy; formed rapidly after sudden influxes of organic material (Miller and Johnson, 1981; Miller, 1991, 2003; Bromley, 1996; Gaillard et al., 1999). The *Zoophycos* tracemaker is interpreted as bioturbating firmer, organic rich substrates with oxygen depleted pore waters (e.g., Rodríguez-Tovar and Uchman, 2004a, b; Rodríguez-Tovar and Dorador, 2014, and references therein). Distribution of *Zoophycos* has been related to Milankovicth orbital scale climatic changes, determining variations in the organic matter content and flux (Rodríguez-Tovar et al., 2011).

Middle and dark grey tone sediments, corresponding to intervals C, F, G, H, I, J, K, and L, reveal, in general, variable intermediate cases between dark/black sediments and the lighter ones. Both types of sediments consist of a well-developed mottled background in the first case with dominance of light color sediments while in the second a mixture between light and dark sediments is observed. In both cases *Planolites* and *Thalassinoides* are the most abundant traces, being light structures dominant in the first case while in dark grey tone sediments dark *Planolites* and *Thalassinoides* are also observed. Dark *Zoophycos* are also registered, especially in the dark grey tone intervals, but dark *Chondrites* are not observed. Middle and dark grey tone sediments could reflect a generalized good bottom and pore-water oxygen conditions and higher abundance in the organic matter content at the surface but also

in the first centimeters of the sediment, allowing bioturbation by shallowest, shallow and middle tiers tracemakers. When input of organic matter content (as indicated by Pexp) is maintained during a comparatively long time (Intervals F, or H to K), deep tier traces, i.e., *Zoophycos*, can be developed, probably reflecting a latter comparatively higher organic matter content and a slight decrease in oxygenation oxygenation related to the presence of the poorly ventilated and benthic $\delta^{13}C$-deplected Antarctic bottom water AABW (Adkins et al., 2005; Hoogakker et al., 2006) (Fig. VIII -5b).

4.2. Environmental conditions during MIS 13-11 and the macrobenthic and foraminiferal record

The benthic foraminifer concentration in the sediments and variations of the planktonic foraminifer assemblages suggest significant changes in surface water productivity and food supply to the sea floor occurring in the Portuguese margin during MIS 12 and 11 that could be correlated with the registered changes in facies and trace fossil assemblages (Fig. VIII -5). Similar changes occurred across the more recent Terminations IV, II and I (Grunert et al., 2015; Rodríguez-Tovar et al., 2015).

Benthic communities living at the sea floor are limited by the flux of organic carbon reaching the sea floor that, in turn, are a function of Pexp and oxygen content along the water column and interstitial waters within the sediments. Higher densities of benthic foraminifers in bottom sediments have been related to higher rates of organic carbon supply to the sea floor, both in the same Site U1385 (Grunert et al., this issue; Rodríguez-Tovar et al., this issue) and in other locations (Schmiedl et al., 1997; Wollenburg et al., 2004; Mojtahid et al., 2009).

A trend of increased productivity both primary, according to coccolithophores (NAR) and alkenones data (Maiorano et al., 2015), and secondary, according to planktonic foraminifer-reconstructed Pexp (Fig. VIII -5g-h), occurred during the final stage of MIS 13 coinciding with warm SST inferred from the Ca/Ti record in our site (Hodell et al., 2015). Low abundance of the coccolithophore *Florisphaera profunda* (Maiorano et al., 2015), suggests a less stratified upper water column. During MIS 11 Pexp was very low and both intervals coincided with the presence of light-color sediments as well as with the continuous presence of light *Planolites* and

Thalassinoides in the differentiated interval A and M (Fig. VIII-5). By contrast, during MIS 12 Pexp is higher, especially in the early part, but decreases towards the end of the stage. Benthic foraminifer accumulation rates do not follow this trend. This decoupling between Pexp, and benthic accumulation rates can be the result of the changing conditions of water column oxidation that are mainly reflected by the benthic $\delta^{13}C$ record. The high benthic $\delta^{13}C$ during MIS 11 and MIS13 reflects the high bottom water oxygenation during these interglacial periods. Higher bottom water ventilation tends to decrease the accumulation of organic matter in the sediments and therefore reduce food availability for the macrobenthic and microbenthic communities.

Microbenthic fauna proliferated during the glacial stage as reflected by the higher benthic foraminifer accumulation rates, which can reach values over 800 individuals/cm^2/ky. Values of Pexp were very low at the final part of MIS 13 and coincide with the presence of light-color sediments as well as by the continuous presence of light *Planolites* and *Thalassinoides* in the differentiated interval A (Fig. VIII-5), but afterwards the organic matter supply increased rapidly and maintained very high until Termination V, as indicated by darker sediments and the presence of *Zoophycos* and *Chondrites*. Similar enhanced fluxes of organic matter occurred also in the South Atlantic upwelling region during this glacial period (Schmiedl and Mackensen, 1997). This high organic carbon flux to the bottom, combined with adequate bottom water ventilation, allowed an eutrophic environment expressed by high benthic foraminifer accumulation rates. Nevertheless, high amounts of organic matter reaching the bottom could reduce the availability of oxygen and produce a subsequent impoverishment of the benthic habitat when bottom water ventilation is low. These conditions happened during short intervals along MIS 12 and in Termination V, and are registered by the micro benthos, as an increase in Export Productivity coupled with a decrease in benthic foraminifer accumulation rate (Fig. VIII-5). Macrobenthos also reveals the punctual pulse (increasing) in organic matter reaching the bottom, by the record of *Spirophyton* and *Zoophycos*, and the associated decrease in oxygen availability mainly revealed by the presence of *Chondrites*, observed in the intervals B and D (Fig. VIII-5). Differentiation of several intervals (A to L) during the ending of MIS 13 and the whole MIS 12, based on the trace fossil record

agree with the idea that tracemakers are more sensitive than foraminifers to depth variations in the redox boundary in near-surface sediments leading to the movement of trace-fossil tiers, as indicated by Baas et al. (1998) and also recently demonstrated by Rodríguez-Tovar et al. (this issue).

By contrast with MIS 12, lower benthic foraminifer accumulation rates during MIS11 indicate an oligotrophic environment at the bottom and are consistent with lower inputs of organic carbon inferred from total alkenone accumulation (Maiorano et al., 2015) and planktonic foraminifer Pexp, as well as with low NAR (Maiorano et al., 2015). This oligotrophic environment is characteristic of peak interglacial periods in this region, as studies on sediments ranging from MIS 6 to the Holocene show (Pailler and Bard, 2002). Oxygen consumption in deep sea waters during MIS 11 due to the weak organic carbon supply was low which, together with the presence of the more ventilated North Atlantic Deep Water (NADW) as can be inferred from the high values of benthic $\delta^{13}C$ (Fig. VIII-5b), resulted in higher oxygen content of bottom waters. This agrees with the lighter color of the sediments in the differentiated interval M, as well as by the continuous presence of light *Planolites* and *Thalassinoides*. This higher bottom-water oxygen concentration during the interglacial compared to the previous glacial maximum occurred on the Portuguese margin also during the last two climatic cycles (Hoogakker et al., 2015), and can be related to increased ventilation linked to a reorganization of ocean circulation after deglaciations (McManus et al., 2004). Oscillations in Pexp during this interglacial produced fluctuations of the organic matter content in the bottom, which is registered in the macrobenthos by the presence of dark *Planolites* and *Thalassinoides*, and the local record of *Nereites*. North Atlantic coccolithophore analyses allow envisaged a relationship between lighter color sediments and high coccolith content in the MIS 11 (Amore et al., 2012; Marino et al., 2014; Maiorano et al, 2015).

The low availability of organic matter for benthic macro and micro fauna along MIS 11 could evidence a possible stratification of the superficial water masses in the area, as indicated by higher percentage of the coccolithophore *Florisphaera profunda* compared with the previous interglacial (Maiorano et al., 2015), or be related to a reduced input of land-derived nutrients during the sea level highstand (Rodrigues et

al., 2011). Such possibility should be explored with the study of planktonic fauna and the evolution of the sea surface conditions for the same period in the same site.

In a few cases, trace fossil assemblage in sediments corresponding to MIS 12 and MIS 11 has been characterized. At the eastern Mediterranean Sea, and in relation with the ichnological response to late Quaternary sapropel formation, a detailed trace fossil analysis was conducted on two cores from the last 400 ka, involving at the base of MIS 11 (Löwemark et al., 2006). As a general pattern, the sediment in the two cores is characterized by mottled burrows, with few trace fossils of *Scolicia*, *Thalassinoides*, *Chondrites*, and *Trichichnus*, attributed to well-oxygenated and warm bottom waters in an oligotrophic environment typical for non-sapropel times (Löwemark et al., 2006). Recently, variability in trace fossil abundance and diversity associated to glacial-interglacial cycles, including MIS 11, was recognized in Late Quaternary sediment cores from the Artic Ocean; during interglacial periods the increase food flux, rather than changes in deep water circulation, is responsible of higher abundance and diversity (i.e., *Scolicia*, *Planolites* or *Nereites*), while in glacial interval characterized by extremely low food flux consist of impoverished ichnofauna dominated by *Trichichnus* and *Chondrites* (Löwemark et al., 2012).

Obtained results allow addressing interpretations on local (?) paleocenographic dynamics. Although higher resolution climatic records need to be carried out in this time period, benthic $\delta^{13}C$ data prove that the evolution of macrobenthic tracemaker community during MIS 12 and 11 responded to major changes in bottom water ventilation probably linked to variations in deep water thermohaline circulation, determining variations in oxygen and food availability.

During glacial MIS 12 a higher planktonic foraminifer-reconstructed Pexp from surface waters, together with reduced deep water formation in the North Atlantic probably resulted in higher accumulation rates of organic matter in the sea floor, favoring the developing of macrobenthic communities typically living in these environments, characterized by comparatively high food, and low oxygen availability. This was probably more intense at some particular time periods such as intervals B and D that may be linked to times of extremely poor bottom-water ventilation associated with cooling events at surface. In particular, dark intervals during MIS 12 show low

Ca/Ti ratios (figure VIII-5c) that are usually associated to cool stadials in the Portuguese margin (Hodell et al. 2013b, 2015). The low benthic $\delta^{13}C$ values during MIS 12, especially in the dark intervals, indicate low bottom water ventilation probably due to a higher influence of AABW during this time period. Low bottom water oxygenation favored the preservation of organic matter, increasing food availability for the benthic macrofauna, even though the flux of organic matter from the surface was low.

By contrast, intense North Atlantic deep water formation during MIS 11 (interval M) (Poirier and Billups, 2014), and probably late MIS 13 (interval A), together with lower export production at surface led to more oxygenated bottom waters in the Portuguese margin, determining a well-developed deep-sea tiered assemblage.

Near Termination V an extremely low sedimentation rate has been recognized based on the chronology elaborated for this site (Hodell et al. this issue). Around 30 ky are condensed in the lowermost 40 cm at the base of MIS 11 (bottom of interval M), with a more extreme condensation recorded in the first 5 cm at the base of interval.

5. CONCLUSIONS

The present study including facies characterization, ichnological composition and foraminifer analysis, allowed interpretation of deep-sea paleoenvironmental conditions during the transition MIS 13/12, MIS 12 and MIS 11.

A generalized context of well-oxygenated bottom and pore-waters, as well as abundance of food in the sediment for macrobenthic tracemaker community can be interpreted, with marked changes in these paleoenviromental factors as revealed by variations in composition and distribution of trace fossils according to the differentiated intervals A to M.

Benthic foraminifer concentration in the sediments and variations of the planktonic foraminifer assemblages suggest significant changes in surface productivity and food supply to the sea floor during MIS 12 and 11 that could be correlated with the registered changes in facies and ichnology.

The end of MIS 13 is characterized by very low values of annual export productivity, that together with the presence of light-color sediments and the continuous presence of light *Planolites* and *Thalassinoides* at interval A, reveals

relatively low organic carbon flux to the bottom and high oxygen conditions. These initial conditions were changed during development of MIS 12, showing the rapid increase in the organic matter supply and then remaining very high until Termination V, determining a eutrophic environment, as is revealed by high benthic foraminifer accumulation rates. This change and the associated reduced availability of oxygen, correlate with the record of *Spirophyton* and *Zoophycos*, and the presence of *Chondrites*, observed in the intervals B and D. During MIS 11 lower benthic foraminifer accumulation rates are registered suggesting an oligotrophic environment at the bottom, associated with lower inputs of organic carbon, and high oxygen content of bottom waters, in agreement with the lighter color of the sediments as well as the continuous presence of light *Planolites* and *Thalassinoides* at the interval M.

In conclusion, the evolution of macrobenthic tracemaker community during MIS 13 to 11 responded to major changes in bottom water ventilation probably linked to variations in North Atlantic deep-water thermohaline circulation.

Table VIII-1

Differentiated intervals with lithological and ichnological features.

Interval (thickness/location)	Facies color	Contacts	Background	Light Traces	Dark traces	Cross-cutting relationships
A (75 cm): from 150 to around 75 cm of U1385 7H4	Light tone grey	Bioturbated upper contact	Mottled background	Diffuse *Thalassinoides* (l*Th*) & *Planolites* (l*Pl*)	*Chondrites* (d*Ch*) from 89 to 75 cm	d*Ch* crosscutting l*Th* & l*Pl*
B (14 cm): from 75 to 61 cm of U1385 7H4	Dark/black	Gradual upper contacts	Mottled background	*Thalassinoides* from 67 to 61 cm	Dominant *Chondrites* (d*Ch*). *Planolites* (d*Pl*) & *Thalassinoides* (d*Th*) at the base	*dCh* crosscutting d*Th* & d*Pl*
C (43 cm): from 61 to 18 cm of U1385 7H4	Middle dark tone grey	Bioturbated upper contact	Mottled background	Diffuse *Thalassinoides* (l*Th*) and *Planolites* (l*Pl*)	Dominant *Chondrites* (d*Ch*), *Planolites* (d*Pl*), *Thalassinoides* (d*Th*), *Spirophyton* (d*Sp*) & *Zoophycos* (d*Zo*)	Dark traces crosscutting light traces & d*Ch* crosscutting d*Pl*, d*Tha* & d*Sp*
D (13 cm): from 18 to 5 cm of U1385 7H4	Dark/black	More or less shap upper contact			Dominant *Chondrites* (d*Ch*) & *Zoophycos* (d*Zo*). *Thalassinoides* (d*Th*) at the base	*dCh* crosscutting d*Th*
E (35 cm): from 5 cm of U1385D 7H4 to 119 cm of U1385 7H3	Light tone grey	Sharp upper contact, channel morphology	Mottled background, especially on top	Discrete, dominant *Thalassinoides* (l*Th*), and few *Planolites* (l*Pl*)		
F (58 cm): from 119 to 61 cm of U1385 7H3	Very dark tone grey, with increasing darker upward	Sharp upper contact	Mottled background	*Planolites* (l*Pl*), on top	*Planolites* (d*Pl*) &*Thalassinoides* (d*Th*), then *Zoophycos* (d*Zo*). Probable *Thalassinoides*-like (d*Th*-l)	d*Zo* cross-cutting d*Th* on top
G (74 cm): from 61 of U1385 7H3 to 137 cm of U1385 7H2	Middle dark tone grey, with a thick (56 cm) darker horizon at the middle part	Bioturbated upper contact	Mottled background at the lighter parts	*Thalassinoides* (l*Th*) and *Planolites* (l*Pl*) as exclusive in the lighter part, and also in the upper part of the darker horizon	Diffuse, abundant *Zoophycos* (d*Zo*), but also *Thalassinoides* (d*Th*-l), and probable *Planolites* (*dPl*) in the darker horizon *Alcyonidiopsis* (d*Al*), *Chondrites* (d*Ch*), *Planolites* (d*Pl*), *Thalassinoides* (d*Th*) & *Zoophycos* (d*Zo*) in the upper light interval, coming from the next dark interval	d*Zo* cross-cutting d*Th* *dCh* cross-cutting the rest of traces
H (33 cm): from 137 to 104 cm of U1385 7H2	Very dark tone grey	Bioturbated upper contact	Mottled background	Probable *Thalassinoides* (l*Th*) on top	Dominant, near exclusive, *Zoophycos* (d*Zo*)	
I (12 cm): from 104 to 92 cm of U1385 7H2	Middle dark tone grey	Sharp/bioturbated upper contact? Minor erosion?	Mottled background	*Planolites* (l*Pl*) & probable *Thalassinoides* (l*Th*)	*Planolites* (d*Pl*), *Thalassinoides* (d*Th*) & dominant, diffuse, *Zoophycos* (d*Zo*)	d*Zo* cross-cutting d*Pl* and d*Th*
J (18 cm): from 92 to 74 cm of U1385 7H2	Very dark greyish/blue/pink	Mixture of sediments Sharp/bioturbated upper contact?	Mottled background	*Thalassinoides* (l*Th*) & *Planolites* (l*Pl*)	Diffuse *Planolites* (d*Pl*) *Thalassinoides*,(d*Th*) and *Zoophycos* (d*Zo*)	d*Zo* cross-cutting d*Th*
K (47 cm): from 74 to 27 cm of U1385 7H2	Middle to very dark tone grey/pink	Darker color upward. Sharp upper contact?	Mottled background	Diffuse *Planolites* (l*Pl*) & *Thalassinoides* (l*Th*)	Diffuse *Zoophycos* (d*Zo*)	
L (12 cm): from 27 to 15 cm of U1385 7H2	Very dark greyish/blue/pink	Gradual contact to lighter colour & decreasing bioturbation	Mottled background	*Thalassinoides* (l*Th*) & *Planolites* (l*Pl*), sinuous traces	*Planolites* (d*Pl*), sinuous, bifurcate traces	
M (165 cm); from 15 cm of U1385D 7H2 to 0 of U1385D 7H1	Light tone grey with darker intercalation	Gradual alternations in color	Mottled background	Diffuse *Planolites* (l*Pl*), *Thalassinoides* (l*Th*) & local *Nereites* (l*Ne*)	Diffuse *Planolites* (d*Pl*) and *Thalassinoides* (d*Th*), probably *Zoophycos* (d*Zo*),	

CHAPTER IX

MILLENNIAL TIMESCALE CLIMATE VARIATIONS FROM MARINE ISOTOPE STAGE 13 TO 11

CHAPTER IX

MILLENNIAL TIMESCALE CLIMATE VARIATIONS FROM MARINE ISOTOPE STAGE 13 TO 11 (*)

* This Chapter is based on: **Martin-Garcia, G.M.**, Sierro, F.J., Abrantes, F., Flores, J.A., Hodell, D.A. Orbital and millennial timescale climate variability in the Northeast Atlantic across marine isotope stages MIS 21 to 13: Insights from Site IODP-U1385. *Climate of the past* (In preparation)

ABSTRACT

Using a high-resolution record of planktonic foraminifer assemblages from IODP Site U1385 (37º34.285´N, 10º7.562´W; 2585 m depth) covering a time interval between 530 and 395 ka, we reconstruct millennial scale climate variation from MIS 13 to MIS 11 in the Portuguese margin. Sea surface temperature (SST) in the region registered abrupt climate changes similar to Dansgaard-Oeschger events of Late Pleistocene. Seven sequences (Bond cycles) of progressive cooling happened in the North Atlantic during MIS 13 – 12 that were registered in the Iberian margin by both microfaunal assemblages, Ca/Ti ratios and planktonic and benthic isotopic records. These cycles can be correlated with the synthetic record of Greenland climate and, during MIS 12, the final cooling of each sequence coincided with a Heinrich-type event recorded in high latitude North Atlantic. We demonstrate that the cooling events in the mid-latitude ocean are related with the advance of the Arctic front, via reduction of deep-water formation in the North Atlantic and associated weakening of thermohaline circulation.

1. INTRODUCTION

During most recent glacial cycles, a series of high-frequency (~1.5-3 ky) temperature swings termed Dansgaard–Oeschger (D–O) oscillations registered in the Greenland ice-core records (Dansgaard et al., 1993; Grootes et al., 1993); the final event coincided with the Younger Dryas (e.g. Bond et al., 1992). These stadial-interstadial oscillations appear to be grouped in sequences – known as “Bond cycles” (e.g., Broecker et al., 1990) – of progressively cooler events, the end of each sequence marked by the deepest cooling. Most of Heinrich events happened at the end of the colder phase of a Bond cycle and were followed by warming to almost interglacial temperatures (e.g. Bond et al., 1992; Wright and Flower, 2002).

Numerous studies spanning late Pleistocene have related millennial-scale cooling events in the North Atlantic with changes in the strength of the thermohaline circulation (e.g., Hemming, 2004; Alley, 2007). Reduced formation of deep water in the North Atlantic would result in stratification of the water column, reduction of thermohaline circulation rate and spread of cold water across the whole North

Atlantic. Such deep cooling events have been recorded as far south as the Portuguese margin since the last glacial cycle (Bard et al., 2000) back to MIS 21 (Martin-Garcia et al., 2015). During the last glacial, these events of general cooling in the Northern Hemisphere were related with warming in Antarctica (Blunier et al., 1998) by the so-called see-saw mechanism (Stocker and Johnsen, 2003), which consisted in changes in the interhemispheric heat transport in response to changes in the strength of the meridional overturning circulation. However, the occurrence of this mechanism during older glacials is not well supported by data.

The southwester Iberian margin has been proven a key area to reconstruct millennial-scale climate variability. Nick Shackleton was the first in highlighting the global importance of a specific area of this margin (Shackleton et al., 2000) that has ever since been known as the Shackleton site. This area has a high sedimentation rate, which allows a high-resolution climatic record. Its depth allows the presence of the same bottom water masses than in the rest of the basin. In consequence, sediments in this area generate climatic signals that can be consistently used to interpret basin-wide climatic phenomena. Studies for the most recent climatic cycles proved that the benthic $d^{18}O$ variation was similar to the Antarctic temperature record, while the planktonic isotopic signal and reconstructed sea surface temperature (SST) resembled the Greenland ice $d^{18}O$ (Shackleton et al., 2000; Martrat et al., 2007; Skinner et al., 2007). Hodell et al. (2011b) demonstrated that sediment composition in this region records orbital-scale and millennial-scale climate variation - the ratio Ca/Ti reflecting the proportion between carbonate and detrital components of the sediment. Cold events are recorded by low values ratios, either because of a decrease in biogenic production (Hodell et al., 2013b), or because increased detrital sedimentation (Lebreiro et al., 2009).

In this work we study planktonic foraminifer assemblages, Ca/Ti record, as well as both benthic and planktonic isotopes from sediment core IODP-U1385, in the Shackleton site, to reconstruct millennial-scale climate variations from MIS 13 to MIS 11 and their relation with global climate. This time period was selected for three reasons. (1) Although numerous climatic records show that MIS 12 was the most severe glacial during the Pleistocene (e.g. Helmke and Bauch, 2003; Lisiecki and

Raymo, 2005), sea surface temperature (SST) recorded in site U1385 was not so cold as that recorded during previous glacials in the same site (Martin-Garcia et al.,2015). (2) MIS 13 was an unusual interglacial in which interglacial optimum happened at the end of the stage, not at the beginning both in terms of minimum global ice volume (Lisiecki and Raymo, 2005) and SST recorded in site U1385 (Martin-Garcia et al.,2015). (3) The published time scale for U1385 (Hodell et al., 2015) identified a hiatus in the vicinity of Termination V whose spanning age needed to be constrained.

2. MATERIAL AND METHODS

Sediments at Site U1385 define a single lithological unit dominated by calcareous muds and calcareous clays, with varying proportions of biogenic carbonate (23% - 39%) and terrigenous sediment. Pelagic sedimentation prevails during interglacials, while terrigenous input is enhanced during glacials (Stow et al., 2012). Cyclic variations in physical properties and color reflect changes in the proportion of biogenic carbonate and detrital material delivered to the site (Hodell el al., 2013b).

This study covers a section from the secondary splice U1385D/E (Hodell et al., 2013a) between 54.60 and 67.53 crmcd (corrected revised meters composite depth) (MIS 11 - MIS 13). For the intervals 54.60–55.14 and 60.65–67.53 crmcd, sampling was performed every 20 cm, and for the interval in between samples were taken at an average 4.4 cm separation. The estimated average resolution for each interval down core is 1.3, 0.33 and 1.02 ky.

A total of 164 samples (1 cm-thick) were freeze-dried, weighed and washed over a 63 μm mesh sieve. The >63 μm residue was dried, weighed and sieved again to separate and weigh the >150 mm fraction. Counts of detrital particles were conducted on the whole of this fraction, while counts of planktonic foraminifer taxa and planktonic foraminifer fragments were conducted on representative subsamples of this sediment fraction containing at least 300 whole specimens. Twenty-eight species and ten morphotypes (Kennett and Srinivasan, 1983) of planktonic foraminifers have been identified (Appendix I) and their relative abundances, calculated.

Sea surface temperature (SST) values (annual, winter, summer and seasonality) were reconstructed according to the Artificial Neural Network (ANN) method, using a

back propagation neural network system (Malmgren et al., 2001) to compare our fossil planktonic foraminifers assemblages with a set of 10 neural networks of the MARGO North Atlantic database, as described in Kucera et al. (2005). The average value of the 10 different SST reconstructions obtained for each component (winter, summer, annual and seasonality) was used as the final SST reconstruction.

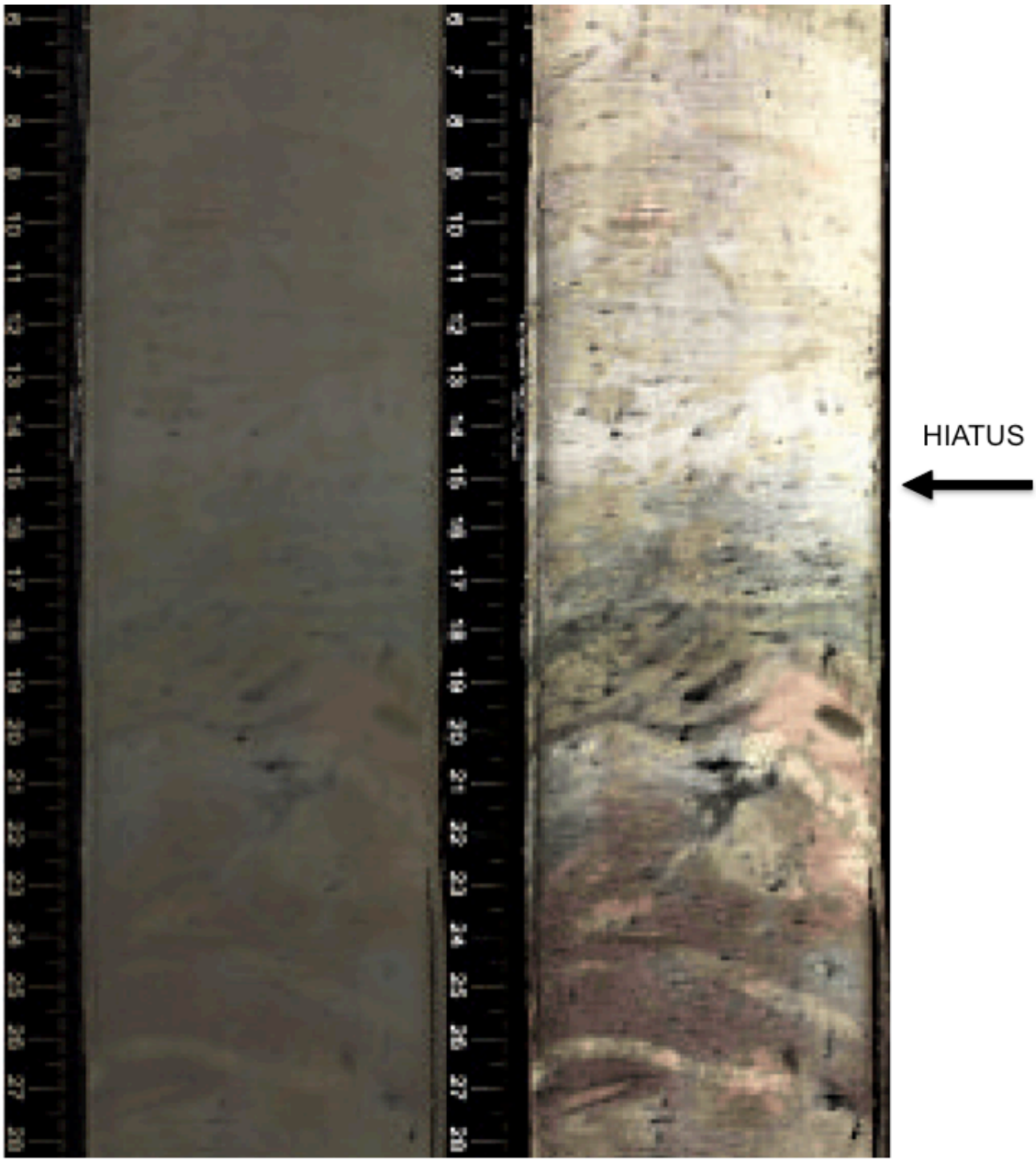

Figure IX - 1. Detail from core U1385D-7H-2, showing the identified hiatus. The right part of the panel was obtained after digital image treatment. The photography has been taken from Rodríguez-Tovar et al. (2015).

2.1. Age model

The age model of the studied section is modified from the one firstly published for site U1385 (Hodell et al., 2015) using the correlation of the benthic oxygen isotope record to the global benthic LR04 isotope stack (Lisiecki and Raymo, 2005). Due to the low resolution of the LR04 stack, additional control points were added based on the North Atlantic core U1308 (Table IX-I). A hiatus has been identified at 55.73 crmcd (Fig. IX-1), marked by a sharp transition in colour and other sediment characteristic that have been used to define distinct intervals (Rodriguez-Tovar et al., 2015). The age of the sediments limiting the hiatus was calculated using the extrapolated sedimentation rate. According to our age model this hiatus spans from 431.09 to 400.87 ka. As a consequence, Termination V and the interglacial optimum of MIS 11 were not recorded in site U1385, according to both isotopic (Fig. IX-2), and microfaunal data (Fig. IX-3). At the base of the hiatus, the percentage of the polar species Neogloboquadrina pachyderma sin was 4.22%, very low when compared to values recorded in the same site during previous Terminations (8-49%) by Martin-Garcia et al. (2015). Above the hiatus, the recorded percentages of warm microfauna were lower than during interglacial MIS 13 optimum (Fig. IX-3d) and much lower than the ~45% recorded in nearby site MD01-2443 during MIS 11 optimum (de Abreu et al., 2005).

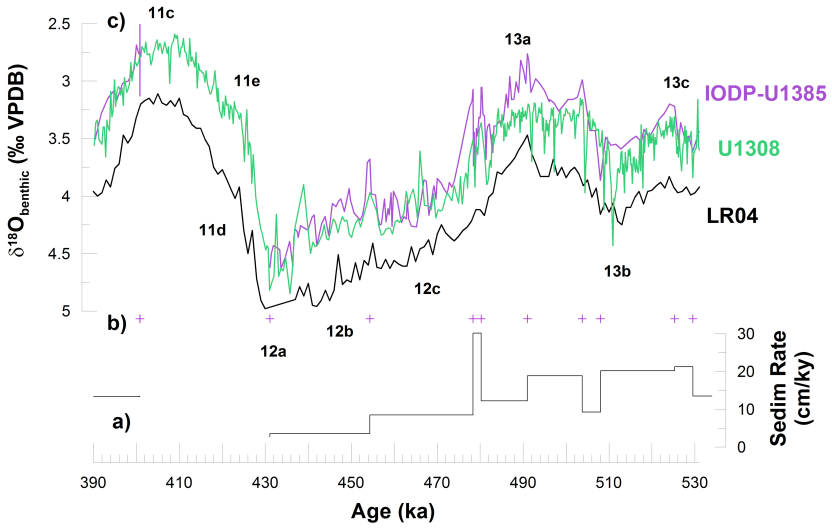

Figure IX - 2. Age model for the study interval. (a) Sedimentation rate in cmky^{-1}. (b) Age control points (see Table I for details). (c) Benthic $\delta^{18}O$ profiles from LR-04 stack (Lisiecki and Raymo, 2005) in black, from IODP-U1308 (Hodell et al., 2008) in green, and from IODP-U1385 (Hodell et al., 2015) in purple. Substages are named according to Railsback et al. (2015).

3. RESULTS

3.1. Planktonic foraminifer results

This study focuses on species and assemblages that can be directly used to monitor past changes in climatic conditions in North Atlantic surface water.

The polar species *Neogloboquadrina pachyderma* sinistral (Nps), with a temperature tolerance range between –1 and 8 ºC and an optimum of 2 ºC (Tolderlund and Bé, 1971), has been extensively used within the North Atlantic as a proxy for climate cooling (Ruddiman et al., 1986; Bond et al., 1993) and to monitor southward penetrations of very cold water masses of polar origin, usually associated to iceberg discharges and/or migrations of the arctic front (AF) (eg., Bond et al., 1992; Cayre et al., 1999; de Abreu et al., 2003; Eynaud et al., 2009; Martin-Garcia et al., 2015). At present, this species is absent from plankton tows (Ottens, 1991) and surface sediments (Pflaumann et al., 2003) (Simmax database) collected in the study area. In our study interval this species keeps low relative abundance during both the glacial and interglacial stages. Percentages are higher than 15 % only at 454.68 ka and at 504.52 ka, in coincidence with a decrease in benthic $\delta^{18}O$ of 0.5‰ (Fig. IX-3b).

Turborotalita quinqueloba (Tq) has a temperature tolerance range of 4.6ºC – 10.8ºC, with an optimum of 12ºC and is usually associated to high phytoplankton productivity (Bé, 1977; Johannessen et al., 1994). High percentages of this species are found south of Iceland (Pujol, 1980), and its maximal abundance has been recognized as associated with the Arctic front (Cayre et al., 1999; Wright and Flower, 2002). In the study interval, higher percentages of Tq occur during the glacial substage MIS 13b and its subsequent deglaciation, as well as during MIS 12c (Fig. IX-3c).

Globigerinoides ruber (Gr), which can tolerate a wide range of salinity (Bijma et al., 1990), is a surface dweller of subtropical waters (ENACWst) transported by the AzC to the Northeast Atlantic (eg. Ottens, 1991) and it is present today in the site during non-upwelling months (Salgueiro et al., 2008). Highest percentages of this species occurred

during the transition MIS 13b/a and during interglacial MIS 13a, coinciding with the presence of the pink morphotype (Fig. IX-3d-e).

The group of warm surface water species as defined in the Gulf Stream area (Vautravers et al., 2004) includes only tropical mixed layer dwelling species. Most of these species live in the warm waters south of the Azores front (AzF) and have been used to trace the influence of tropical waters originating in the Gulf Stream on the region after the upwelling season (Vautravers and Shackleton, 2006). Postupwelling conditions in Site U1385 remained relatively warm during most of the study interval. Interglacial MIS 13 was the richest in tropical species; maximum percentages of this assemblage occurred during the early phases of ice sheets growth during MIS 13c and 13a, as well as during the deglaciation of substage MIS 13b (Fig. IX-3d).

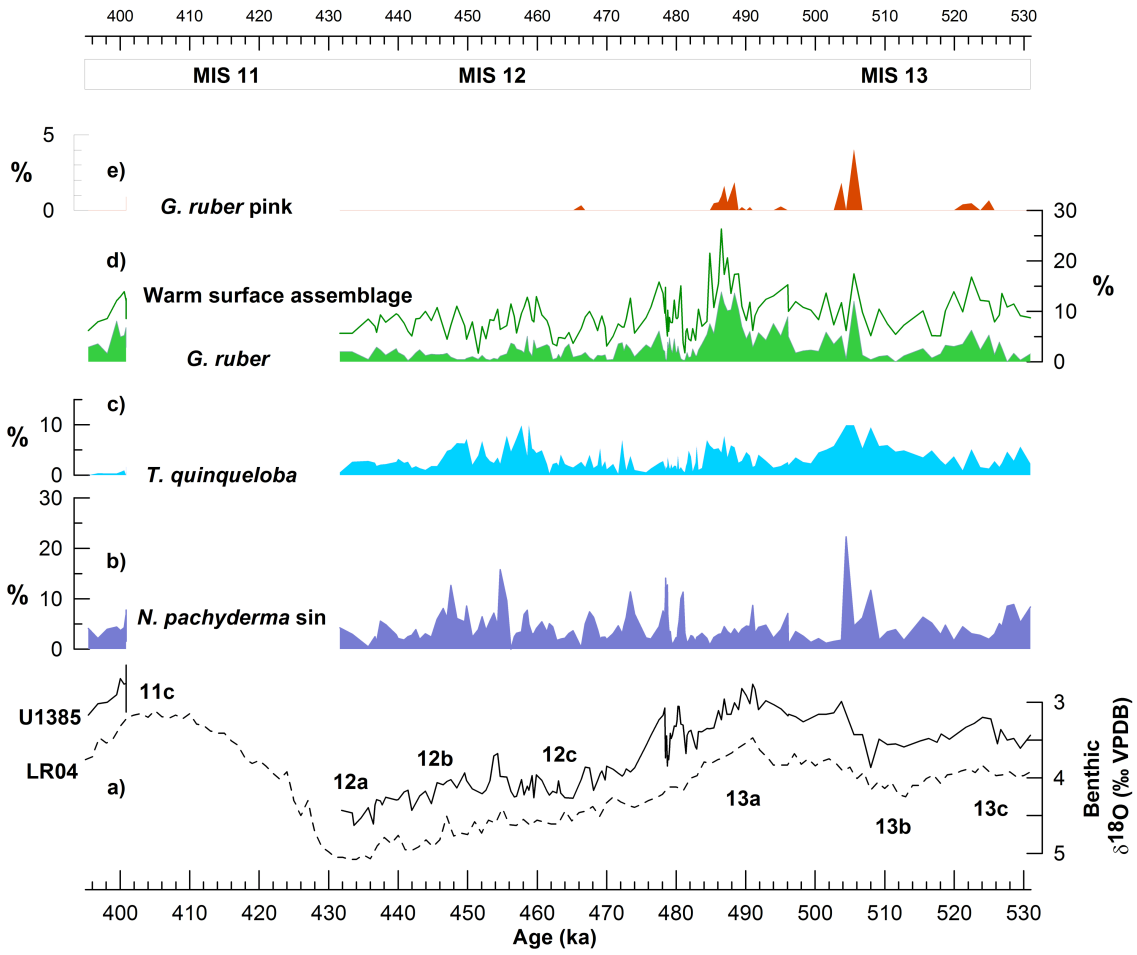

Figure IX - 3. Microfaunal results from IODP-U1385. (a) Benthic $\delta^{18}O$ profile: LR-04 stack (Lisiecki and Raymo, 2005) in dashed line, and record from U1385 (Hodell et al., 2015); substages are named according to Railsback et al. (2015). (b) Relative abundance of the planktonic foraminifer polar species *Neogloboquadrina pachyderma* sinistral. (c) Percentage of *Turborotalita quinqueloba*. (d) Relative abundance of the subtropical species *Globigerinoides ruber* (solid green) and of the warm surface assemblage as defined by Vautravers et al. (2004). (e) Relative abundance of the pink morphotype of *G. ruber*.

3.2. Sea Surface Temperature reconstruction

We estimated SST based on faunal counts for the coldest (winter) and warmest months.

At present, at this site, the warmest month is August (20.5 ºC; Locarnini et al., 2010) coinciding with the end of the upwelling. However, except for MIS 11, SST in the area was generally colder during the study interval (16.4 ºC annual mean) than at present (18 ºC; Locarnini et al., 2010). Summer temperature (SSTsum) oscillated between 14.6 and 21.9 ºC while winter values (SSTw) varied between 9 and 17.9 ºC (Fig. IX-4c). Seasonality was generally higher during MIS 12 than during both interglacials, and higher values coincided with lower SSTw, that is, cooling events on site U1385 occurred mainly in winter, while in the warmest season surface water kept similar values during the study interval (Fig. IX-4c-d). The widest SST oscillations (~8 ºC), as well as the coldest events (SSTw ~9 ºC), happened during the MIS 13b/a transition and during the glacial inception at the end of MIS 13a. During the rest of interglacial MIS 13 and during MIS 11 SST fluctuations were of lesser amplitude (≤ 3 ºC), and during MIS 12 SST oscillations displayed intermediate width (≤ 5.5 ºC). This difference in the amplitude of temperature oscillations was also recorded by the Ca/Ti ratio (Hodell et al., 2015) (Fig. IX-4b).

3.3. Ice Rafted Debris (IRD)

Considerable amount of detrital material particles was recorded ~455 ka. The rest of the study interval show none or very low amount of IRD (Fig. IX-5f).

Several IRD events have been recorded in the Portuguese margin during MIS 12 (Voelker et al., 2010; Rodrigues et al., 2011), but at northern locations than site U1385.

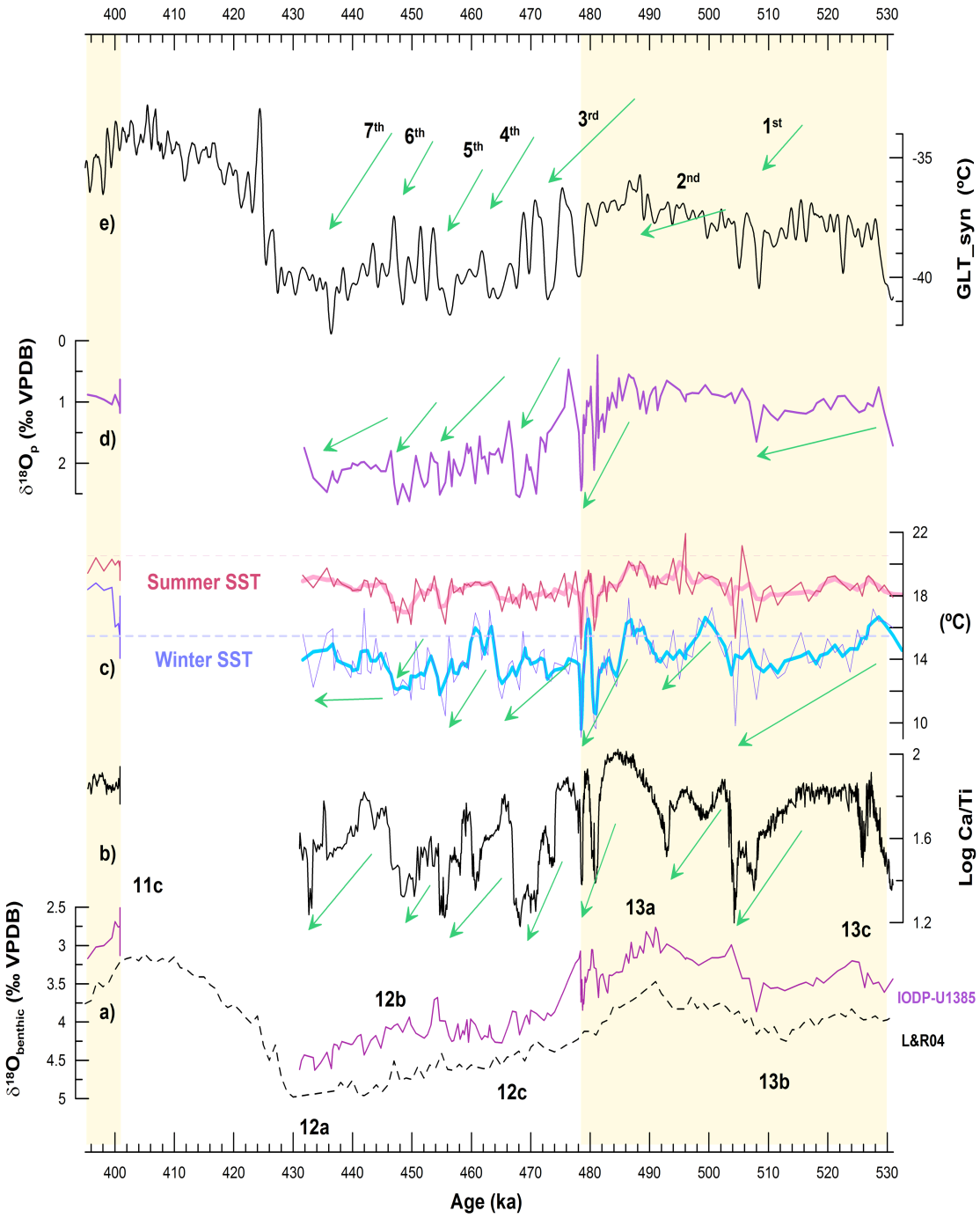

Figure IX - 4. Comparison between SST records from site IODP-U1385 and the synthetic record of Greenland climate. (a) Benthic $\delta^{18}O$ profile: LR-04 stack (Lisiecki and Raymo, 2005) in dashed line, and record from U1385 (Hodell et al., 2015). Substages are named according to Railsback et al. (2015). (b) Log Ca/Ti record (Hodell et al., 2015). (c) Foraminifer-based SST and 3-points moving average: winter (blue) and summer (red). Present-day values (Locarnini et al., 2010) are represented in dashed line. (d) Planktonic $\delta^{18}O$ profile (Hodell et al., 2015). (e) Reconstructed temperature for Greenland (Barker et al., 2011). Yellow bands mark interglacial stages and green arrows represent observed climatic sequences.

4. DISCUSSION

4.1. Climate variations during interglacial MIS 13

Numerous studies have established that in the mid-latitude North Atlantic, stadials coinciding with Heinrich events were more pronounced than other stadial and interstadial temperature fluctuations (e.g., Bond et al. 1999; Labeyrie, 2000). On the SW Iberian margin, SST was lower by 10ºC during HEs of MIS 3 (Vautravers and Shackleton, 2006) and Heinrich-type (H-type) events of MIS 20 and MIS 15b (Martin-Garcia et al., 2015). It has been noticed that most of Heinrich events occurred at the end of the so-called Bond cycles. These cycles were first identified during MIS 3-2 as a series of high-frequency SST variations superimposed on HE 1-6, five of which occurred at the end of the cool phase of a Bond cycle and were followed by warming to almost interglacial temperatures (Bond et al., 1992); such cycles have also been identified in the northern Atlantic during MIS 16 (Wright and Flower, 2002; Hodell et al., 2008) and in mid-latitude site U1313 also during MIS 12 (Naafs et al., 2014).

Main cooling events recorded in site U1385 during both MIS 13 and MIS 12 occurred at the end of similar progressive cooling sequences (fig. IX-4) and were marked by ≥4.7% of the polar species Nps, usually accompanied by an increase in the percentage of the subpolar Tq. All of them were followed by sharp and steep SST rise (Fig. IX-5d-e), which is a characteristic of H-type events recorded in the same site from MIS 21 to MIS 14 (Martin-Garcia et al., 2015) and also of HE occurring at the end of Bond cycles (Bond et al., 1992).

As interglacial MIS 13 progressed, North Atlantic surface water experienced sharp and high-amplitude temperature oscillations, especially during winter (Fig. IX-4c). Two cooling sequences were recorded by both SSTw and Ca/Ti, while SSTsum and planktonic $\delta^{18}O$ recorded only the first one, which lasted more and reached colder SST (Fig. IX-4b-d) than the second one. This first Bond cycle coincided with the ice-building phase between MIS 13c-b, according to benthic $\delta^{18}O$, and finished with the most pronounced cooling event recorded in Site U1385 during the whole study interval, which occurred linked to the deglaciation of MIS 13b (Fig. IX-4c). This event consisted in two deep cooling phases separated by a short-lived, high-amplitude warming. The first phase, ~508 ka, coincided with a sharp and important decrease in $\delta^{13}C$ and an

increase of 0.4‰ in benthic $\delta^{18}O$ while the subsequent warming, which reached the highest SST values of MIS 13, coincided with a steep increase of $\delta^{13}C$, (Fig. IX-5a,b,d). As deglaciation completed, according to benthic $\delta^{18}O$ data, the fresh water input reduced the NADW formation, which resulted in the advection of subpolar water to the mid-latitude ocean and the occurrence o a new, colder event ~504.4 ka. It was during this second cooling phase that highest percentages of the polar species Nps for the whole study interval were recorded in site U1385 (Fig. IX-5e).

Nearby site MD03-2699 also registered the advection of subpolar water during a prolonged interval at the time (Rodrigues et al., 2011), coinciding with the first cooling cycle recorded in site U1385

The second climate sequence was better registered by SSTw and Ca/Ti than by other records (Fig. IX-4). It coincided with the final phase of reduction of ice volume of MIS 13a. Towards the end of this phase the NADW formation weakened slightly, according to the light decrease of $\delta^{13}C$ (Fig. IX-5b), which resulted in the advection of subpolar water to the Iberian margin in winter, while postupwelling conditions remained relatively warm. The final cooling of this cycle was not the coldest one, but it was marked by a peak in Nps and coincided with a IRD layer recorded in the mid-latitude site U1313 (Stein et al., 2009) (Fig. IX-5d,g)

When comparing with the reconstructed temperature for Greenland (GLTsyn) (Barker et al., 2011), a similar pattern to that recorded in site U1385 can be identified, with high-amplitude Dansgaard-Oeschger oscillations that define a cooling sequence towards MIS 13b, and progressively warmer temperatures toward MIS 13a. During this prolonged warming a shorter, less marked cooling cycle was recorded previous to the pronounced warming of the interglacial optimum that also initiates the following cycle (Fig. IX-4e).

Figure IX - 5. (a) Benthic $\delta^{18}O$ profile: LR-04 stack (Lisiecki and Raymo, 2005) in dashed line, and record from U1385 (Hodell et al., 2015). Substages are named according to Railsback et al. (2015). (b) Benthic $\delta^{13}C$ from U1385 (Hodell et al., 2015); filling indicates typical values for Antarctic Bottom Water (AABW) according to Adkins et al. (2005). (c) Log Ca/Ti from U1385 (Hodell et al., 2015). (d) Winter SST; filling represents average value for the studied period. (e) Relative abundance of the polar species *Neogloboquadrina pachyderma* sinistral

(Nps) (blue) and percentage of the addition of Nps + *Turborotalita quinqueloba* (pink). (f) IRD recorded in site U1385. (g) Bulk benthic δ ^{18}O from site U1308 (crimsom) marking H-type events (Hodell et al., 2008). (h) Reconstructed temperature for Greenland (Barker et al., 2011). Green bands mark the final cooling event of each Bond cycle.

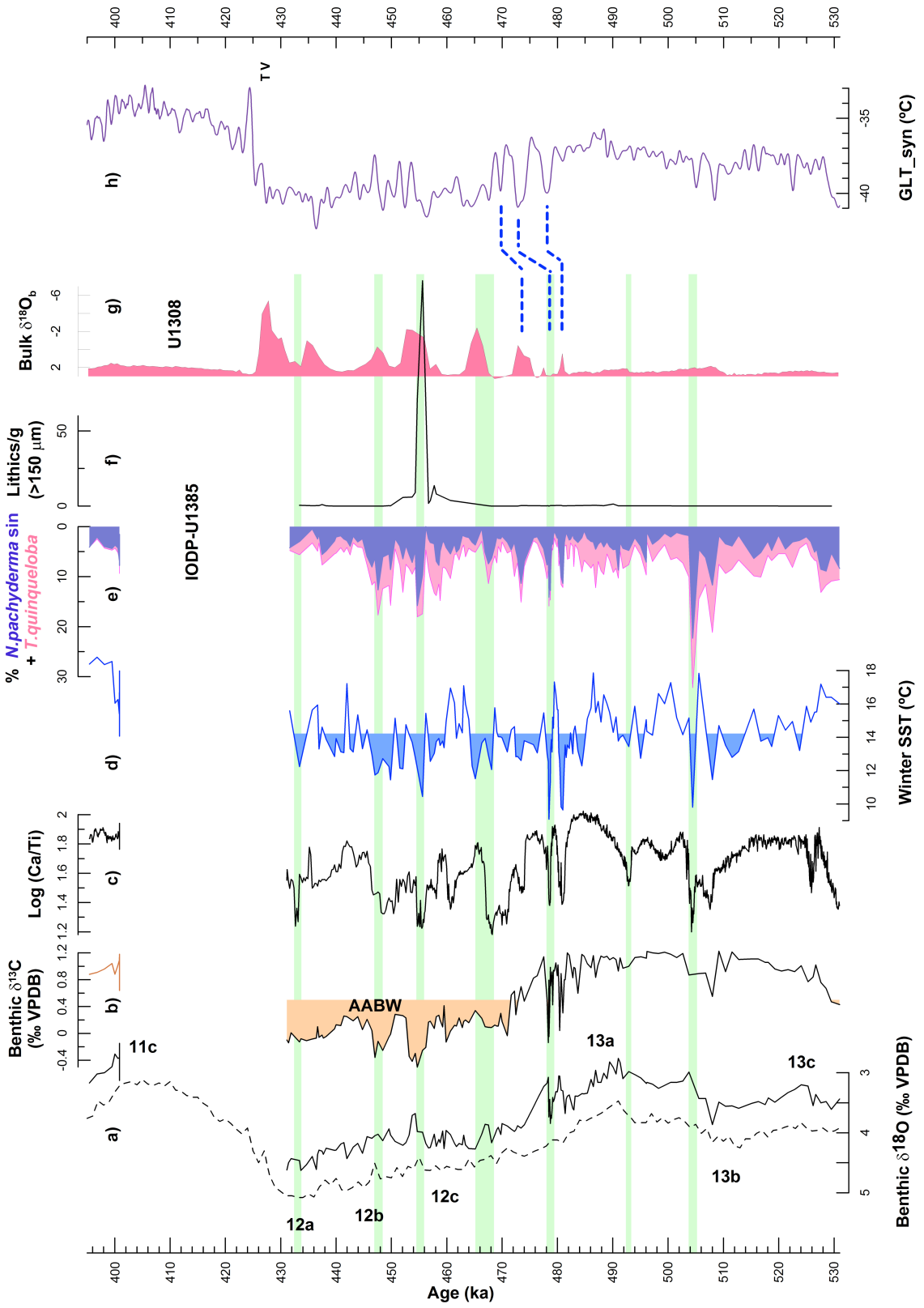

4.2. Glacial inception and climate variations during MIS 12

Millennial climate variability during MIS 12 shows the occurrence of five sequences of progressive cooling, sequences 3nd to 7th in figure 5, that again share many similarities with Bond cycles. Each sequence is characterized by more intense cooling events towards its end, culminating with a major cooling (Fig. IX-5d), and is followed by a warming episode. The five identified climate sequences coincided with five vaguely recorded stages of gradual increase in benthic $\delta^{18}O$ that was interrupted, or decreased, towards the end of each sequence. This expression in the benthic $\delta^{18}O$ record points to a relationship between these climate sequences and stages of ice volume increase during the glaciation of MIS 12.

The first sequence started with a pronounced warming event that occurred at glacial inception of MIS 12 as illustrated by the onset of increasing benthic $\delta^{18}O$ values. Winter and summer SST in site U1385 margin were among the highest during the studied period. This warming event was also recorded by the highest Ca/Ti values during the whole interval (Fig. IX-4a-c). Cooling at site U1385 only started ~3 ky after the glacial inception. By contrast, at higher latitudes of the NW Atlantic the onset of glaciation is recorded by an abrupt drop in SST from 12 to 3 ºC (Alonso-Garcia et al. 2011). This suggests a marked thermal gradient between the northern and middle latitudes or the northwest and northeast regions of the Atlantic when ice sheets started to expand and is similar to the scenario described for more recent glacial cycles (Barker et al., 2015). This seems to point to a rapid southeast-wards migration of the Arctic Front at glacial inception, displacing the influence of the warmer waters of the North Atlantic current to more eastern or southeastern positions, especially the southwester margins of Europe.

Three ky after the glacial inception, SST at the Portuguese margin started to gradually drop to culminate the first climate sequence of this glacial with two pronounced cooling events separated by a warming episode, which is recorded in site U1385 by SST, planktonic $\delta^{18}O$ and Ca/Ti (Fig. IX-6c-e). The initial part of this sequence, during the early stage of ice sheets growth, characterized by still relatively intense NADW formation and vigorous AMOC as recorded by the relatively high benthonic $\delta^{13}C$ values (Fig. IX-5b,d). This suggests that during the glacial inception, when as the AF

advanced southeastwards, the area of formation of NADW also migrated towards the east or southeast and remained active even after the ice volume had reached fully glacial levels (Fig. IX-5a-b). This would have diverted the NAC eastwards but allowed the arrival of warm water to the northern ocean, where the continuous supply of water vapour would have helped in the building of ice sheets. Only at ~481 and ~478.5 ka, coinciding with the final cooling events of the sequence, two very short and abrupt decreases in benthic $\delta^{13}C$ were recorded (Fig. IX-6), signalling abrupt and brief interruptions of the AMOC and reduced NADW at site U1385. These two cooling events were characterized by the first two marked drops in the benthicδ $\delta^{18}O$ record, which could be related to events of ice-sheet retreat or to higher influence of the ^{18}O-depleted Antarctic bottom Water (AABW) in site U1385 during these episodes. This would be in line with the evolution of the AF proposed by Barker et al. (2015) for more recent glacials, in which a gradual cooling pushed the southward migration of the front until a threshold point, after which an abrupt shift even southwards occurred with associated stadial conditions.

Although the percentage of Nps was lower during these two events than during the cooling at ~504.4, SST was colder (Fig. IX-5d-e). This apparent contradiction could be related with the occurrence of cooling during the glacial inception or during the interglacial, and be in line with the generally lower SST recorded off

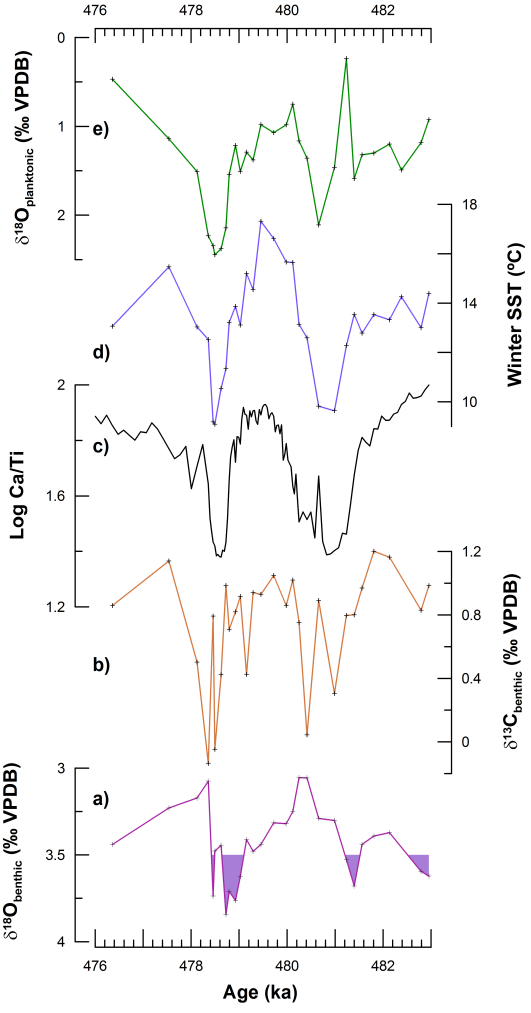

Figure IX - 6. MIS 12 glacial inception. (a) Benthic $\delta^{18}O$ profile. (b) Benthic $\delta^{13}C$ (c) Log Ca/Ti. (d) Winter SST. (e) Planktonic $\delta^{18}O$.

Iberia during glacials in comparison to interglacials (e.g.: Martrat et al., 2007; Rodrigues et al., 2011; Martin-Garcia et al., 2015).

The combined relative abundance of the polar species Nps and the subpolar Tq during MIS 12 (Fig. IX-5e) suggest that the AF was distant from the site for the whole period. Variation of this assemblage also reveals less influence of water of subpolar origin during glacial MIS 12 than during MIS 13b/a, although SST was generally colder during MIS 12 than during both interglacials, especially in winter months. Contrary to this, site U1313 recorded sequences of increasingly colder SST towards the glacial maximum, the three last stadials coinciding with a H-type event (Naafs et al., 2014). This suggests that the AF during MIS 12 acquired a southwest-northeast position and a west-east thermal gradient developed in the North Atlantic during MIS 12b-a, as well as the pre-existing north-south one.

The four cooling sequences similar to Bond cycles that occurred after the glacial inception, were registered by different amplitude changes both in Ca/Ti, SSTw and planktonic $\delta^{18}O$ records, and can be correlated to those in the GLT synthetic record of Barker et al. (2011) (Fig. IX-4). The first of these sequences (sequence 4^{th} in Fig.IX-4) coincided with a period of rapid growing of ice sheets after the glacial inception and ended with a sharp and pronounced increase of ^{18}O-depleted bottom water mass. During this cycle the NADW formation decreased rapidly, producing the surface advection to the mid-latitude ocean of subpolar water, cold and rich in Nps; in the bottom the weakened AMOC allowed the arrival of AABW to site U1385 (Fig. IX-5a-b,d-e). The last, more pronounced cooling of this sequence coincided with a HE recorded in the northern site U1308 (Hodell et al., 2008) as well as in the mid-latitude site U1313 (Stein et al., 2009) (fig. IX-5d,g-h).

The following cycle (sequence 5^{th} in Fig. IX-4) began with a pronounced warming that reached interglacial values, as is typical in Bond cycles (Bond et al., 1992), and was formed by four progressively colder climate oscillations, culminating with the greatest SST drop (5ºC) of MIS 12 and the only H-type event recorded in the site for the study period (Fig. IX-5d,f). This pattern was similar to that observed in other North Atlantic sites for several HE occurring during MIS 3 (Bond and Lotti, 1995). The increase in percentage of Nps recorded during this event in our site was not very great,

considering the high amount of IRD recorded (Fig. IX-5e-f). IRD layers were also recorded during this event in the subpolar site U1308 (Hodell et al., 2008) and also in the mid-latitude site U1313 (Stein et al., 2009) (Fig. IX-5g-h). A sharp decrease of the AMOC was recorded by a reduction of 0.77‰ in $\delta^{13}C$ from site U1385 (Fig. IX-5b).

Sequence 6th was the shortest and generally coldest of the studied interval (Fig. IX-4). Initial SSTw was much colder than present-day value, but the final cooling was milder than those of preceding sequences. In terms of bottom circulation this climate sequence characterized by two episodes of rapid weakening of the NADW formation that occurred at the transition from sequence 5th to 6th and towards the end of this cycle. These two episodes were recorded by the lowest values of benthic $\delta^{13}C$ throughout MIS 13 and 12, which can be related to larger influence of AABW in site U1385 (Fig. IX-5a-b). The last of these two episodes was registered at nearby site MD03-2699 by the advection of subpolar water during the last and prolonged cooling of this cycle (Rodrigues et al., 2011) that coincided also with a HE recorded in site U1308 (Hodell et al., 2008) (Fig. IX-5g).

The last sequence of this glacial coincided with the last stage of ice sheets growth towards the glacial maximum (Fig. IX-4) and was characterized by lower variability and lesser cooling. Planktic $\delta^{18}O$ and SSTsum show the less variability. SST registered an increasing trend toward the glacial maximum, but again a cooling event marked the end of the sequence and was registered by low SSTw and Ca/Ti. During this prolonged and gradual increase of ice volume a weakening of the NADW seems to have occurred, as reflected by the gradual lowering of the benthic $\delta^{13}C$, however no abrupt disruptions were observed (Fig. IX-5b). The last part of this sequence coincided with a HE recorded in the northern site U1308 (Hodell et al., 2008).

In a similar way to what has been recorded in more recent glacial cycles (Margari et al., 2014), climate oscillations during MIS 12 were of wider amplitude during the expansion of ice sheets; by contrast, the reduction of climate variability when approaching glacial maximum led to a more stable glacial state that culminated into one of the most extremely pronounced Quaternary glaciations that was MIS 12 (e.g. Helmke and Bauch, 2003; Lisiecki and Raymo, 2005). Generally cold climate with very cold and dry winters happened over Iberia during MIS 12, according to pollen records

from the same site (Sánchez-Goñi et al., 2016), which were similar to those observed in the region during other periods of large ice volume like MIS 2, MIS 4 and MIS 6.4 (Fletcher et al., 2010; Margari et al., 2014).

Major cooling events recorded in site U1385 during MIS 13 and MIS 12 can be correlated with stadials in GLTsyn (Barker et al., 2011) (Fig. IX-5d,h) - the possible lags due to the different chronological framework of both records - and, with exceptions, also with high values of temperature reconstructions from Antarctica (Jouzel et al., 2007). This suggests that the see-saw mechanism (Stocker and Johnsen, 2003; Schmittner and Galbraith, 2008), by which disruptions in the AMOC caused by iceberg discharges into the North Atlantic led to cooling in the Northern Hemisphere and warming in Antarctica since MIS 6 (Blunier et al., 1998; Hemming, 2004; Margari et al., 2010), was also a characteristic feature during MIS 13 and MIS 12. This interpretation is supported by the coincidence of cooling events with steep decreases and/or low values of $\delta^{13}C$ recorded in U1385 (Fig. IX-5b,d).

4.3. Climate variations during MIS 11c

The short interval of MIS 11c recorded in site U1385 was characterized by very stable climate with warm winters (Fig. IX-4c) and especially, very low seasonality, in line with the low eccentricity and reduced precession at the time (Laskar et al., 2004). These climatic conditions led to the weakening of the regional upwelling system registered in site U1385 at the time (Rodríguez-Tovar et al., 2015). In the Iberian Peninsula, warm winters and increased humidity allowed the rapid expansion of vegetation, mainly Mediterranean forest (Tzedakis et al., 2009; Sánchez Goñi et al., 2016).

During this interval, SST variations recorded in our site are very similar to the pattern observed in the GLTsyn record (Barker et al., 2011), in line with the strong climate connection between low and high latitudes noticed between different North Atlantic locations across MIS 11 (Helmke et al., 2008).

4.4. Variation of the influence of subtropical waters on Site U1385

Variations in the warm surface-water assemblage (Fig. IX-7d) show that at the northern edge of the subtropical area, post-upwelling conditions remained relatively warm during most of the study interval, and especially warm during the early stage of ice sheets growth. This suggests an increasing influence of tropical water via reinforcement of the AzC, at least on the post-upwelling season, during the intervals of ice sheets growth. Such warm conditions could be the consequence of subtropical warming, by a similar mechanism to that proposed for more recent isotope stages when heat was stored in the subtropical region as a consequence of the reduction of the AMOC and the subsequent cooling of high latitudes (Rühlemann et al., 1999; Huls and Zahn, 2000). Warm surface assemblage variations are almost symmetrical to those of benthic $\delta^{18}O$ (Fig. IX-7a,d), which points toward a connection between the presence of subtropical fauna in mid-latitude North Atlantic and the ice sheet volume. Southward migrations of the Arctic front probably related to a change in the region of formation of NADW towards a more eastern or southern location promoted the continuous flow of the NAC and AzC towards the southwestern European margin while intense cooling prevailed in the NW Atlantic.

This scenario was very evident during the climatic optimum of interglacial MIS 13a, when warmest SST occurred ~3 ky after the minimum ice volume and coincided with the new expansion of ice sheets, according to the benthic $\delta^{18}O$ record. Maximal values of summer boreal energy (Huybers, 2006) happening during this climatic optimum produced the warmest interstadial in the North Hemisphere during both MIS 13 and 12 and kept the polar ocean free of ice, allowing the northward migration of the subtropical gyre and the increase of subtropical species in the mid-latitude North Atlantic.

During the transition MIS 12b/a ice sheet growth was not accompanied by the southward migration of the subtropical gyre, as no relevant decrease in surface warm microfauna is recorded. The most probable explanation is that the AMOC, although weakened, remained active and thus no further disturbance of North Atlantic surface circulation was produced during the glacial maximum, at least in the eastern North

Atlantic. This interpretation is corroborated by values of $\delta^{13}C$ at the time, which were ~0.5 ‰ higher than during other intervals of MIS 12 (Fig. IX-7b-d).

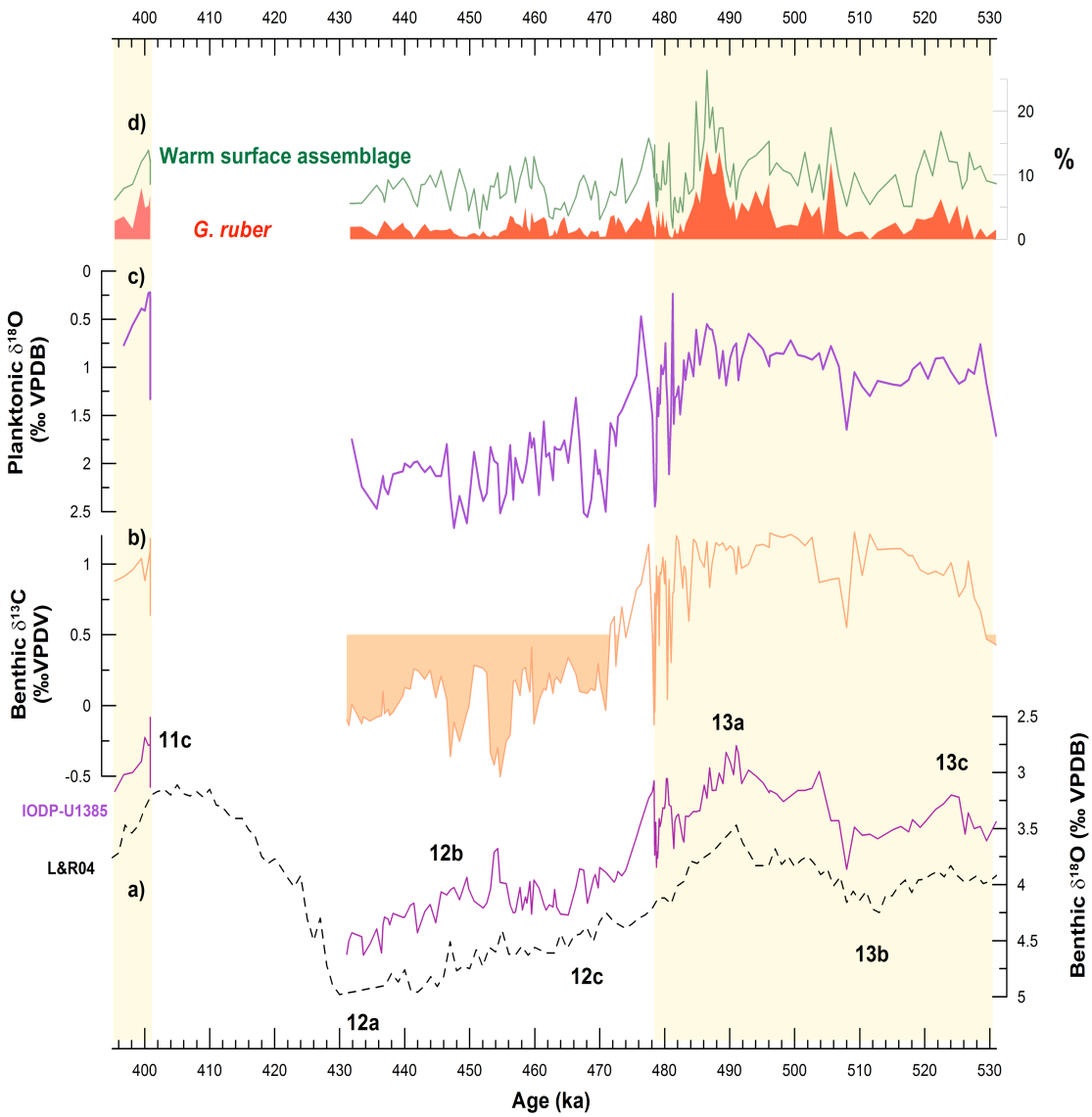

Figure IX - 7. (a) Benthic $\delta^{18}O$ profile: LR-04 stack (Lisiecki and Raymo, 2005) in dashed line, and record from U1385 (Hodell et al., 2015). Substages are named according to Railsback et al. (2015). (b) Benthic $\delta^{13}C$ from U1385 (Hodell et al., 2015); filling indicates typical values for Antarctic Bottom Water (AABW) according to Adkins et al. (2005). (c) Planktonic $\delta^{18}O$ profile (Hodell et al., 2015) (d) Relative abundance of the subtropical species *Globigerinoides ruber* (solid red) and of the warm surface assemblage as defined by Vautravers et al. (2004) (green line).

6. CONCLUSIONS

Our high-resolution study of the evolution of planktonic foraminiferal assemblages and reconstructed SST from the Shackleton Site, as well as the comparison of our results with both benthic and planktonic isotope records and Ca/Ti data from the same Site (Hodell et al., 2015), allows the characterization of climatic conditions in the North Atlantic from MIS 13 to 11. SST was generally colder than today off the southwestern Iberian margin, especially during the warmest months, which showed higher SST than today only during peak interglacial optima. Less pronounced cooling was recorded in this site during MIS 13-11, than during MIS 20 or MIS 15 (Martin-Garcia et al., 2015).

During MIS 12 surface water in the mid-latitude ocean was generally colder than during interglacials, with reduced seasonality and less amplitude SST fluctuations, especially in the warmest months. Climate oscillations were greater during the expansion of ice sheets, while the reduction of climate variability prior the glacial maximum led to one of the most pronounced glaciations of the last million years.

MIS 11c was characterized by climatic stability, with warm winters and very low seasonality, in line with the low eccentricity and reduced precession at the time. These climatic conditions led to the weakening of the regional upwelling system and the stratification of surface water recorded in site U1385 (Rodríguez-Tovar et al., 2015).

Millennial climate variability from MIS 13 to MIS 11 shows the occurrence of seven sequences of progressive cooling; each sequence culminated with a major cooling event and was followed by a warming episode. These sequences are similar to Bond cycles defined for the late Pleistocene and most of the final cooling events recorded in site U1385 coincided with H-type events registered in northern sites. These identified climate sequences coincided with vaguely recorded stages of gradual increase in benthic $\delta^{18}O$ that was interrupted, or decreased, towards the end of each sequence. Such sequences can also be identified in the reconstructed record of Greenland temperature (GLTsyn of Barker et al., 2011). Major cooling coincided with steep reduction and/or low AMOC, Greenland stadials and, with exceptions, also with high temperature over Antarctica. This suggests that the see-saw mechanism was also a characteristic feature during the fifth climatic cycle.

A lag between SST and ice volume, as informed by benthic $\delta^{18}O$, was clearly recorded both during MIS 13 and the subsequent glacial inception. Warmest SST during MIS 13a occurred ~4.5 ky after the minimum ice volume, and SST began to decrease again only ~3 ky after the new ice growth phase. During this glacial inception a very steep SST gradient developed between the northwest Atlantic and the mid-latitude ocean in response to the advance of the AF toward the east or the southeast.

Variations of planktonic foraminifer assemblages in this site indicate a strong connection between the presence of warm surface water off Iberia and migration of the AF. The advance of the AF over the northern Atlantic would displace the subtropical gyre southwards, while episodes of retreat of the AF would allow the northward migration of the gyre and the arrival of warm water masses to more northern latitudes. During the transition MIS 12b/a the increase in ice volume was not accompanied by the southward migration of the subtropical gyre, which indicates that the North Atlantic surface circulation was not greatly disturbed in the eastern margin, probably because the AF had a southwest-northeast orientation and the locus of deep water formation was not affected during this period. This interpretation is supported by values of $\delta^{13}C$ ~0.5 ‰ higher than in other intervals of MIS 12, which suggests a reduced but still active AMOC at the time, compared with other intervals of the same glacial period.

Table IX- I: Age model for Core IODP-U1385 (for MIS 11, 12 and 13)

Core Depth (crmcd)	Age (ka B.P.)	Proxies used for correlation	Source
51.506	372.21	Benthic $\delta^{18}O$ LR04 stack[(a)]	Lisiecki and Raymo (2005)
55.322	400.84	Benthic $\delta^{18}O$ LR04 stack	Lisiecki and Raymo (2005)
55.728	400.87	Extrapolated sedimentation rate	This work
55.737	431.09	Extrapolated sedimentation rate	This work
55.753	431.10	Benthic $\delta^{18}O$ LR04 stack[(a)]	Lisiecki and Raymo (2005)
56.58	454.33	Benthic $\delta^{18}O$ U1308	Hodell et al. (2008)
58.62	478.36	Benthic $\delta^{18}O$ U1308	Hodell et al. (2008)
59.19	480.25	Benthic $\delta^{18}O$ U1308	Hodell et al. (2008)
60.50	491.00	Benthic $\delta^{18}O$ LR04 stack	Lisiecki and Raymo (2005)
62.83	503.76	Benthic $\delta^{18}O$ U1308	Hodell et al. (2008)
63.53	508.00	Benthic $\delta^{18}O$ LR04 stack	Lisiecki and Raymo (2005)
66.43	525.265	Benthic $\delta^{18}O$ LR04 stack	Lisiecki and Raymo (2005)
67.33	529.50	Benthic $\delta^{18}O$ U1308	Hodell et al. (2008)
67.93	533.93	Benthic $\delta^{18}O$ LR04 stack[(a)]	Lisiecki and Raymo (2005)

(a) Age control point published by Hodell et al. (2015)

CAPÍTULO IX

CONCLUSIONES / CONCLUSIONS

CAPÍTULO IX

CONCLUSIONES / CONCLUSIONS

CONCLUSIONES

El estudio de las asociaciones de foraminíferos planctónicos procedentes del sondeo U1385 en el margen atlántico ibérico, así como la comparación de los resultados obtenidos con datos de $\delta^{18}O$, tanto bentónicos como planctónicos, y el registro de Ca/Ti del mismo sitio (Hodell et al., 2015), permite la caracterización climática y paleoceanográfica del Atlántico Norte de los estadios isotópicos (MIS) 21 al 11. A continuación se presentan las principales conclusiones obtenidas para este intervalo.

Todas las desglaciaciones registradas en el margen portugués, tanto las Terminaciones (particularmente T IX y VIII) como las transiciones glacial/interglacial entre subestadios (MIS 21b/a, MIS 18e/d y especialmente MIS 15b/a), muestran una prominente oscilación climática que puede alcanzar los 10 ºC de variación. Esta importante oscilación térmica durante las desglaciaciones coincide con un cambio notable en las asociaciones de foraminíferos planctónicos, pasando rápidamente de una alta abundancia relativa de la especie polar Nps a una alta abundancia relativa de la Asociación subtropical. Estas oscilaciones térmicas de alta amplitud se produjeron como consecuencia de importantes reorganizaciones de la circulación superficial y profunda en el Atlántico Norte provocadas, a su vez, por aportes de agua dulce al océano cuando las masas de hielo del hemisferio norte comenzaron a retirarse. La reducción de salinidad superficial paralizó la formación de aguas profundas en el Atlántico Norte y, como consecuencia, el aporte de calor hacia latitudes altas y la llegada de aguas cálidas al margen oriental del giro subtropical, lo que provocó el aporte de aguas subpolares al margen occidental ibérico. Esta situación cambió rápidamente tras cesar la perturbación del agua dulce. La reiniciación de la formación de NADW reactivó la circulación profunda y condujo a una intensificación de la NAC y la llegada de aguas cálidas al margen ibérico.

La comparación con registros de temperatura oceánica superficial a latitudes altas del Atlántico Norte revela el desarrollo de un acusado gradiente térmico latitudinal entre el Atlántico Norte subtropical y el polar a medida que las masas de hielo del hemisferio norte se van formando. Este acusado gradiente proporciona una fuente de vapor de agua que podría favorecer el crecimiento de las masas de hielo.

Durante el intervalo MIS 13-11, la temperatura oceánica superficial del margen SW ibérico era, en general, más fría que en la actualidad, en especial durante los meses más cálidos. La temperatura oceánica superó los valores actuales sólo durante cortos intervalos de los óptimos interglaciales. Los enfriamientos registrados en el U1385 durante el intervalo MIS 13-11 fueron menos pronunciados que los registrados durante MIS 20 ó MIS 15.

Durante MIS 12 el agua superficial en latitudes medias era, en general, más fría que durante los interglaciales, con baja estacionalidad y menor amplitud de oscilación térmica, especialmente durante los meses cálidos. Las oscilaciones climáticas eran mayores durante la expansión de las masas de hielo y se cree que la disminución de la variación climática antes del máximo glacial condujo a una de las glaciaciones más pronunciadas del último millón de años.

El MIS 11c se caracterizó por estabilidad climática, inviernos templados y muy baja estacionalidad, como corresponde a una baja excentricidad y precesión reducida. Tales condiciones climáticas provocaron la estratificación del agua superficial y el debilitamiento del sistema de upwelling regional en la zona de estudio.

Las variaciones climáticas desde el MIS 13 al MIS 11 muestran la existencia de siete secuencias climáticas formadas por episodios progresivamente más fríos y que culminaban con un enfriamiento importante que era seguido por un repentino y drástico calentamiento. Dichas secuencias son similares a los ciclos Bond descritos en el Pleistoceno superior y la mayor parte de los episodios finales de enfriamiento registrados en el U1385 coincidieron con eventos tipo Heinrich registrados en altas latitudes del océano Atlántico. Estas secuencias climáticas se corresponden con períodos de incremento gradual en el registro de $\delta^{18}O$ que se interrumpe, o disminuye, hacia el final de cada secuencia; también se corresponden con secuencias similares en del registro sintético de temperatura sobre Groenlandia (GLTsyn of Barker et al., 2011).

Los principales enfriamientos coincidieron con la abrupta disminución y/o valores bajos de la AMOC, estadiales sobre Groenlandia y, salvo excepciones, también con alta temperatura sobre Antártica. Esto sugiere que el modelo en dientes de sierra, que explica las oscilaciones climáticas del último ciclo glacial, funcionó también durante el quinto ciclo climático.

Durante el MIS 13 y el inicio de la siguiente glaciación se registró un claro desfase entre las variaciones de SST y el volumen del hielo, según el $\delta^{18}O$ bentónico. Los valores más altos de SST durante MIS 13a se alcanzaron ~4.5 ky después del mínimo volumen de hielo, y la SST empezó a descender de nuevo ~3 ky después del inicio de la nueva fase del crecimiento del hielo. Durante este inicio glacial se formó un gradiente térmico superficial muy acusado entre el Atlántico NW y latitudes medias, en respuesta al avance del AF en dirección este o el sureste.

Las variaciones de las asociaciones de foraminíferos planctónicos del U1385 indican una fuerte conexión entre la presencia del agua cálida superficial en el margen Ibérico y la migración del AF. El avance del frente ártico en latitudes altas produciría el desplazamiento hacia el sur del giro subtropical, mientras que los episodios del retroceso del AF permitirían la migración hacia el norte de dicho giro y la llegada de masas superficiales cálidas a latitudes más altas. Durante la transición MIS 12b/a el aumento en volumen del hielo no se acompañó de la migración hacia el sur del giro subtropical, lo que indica que la circulación superficial de Atlántico Norte se mantuvo sin grandes alteraciones en el margen del este, probablemente debido a que el AF tenía una orientación sudoeste-noreste y el lugar de hundimiento de aguas no resultó afectado durante este período. Esta interpretación se respalda por valores del $\delta^{13}C$, que son ~0.5‰ más altos que durante otros intervalos del MIS 12, lo que sugiere la existencia de una AMOC reducida, pero aún activa comparada con otros intervalos del mismo período glacial.

El margen suroeste ibérico es muy sensible a los cambios en la distribución de las corrientes del Atlántico Norte y las masas de agua, así como a los cambios en la posición de los frentes ártico y subtropical. Las variaciones en la abundancia de las asociaciones de microfauna asociadas a las diversas corrientes del Atlántico Norte indican un cambio en la circulación general de esta parte del océano durante el estadio

MIS 16. Antes del MIS 16, cuando la posición del frente Ártico (AF) era más meridional, tanto durante los glaciales como los interglacials, la circulación del Atlántico Norte estaba condicionada por la migración del AF hacia el sur conforme avanzaba las condiciones glaciales. Durante los máximos glaciales de MIS 20 y MIS 18, coincidiendo con la posición más meridional del AF, la corriente del Atlántico Norte (NAC) quedó desviada hacia el sur y adquirió una posición casi puramente oeste-este, lo que produjo un menor transporte de calor a latitudes altas. Durante estos dos estadios glaciales, especialmente durante MIS 20, la corriente subtropical de las Azores aportaba aguas subtropicales cálidas a lo largo del margen ibérico, fluyendo superficialmente sobre las aguas más frías que llegaban procedentes de latitudes subpolares en dirección sur.

En el margen ibérico el cambio de posición del AF quedó registrado en torno a los 655 ka mediante el descenso en porcentaje de la especie polar *Neogloboquadrina pachyderma* (sinistral) y el incremento de la especie subpolar, *Turborotalita quinqueloba*.

Desde el MIS 16 la circulación general del Atlántico Norte estaba menos condicionada por las diferentes posiciones del AF que en estadios anteriores. Durante MIS 14 la NAC llegaba con mayor intensidad a latitudes altas, coincidiendo con el avance de la glaciación. Desde el MIS 16, la microfauna característica de la NAC dominó la asociación registrada en el margen oriental subtropical, indicando una reactivación importante de la corriente de Portugal, rama descendente de la NAC, a lo largo del margen Ibérico. Esta corriente produciría el desvío del agua cálida superficial hacia mar abierto y, en consecuencia, la disminución en el porcentaje de especies cálida en el U1385.

La evolución de las comunidades bentónicas durante el intervalo MIS 13 al 11 responde a importantes cambios en la ventilación del fondo, probablemente ligada a variaciones en la circulación termohalina profunda del Atlántico Norte.

Las condiciones ambientales del fondo para el intervalo de tiempo MIS 13 - 11 se pueden interpretar como de buena oxigenación, tanto del fondo como del agua intersticial del sedimento, así como de abundancia de nutrientes para las comunidades bentónicas.

La concentración de foraminíferos bentónicos y las variaciones en las asociaciones de planctónicos, sugieren cambios significativos en la productividad superficial y el aporte de nutrientes al fondo oceánico durante MIS 13-11 que pueden correlacionarse con los cambios registrados de icnofacies.

El final del MIS 13 se caracteriza por valores muy bajos de la productividad anual exportada, lo que conjuntamente con la presencia de sedimentos claros indica un flujo relativamente bajo de carbono orgánico hacia el fondo, así como buena oxigenación. Estas condiciones iniciales cambiaron durante el MIS 12, con un rápido incremento del aporte de materia orgánica, que mantuvo altos valores hasta la Terminación V. Durante este tiempo las condiciones eran eutróficas, como indica la elevada tasa de acumulación de foraminíferos bentónicos. Durante MIS 11 se registró una menor tasa de acumulación de foraminíferos bentónicos, lo que sugiere un ambiente oligotrófico en el fondo asociado a menores aportes de carbono orgánico y alto contenido de oxígeno en el fondo, lo que produjo sedimentos de color más claro.

CONCLUSIONS

The study of the variation of planktonic foraminifers assemblages and SST from the Shackleton site during the middle Pleistocene, as well as the comparison of results with both benthic and planktonic $\delta^{18}O$ records and Ca/Ti data from the same Site (Hodell et al., 2015), allows the characterization of climatic and palaeoceanographic conditions in the North Atlantic back to the ninth climatic cycle (867 ka). Main conclusions for marine isotope stages MIS 21 to 11 are the following:

All deglaciations on the Portuguese margin, both Terminations (particularly T IX and VIII) and the transitions from glacial to interglacial substages (MIS 21b/a, MIS 18e/d and especially MIS 15b/a), show a prominent (up to 10ºC in amplitude) cold-warm climate oscillation. This high amplitude variation in temperature during deglaciations is recorded by a remarkable change in the planktonic foraminifer assemblages from high relative abundance of the polar species Nps to high relative abundance of the subtropical association. These high amplitude oscillations in temperature were the result of major reorganizations of Sea surface and deep water

circulation in the North Atlantic triggered by freshwater releases to the Ocean when Ice sheets in the northern Hemisphere started to retreat. Reduced salinities at surface shutdown NADW formation and reduced the northward advection of heat and the transport of warm waters to the eastern margin of the subtropical gyre, causing the advection of subpolar waters to the SW Iberian margin. This scenario rapidly changed when the freshwater perturbation stopped. The re-initiation of NADW formation enhanced the strength of the AMOC leading to an intensification of the NAC and the flux of warm waters to the Iberian margin.

The comparison with SST records from higher latitudes of the North Atlantic reveals the development of a steeper latitudinal SST gradient between the sub-tropical and the sub-polar North Atlantic as ice sheets were growing in the northern Hemisphere, providing a source of water vapour that could promote the growth of ice sheets.

During the interval between MIS 13-11, SST was generally colder than today off the southwester Iberian margin, especially during the warmest months, which showed higher SST than today only during peak interglacial optima. Less pronounced cooling was recorded in this site during MIS 13-11, than during MIS 20 or MIS 15.

During MIS 12 surface water in the mid-latitude ocean was generally colder than during interglacials, with reduced seasonality and less amplitude SST fluctuations, especially in the warmest months. Climate oscillations were greater during the expansion of ice sheets, while the reduction of climate variability prior the glacial maximum led to one of the most pronounced glaciations of the last million years.

MIS 11c was characterized by climatic stability, with warm winters and very low seasonality, in line with the low eccentricity and reduced precession at the time. These climatic conditions led to the weakening of the regional upwelling system and the stratification of surface water recorded in site U1385.

Millennial climate variability from MIS 13 to MIS 11 shows the occurrence of seven sequences of progressive cooling; each sequence culminated with a major cooling event and was followed by a warming episode. These sequences are similar to Bond cycles defined for the late Pleistocene and most of the final cooling events recorded in site U1385 coincided with H-type events registered in northern sites. These identified

climate sequences coincided with vaguely recorded stages of gradual increase in benthic $\delta^{18}O$ that was interrupted, or decreased, towards the end of each sequence. Such sequences can also be identified in the reconstructed record of Greenland temperature (GLTsyn of Barker et al., 2011). Major cooling coincided with steep reduction and/or low AMOC, Greenland stadials and, with exceptions, also with high temperature over Antarctica. This suggests that the see-saw mechanism was also a characteristic feature during the fifth climatic cycle.

A lag between SST and ice volume, as informed by benthic $\delta^{18}O$, was clearly recorded both during MIS 13 and the subsequent glacial inception. Warmest SST during MIS 13a occurred ~4.5 ky after the minimum ice volume, and SST began to decrease again only ~3 ky after the new ice growth phase. During this glacial inception a very steep SST gradient developed between the northwest Atlantic and the mid-latitude ocean in response to the advance of the AF toward the east or the southeast.

Variations of planktonic foraminifer assemblages in this site indicate a strong connection between the presence of warm surface water off Iberia and migration of the AF. The advance of the AF over the northern Atlantic would displace the subtropical gyre southwards, while episodes of retreat of the AF would allow the northward migration of the gyre and the arrival of warm water masses to more northern latitudes. During the transition MIS 12b/a the increase in ice volume was not accompanied by the southward migration of the subtropical gyre, which indicates that the North Atlantic surface circulation was not greatly disturbed in the eastern margin, probably because the AF had a southwest-northeast orientation and the locus of deep water formation was not affected during this period. This interpretation is supported by values of $\delta^{13}C$ ~0.5 ‰ higher than in other intervals of MIS 12, which suggests a reduced but still active AMOC at the time, compared with other intervals of the same glacial period.

The southwester Iberian margin is highly sensitive to changes in the distribution of North Atlantic currents and water masses, as well as to changes in the position of arctic and subtropical fronts. Variations in abundance of microfaunal assemblages associated to different water masses indicate a change in the general North Atlantic circulation during MIS 16. Previous to MIS 16, when the arctic front (AF) was located at

a more southerly position during both glacials and interglacials, the North Atlantic circulation was determined by its southward migration as glacial conditions progressed. During peak glacial conditions of MIS 20 and MIS 18, coinciding with the southernmost position of the AF, the North Atlantic Current (NAC) was diverted southward and followed and almost pure west to east drift, transporting less heat to high latitudes. During these two glacials, especially during MIS 20, the Azores current (AzC) transported warm subtropical waters along the Iberian margin superficially over waters of polar origin.

Off Iberia, the shift in the AF position was recorded at ~655 ka by the decrease of relative abundance of the polar species *Neogloboquadrina pachyderma* (sinistral) and the increase of the subpolar one, *Turborotalita quinqueloba*. Since MIS 16, the general circulation across the North Atlantic was lesser influenced by the different positions of the AF than before. The NAC reached high latitudes more frequently during MIS 16 than during previous glacials, and during MIS 14 the NAC became more important in the subpolar North Atlantic as glacial conditions progressed. In the subtropical eastern boundary the faunal assemblage associated with the NAC became the most abundant since MIS 16, which indicates that the PC became stronger along the Iberian margin and diverted warmer water offshore, reducing the relative abundance of warm surface-dwelling species in site U1385.

The evolution of benthic communities during MIS 13 to 11 responded to major changes in bottom water ventilation probably linked to variations in North Atlantic deep-water thermohaline circulation.

During MIS 13 - 11, a generalized context of well-oxygenated bottom and pore-waters, as well as abundance of food in the sediment for benthic communities can be interpreted, with marked changes in these paleoenviromental factors as revealed by variations in composition and distribution of trace fossils.

Benthic foraminifer concentration in the sediments and variations of the planktonic foraminifer assemblages suggest significant changes in surface productivity and food supply to the sea floor during MIS 13 and 11 that could be correlated with the registered changes in facies and ichnology.

The end of MIS 13 is characterized by very low values of annual export productivity, which together with the presence of light-color sediments, reveals relatively low organic carbon flux to the bottom and high oxygen conditions. These initial conditions were changed during development of MIS 12, showing the rapid increase in the organic matter supply and then remaining very high until Termination V, determining a eutrophic environment, as is revealed by high benthic foraminifer accumulation rates. During MIS 11 lower benthic foraminifer accumulation rates are registered suggesting an oligotrophic environment at the bottom, associated with lower inputs of organic carbon, and high oxygen content of bottom waters, in agreement with the lighter color of the sediments as well as the continuous presence of light *Planolites* and *Thalassinoides* at the interval M.

BIBLIOGRAFÍA

REFERENCES

BIBLIOGRAFÍA

REFERENCES

Abe-Ouchi, A., Saito, F., Kawamura, K., Raymo, M.E., Okuno, J.i., Takahashi, K., Blatter, H., 2013. Insolation-driven 100,000-year glacial cycles and hysteresis of ice-sheet volume. Nature 500, 190-193

Abrantes, F., 1991. Increased upwelling off Portugal during the last deglaciation: Diatom evidence. Mar. Micropaleontol. 17, 285-310

Abrantes, F., 1992. Paleoproductuvity oscillations during the last 130 ka along the Portuguese and NW African margins, in *Upwelling Systems: Evolution Since the Early Miocen*, ed. C.P. Summerhayes, W.L. Prell and K.C. Emeis, Geol. Soc. Spec. Publ., 64, 499-510

Abrantes, F., Loncaric, N., Moreno, J., Mil-Homens, M., Pflaumann, U., 2001. Paleoceanographic conditions along the Portuguese margin during the last 30 ka: A multiple proxy study. Comun. Inst. Geol. Min. Portugal 88, 161-184

Adkins, J., 2013. The role of deep ocean circulation in setting glacial climates. Paleoceanography, 28, 539-561

Allen, J.R.M., Brandt, U., Brauer, A., Hubberten, H.W., Huntley, B., Keller, J., Kraml, M., Mackensen, A., Mingram, J., Negendank, J.F.W., Nowaczyk, N.R., Oberhansli, H., Watts, W.A., Wulf, S., Zolitschka, B., 1999. Rapid environmental changes in southern Europe during the last glacial period. Nature 400, 740-742

Alonso-Garcia, M., Sierro, F.J., Flores, J.A., 2011a. Arctic front shifts in the subpolar North Atlantic during the Mid-Pleistocene (800–400 ka) and their implications for ocean circulation. Palaeogeog. Palaeoclimatol. Palaeoecol. 311, 268-280

Alonso-Garcia, M., Sierro, F.J., Kucera, M., Flores, J.A., Cacho, I., Andersen, N., 2011b. Ocean circulation, ice sheet growth and interhemispheric coupling of millennial climate variability during the mid-Pleistocene (ca 800–400 ka). Quat. Sci. Rev. 30, 3234-3247

Amore, F.O., Flores, J.A., Voelker, A.H.L., Lebreiro, S.M., Palumbo, E., Sierro, F.J., 2012. A Middle Pleistocene Northeast Atlantic coccolithophore record: Paleoclimatology and paleoproductivity aspects. Marine Micropeleontology 90-91, 44-59, doi:10.1016/j.marmicro.2012.03.006

Baas, J., Schönfeld, J., Zahn, R., 1998. Mid-depth oxygen drawdown during Heinrich events: evidence from benthic foraminiferal community structure, trace-fossil tiering, and benthic $\delta^{13}C$ at the Portuguese Margin. Marine Geology 152(1), 25-55

Bard, E., Rostek, F., Turon, J.L., Gendreau, S., 2000. Hydrological impact of Heinrich Events in the Subtropical Northeast Atlantic. Science 289, 1321-1324, doi:10.1126/science289.5483,1321

Barker, S., Knorr, G., Edwards, R.L., Parrenin, F., Putnam, A.E., Skinner, L.C., Wolff, E., Ziegler, M., 2011. 800,000 Years of Abrupt Climate Variability. Science, 334, 347, doi:10.1126/science.1203580

Bauch, D., Carstens, J., Wefer, G., 1997. Oxygen isotope composition of living *Neogloboquadrina pachyderma* (sin) in the Arctic Ocean. Earth and Planetary Science Letters 146, 47-58

Bé, A.W.H., 1977. Recent planktonic foraminifera, in Oceanic Micropaleontology, 1, edited by Ramsay, A.T.S., pp. 1-100, Elsevier, New York.

Bé, A.W.H., Tolderlund, D.S., 1971. Distribution and ecology of living planktonic foraminifera in surface waters of the Atlantic and Indian Oceans, In: Funnell, B., Riedel, W.R. (Eds.), The Micropaleontology of the Oceans. Cambridge Univ. Press. London, 105-149

Bijma, J., Faber, W., Hemleben, C., 1990. Temperature and salinity limits for growth and survival of some planktonic foraminifers in laboratory cultures. J. Foraminiferal Res. 20, 95-116

Black, D.E. et al., 1999. Eight centuries of North Atlantic Ocean variability. Science 286, 1709-1713

Böhm, E., Lippold, J., Gutjahr, M., Frank, M., Blaser, P., Antz, B., Fohlmeister, J., Frank, N., Andersen, M.B., Deininger, M., 2014. Strong and deep Atlantic meridional overturning circulation during the last glacial cycle. doi:10.1038/nature14059

Bond, G.C. and Lotti, R., 1995. Iceberg discharges into the North Atlantic on millennial time scales during the last glaciation. Science 267, 1005-1010

Bond, G., Heinrich, H., Broecker, W., Labeyrie, L., McManus, J., Andrews, J., Huon, S., Jantschik, R., Clasen, S., Simet, C., Tedesco, K., Klas, M., Bonani, G., Ivy, S., 1992. Evidence for massive discharges of icebergs into the North Atlantic ocean during the last glacial period. Nature 360, 245-249, doi:10.1038/360245a0

Boyle, E., Keigwin, L., 1987. North Atlantic thermohaline circulation during the past 20,000 years linked to high-latitude surface temperature. Nature 330, 35-40

Brambilla, E., Talley, L.D., 2008. Subpolar Mode Water in the northeastern Atlantic: 1. Averaged properties and mean circulation. J. Geophys. Res. 113, C04025, doi:10.1029/2006JC004062

Brierley, C.M., Fedorov, A.V., 2010. The relative importance of meridional and zonal SST gradients for the onset of the ice ages and Pliocene-Pleistocene climate evolution. Paleoceanography 25, PA2214, doi:2210.1029/2009PA001809

Broecker, W.S., 1994. Massive iceberg discharges as triggers for global climate change. Nature 372, 421-424

Broecker, W. S., Peteet, D.M., Rind, D., 1985. Does the ocean-atmosphere system have more than one stable mode of operation? Nature 315, 21-26

Broecker, W. S., Kennett, J. P., Flower, B. P., Teller, J. T., Trumbore, S., Bonani, G., Wolfli, W., 1989. Routing of meltwater from the Laurentide Ice Sheet during the Younger Dryas cold episode. Nature 341, 318-321

Broecker, W.S., Bond, G., Millie, K., Geotges, B., Willy, W., 1990. A salt oscillator in the glacial Atlantic?, 1, The concept. Paleoceanography 5, 469-477

Broecker, W.S., Bond, G., Klas, M., Clark, E., McManus, J., 1992. Origin of the nothern Atlantic´s Heinrich events. Climate Dynamics 6, 265-273

Bromley, R.G., 1996. Trace Fossils. Biology, Taphonomy and Applications, Second edition. Chapman & Hall, London

Bromley, R.G., Hanken, N.M., 2003. Structure and function of large, lobed *Zoophycos*, Pliocene of Rhodes, Greece. Palaeogeography, Palaeoclimatology, Palaeoecology 192, 79-100

Brongniart, A.T., 1823. Observations sur les Fucoïdes. Mémoire. Société d'Historie Naturelle de Paris 1, 301-320

Calvo, E., Villanueva, J., Grimalt, J.O., Boelaert, A., Labeyrie, L., 2001. New insights into the glacial latitudinal temperature gradients in the North Atlantic. Results from $U^{k'}_{37}$ sea surface temperatures and terrigenous inputs, Earth Planet. Sci. Lett., 188 (3-4), 509-519, doi:10.1016/S0012-821X(01)00316-8

Candy, I., Coope, G.R., Lee, J.R., Parfi tt, S.A., Preece, R.C., Rose, J., Schreve, D.C., 2010, Pronounced warmth during early middle Pleistocene interglacials: Investigating the Mid-Brunhes Event in the British terrestrial sequence. Earth-Science Reviews 103, 183-196

Candy, I., Schreve, D.C., Sherriff, J., Tye, G.J., 2014. Marine Isotope Stage 11: Palaeoclimates, palaeoenvironments and its role as an analogue for the current interglacial. Earth-Science Reviews 128, 18-51

Cayre, O., Lancelot, Y., Vincent, E., 1999. Paleoceaanographic reconstructions from planktonic foraminifera ogg the Iberian Margin: Temperature, salinity and Heinrich events. Paleoceanography, 14 (3), 384-396

Chaisson, W.P., Poli, M.S., Thunell, R.C., 2002. Gulf Stream and Western boundary undercurrent variations during MIS10-12 at Site 1056, Blake-Bahama Outer Ridge. Marine Geology 189, 79-105

Channell, J.E.T., Hodell, D.A., Romero, O., Hillaire-Marcel, C., de Vernal, A., Stoner, J.S., Mazaud, A., and Roehl, 2012. IODP Site U1302-U1303 (Orphan Knoll): Correlation of Brunhes detrital-layer stratigraphy into the North Atlantic. *Earth Planet. Sci. Letts.* 317-318, 218-230

Chapman, M.R., Shackleton, N.J., Zhao, M., Eglinton, G., 1996. Faunal and alkenone reconstructions of subtropical North Atlantic surface hydrography and paleotemperature over the last 28 kyr. Paleoceanography, 11 (3), 343-358

Chapman, M.R., Shackleton, N.J., 1998. Millennial-scale fluctuations in North Atlantic heat flux during the last 150,000 years. Earth and Planetary Science Letters 159, 57-70

Clark, P.U., Pollard, D., 1998. Origin of the Middle Pleistocene Transition by Ice Sheet Erosion of Regolith. Paleoceanography 13, 1-9, doi:10.1029/1097pa02660.

Clark, P.U., Archer, D., Pollard, D., Blum, J.D., Rial, J.A., Brovkin, V., Mix, A.C., Pisias, N.G., Roy, M., 2006. The middle Pleistocene transition: characteristics, mechanisms, and implications for long-term changes in atmospheric pCO2. Quat. Sci. Rev. 25, 3150-3184

CLIMAP Project Members, 1976. The surface of the ice-age Earth. Science 191, 1131–1137

CLIMAP Project Members, 1981. Seasonal Reconstructions of the Earth's Surface at the Last Glacial Maximum. Geol. Soc. Am. Map and Chart Ser., MC-36, Geol. Soc. of Am., Boulder, Colorado

Coelho, H., Neves, T., White, M., Leitpo, P., Santos, A., 2002. A model for ocean circulation on teh Iberian coast. Journal of Marine Sustems 32, 181-198

Cortijo, E., Yiou, P., Labeyrie, L., Cremer, M., 1995. Sedimentary record of rapid climatic variability in the North Atlantic Ocean during the last glacial cycle. Pleoceanography 10, 911-926

Dansgaard, W., Johsen, S.J., Clauser, H.B., Kahl, J., Gundestrup, N.S., Hommer, C.U., Huidberg, C.S., Steffensen, J.P., Svernbjornsdottir, A.E., Jouzel, J., Bond, G., 1993. Evidence for general instability of past climate from a 250 kyr ice-core record. Nature 364, 218-220

de Abreu, L., Shackleton, N.J., Schönfeld, J., Hall, M.A., Chapman, M., 2003. Millennial-scale oceanic climate variability off the western Iberian margin during the last two glacial periods. Mar. Geol., 196, 1-20

de Abreu, L., Abrantes, F., Shackleton, N.J., Tzedakis, P.C., McManus, J.F., Oppo, D.W., Hall, M.A., 2005. Ocean climate variability in the eastern North Atlantic during interglacial marine isotope stage 11: A partial analogue to the Holocene? Paleoceanography 20, doi:10.1029/2004PA001091

Denton, G.H., Anderson, R.F., Toggweiler, J.R., Edwards, R.L., Schaefer, J.M., Putnam, A.E., 2010. The Last Glacial Termination. Science 328, 1652-1656

Desprat, S., Sanchez-Goni, M.F., Turon, J.L., McManus, J.F., Loutre, M.F., Duprat, J., Malaize, B., Peyron, O., Peypouquet, J.P., 2005. Is vegetation responsible for glacial inception during periods of muted insolation changes? Quaternary Science Reviews 24, 1361-1374

de Vargas, C., Renaud, S., Hilbrecht, H., Pawlowski, J., 2001. Pleistocene adaptive radiation in Globorotalia truncatulinoides: genetic, morphologic, and environmental evidence. Paleobiology 27, 104–125

Dickson, R., Lazier, J., Meinke, J., Thines, P., Swift, J., 1996. Long term coordinated changes in the convective activity of the North Atlantic. Progr. Oceanogr. 38, 241-295

Dokken, T., Jansen, E., 1999. Rapid changes in the mechanism of ocean convection during the last glacial period. Nature 401, 458-461

Dorador, J., Rodríguez-Tovar, F.J., 2014. A novel application of quantitative pixels analysis to trace fossil research in marine cores. Palaios 29, 533-538

Dorador, J., Rodríguez-Tovar, F.J., IODP Expedition 339 Scientists, 2014a. Quantitative Estimation of Bioturbation Based on Digital Image Analysis. Marine Geology 349, 55-60

Dorador, J., Rodríguez-Tovar, F.J., IODP Expedition 339 Scientists, 2014b. Digital image treatment applied to ichnological analysis of marine core sediments. Facies 60(1), 39-44

Droxler, A.W.; Poore, R.Z.; Burckle, L.H., 2003. Earth's Climate and Orbital Eccentricity: The Marine Isotope Stage 11 Question. In: Droxler, A.W., Poore, R.Z., Burckle, L.H. (Eds.), Geophy. Monograph Series 137, AGU, Washington, D.C., 240 pp

Duarte, J. C., Rosas, F. M., Terrinha, P., Schellart, W. P., Boutelier, D., Gutscher, M. A., and Ribeiro, M. A.,2013. Are subduction zones invading the Atlantic? Evidence from the southwest Iberia margin. Geology, doi:10.1130/G34100.1

Duprat, J., 1983. Les Foraminifères planctoniques du Quaternaire terminal d´un domaine pèricontinental (Golfe de Gascogne Côtes Ouest-Iberiques Mer d´Alboran): Ecologie-Biostratigraphie. Bull., Ins. Gèol. Bassin d´Aquitaine 33, 71-150

Ekdale, A., 1992. Muckraking and mudslinging: the joys of deposit-feeding. In: Maples, C.G., West, R.R. (Eds.), Trace Fossils. Short Courses in Paleontology. Paleontological Society, pp. 145-171

Ekdale, A.A., Bromley, R.G., Pemberton, S.G., 1984. Ichnology: The Use of Trace Fossils in Sedimentology and Stratigraphy. Short Course, 15. Society of Economics Paleontologists and Mineralogists, 316 pp

Elderfield, H., Ferretti, P., Greaves, M., Crowhurst, S., McCave, I.N., Hodell, D., Piotrowski, A.M., 2012. Evolution of Ocean Temperature and Ice Volume Through the Mid-Pleistocene Climate Tansition. Science 337, 704-709, doi:10.1126/science.1221294

EPICA community members, 2004. Eight glacial cycles from an Antarctic ice core. Nature, 429, 623

Expedition 339 Scientists, 2012. Mediterranean outflow: environmental significance of the Mediterranean Outflow Water and its global implications. IODP Prel. Rept., 339. doi:10.2204/iodp.pr.339.2012

Expedition 339 Scientists, 2013a. Site U1385. *In* Stow, D.A.V., Hernández-Molina, F.J., Alvarez Zarikian, C.A., and the Expedition 339 Scientists, *Proc. IODP,* 339: Tokyo (Integrated Ocean Drilling Program Management International, Inc.).

doi:10.2204/iodp.proc.339.103.2013 Expedition 339 Scientists, 2013b. Expedition 339 summary. In: Stow, D.A.V., Hernández-Molina, F.J., Alvarez-Zarikian, C.A.,

Expedition 339 Scientists (Eds.), Proceedings of the Integrated Ocean Drilling Program, Tokyo (Integrated Ocean Drilling Program Management International, Inc.), doi: 10.2204/iodp.proc.339.101.2013.

Eynaud, F., de Abreu, L., Voelker, A., Schönfeld, J., Salgueiro, E., Turon, J.L., Penaud, A., Toucanne, S., Naughton, F., Sanchez-Goñi, M.F., Malaizé, B., Cacho, I., 2009. Position of the Polar Front along the western Iberian Margin during key cold episodes of the last 45 ka. Geochem. Geophys. Geosyst. 10, Q07U05, doi:10.1029/2009GC002398

Fairbanks, R.G., Wiebe, P.H., Bé, A.W.H., 1980. Vertical distribution and isotopic composition of living planktonic foraminifera in the Western North Atlantic. Science 207, 61-63

Ferretti, P., Crowhurst, S.J., Hall, M.A., Cacho, I., 2010. North Atlantic millennial scale climate variability 910,000 to 790,000 years and the role of the equatorial insolation forcing. Earth and Planetary Science Letters 293, 28-41, doi:10.1016/j.epsl.2010.02.016

Fiúza, A.F.G., Hamann, M., Ambar, I., Díaz del Río, G., González, N. Cabanas, J.M., 1998. Water masses and their circulation off western Iberia during May 1993. Deep-Sea Research 45, 1127-1160

Flower, B.P., Oppo, D.W., McManus, J.F., Venz, K.A., Hodell, D.A., Cullen, J.L., 2000. North Atlantic intermediate to deep water circulation and chemical stratification during the past 1 Myr. Paleoceanography 15, 388-403

Frey, R.W., Curran, A.H., Pemberton, G.S., 1984. Tracemaking activities of crabs and their environmental significance: the ichnogenus *Psilonichnus*. Journal of. Paleontology 58, 511–528

Fu, S., 1991. Funktion, Verhalten und Einteilung fucoider und lophoctenoider Lebensspuren. Courier Forschungsinstitut Senckenberg 135, 1-79

Fürsich, F., 1973. A revision of the trace fossils *Spongeliomorpha*, *Ophiomorpha* and *Thalassinoides*. Neues Jahrbuch für Geologie und Paläontologie, Monatshefte, 12, 719-735

Gaillard, C., Hennebert, M., Olivero, D., 1999. Lower Carboniferous *Zoophycos* from the Tournai area (Belgium): environmental and ethologic significance. Geobios 32, 513-524

Giannini, A., Cane, M., Kushnir, Y., 2001. Interdecadal changes in the ENSO teleconnection to the Caribbean region and the North Atlantic Oscillation. J. Clim. 14, 2867-2879

Grimm, E.C., Jacobson, G.L., Watts, B.C.S., Hansen, K.A.M., 1993. A 50,000-year record of climate oscillations from Florida and its temporal correlation with the Heinrich Events. Science 261 , 198-200, doi:10.1126/science.261.5118.198

Grootes, P.M., Stuiver, M., White, J.W.C., Johnsen, S., Jouzel, J., 1993. Comparison of oxigen isotope records from the GISP2 and GRIP Greenland ice cores. Nature 255, 522-554

Heinrich, H., 1988. Origin and consequences of cyclic ice rafting in the Northeast Atlantic Ocean during the pasta 130,000 yrs. Quaternary Research 29, 142-152

Hemleben C., Spindler M. & Anderson O.R., 1989. Modern Planktonic Foraminifera. Springer-Verlag, New York, 1-363

Herman, Y., 1972. Globorotalia truncatulinoides: a palaeo-oceanographic indicator. Nature 238, 394–396

Hernandez-Almeida, I., Sierro, F.J., Cacho, I., Flores, J.A., 2012. Impact of suborbital climate changes in the North Atlantic on ice sheet dynamics at the Mid-Pleistocene Transition. Paleoceanography 27, PA3214

Hernandez-Almeida, I., K. R. Bjoklund, F. J. Sierro, G. M. Filippelli, I. Cacho, and J. A. Flores, 2013. A high resolution opal and radiolarian record from the subpolar North Atlantic during the Mid-Pleistocene Transition (1069–779 ka): Paleoceanographic implications, Palaeogeogr.Palaeoclimatol. Palaeoecol., doi:10.1016/j.palaeo.2011.05.049.

Hernández-Molina, F.J., Serra, N., Stow, D.A.V., Llave, E., Ercilla, G., Van Rooij, D., 2011. Along-slope oceanographic processes and sedimentary products around the Iberian margin. Geo-Mar Lett. 31, 315-341, doi:10.1007/s00367-011-0242-2

Hernández-Molina, F.J., Stow, D., Alvarez-Zarikian, C. and Expedition IODP 339 Scientists, 2013. IODP Expedition 339 in the Gulf of Cadiz and off West Iberia: decoding the environmental significance of the Mediterranean outflow water and its global influence. Sci. Dril. 16, 1-11, doi:10.5194/sd-16-1-2013

Hodell, D.A., Channell, J.E.T., Curtis, J.H., Romero, O.E., Röhl, U., 2008. Onset of "Hudson Strait" Heinrich events in the eastern North Atlantic at the end of the middle Pleistocene transition (~640 ka)? Paleoceanography 23, doi:10.1029/2008PA001591

Hodell, D.A.,Lourens, L., Stow, D. A. V., Hernández-Molina, J., Alvarez Zarikian, C. A., and the Shackleton Site Project Members, 2013a. The “Shackleton Site” (IODP Site U1385) on the Iberian Margin, *Scientific Drilling*, 16, 13–19

Hodell, D., Crowhurst, S., Skinner, L., Tzedakis, P.C., Margari, V., Channell, J.E.T., Kamenov, G., Maclachlan, S., Rothwell, G., 2013b. Response of Iberian Margin sediments to orbital and suborbital forcing over the past 420 ka., Paleoceanography 28 (1), 185-199, doi: 10.1002/palo.20017

Hodell, D., Lourens, L., Crowhurst, S., Konijnendijk, T., Tjallingii, R., Jiménez-Espejo, F., Skinner, L, Tzedakis, PC. and the Shackleton Site Project Members, 2015. A reference time scale for Site U1385 (Shackleton Site) on the SW Iberian Margin. Global and planetary Change 133, 49-64, doi:10.1016/j.gloplacha.2015.07.002

Hoogakker, B.A., Elderfield, H., Schmiedl, G., McCave, I.N., Rickaby, R.E., 2015. Glacial-interglacial changes in bottom-water oxygen content on the Portuguese margin. Nature Geoscience 8, 40-43, doi:10.1038/ngeo2317

Huber, C., Leuenberger, M., Spahni, R., Flückiger, J., Schwander, J., Stocker, T.F., Johnsen, S., Landais, A., Jouzel, J., 2006. Isotope calibrated Greenland temperature record over marine isotope stage 3 and its relation to CH_4. Earth and Planetary Science Letters 243 (3-4), 504-519, doi:10.1016/j.epsl.2006.01.002

Huls, M., Zahn, R., 2000. Millennial-scale sea surface temperature variability in the western tropical North Atlantic from planktonic foraminifera census counts. Paleoceanography 15(6), 659-678

Hurrell, J.W., 1995. Decadal trends in the North Atlantic Oscillation: Regional temperaturas and precipitation. Science 269, 676-679

Huybers, P., 2006. Early Pleistocene glacial cycles and the integrated summer insolation forcing. Science 313, 5786 (708-511), doi:10.1126/science.1125249

Huybers, P., 2007. Glacial variability over the last two million years: an extended depth-derived agemodel, continuous obliquity pacing and the Pleistocene progression. Quaternary Science Reviews 26, 37-55

Huybers, P., 2011. Combined obliquity and precession pacing of late Pleistocene deglaciations. Nature 480, 229-232

Huybers, P., Wunsch, C., 2003. Rectification and precession-period signals in the climate system. Geophys. Res. Lett. 30, doi:10.1029/2003GL017875

Imbrie, J., Kipp, N.G., 1971. A new micropaleontological method for quantitative paleoclimatology: application to a late Pleistocene Caribbean core. In: Turekian, K.K. (Ed.), The Late Cenozoic Glacial Ages. Yale University Press, New Haven, pp. 71–181

Imbrie, J., Boyle, E.A., Clemens, S.C., Kutzbach, J., Martinson, D.G., McIntyre, A., Mix, A.C., Molfino, B., Morley, J.J. Peterson, L.C., Pisias, N.G., Prell, W.L., Raymo, M.E., Shackleton, N.J., Toggweiler, J.R., 1992. On the Structure and Origin of Major Glaciation Cycles 1. Linear responses to Milankovitch forcing. Paleoceanography 7, 701-738

Imbrie, J., Berger, A., Boyle, E.A., Clemens, S.C., Duffy, A., Howard, W.R., Kukla, G., Kutzbach, J., Martinson, D.G., McIntyre, A., Mix, A.C., Molfino, B., Morley, J.J. Peterson, L.C, Pisias, N.G., Prell, W.L., Raymo, M.E., Shackleton N.J., Toggweiler, J.R., 1993. On the structure and origin of major glaciation cycles: 2. The 100,000-year cycle. Paleoceanography 8, 699-735, doi:10.1029/93PA02751

Jiménez-Amat, P., Zahn, R., 2015. Offset timing of climae oscillations during the last two glacial-interglacial transitions connected with large-scale freshwater perturbation. Paleoceanography 30-6, doi:10.1002/2014PA002710

Johannessen, T., Jansen, E., Flatoy, A., Ravelo, A.C., 1994. The relationship between surface water masses, oceanographic fronts and paleoclimatic proxies in surface

sediments of the Greenland, Iceland, Norwegian seas. NATO ASI Series, 117, edited by Zahn, R. et al., Springer-Verlag, New York, 61-85.

Jouzel, J., Masson-Delmotte, V., Cattani, O., Dreyfus, G., Falourd, S., Hoffmann, G., Minster, B., Nouet, J., Barnola, J.M., Chappellaz, J., Fischer, H., Gallet, J.C., Johnsen, S., Leuenberger, M., Loulergue, L., Luethi, D., Oerter, h., Parrenin, F., Raisbeck, G., Raynaud, D., Schilt, A., Schwander, J., Selmo, E., Souchez, R., Spahni, R., Stauffer, B., Steffensen, J.P., Stenni, B., Stocker, T.F., Tison, J.L., Wener, M., Wolff, E.W., 2007. Orbital and millennial Antarctic climate variability over the past 800,000 years. Science 317, 793-796, doi:10.1126/science,1141038

Kandiano, E.S., Baunch, H.A., 2007. Phase realationship and surface water mass change in the Northeast Atlantic during Marine Isotope Stage 11 (MIS11). Quaternary Res. 68, 445-455

Keighley, G., Pickerill, R.K., 1995. The ichnotaxa *Palaeophycus* and *Planolites*: Historical perspectives and recommendations. Ichnos: An International Journal for Plant and Animal Traces 3(4), 301-309

Kennett, J.P., Srinivasan, M.S., 1983. Neogene Planktonic Foraminifera. A Phylogenetic Atlas. Hutchinson Ross Publishing Company, New York.

Kennett, J.P., Cannariato, K.G., Hendy, I.L., Behl, R.J., 2000. Carbon isotopic evidence for methane hydrate Instablity during Quaternary interstadials. Science, 288 (5463): 128-133

King, A.L., Howard, W.R., 2005. D18O seasonality of planktonic foraminifera from Southern Ocean sediment traps: Latitudinal gradients and implications for paleoclimate reconstructions. Marine Micropaleontology 56, 1-24

Kipp, N., 1976. New transfer function for estimating past sea-surface conditions from seabed distribution of planktonic foraminiferal assemblages in the North Atlantic, in *Investigation of Late Quaternary Paleoceanography and Paleoclimatology*, edited by R.M. Cline and J.D. Hays, Mem. Geol. Soc. Am. 145, 3-41

Kleiven, H.F., Jansen, E., Curry, W.B., Hodell, D.A., Venz, K.A., 2003. Atlantic Ocean thermohaline circulation changes on orbital to suborbital timescales during the mid-Pleistocene. Paleoceanography 18, 1008

Kleiven, H.F., Hall, I.R., McCave, I.N., Knorr, G., Jansen, E., 2011. Coupled deep-water flow and climate variability in the middle Pleistocene North Atlantic. Geology 39, 343-346 Kotake, N., 1989. Paleoecology of the *Zoophycos* producers. Lethaia 22, 327-341

Kohfeld, K.E., Faibanks, R.G., Smith, S.L., Walsh, I.D., 1996. Neogloboquadrina pachyderma (sinistral coiling) as paleoceanographic tracers in polar oceans: evidence from Northeast Water Polynya tows, sediment traps, and surface sediments. Paleoceanography 11, 679–699

Kucera, M., Darling, K.F., 2002. Genetic diversity among modern planktonic foraminifer species: its effect on paleoceanographic reconstructions. Philosophical Transactions of the Royal Society London A 360, 695–718

Kucera, M., Weinelt, M., Kiefer, T., Pflaumann, U., Hayes, A., Weinelt, M., Chen, M., Mix, AlC., Barrows, T.T., Cortijo, E., Duprat, J., Juggins, S., Waelbroeck, C., 2005. Reconstruction of sea-surface temperatures from assemblages of planktonic foraminifera: multi-technique approach based on geographically constrained calibration data sets and its application to glacial Atlantic and Pacific Oceans. Quat. Sci. Rev., 24, 951-998, doi:10.1016/j.quascirev.2004.07.014

Laskar, J., Robutel, P., Joutel, F., Gastineau, M., Correia, A.C.M., Levrard, B., 2004. A long-term numerical solution for the insolation quantities of the Earth. Astronomy and Astrophysics 428, 1, doi: 10.1051/0004-6361:20041335

Lebreiro, S.M., Moreno, J. C., McCave, I.N., Weaver, P.P.E., 1996. Evidence for Heinrich layers off Portugal (Tore Seamount: 39ºN, 12ºW). Marine Geology 131, 47-56, doi:10.1016/0025-3227(95)00142-5

Lebreiro, S.M., Moreno, F.C., Abrantes, F., Pflaumann, U., 1997. Productivity and paleoceanographic implications on the Tore Seamount (Iberian Margin) during the last 225 kyr: Foraminiferal evidence. Paleoceanography 12, 5, 718-727

Leuschner, D.C., Sirocko, F., Grootes, P.M., Erlenkeuser, H., 2002. Possible influence of *Zoophycos* bioturbation on radiocarbon dating and environmental interpretation. Marine Micropaleontology 46, 111-26

Levy, A., Mathieu, R., Poignant, A., Rousset-Moulinier, M., Ubaldo, M.L., Lebreiro, S., 1995. Present-day foraminifera of the Portuguese continental margin inventory and distribution. Mem. Inst. Geol. Min. Portugal 32, 166

Lisiecki, L.E., Raymo, M.E., 2005. A Pliocene-Pleistocene stack of 57 globally distributed benthic $d^{18}O$ records. Paleoceanography, 20, PA1003, doi:10.1029/2004PA001071

Lisiecki, L.E., Raymo, M.E., 2007. Plio-Pleostocene climate evolution: trends and transitions in glacial cycle dynamics. Quaternary Science Reviews 26, 56-69

Locarnini, R. A., Mishonov, A.V., Antonov, J.I., Boyer, T.P., Garcia, H.E., Baranova, O.K., Zweng, M.M., Johnson, D.R., 2010. World Ocean Atlas 2009, Volume 1: Temperature. S. Levitus, Ed. NOAA Atlas NESDIS 68, U.S. Government Printing Office, Washington, D.C., 184 pp.

Lohmann, G.P., Schweitzer, P.N., 1990. Globorotalia truncatulinoides: growth and chemistry as probes of the past thermocline: 1. Shell size. Paleoceanography 5, 55–75

Loulergue, L., Schilt, A., Spahni, R., Masson-Delmotte, V., Blunier, T., Lemieux, B., Barnola, J.M., Raynaud, D., Stocker, T.F., Chappellaz, J., 2008. Orbital and millennial-scale features of atmospheric CH_4 over the past 800,000 years. Nature, 453, 383, doi:10.1038/nature06950

Löwemark, L., 2015. Testing ethological hypotheses of the trace fossil *Zoophycos* based on Quaternary material from the Greenland and Norwegian Seas. Palaeogeography, Palaeoclimatology, Palaeoecology 425, 1-13.

Löwemark, L., Grootes, P.M., 2004. Large age differences between planktic foraminifers caused by abundance variations and *Zoophycos* bioturbation. Paleoceanography 19, PA2001 1–9

Löwemark, L., Schäfer, P., 2003. Ethological implications from a detailed X-ray radiograph and ^{14}C-study of the modern deep-sea *Zoophycos*. Palaeogeography, Palaeoclimatology, Palaeoecology 192, 101-121

Löwemark, L., Werner, F., 2001. Dating errors in high-resolution stratigraphy: a detailed X-ray radiograph and AMS-^{14}C study of *Zoophycos* burrows. Marine Geology 177

Löwemark, L., Lin, I.-T., Wang, C.-H., Huh, C.-A., Wei, K.-Y., Chen, C.-W., 2004. Ethology of the *Zoophycos*-producer: Arguments against the gardening model from δ^{13}Corg evidences of the spreiten material. TAO 15, 713-725

Löwemark, L., Lin, Y., Chen, H.-F., Yang, T.-N., Beier, C., Werner, F., Lee, C.-Y., Song, S.-R., Kao, S.-J., 2006. Sapropel burn-down and ichnological response to late Quaternary sapropel formation in two ~400 ky records from the eastern Mediterranean Sea. Palaeogeography, Palaeoclimatology, Palaeoecology 239, 406-425

Löwemark, L., O'Regan, M., Hanebuth, T., Jakobsson, M., 2012. Late Quaternary spatial and temporal variability in Arctic deep-sea bioturbation and its relation to Mn cycles. Palaeogeography, Palaeoclimatology, Palaeoecology 365, 192-208

Lüthi, D., Le Floch, M., Bereiter, B., Blunier, T., Barnola, J.M., Siegenthaler, U., Raynaud, D., Jouzel, J., Fischer, H., Kawamura, K., Stocker, T.F., 2008. High-resolution carbon dioxide concentration record 650,000-800,000 years before present. Nature, 453, 379. doi:10.1038/nature06949

Maldonado, A., Somoza, L., and Pallarés, L., 1999. The Betic orogen and the Iberian–African boundary in the Gulf of Cádiz: geological evolution (central North Atlantic). Mar. Geol., 155, 9–43, doi:10.1016/S0025-3227(98)00139-X

Malmgren, B.A., and Nordlund, U., 1997. Application of artificial neural networks to paleoceanographic data. Palaeogeography, Palaeoclimatology, Palaeoecology 136, 359-373

Malmgren, B.A., Kucera, M., Nyberg, J., Waelbroeck, C., 2001. Comparison of statistical and artificial neural network techniques for estimating past sea surface temperatures from planktonic foraminifer census data. Paleoceanography 16, 520-530

Mangano, M.G., Buatois, L., West, R.R., Maples, C.G., 2002. Ichnology of a Pennsylvanian equatorial tidal flat – the Stull Shale Member at Waverly, eastern Kansas. Kansas Geological Survey Bulletin 245, 1-133

Margari, V., Skinner, L.C., Tzedakis, P.C., Ganopolski, A., Vautravers, M., Shackleton, N. J., 2010. The nature of millennial-scale climate variability during the past two glacial periods. Nature Geoscience 3, 127-131

Marino, M., Maiorano, P., Tarantino, F., Voelker, A., Capotondi, L., Girone, A., Lirer, F., Flores, J.-A., Naafs, B.D.A., 2014. Coccolithophores as proxy of sea-water changes at orbital-to-millennial scale during middle Pleistocene Marine Isotope Stages 14-9 in North Atlantic core MD01-2446. Paleoceanography 29, 2013PA002574, doi:10.1002/2013PA002574

Martins, M.V.A., Gomes, V.C.R., 2004. Foraminiferos da Margem Continental NW Ibérica: Sistemática, Ecologia e Distribuiçao. Ed. By C. de Sousa Figueiredo Gomes, 377 pp

Martrat, B., Grimalt, J.O., Shackleton, N.J., de Abreu, L., Hutterli, M.A., Stocker, T.F., 2007. Four Climate Cycles of Recurring Deep and Surface Water Destabilizations on the Iberian Margin. Science, 317 (5837), 502-507, doi:10.1126/science.1101706

Marshall, J., Speer, K., 2012. Closure of the meridional overturning circulation through Southern Ocean upwelling. Nature Geosci 5, 171-180

Maslin, M.A., Li, X.S., Loutre, M.F., Berger, A., 1998. The contribution of orbital forcing to the progressive intensification of Northern Hemisphere glaciation. Quatern. Sci. Rev. 17 (4-5), 411-426, doi:10.1016/S0277-3791(97)00047-4

Matzumoto, K., Lynch-Stieglitz, J., 2003. Persistence of the Gulf Stream separation during the Last Glacial Period: Implications for current separation theories. J. Geophys. Res. 108 (C6), 3174, doi:10.1029/2001IJC000861

Maze, J.P., Arhan, M., Mercier, H., 1997. Volume budget of the eastern boundary layer off the Iberian Peninsula. Deep Sea Research Part I: Oceanographic Research Papers 44, 1543-1574

McCartney, M.S. and Talley, L.D., 1982. The Subpolar Mode Water of the North Atlantic Ocean. J. Phys. Oceanogr. 12, 1169-1188

McIntyre, A., Ruddiman, W.F., Jantzen, R., 1972. Southward penetrations of the North Atlantic Polar Front: faunal and floral evidence of large-scale surface water mass movements over the last 225,000 years. Deep-Sea Res. 19, 61-77

McIntyre, A. et al., 1976. Glacial North Atlantic 18,000 years ago: A CLIMAP reconstruction. Geo. Soc. Am. Bull. 145, 43-76

McManus, J.F., Oppo, D.W., Cullen, J.L., 1999. A 0.5-million.year record of millennial. scale climate variability in the North Atlantic. Science, 283 (5404) 971-975, doi:10.1126/science.283.5404.971

McManus, J.F., Francois, R., Gherardi, J., Keigwin, L., Brown-Leger, S., 2004. Collapse and rapid resumption of Atlantic meridional circulation linked to deglacial climate change. Nature 428, 834-837

Mena, A., 2013. Paleoceanography and paleoclimatic evolution of the Galicia Interior Basin (NW Iberian Peninsula) during the past 60 ka. PhD Thesis, Universidad de Vigo

Miao, Q., Thunell, R.C., Anderson, D.M., 1994. Glacial-Holocene carbonate dissolution and sea surface temperatures in the South China and Sulu Seas. Paleoceanography 9, 269-290

Milankovitch, M., 1941. Canon of insolation and the ice-age problem. Royal Serbian Sciences Special Publication. Section of Mathematical and Natural Sciences, 33: 633

Miller, M.F., 1991. Morphology and palaeoenvironmental distribution of Paleozoic *Spirophyton* and *Zoophycos*: Implications for the *Zoophycos* ichnofacies. Palaios 6, 410-425

Miller, M.F., 2003. Styles of behavioral complexity recorded by selected trace fossils. Palaeogeography, Palaeoclimatology, Palaeoecology 192, 33-43

Miller, M.F., Johnson, K.G., 1981. *Spirophyton* in alluvial-tidal facies of the Castkill deltaic complex: possible biological control of ichnofossil distribution. Journal of Paleontology 55, 1016-1027

Mohtadi, M., Hebbeln, D., 2004. Mechanisms and variations of the paleoproductivity off northern Chile (24ºS-33ºS) during the last 40,000 years. Paleoceanography 19, PA20223, doi:10.1029/2004PA001003

Mojtahid, M., Jorissen, F., Lansard, B., Fontanier, C., Bombled, B., Rabouille, C., 2009. Spatial distribution of live benthic foraminifera in the Rhone prodelta: faunal response to a continental-marine organic matter gradient. Marine Micropaleontology 70, 177-200

Mortyn, P.G., Charles, CD., 2003. Planktonic foraminiferal depth habitat and d18O calibrations: Plankton tow results from the Atlantic sector of the Southern Ocean. Paleoceanography 18, 1037, doi:10.1029/2001PA000637

Mulitza, S., Dürkoop, A., Hale, W., Wefer, G., Niebler, H.S., 1997. Planktonic foraminifera as recorders of past surface-water stratification. Geology 25, 335–338

Müller, P.J., Kirst, G., Ruhland, G., von Storch, I., Rosell-Melé, A., 1998. Calibration of the alkenone paleotemperature index Uk´37 based on core-tops from the easten South Atlantic and the global ocean (60ºN-60ºS). Geochim. Cosmochim. Acta, 62 (10), 1757-1772, doi:10.1016/S0016-7037(98)00097-0

Naafs, B.D.A., Stein, R., Hefter, J., Khélifi, N., De Schepper, S., Haug, G.H., 2010. Late Pliocene changes in the North Atlantic Current. Earth and Planetary Science Letters 298, 434-442, doi:10.1016/j.epsl.2010.08.023

Naafs, B.D.A., Hefter, J., Ferretti, P., Stein, R., Haug, G.H., 2011 (a). Sea surface temperatures did not control the first occurrence of Hudson Strait Heinrich Events during MIS 16. Paleoceanography, 26, doi:10.1029/2011PA002135

Naafs, B.D.A., Hefter, J., Ferretti, P., Stein, R., Haug, G.H., 2011 (b). Biomarker abundance in MIS 16 of IODP Site 306-U1313. doi:10.1594/PANGAEA.757948

Olson, H.C. and Smart, C.W., 2004. Pleistocene climatic history reflected in planktonic foraminifera from ODP Site 1073 (Leg174A), New Jersey margin, NW Atlantic Ocean. Mar. Micropaleontol., 51, 213-238.

Ottens, J.J., 1991. Planktic foraminifera as North Atlantic watermass indicators. Oceanol. Acta, 14, 123-140.

Ottens, J.J., 1992. Planktic foraminifera as indicators of ocean envitonments in the northeast Atlantic. Ph. D. Thesis, Univ. of Amsterdam, Amsterdam

Paillard, D., Labeyrie, L., Yiou, P., 1996. Macintosh program performs time-series analysis. Eos Trans. AGU 77, 379

Pailler, D., Bard, E., 2002. High frequency palaeoceanographic changes during the past 140,000 years recorded by the organic matter in sediments off the Iberian Margin. Palaeogeography, Palaeoclimatology, Palaeoecology 181, 431-452

Peliz, A., Dubert, J., Santos, A.M.P., Oliveira, P.B., Le Cann, B., 2005. Winter upper ocean circulation in the Western Iberian Basin - Fronts, eddies and poleward flows: an overview. Deep Sea Research Part I: Oceanographic Research Papers 52, 621-646, doi:10.1016/j.dsr.2004.11.005

Pemberton, S.G., Frey, R.W., 1982. Trace fossil nomenclature and the *Planolites-Palaeophycus* dilema. Journal of Paleontology 56(4), 843-881

Peterson,L.C., Haug, G.H., Hughen, K.A., Tohl, U., 2000. Tapid changes in the tropical hydrologic cycle of the tropical Atlantic during the last glacial. Science 290, 1947-1951

Pflaumann, U., Duprat, J., Pujol, C., Labeyrie, L.D., 1996. SIMMAX: a modern analog technique to deduce Atlantic sea surface temperatures from planktonic foraminifera in deep-sea sediments. Paleoceanography 11 (1), 15-35

Pflaumann, U., Sarnthein, M., Chapman, M., de Abreu, L., Funnell, B., Huels, M., Kiefer, T., Maslin, M., 2003. Glacial North Atlantic: sea-surface conditions reconstructed by GLAMAP 2000. Paleoceanography 18, 1065, doi:1010.1029/2002PA000774

Pisias, N.G., Clark, P.U., Brook, E.J., 2010. Modes of global climate variability during Marine Isotope Stage 3 (60-26 ka). J.Clim. 23 (6), 1581-1588, doi:10.1175/2009JCLI3416,1

Poirier, R.K., Billups, K., 2014. The intensification of northern component deepwater formation during the mid-Pleistocene climate transition. Paleoceanography 29, 1046-1061, doi:10.1002/2014PA002661

Prell, W.L., 1984. Monsoonal climate of the Arabian Sea during the Late Quaternary. A response to changing solar radiation, in *Milankovitch and Climate*, edited by A. L. Berger et al., pp. 349-366, Springer, New York.

Prell, W.L., 1985. The stability of low-latitude sea-surface temperatures, an evaluation of the CLIMAP reconstruction with emphasis on the positive SST anomalies. Rep. TR025, US Dept. of Energy, Washington, DC

Prell, W., Martin, A., Cullen, J., Trend, M., 1999. The Brown University Foraminiferal Data Base. IGBP PAGES/World Data Center-A for Paleoclimatology, Data Contribution Series, 1999-1027. NOAA/NGDC Paleoclimatology Program, Boulder, CO, USA

Pujol, C.(1980),Lesforaminife`resplanctoni- ques de l'Atlantique Nord au Quaternaire: Ecologie Stratigraphie Environnement, thesis, Univ. Bordeaux I, Talence, France

Rahmstorf, S., 2002. Ocean circulation and climate during the past 120,000 years. Nature 419, 207-214

Railsback, L.B., Gibbard, P.L., Head, M.J., Voarintsoa, N.R.G., and Toucanne, S., 2015. An optimized scheme of lettered marine isotope substages for the last 1.0 million years, and the climatostratigraphic nature of isotope stages and substages. Quaternary Science Reviews 111, 94-106

Ravelo, A.C., Fairbanks, R.G., 1992. Oxygen isotopic composition of multiple species of planktonic foraminifera. Paleoceanography 7, 815–831

Raymo, M.E., Oppo, D.W. Curry, W.V., 1997. The mid-Pleistocene climate transition: A deep sea carbon isotopic perspective. Paleoceanography 12, 546-559

Raynaud, D., Loutre, M.F., Ritz, C., Chappellaz, J., Barnola, J.M., Jouzel, J., Lipenkov, V.Y., Petit, J.R., Vimeux, F., 2003. Marine Isotope Stage (MIS) 11 in the Vostok ice core: CO2 forcing and stability of East Antarctica, In: Droxler, A.W., Poore, R.Z., Burkle, L.H. (Eds.) Earth´s Climate and Orbital Eccentricity. The marine Isotope Stage 11 Question. Geophysical Monograph, 137. American Geophysical Union, Washington D.C., pp. 27-40

Renaud, S., Schmidt, D., 2003. Habitat tracking as a response of the planktic foraminifer Globorotalia truncatulinoides to environmental fluctuations during the last 140 ka. Marine Micropaleontology 49, 97–122

Reynolds, L., Thunell, R.C., 1985. Seasonal succession of planktonic foraminifera in the subpolar North Pacific. Journal of Foraminiferal Research 15, 282-301

Reynolds, L., Thunell, R.C., 1989. Seasonal succession of planktonic foraminifera; results from a four-year time-series sediment trap experiment in the Northeast Pacific. Journal of Foraminiferal Research 19, 253-267

Rios, A.F., Perez, F.F., Fraga, F., 1992. Water Masses in the Upper and Middle North-Atlantic Ocean East of the Azores. Deep-Sea Res. Pt. A, 39, 645-658

Roberts, N., Piotrowski, A., McManus, J., Keigwin, L., 2010. Synchronous deglacial overturning and water mass source changes. Science 327, 75-78

Rodo, W., Baert, E., Comin, F.A., 1997. Variations in seasonal rainfall in southern Europe during the present century: Relationships with the North Atlantic Oscillation and the El Niño-Southern Oscillation. Climate Dynamics 13, 275-284

Rodrigues, T., Voelker, A.H.L., Grimalt, J.O., Abrantes, F., Naughton, F., 2011. Iberian Margin sea surface temperature during MIS15 to 9 (580-300 ka): Glacial suborbital variability versus interglacial stability. Paleoceanography 26, 1-16, doi:10.1029/2010PA001927

Rodríguez-Tovar, F.J., Dorador, J., 2014. Ichnological analysis of Pleistocene sediments from the IODP Site U1385 “Shackleton Site” on the Iberian Margin: Approaching palaeoenvironmental conditions. Palaeogeography, Palaeoclimatology, Palaeoecology 409, 24-32

Rodríguez-Tovar, F.J., Dorador, J., in press. Ichnofabric characterization in cores: a method of digital image treatment. Annales Societatis Geologorum Poloniae

Rodríguez-Tovar, F.J., Uchman, A., 2004a. Trace fossils after the K–T boundary event from the Agost section, SE Spain. Geological Magazine 141, 429-440

Rodríguez-Tovar, F.J., Uchman, A. 2004b. Ichnotaxonomic analysis of the Cretaceous/Palaeogene boundary interval in the Agost section, south-east Spain. Cretaceous Research 25, 635-647

Rodríguez-Tovar, F.J., Uchman, A., 2006. Ichnological analysis of the Cretaceous–Palaeogene boundary interval at the Caravaca section, SE Spain. Palaeogeography, Palaeoclimatology, Palaeoecology 242, 313-325

Rodríguez-Tovar, F.J., Uchman, A., 2008. Bioturbational disturbance of the Cretaceous–Palaeogene (K–Pg) boundary layer: implications for the interpretation of the K–Pg boundary impact event. Geobios 41, 661-667

Rodríguez-Tovar, F.J., Uchman, A., 2010. Ichnofabric evidence for the lack of bottom anoxia during the Lower Toarcian Oceanic Anoxic event in the Fuente de la Vidriera section, Betic Cordillera, Spain. Palaios 25, 576-587Rogerson, M., Rohling, E.J., Weaver, P,P,E., Murray, J., 2004. The Azores Front since the last Glacial Maximum. Earth Planet. Sci. Lett. 222, 779-789

Roucoux, K.H., de Abreu, L., Shackleton, N.J., Tzedakis, P.C., 2005. The response of NW Iberian vegetation to North Atlantic climate oscillations during the last 65 kyr. Quaternary Science Reviews, 24, 1637-1653, doi:10.1016/j.quascirev.2004.08.022

Ruddiman, W.F., Bowles, F.A., 1977. Late Quaternary deposition of ice-rafted sand in the sub-polar North Atlantic (lat 40º to 65ºN). Geol. Soc. Am. Bull. 88, 1813-1827

Ruddiman, W.F., McIntyre, A., 1981. Oceanic mechanisms for amplification of the 23,000-year cycle. Science 212, 617-627

Ruddiman, W.F., Raymo, M.E., Martinson, D.G., Clement, B.M., Backman, J., 1989. Sea surface temperature reconstruction of DSDP Site 94-607 in the North Atlantic. doi:10.1594/PANGAEA.52373

Ruddiman, W.F., 2003. Orbital insolation, ice volume and greenhouse gases. Quaternary Science Reviews, 22 (15-17); 1597-1629

Ruddiman, W.F., 2006. Ice-driven CO_2 feedback on ice volume. Clim. Past 2, 43-55

Rühlemann, C., Mulitza, S., Müller, P.J., Wefer, G., Zahn, R., 1999. Warming of the tropical Atlantic Ocean and slowdown of thermohaline circulation during the last deglaciation. Nature 402, 511-514, doi:10.1038/990069

Salgueiro, E., Voelker, A., Abrantes, F., Meggers, Pflaumann, U., Loncaric, N., González-Álvarez, R., Oliveira, P., Bartels-Jónsdóttir, H.B., Moreno, J., Wefer, G. 2008. Planktonic foraminifera from modern sediments reflect upwelling patterns off Iberia: Insights from a regional transfer function. Marine Micropaleontology 66, 135-164, doi:10.1016/j.marmicro.2007.09.003

Salgueiro, E., Voelker, A.H.L., de Abreu, L., Abrantes, F., Meggers, H., Wefer, G., 2010. Temperature and productivity changes off the western Iberian margin during the last 150 ky. Quaternary Science Reviews 29, 680-695, doi:10.1016/j.quascirev.2009.11.013

Sánchez Goñi, M.F., Cacho, I., Turon, J.L., Guiot, J., Sierro, F.J., Peypouquet, J.P., Grimalt, J.O., Shackleton, N.J., 2002. Synchroneity between marine and terrestrial

responses to millennial scale climatic variability during the last glacial period in the Mediterranean region. Clim. Dyn. 19 (1), 95 - 105, doi:10.1007/s00382-001-0221-x

Sánchez Goñi, M.F., Landais, A., Fletcher, W.J., Desprat, S., Duprat, J., 2008. Contrasting impacts of Dansgaard-Oeschger events over a latitudinal transect modulated by orbital parameters. Quaternary Science Reviews 27, 1136-1151, doi:10.1016/j.quascirev.2008.03.003

Sánchez Goñi, M.F., Bard, E., Landais, A., Rossignol, L., d´Errico, F., 2013. Air-sea temperature decoupling in western Europe during the last interglacial-glacial transition. Nature Geoscience, doi:10.1038/NGEO1924

Sarnthein, M., Winn, K., Jung, S.J.A., Duplessy, J.C., Labeyrie, L., Erlenkeuser, H., Ganssen, G., 1994. Changes in east Atlantic deepwater circulation over the last 30,000 years: eight time slice reconstructions. Paleoceanography 9, 209-267

Schiebel, R., Hemleben, C., 2000. Interannual variability of planktic foraminiferal populations and test flux in the eastern North Atlantic Ocean (JGOFS). Deep Sea Research Part II: Topical Studies in Oceanography 47 (9-11), 1809-1852, doi:10.1016/S0967-0645(00)00008-4

Schiebel, R., Waniek, J., Bork, M., Hemleben, C., 2001. Planktic foraminiferal production simulated by chlorophyll redistribution and entrainment of nutrients. Deep Sea Research Part I: Oceanographic Research Papers 48, 721-740

Schiebel, R., Schmuker, B., Alves, M. Hemleben, C., 2002. Tracking the recent and late Pleistocene Azores front by the distribution of planktic foraminifers. J. Mar.Syst. 37, 213-227

Schieller, A., Milkolajewicz, U., Voss, R., 1997. The stability of North Atlantic thermohaline circulation in a coupled ocean-atmosphere general circulation model. Clim. Dyn. 13, 325-347

Schlirf, M., 2000. Upper Jurassic trace fossils from the Boulonnais (northern France). Geologica et Palaeontologica 34, 145-213

Schmiedl, G., Mackensen, A., 1997. Late Quaternary paleoproductivity and deep water circulation in the eastern South Atlantic Ocean: Evidence from benthic foraminifera. Palaeogeography, Palaeoclimatology, Palaeocology 130, 43-80.

Schmiedl, G., Mackensen, A., Muller, P.J., 1997. Recent benthic foraminifera from the eastern South Atlantic Ocean: Dependence on food supply and water masses. Marine Micropaleontology 32, 249-287.

Schmidt,M.W., Spero, H.J., Lea, D.W., 2004. Links between salinity variation in the Caribbean and North Atlantic thermohaline circulation. Nature 428, 160-163

Schmuker, B. and Schiebel, R., 2002. Planktic foraminifera and hydrography of the eastern and northern Caribbean Sea. Mar. Micropaleontol., 46, 387-403

Schulz, H., con Rad, U., Erlenkeuser, H., 1998. Correlation between Arabian Sea and Greenland climate oscillations of the past 110,000 years. Nature, 393, 54-57

Seilacher, A., 1990. Aberrations in bivalve evolution related to photo-and chemosymbiosis. Historical Biology 3(4), 289-311

Serra, N., Ambar, I., Boutov, D., 2010. Surface expression of Mediterranean Water dipoles and their contribution to the shelf/slope-open ocean Exchange. Ocean Sci 6, 191-209

Shackleton, N.J., Pisias, N.G., 1985. Atmospheric carbon dioxide, orbital forcing and climate. In: E.T. Sundquist and W.S. Broecker (Ed.), The Carbon cycle and atmospheric CO_2: natural variations, Archean to present. American Geophysical Union, Washington, D.C.

Shackleton, N.J., Berger, A., Peltier, W.R., 1990. An alternative astronomical calibration of the lower Pleistocene time scale based on OSP Site 677. Trans. R. Soc. Edinburgh Earth Sci. 81, 251-261

Shackleton, N.J., Hall, M.A., Vincent, E., 2000. Phase relationships between millennial-scale events 64,000-24,000 years ago. Paleoceanoraphy, 15-6, 565-569, doi:10.1029/2000PA000513

Shackleton, N., Fairbanks, R., Chiu, T.C., Parrenin, F., 2004. Absolute calibration of the Greenland time scale: implications for Antarctic time scales and for $\Delta^{14}C$. Quaternary Science Reviews 23(14), 1513-1522

Sierro, F.J., Andersen, N., Bassetti, M.A., Berné, S., Canals, M., Curtis, J.H. Dennielou, B., Flores, J.A., Frigola, J., Gonzalez-Mora, B., Grimalt, J.O., Hodell, D.A., Jouet, G., Pérez-Folgado, M., Scheider, R., 2009. Phase relationship between sea level and abrupt climate change. Quaternary Science Reviews 28, 2867-2881, doi:10.1016/j.quascirev.2009.07.019

Skinner, L. C., and N. J. Shackleton (2006), Deconstructing Termination I and II: revisiting the glaciowustatic paradigm base don deep-water temperatura estimates. Quat. Sci. Rev., 25, 3312-3321Skinner, L.C., Elderfield, H., 2007. Rapid fluctuations in the deep North Atlantic heat budget during the last glacial period. Paleoceanography 22, doi:10.1029/2996PA001338

Skinner, L.C., Shackleton, N.J., Elderfield, H., 2003. Millennial-scale variability of deep-water temperature and $d^{18}O_{dw}$ indication deep-warer source variations in the northeast Atlantic, 0-34 cal. Ka BP. Geochem. Geophys. Geosyst. 4, 1098, doi:10.1029/2003GC000585

Skinner, L.C., Elderfield, H., 2007. Rapid fluctuations in the deep North Atlantic heat budget during the last glacial period. Paleoceanography 22, PA1205, doi:10.1029/2006PA001338

Sousa, J.M., Bricaud, A., 1992. Satellite-derived phytoplankton pigment structures in the Portuguese upwelling area. J. Geophys. Res. 97, 11,343-11,356

Spindler, M., Hemleben, Ch., Salomons, J.B., Smit, L.P., 1984. Feeding behaviour of some planktonic foraminifers in laboratory cultures. Journal of Foraminiferal Research 14, 237-249

Stangeew, E., 2001. Distribution and Isotopic Composition of Living Planktonic Foraminifera *N. pachyderma* (sinistral) and *T.quinqueloba* in High Latitude North

Atlantic, Ph.D. dissertation, Mathematisch-Naturwissenschaftlichen Fakultät. Christian-Albrechts-Universität, Kiel, Germany

Stein, R., Hefter, J., Grützner, J., Voelker, A., Naafs, B.D.A., 2009. Variability of surface water characterstics and Heinrich-like events in the Pleistocene midlatitude North Atlantic Ocean: Biomarker and XRD records from IODP Site U1313 (MIS 16-9). Paleoceanography 24, doi:10.1029/2008PA001639

Stich, D., Serpelloni, E., Mancilla, F.-L., and Morales, J., 2006. Kinematics of the Iberia–Maghreb plate contact from seismic moment tensors and GPS observations, Tectonophysics, 426, 295–317

Stow, D.A.V., Hernández-Molina, F.J., Alvarez-Zarikian, C.A., and Expedition 339 Scientists, 2012. Mediterranean outflow: environmental significance of the Mediterranean Outflow Water and its global implications. IODP Preliminary Report, 339, doi:10.2204/iodp.pr.339.2012

Stow, D.A.V., Hernández-Molina, F.J., Alvarez-Zarikian, C.A., and Expedition 339 Scientists, 2013. Proceedings of the Integrated Ocean Drilling Program, vol. 339, doi:10.2204/iodp.proc.339.103.2013

Stocker, T.F., 1999. Past and future reorganisations in the climate system. Quaternary Science Reviews 19, 301-319

Stuiver, M., Grootes, P.M., 2000. GISP2 oxygen isotope ratios. Quaternary Research 53 (3), 277-284, doi:10.1016/qres.2000.2127

Swift, J., 1986. The Arctic waters. In: Hurdle, B.G. (Ed.). The Nordic Seas. Springer, New York, p. 129-151

Thunnel, R., Sautter, L.R., 1992. Planktonic foraminiferal faunal and stable isotopic indicators of upwelling: Results from sediment trap study in the California Current. In *Evolution of Upwelling Systems Since the Early Miocene*, edited by Summerhayes, C.P., Prell, W.L., Emeis, K.C. Geol. Soc. Spec. Publ. London, pp. 77-91

Thiede,J.,1971. Variations in coiling ratios of Holocene planktonic foraminifera. Deep-Sea Research 18

Toggweiler, J.R., Russell, J.L., Carson, S.R., 2006. Midlatitude westerlies, atmospheric CO2 and climate change during the ice ages. Paleoceanoghraphy, 21 (2)

Tolderlund, D.S., Bé, A.W.H., 1971. Seasonal distribution of planktonic foraminifera in the western North Atlantic. Micropaleontology 17, 297-329

Tzedakis, P.C., Channell, J.E.T., Hodell, D.A., Kleiven, H.F., Skinner, L.C., 2012. Determining the natural length of the current interglacial. Nature Geoscience 5, doi:10.1038/NGEO1358

Tziperman, E., Raymo, M.E., Huybers, P., Wunsch, C., 2006. Consequences of pacing the Pleistocene 100 kyr ice ages by nonlinear phase locking to Milankovitch forcing. Paleoceanography 21

Uchman, A., 1995. Taxonomy and palaeoecology of flysch trace fossils: The Marnoso-arenacea Formation and associated facies (Miocene, Northern Appenines, Italy). Beringeria 15, 1-114

Uchman, A., 1999, Ichnology of the Rhenodanubian Flysch (Lower Cretaceous-Eocene) in Austria and Germany. Beringeria 25, 67-173

Uchman, A., Wetzel, A., 2011. Deep-sea ichnology: the relationships between depositional environment and endobenthic organisms. In: Hüneke, H., Mulder, T. (Eds.), Deep-Sea Sediments, Developments in Sedimentology 63, Elsevier, Amsterdam, pp. 517-555

Vautravers, M. J., and N. J. Shackleton, 2006. Centennial-scale surface hydrology off Portugal during marine isotope stage 3: Insights from planktonic foraminiferal fauna variability, Paleoceanography, 21, PA3004, doi:10.1029/2005PA001144

Vautravers, M.J., Shackleton, N.J., Lopez-Martinez, C., Grimalt, J.O., 2004. Gulf Steam variability during marine isotope stage 3. Paleoeanography 19, PA2011, doi:10.1029/2003PA000966

Vidal, L., Labeyrie, L., Van Weering, T.C.E.,1998. Benthic $d^{18}O$ records in the North Atlantic over the last glacial period (60-10 kyr): evidence for brine formation. Paleoceanography 13 (3), 245-251

Villanueva, J., Calvo, E., Pelejero, C., Grimalt, J.O., Boelaert, A., Labeyrie, L., 2001. A latitudinal productivity band in the Central North Atlantic over the last 270 kyr: an alkenone perspective. Paleoceanography 16, 617-626, doi:610.1029/2000PA000543

Voelker, A.H.L., Rodrigues, T., Billups, K., Oppo, D., McManus, J., Stein, R., Hefter, J., Grimalt, J.O., 2010. Variations in mid-latitude North Atlantic surface water properties during the mid-Brunhes (MIS 9-14) and their implications for the thermohaline circulation. Clim. Past 6, 531-552, doi:10.5194/cp-6-531-2010

Wanner, H., Brönnimann, S., Casty, C., Gyalistras, D., Luterbacher, J., Schmutz, C., Stephenson, D.B., Xoplaki, E., 2001. North Atlantic oscillation-concepts and studies. Surveys in Geophysics 22, 321-382

Watts, W.A., Allen, J.R.M., Huntley,B., 1996. Vegetation history and palaeoclimate of the last glacial period at Logo Grande di Nonticchio, southern Italy. Quaternary Science Reviews 15, 133-153

Wetzel, A., 1991. Ecologic interpretation of deep-sea trace fossil communities. Palaeogeography, Palaeoclimatology, Palaeoecology 85(1-2), 47-69

Wetzel, A., 2002. Modern Nereites in the South China Sea—ecological association with redox conditions in the sediment. Palaios 17(5), 507-515

Wetzel, A., Uchman, A., 2012. Hemipelagic and pelagic basin plains. In: Bromley, R.G., Knaust, D. (Eds.), Trace Fossils as Indicators of Sedimentary Environments. Developments in Sedimentology 64, Elsevier, Amsterdam, pp. 673-701

Wollenburg, J.E., Knies, J., Mackensen, A., 2004. High-resolution paleoproductivity fluctuations during the past 24 kyr as indicated by benthic foraminifera in the

marginal Arctic Ocean. Palaeogeography, Palaeoclimatology, Palaeoecology 204, 209-238

Wooster, W. S., Bakun, A., McLain, D. R., 1976. The seasonal upwelling cycle along the eastern boundary of the North Atlantic, J. Mar. Res., 34(2), 131–141

Wright, A.K., Flower, B.P., 2002. Surface and deep ocean circulation in the subpolar North Atlantic during the mid-Pleistocene revolution. Paleoceanography 17, 1068, doi:10.1029/2002PA000782

Zahn, R., Schönfeld, J., Kudrass, H.R., Park, M.H. Erlenkeuser, H., Grootes, P., 1997. Thermohaline instability in the North Atlantic during meltwater events: Stable isotope and ice-rafted detritus records from core SO75-26KL, Portuguese margin. Paleoceanography 12, 696-710

Zitellini, N., Gràcia, E., Matias, L., Terrinha, P., Abreu, M. A., DeAlteriis, G., Henriet, J. P., Dañobeitia, J. J., Mas- son, D. G., Mulder, T., Ramella, R., Somoza, L., and Diez, S., 2009. The quest for the Africa–Eurasia plate boundary west of the Strait of Gibraltar. Earth Planet. Sc. Lett. 280, 13–50, doi:10.1016/j.epsl.2008.12.005

ANEXOS

APPENDICES

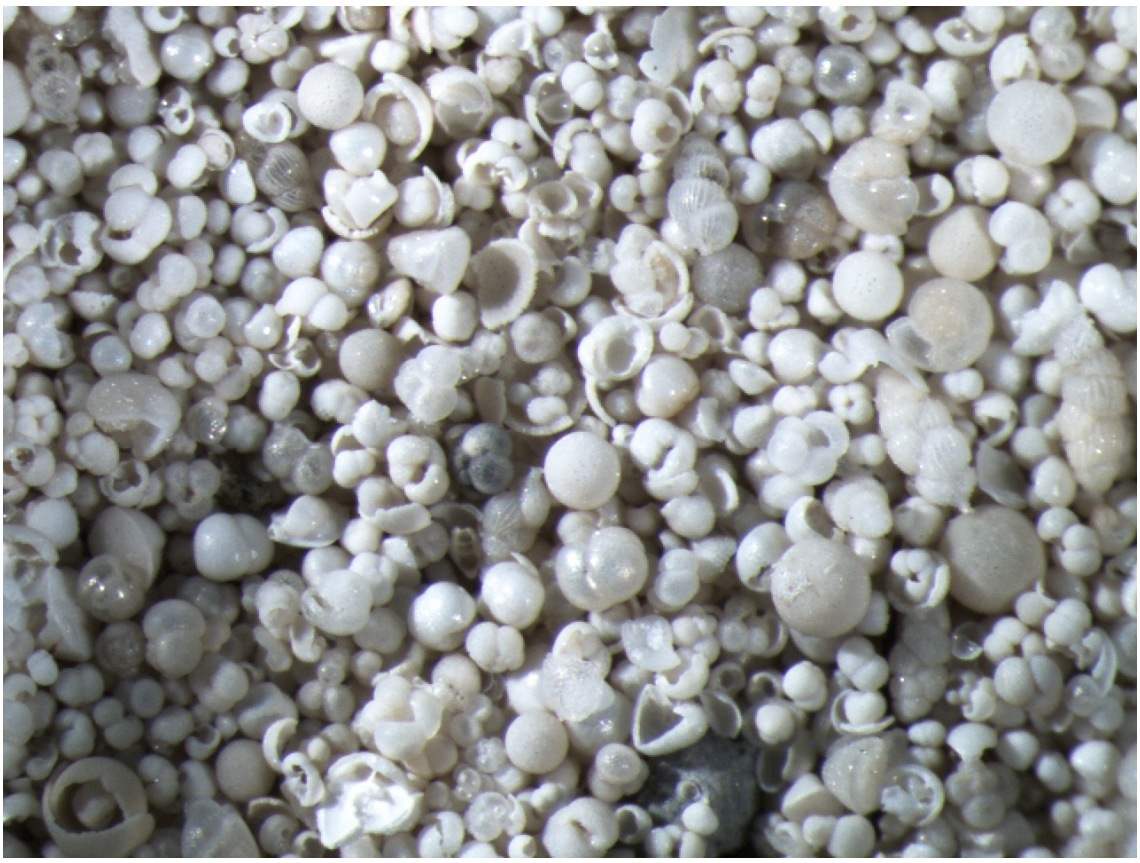

ANEXO I: CLASIFICACIÓN TAXONÓMICA DE LAS ESPECIES IDENTIFICADAS EN EL TESTIGO IODP-U1385 Y ESTUDIADAS PARA ESTA MEMORIA

REINO **PROTOCTISTA**

FILUM PROTOZOA

Subfilum SARCODINA

Clase FORAMINIFERA d´Orbigny, 1826

Orden FOMAMINIIFERIDA Eichwald, 1830

Suborden GLOBIGERININA Delage & Hérouard, 1896

Superfamilia GLOBIGERINOIDEA Carpenter, Parker & Jones, 1862

Familia GLOBIGERINIDAE (Carpenter, Parker & Jones) Schultze, 1877

Subfamilia GLOBIGERININAE (Carpenter, Parker & Jones) Cushman, 1927

Beella Banner and Blow, 1960

B. digitata Brady, 1879

Globigerina d´Orbigny, 1826

G. bulloides d´Orbigny, 1826

G. falconensis Blow, 1959

Globigerinella Cushman, 1927

G. calida Parker, 1962

G. aequilateralis Brady, 1884

= *Globigerina siphonifera* d´Orbigny, 1839

Globigerinoides (d´Orbigny) Cushman, 1927

G. conglobatus (Brady) Parker, 1962

G. ruber (d´Orbigny) Bé, 1967

G. sacculifer (Brady) Bé, 1967

G. tenellus Paker, 1958

Globoturborotalita Hofker, 1976

G. rubescens Hofker, 1956

Globorotaloides Bolli, 1957

G. hexagonus Natland, 1938

Sphaeroidinella Cushman, 1927

S. dehiscens Parker and Jones, 1865

Subfamilia ORBULININAE Schultze, 1854

Orbulina d´Orbigny, 1839

O. universa d´Orbigny, 1839

O. suturalis Broennimann, 1951

Familia TURBOROTALITIDAE Hofker, 1976

Subfamilia TURBOROTALITINAE Hofker, 1976

Turborotalita (Brady) Blow & Banner, 1962

T. quinqueloba Natland, 1938

T. humilis Brady, 1884

Familia GLOBOROTALIIDAE Cushman ,1927

Globorotalia Cushman & Bermúdez, 1949

G. crassaformis Galloway and Wissler, 1927

G. hirsuta (d´Orbigny) Parker, 1962

G. inflata (d´Orbigny) Parker, 1962

G. scitula (Brady) Parker, 1962

G. truncatulinoides (d´Orbigny) Bé, 1967

Neogloboquadrina Bandy et al., 1967

N. dutertrei d´Orbigny, 1839

N. pachyderma (Ehrenberg) Brady, 1884

Familia PULLENIATINIDAE Cushman, 1927

Pulleniatina Cushman, 1927

P. obliquiloculata Parker and Jones, 1865

Superfamilia GLOBOROTALIOIDEA Cushman, 1927

Familia CANDEINIDAE Cushman, 1927

Subfamilia CANDEININAE Cushman, 1927

Candenia d´Orbigny, 1839

C. nitida d´Orbigny, 1839

Subfamilia GLOBIGERINITINAE Bermúdez, 1961

Globigerinita Brönnimann, 1951

G. glutinata (Egger) Parker 1962

G. uvula Ehrenberg, 1861

Tenuitellinata Li, 1987

T. iota Parker, 1962

Subfamilia TENUITELLINAE Banner, 1982

Tenuitella Fleisher, 1974

T. munda Jenkins, 1966

ANEXO II: ESPECIES Y MORFOTIPOS DE FORAMINÍFEROS PLANKTÓNICOS UTILIZADOS PARA RECONSTRUIR LA PALEOTEMPERATURA OCEÁNICA SUPERFICIAL

Beella digitata

Candenia nitida

Globigerina bulloides

Globigerina falconensis

Globigerinella calida

Globigerinella siphonifera (aequilateralis)

Globigerinita glutinata

Globigerinita uvula

Globigerinoides conglobatus

Globigerinoides ruber (pink)

Globigerinoides ruber (white)

Globigerinoides sacculifer (con saco)

Globigerinoides sacculifer (sin saco)

Globorotalia crassaformis (dextrorsa)

Globorotalia crassaformis (sinistrorsa)

Globorotalia hirsuta

Globorotalia inflata

Globorotalia scitula (dextrorsa)

Globorotalia scitula (sinistrorsa)

Globorotalia truncatulinoides (dextrorsa)

Globorotalia truncatulinoides (sinistrorsa)

Globorotaloides hexagonus

Globoturborotalita rubescens

Globoturborrotalita tenella

Neogloboquadrina dutertrei

Neogloboquadrina pachyderma (dextrorsa)

Neogloboquadrina pachyderma (sinistrorsa)

Orbulina universa

Pulleniatina obliquiloculata

Sphaeroidinella dehiscens

Tenuitella munda

Turborotalita humilis

Turborotalia quinqueloba

ANEXO III: ESPECIES Y MORFOTIPOS DE FORAMINÍFEROS PLANKTÓNICOS UTILIZADOS PARA RECONSTRUIR LA PALEOPRODUCTIVIDAD EXPORTADA

Beella digitata

Globigerina bulloides

Globigerina falconensis

Globigerinella calida

Globigerinella siphonifera (aequilateralis)

Globigerinita glutinata

Globigerinoides ruber (rosa)

Globigerinoides ruber (blanco)

Globigerinoides sacculifer

Globigerinoides trilobus

Globorotalia hirsuta

Globorotalia inflata

Globorotalia scitula

Globorotalia truncatulinoides

Globoturborotalita rubescens

Globoturborrotalita tenella

Neogloboquadrina dutertrei

Neogloboquadrina pachyderma (dextrorsa)

Neogloboq. pachyderma (sinistrorsa)

Orbulina universa

Pulleniatina obliquiloculata

Turborotalita humilis

Turborotalia quinqueloba

ANEXO IV: ASOCIACIONES DE FORAMINÍFEROS PLANKTÓNICOS UTILIZADAS PARA IDENTIFICAR LAS DISTINTAS MASAS DE AGUA Y CORRIENTES DEL ATLÁNTICO NORTE

ASOCIACIÓN SUBTROPICAL (Cayre et al., 1999)

Beela digitata
Candenia nitida
Globigerinella aequilateralis
Globigerinoides sps
Globoturborotalita rubescens
Globoturborotalita tenella
Pulleniatina obliquiloculata

CORRIENTE NORD-ATLÁNTIC A (*North Atlantic Current*) (Ottens, 1991)

Globigerina bulloides
Globigerinella siphonifera (aequilateralis)
Globorrotalia inflata
Neogloboquadrina pachyderma (dextrorsa)

CORRIENTE DE LAS AZORES (*Azores Current*) (Ottens, 1991)

Globigerinella siphonifera (aequilateralis)
Globigerinita glutinata
Globigerinoides conglobatus
Globigerinoides ruber
Globorotalia crassaformis
Globorotalia scitula
Globoturborotalita rubescens
Globoturborotalita tenella
Neogloboquadrina dutertrei
Pulleniatina obliquiloculata

CORRIENTE DE LAS AZORES (*Azores Current*) (Salgueiro et al., 2008)

Globigerinoides ruber (blanco)
Globorotalia inflata

ASOCIACIÓN CÁLIDA SUPERFICIAL (Vautravers et al., 2004)

Beela digitata
Globigerina falconensis
Globigerinella siphonifera (aequilateralis)
Globigerinoides ruber
Globigerinoides sacculifer
Globoturborotalita rubescens
Globoturborotalita tenella
Orbulina universa
Pulleniatina obliquiloculata

ANEXO V: LISTADO DE FIGURAS Y TABLAS

ANEXO VI: LISTADO DE ABREVIATURAS Y ACRÓNIMOS UTILIZADOS

A continuación se relacionan alfabéticamente los acrónimos y abreviaturas utilizados en esta memoria. En algunos casos se incluye su traducción al español o una pequeña explicación de su significado.

AABW: *Antarctic Bottom Water*

AF: *Arctic Front*

AMOC: *Atlantic Meridional Overturning Circulation* (circulación profunda en dirección Sur de aguas originadas en el Atlántico Norte)

ANN: *Artificial Neural Networks* (método para reconstruir paleotemperaturas a partir de asociaciones fósiles)

AR: *Accummulation Rate*

AzC: *Azores Current*

AzH: *Azores High-pressure area*

CLIMAP: *Climate Long Range Investigation, Mapping and Prediction*

crmcd: corrected *revised meters of composite depth* (profundidad en metros, revisada y corregida, de la composición realizada utilizando todos los testigos de una localización de sondeo)

EDC: *Epica Dome C* (uno de los sondeos efectuados en hielo Antártico)

ENACW: E*astern North Atlantic Central Water* (masa de agua superficial presente en el Este del Atlántico Norte)

ENACWsp: *Eastern North Atlantic Central Water of subpolar origin*

ENACWst: *Eastern North Atlantic Central Water of subtropical origin*

EPICA: European Project for Ice Coring in Antarctica

FI: *Fragmentation Index*

IODP: *International Ocean Discovery Program*

IPC: *Iberian Poleward Current* (corriente de aguas cálidas en dirección norte formada a lo largo del margen oeste ibérico)

IRD: *Ice Rafted Debris* (material arrastrado por glaciares, que es transportado y depositado mar adentro por témpanos flotantes)

ITCZ: *Intertropical Convergence Zone*

ka: *kilo-annii*

ky*: kilo-years*

LDW: *Lower Deep Water* (agua abisal compuesta principalmente por *AABW*)

LGM: *Last Glacial Maximum*

LNADW: *Lower North Atlantic Deep Water*

LR04 / L&R-04: Benthic $d^{18}O$ stack (Lisiecki and Raymo, 2005)

LSW: *Labrador Sea Water* (masa de agua fría y profunda originada en el Labrador y que circula en el Atlántico Norte a profundidades medias)

MARGO: *Multiproxy Approach for the Reconstruction of the Glacial Ocean surface*

MAT: *Modern Analog Technique* (técnica para reconstruir condiciones oceanográficas de registros fósiles: temperatura de aguas superficiales, productividad, etc.)

MIS: *Marine Isotope Stage*

NAC: *North Atlantic Current*

NACW: *North Atlantic Central Water* (masa de agua superficial en el Atlántico Norte que llega hasta los 500-600 m de profundidad)

NADW: *North Atlantic Deep Water* (masa de agua más profunda originada en el Atlántico Norte; fluye sobre la *LDW*)

NHG: *Northern Hemisphere Glaciation*

NAO: *North Atlantic Oscillation*

ODP: *Ocean Drilling Program*

PC: *Portugal Current* (rama en dirección sur de la *NAC* a lo largo del margen ibérico)

PF: *Polar Front*

rmcd: *revised meters of composite depth* (profundidad en metros revisada de la composición realizada utilizando todos los testigos de una localización de sondeo)

SST: *Sea Surface Temperature*

VPDB: *Vienna Pee Dee Belemnite*

ANEXO VII: COPIA DE LOS ARTÍCULOS PUBLICADOS

SEVERE COOLING EPISODES AT THE ONSET OF DEGLACIATIONS ON THE SOUTHWESTERN IBERIAN MARGIN FROM MIS 21 TO 13 (IODP SITE U1385)

Gloria Maria Martin-Garcia, Montserrat Alonso-Garcia, Francisco J Sierro, David A Hodell, José A Flores

Global and Planetary Change 135 (2015), doi: 10.1016/j.gloplacha.2015.11.001

RESPONSE OF MACROBENTHIC AND FORAMINIFER COMMUNITIES TO CHANGES IN DEEP- SEA ENVIRONMENTAL CONDITIONS FROM MARINE ISOTOPE STAGE (MIS) 12 TO 11 AT THE "SHACKLETON SITE"

Francisco J. Rodríguez-Tovar, Javier Dorador, Gloria M. Martin-Garcia, Francisco J. Sierro, José A. Flores, David A. Hodell

Global and Planetary Change 133 (2015), doi: 10.1016/j.gloplacha.2015.08.012

Global and Planetary Change 135 (2015) 159–169

Contents lists available at ScienceDirect

Global and Planetary Change

journal homepage: www.elsevier.com/locate/gloplacha

Severe cooling episodes at the onset of deglaciations on the Southwestern Iberian margin from MIS 21 to 13 (IODP site U1385)

Gloria M. Martin-Garcia [a,*], Montserrat Alonso-Garcia [b], Francisco J. Sierro [a], David A. Hodell [c], José A. Flores [a]

[a] Departamento de Geología, Universidad de Salamanca, Salamanca, Spain
[b] Div. de Geologia e Georecursos Marinhos, Instituto Português do Mar e da Atmosfera, Lisboa, Centro de Ciencias do Mar, Univ. Algarve, Faro, Portugal
[c] Godwin Laboratory for Palaeoclimate Research, Department of Earth Sciences, University of Cambridge, UK

ARTICLE INFO

Article history:
Received 27 March 2015
Received in revised form 3 November 2015
Accepted 5 November 2015
Available online 7 November 2015

Keywords:
North Atlantic
Iberian margin
Deglaciations
Millennial-scale SST variability
Pleistocene
Planktonic foraminifers

ABSTRACT

Here we reconstruct past sea surface water conditions on the SW Iberian Margin by analyzing planktonic foraminifer assemblages from IODP Site U1385 sediments (37°34.285′N, 10°7.562′W; 2585 m depth). The data provide a continuous climate record from Marine Isotope Stages (MIS) 21 to 13, extending the existing paleoclimate record of the Iberian Margin back to the ninth climatic cycle (867 ka). Millennial-scale variability in Sea Surface Temperature (SST) occurred during interglacial and glacial periods, but with wider amplitude (>5 °C) at glacial onsets and terminations. Pronounced stadial events were recorded at all deglaciations, during the middle Pleistocene. These events are recorded by large amplitude peaks in the percentage of *Neogloboquadrina pachyderma* sinistral coincident with heavy values of planktonic $\delta^{18}O$ and low Ca/Ti ratios. This prominent cooling of surface waters along the Portuguese margin is the result of major reorganizations of North Atlantic surface and deep-water circulation in response to freshwater release to the North Atlantic when ice sheets collapse at the onset of deglaciations. In fact, most of these cooling events occurred at times of maximum or increasing northern Hemisphere summer insolation. The slowdown of deep North Atlantic deep-water formation reduced the northward flow of the warm subtropical North Atlantic Drift, which was recorded on the Iberian margin by enhanced advection of northern cold subpolar waters. Following each episode of severe cooling at the onset of deglaciations, surface water experienced abrupt warming that initiated the climatic optimum during the early phase of interglacials. Abrupt warming was recorded by a sudden increase of the subtropical assemblage that indicates enhanced northward transport of heat through the North Atlantic Drift. At the onset of glaciations, SST along the Portuguese margin remained relatively warm while the surface waters of the North Atlantic experienced cooling, generating a large latitudinal SST gradient.

1. Introduction

The western Iberian margin has proven to be a crucial location for the comprehensive evaluation of millennial climate variability between hemispheres over the late Pleistocene, offering a direct comparison with Antarctic and Greenland ice core records (e.g. Shackleton et al., 2000; Martrat et al., 2007). A large number of studies have been conducted using piston cores from this area to partially characterize the last six climatic cycles (Cayre et al., 1999; Bard et al., 2000; de Abreu et al., 2003; Roucoux et al., 2005; Vautravers and Shackleton, 2006; Martrat et al., 2007; Rodrigues et al., 2011).

The western part of the Iberian Peninsula is very sensitive to variations in the North Atlantic surface circulation dynamics. The Iberian margin is located in a key region characterized by the interplay of subpolar waters brought by the Portugal Current, which constitutes the descending branch of the North Atlantic Drift, and subtropical waters brought by the Azores Current. Changes in the intensity of the northward flow of the North Atlantic Drift drive a deep impact on the north Atlantic subpolar and subtropical gyres, as well as on the position of the Polar, Arctic and subtropical fronts.

For the last climatic cycles various studies have illustrated the relationship between ice sheets instabilities in the northern Hemisphere and the southward migrations of the Arctic Front (AF) as far south as the Iberian margin (Bard et al., 2000) via the recirculation of cold water through the subtropical gyre eastern currents. Millennial-scale oscillations of Sea Surface Temperature (SST) at the Portuguese margin have been related to changes in North Atlantic surface circulation driven by freshwater perturbations at high latitudes (eg., Lebreiro et al., 1996, 1997; Zahn et al., 1997; Cayre et al., 1999; de Abreu et al., 2005; Vautravers and Shackleton, 2006; Martrat et al., 2007; Eynaud et al., 2009; Rodrigues et al., 2011). These oscillations also affected the continental climate across southern Europe via atmosphere–ocean coupling (Allen et al., 1999; Roucoux et al., 2005; Sánchez Goñi et al., 2008, 2013).

* Corresponding author.
E-mail address: gm.martin@usal.es (G.M. Martin-Garcia).

http://dx.doi.org/10.1016/j.gloplacha.2015.11.001
0921-8181/

During the last glacial cycle a series of layers with high abundances of the polar species *Neogloboquadrina pachyderma* sinistral (Nps) were recorded along the Portuguese margin during Heinrich events (e.g., Lebreiro et al., 1997; de Abreu et al., 2003). In certain sites those layers also contained important amounts of Ice rafted debris (IRD) although the presence or absence of IRD rich layers off the Iberian margin during these events depends on the proximity to the shore. Sites located further offshore usually record IRD layers (Lebreiro et al., 1996; Bard et al., 2000) whereas sites nearshore rarely register them (Zahn et al., 1997).

At the same time, the Portuguese margin provides an excellent location to monitor past changes in deep water circulation and heat and salt exchange between Hemispheres (Hodell et al., 2013a). Millennial-scale oscillations in surface circulation recorded along the Portuguese margin were linked to significant changes in deep water circulation. Shutdown or reduced deep water formation in the North Atlantic in response to freshwater perturbations is registered in the SW Iberian margin by reduced flux of the North Atlantic Deep Water (NADW) and a rapid replacement by the northward flux of the Antarctic Bottom Water (AABW) (Shackleton et al., 2000; Skinner et al., 2003).

Before Integrated Ocean Drilling Program (IODP) Expedition 339 the existing sediment cores in the western Iberian margin only provided climatic and oceanographic reconstructions back to late Marine Isotope Stage 15 (e.g. Bard et al., 2000; Rodrigues et al., 2011). The sediment cores from Site U1385 (Shackleton Site), retrieved during Expedition 339, allow us to extend the record back to 870 ka and investigate the response of the mid-latitude eastern North Atlantic to climatic changes during the interval between 870 and 490 ka. In this work we studied planktonic foraminifer assemblages and combined them with the oxygen isotopes records from IODP Site U1385 to reconstruct the history of sea surface temperature on the southwest Iberian Margin from MIS 21 to MIS 13, thereby extending the existing record in the area back to the ninth climatic cycle.

Given that previous works suggested the Iberian Margin can play a pivotal role in understanding the millennial-scale climate variability during the last glacial cycle (Shackleton et al., 2000, Vautravers and Shackleton, 2006), in this work we aim to study the suborbital climate variability at this location during the last part of the middle Pleistocene transition (MPT, ~1250–700 ka; Clark et al., 2006) and state the influence that subpolar North Atlantic climatic oscillations and meridional SST gradients had on climatic events during and since the emergence of the 100-ka cycles.

2. Regional and oceanographic setting

IODP Site U1385 was drilled at the "Shackleton site", off the western Iberian margin (37°34.284′N, 10°7.562′W), at 2578 m water depth.

The western Iberian margin lies at present under the influence of several distinct water masses, which have been clearly identified and characterized (e.g. Fiúza et al., 1998; Peliz et al., 2005; Serra et al., 2010). These are, from top to bottom: the *North Atlantic Central Water* (NACW), reaching around 500–600 m depth and characterized by a complex circulation pattern; the *Mediterranean Outflow Water*, warm and very saline, between the NACW and 1500 m; the *Labrador Sea Water* (LSW) can reach 2200 m depth, depending on the density difference with the *Northeast Atlantic Deep Water* (NEADW), which flows down to 4000 m depth; and, across the lower slope and abyssal plains, the *Lower Deep Water*, composed mainly of Antarctic Bottom Water (AABW). The studied site (Fig. 1) is currently under the influence of NACW at the surface and NEADW at the sea floor. Surface water circulation in the area is determined by the eastern gyre of the North Atlantic (Eastern North Atlantic Central Water or ENACW) which consists of two branches, the Portugal Current in the north, of sub polar origin, and the Azores Current in the south, of subtropical origin. The general distribution of water masses is influenced by the seasonal migration of the Azores anticyclonic cell and its associated large-scale wind pattern. In summer, strong northerly Trade winds along west Iberia induce a coastal upwelling of the deeper layers of ENACW.

3. Material and methods

Sediments at Site U1385 define a single lithological unit dominated by calcareous muds and calcareous clays, with varying proportions of biogenic carbonate (23%–39%) and terrigenous sediment. Pelagic sedimentation prevails during interglacials, while terrigenous input is enhanced during glacials; however, sedimentation rates remain high (~10 cm/ka) for glacial and interglacial periods (Stow et al., 2012). Occasional occurrence of ice rafted debris (IRD) is also recorded. Cyclic variations in physical properties and color reflect cyclic changes in the proportion of biogenic carbonate and detrital material delivered to the site (Hodell et al., 2013b).

This study covers a section from the secondary splice U1385D/E (Hodell et al., 2013a) between 59.95 and 99.84 crmcd (corrected revised meters composite depth) (MIS 21–MIS 13). Samples for the microfaunal analysis were taken every 20 cm, providing an average estimated 1.76-ka resolution record. A total of 210 samples 1 cm thick were dried, weighed and washed over a 63 μm mesh sieve. The >63 μm residue was dried, weighed and sieved again to separate and weigh the >150 μm fraction. Census counts of planktonic foraminifera taxa and of planktonic foraminifer fragments were conducted on the sediment fraction larger than 150 μm, using a stereomicroscope. Each sample was successively split until a minimum of 300 specimens was obtained. A total of twenty-eight species and ten morphotypes (Kennett and Srinivasan, 1983) of planktonic foraminifers have been identified (Appendix A) and their relative abundances, calculated, as well as the number of specimens per gram of dry sediment. To monitor carbonate dissolution, planktonic foraminifer fragmentation index was calculated as percentage of test fragments related to the total amount of fragments plus specimens (Thunell, 1976).

Sea surface temperature (SST) values (annual, winter, summer and seasonality -difference between winter and summer parameters) were reconstructed according to the Artificial Neural Network (ANN) method, using a back propagation neural network system (Malmgren et al., 2001) to compare our fossil planktonic foraminifera assemblages with MARGO North Atlantic database. We used the commercial software NeuroGenetic Optimiser v2.6 (Biocomp), as described in Kucera et al. (2005), who calculate an error of prediction of 1.02 °C. The same set of 10 neural networks as in Kucera et al. (2005) was used in this study, providing 10 different SST reconstructions for each component (winter, summer, annual and seasonality). The average value of these ten estimations was used as the final SST reconstruction. Additionally, in order to calculate a similarity index and corroborate the ANN results, we applied a Modern Analog Technique (Prell, 1985) on the fossil data using the same MARGO modern dataset as was used for the training of the ANN (Kucera et al., 2005). The same methodology has been followed to reconstruct winter SST of Site U1314, using the same planktonic foraminifer assemblages as in Alonso-Garcia et al. (2011b). Site U1314 (~1 ka resolution) has been included in this work to better compare with the subpolar North Atlantic.

The age model of the studied section is based on the correlation of the benthic oxygen isotope record to the global benthic LR04 isotope stack (Lisiecki and Raymo, 2005) (see Hodell et al., 2015).

4. Results

Preservation in the studied interval is analyzed considering the planktonic foraminifer fragmentation index. This index remains generally lower than 20% (Fig. 2g), which informs of a very good preservation in the samples, except for some short intervals of increased dissolution. Nevertheless, the fragmentation index did not surpass the 40% threshold above which planktonic foraminifer assemblages

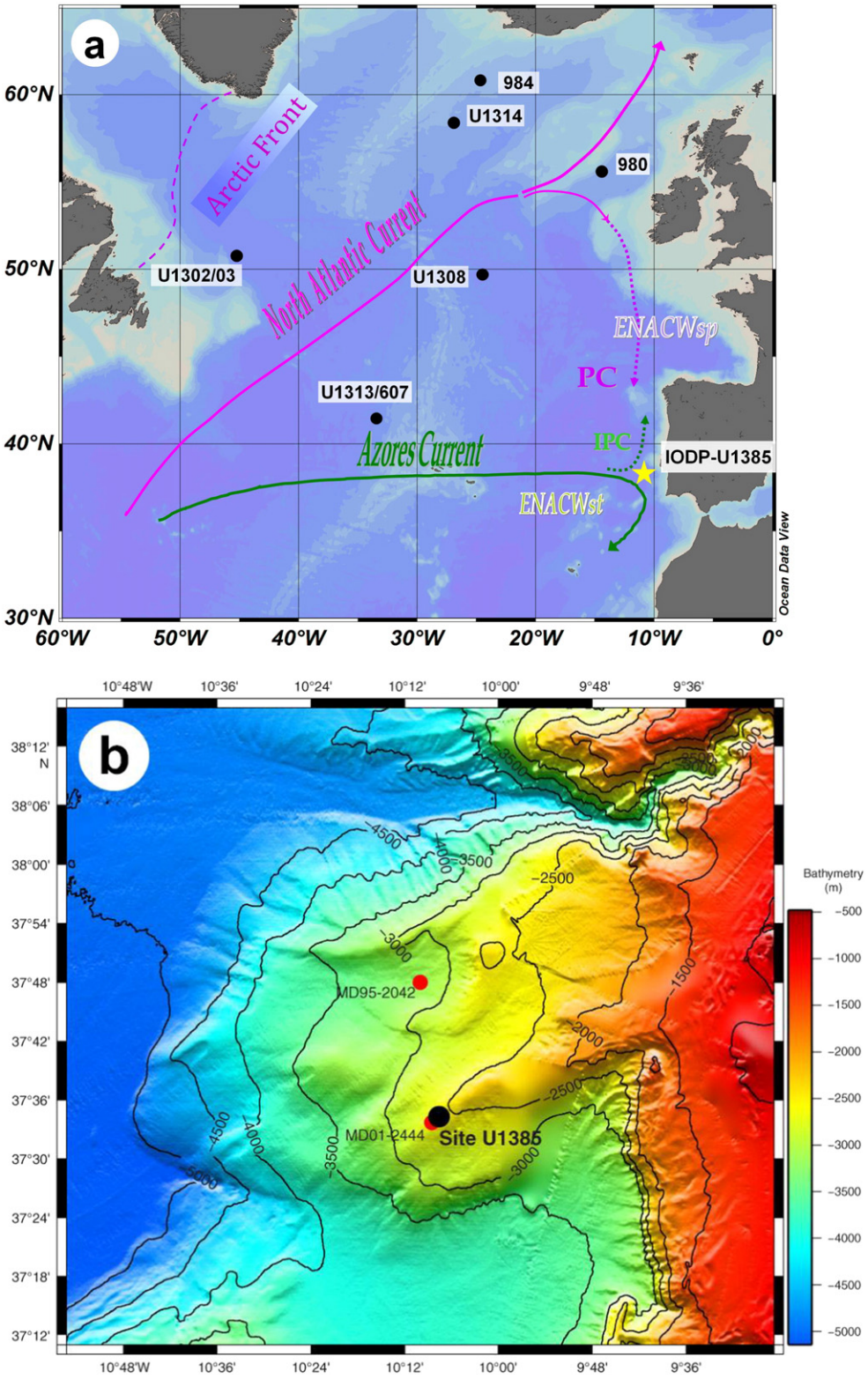

Fig. 1. (a) Map showing the location of Site IODP-U1385 in the Iberian margin and its oceanographic setting (Position of the Arctic Front, from: Swift, 1986 and Pflaumann et al., 2003). *PC*: Portugal Current; IPC: Iberian Poleward Current; *ENACWsp*: Eastern North Atlantic Central Water of subpolar origin; *ENACWst*: Eastern North Atlantic Central Water of subtropical origin. Other cores mentioned in this paper are also shown. (b) Bathymetric map of the southwester Iberian margin showing the position of Site U1385 and nearby piston Cores MD01-2444, located at approximately the same position as Site U1385, and MD95-2042 (After Hodell et al., 2013a).

begin to suffer modifications due to dissolution (Miao et al., 1994). Therefore, we can assume that the assemblages used for this work are not modified by dissolution and they are suitable to infer water mass properties.

Planktonic foraminifer accumulation rate ranges between 500 and 49,800 specimens per gram of dry sediment and ka, lowest values corresponding to levels of high bioturbation, where metallic deposits conform most of the coarse fraction of the sediment.

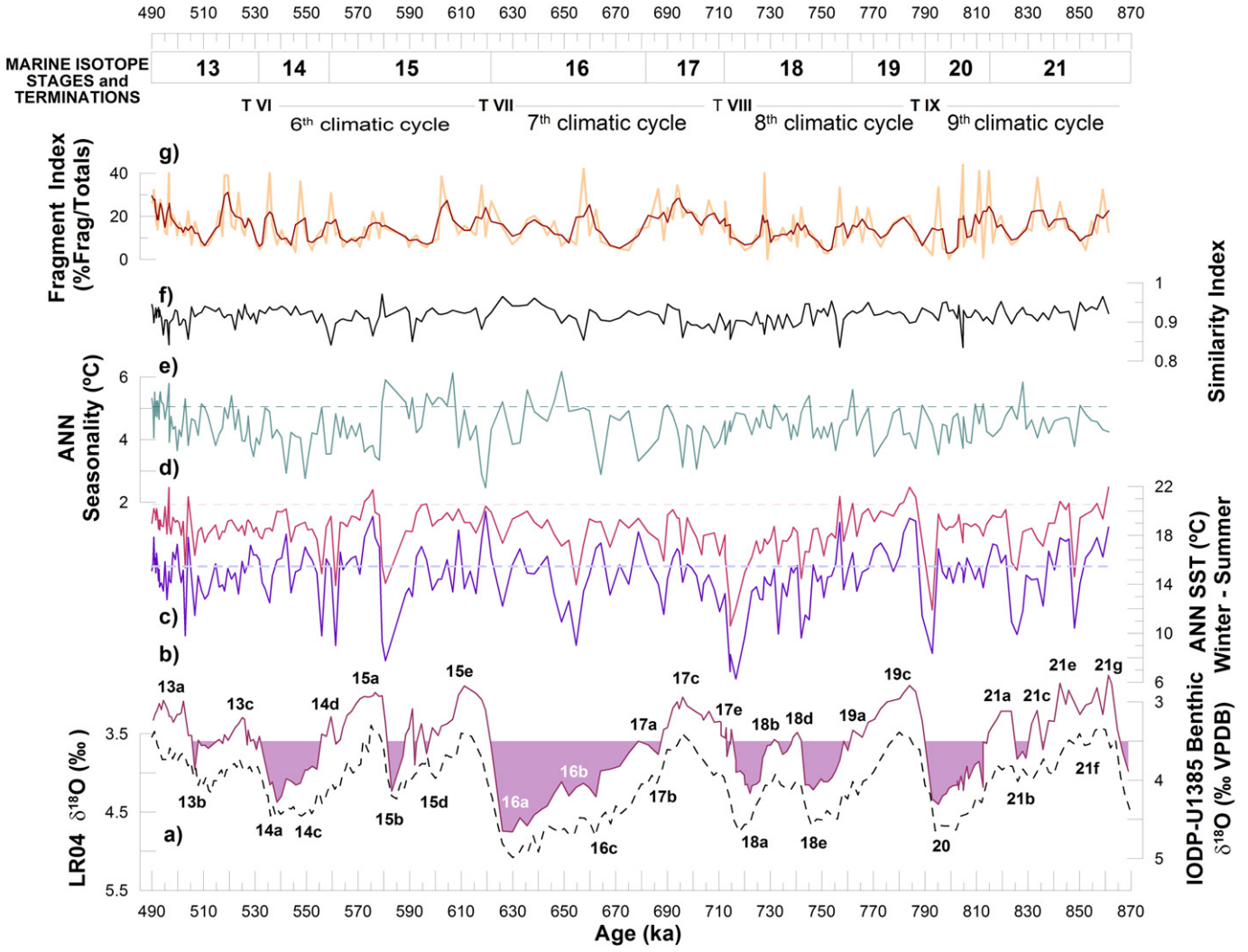

Fig. 2. Down-core results for stages 13 to 21 from IODP-U1385 and comparison with global LR04 benthic stack. (a) Age control points used to correlate both stacks (marked with crosses). (b) Benthic $\delta^{18}O$ profiles from LR-04 stack (Lisiecki and Raymo, 2005) in dashed line, and from U1385 (Hodell et al., 2015); filling enhances the ice volume threshold separating stable and unstable climatic regimes, which has been identified for the North Atlantic in $\delta^{18}O$ value of 3.5 ‰ (McManus et al., 1999). This threshold has been used to locate in the core the limits between glacial and interglacial conditions and determine the duration of climatic cycles. Substages are named according to Railsback et al. (2015). U1385 benthic $\delta^{18}O$ record shows a much higher variability and around 0.5 ‰ VPDB lower values than the global stack. (c) Winter ANN-reconstructed sea surface temperature. (d) Summer ANN-reconstructed sea surface temperature. Both winter and summer records are compared with present day temperatures on the site (horizontal dashed lines) from Locarnini et al. (2010). (e) ANN-reconstructed seasonality compared with present-day seasonality on the site (dashed line). (f) MAT-reconstructed similarity index (Prell, 1985) between fossil planktonic foraminifer assemblage in Site U1385 and MARGO dataset (Kucera et al., 2005). (g) Planktonic foraminifer fragmentation index (number of test fragments related to the total amount of fragments plus specimens) (Thunell, 1976) and averaged with a 3-point running mean.

4.1. Planktonic foraminifer results

The microfaunal analysis focuses on species and assemblages that can be directly used to monitor any change in climatic or oceanographic conditions in North Atlantic surface water.

The species *Neogloboquadrina pachyderma* sinistral (Nps), with a temperature tolerance range between −1 and 8 °C and an optimum of 2 °C (Bé and Tolderlund, 1971; Tolderlund and Bé, 1971; Bauch et al., 1997; Pflaumann et al., 2003), is particularly abundant in the Arctic water (Johannessen et al., 1994). This species has been used to monitor southward penetrations of polar water masses, usually associated with iceberg discharges in mid-latitude North Atlantic (eg., Bond et al., 1992) as well as in the Portuguese margin (Cayre et al., 1999; de Abreu et al., 2003; Vautravers and Shackleton, 2006; Eynaud et al., 2009). This species ranges from 0% to a maximum of almost 50% during MIS 18. The species is more abundant before MIS 16 where high values occurred during interglacials, except for MIS 19, as well as glacials (Fig. 3e).

The subtropical assemblage (Ottens, 1991) consists mainly of species of *Globigerinoides* genus and it is usually linked to the subtropical

Fig. 3. Comparison between IODP-U1385 record and orbital parameters. (a) Benthic $\delta^{18}O$ profile: LR-04 stack (Lisiecki and Raymo, 2005) in dashed line, and record from U1385 (Hodell et al., 2015); filling enhances the ice volume threshold separating stable and unstable climatic regimes (McManus et al., 1999). Substages are named according to Railsback et al. (2015) (b) Planktonic foraminifer *Globigerina bulloides* $\delta^{18}O$ record from U1385 (Hodell et al., 2015). (c) Log Ca/Ti record from U1385 (Hodell et al., 2015) (d) Winter SST for Site U1385 (values above average are shaded). (d) Relative abundance of the planktonic foraminifer polar species *Neogloboquadrina pachyderma* sinistral in U1385. (e) Relative abundance of the subtropical assemblage (Ottens, 1991) in U1385. (g) Orbital parameters: obliquity (Laskar et al., 2004) (black) and 65 °N 21st June Insolation values (W/m^2) (blue) (Huybers, 2006) and integrated summer energy at 65 °N (>275 W/m^2) (red) (Huybers, 2006). Vertical bands mark pronounced cooling coinciding with deglaciations; gray bands mark events close to obliquity maxima and green bands mark the exceptions (no obliquity maxima or no deglaciation). Blue lines mark other pronounced cooling not linked either with deglaciations or with obliquity maxima.

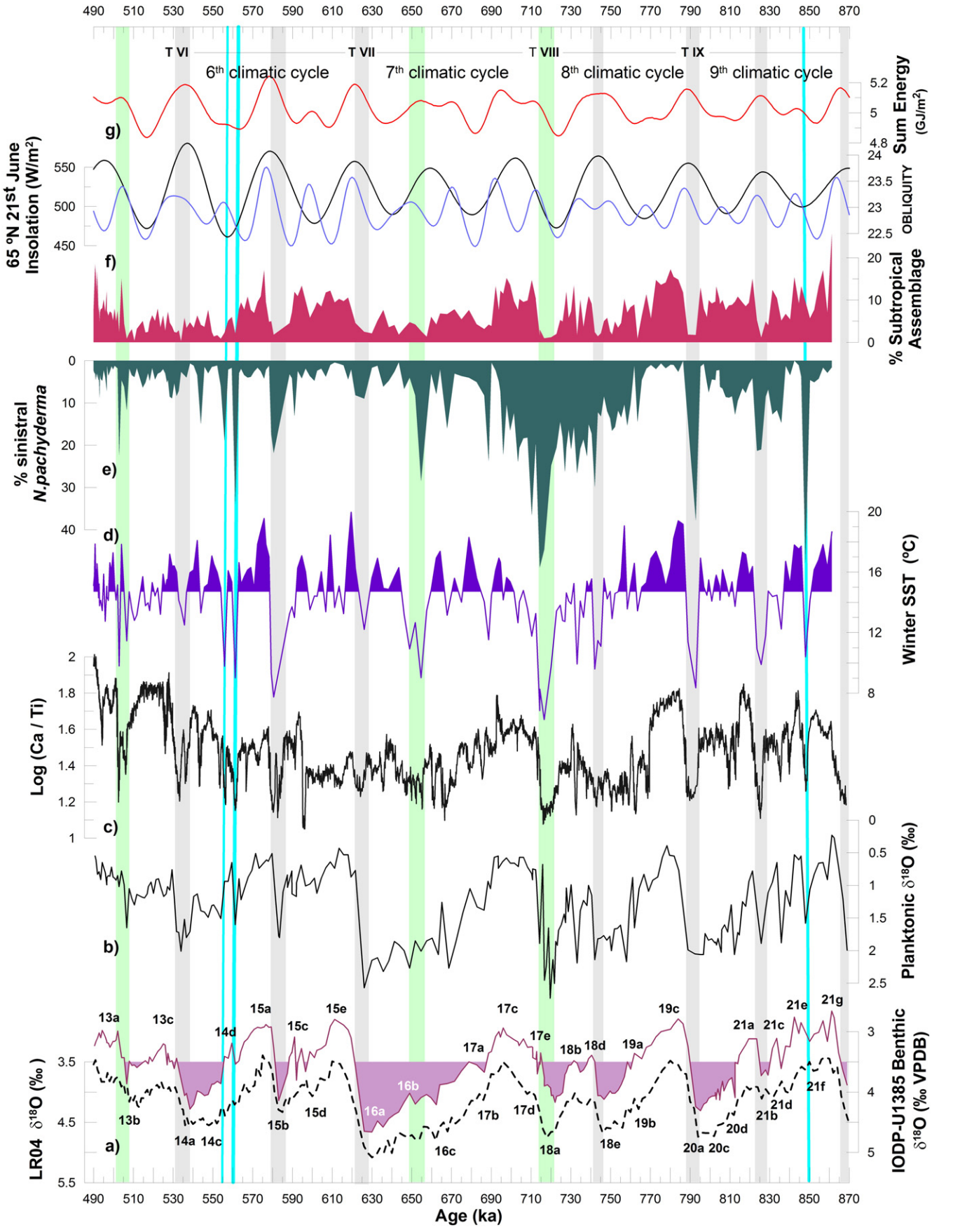
T VI
T VII
T VIII
T IX
6th climatic cycle
7th climatic cycle
8th climatic cycle
9th climatic cycle
65 °N 21st June Insolation (W/m²)
Sum Energy (GJ/m²)
OBLIQUITY
% Subtropical Assemblage
% sinistral N.pachyderma
Winter SST (°C)
Log (Ca / Ti)
Planktonic δ18O (‰)
LR04 δ18O (‰)
IODP-U1385 Benthic δ18O (‰ VPDB)
Age (ka)

branch of ENACW, transported to the Northeast Atlantic by the Azores Current, which flows northward over the site during non-upwelling months (Peliz et al., 2005). Variations in the abundance of the subtropical assemblage (Fig. 3f) are consistent with climatic cycles. Variations in the subtropical assemblage resemble the planktonic $\delta^{18}O$ record, during both glacial and interglacial periods (Fig. 3).

4.2. Sea surface temperature variations

The similarity index of MAT (Fig. 2f) ranges between 0.9 and 1 for almost all the interval, suggesting that the studied samples are well represented in the modern dataset and that SST reconstructions (Fig. 2) are not affected by no-analog artifacts (Kucera et al., 2005).

In general, winter SST off the southwestern Iberian Margin resemble the planktonic oxygen isotope variations (Fig. 3, b and d). Minimum temperature occurred during Terminations or during glacial inceptions. SST in the area was generally colder during the studied interval (mean annual value, 16.6 °C) than at present (18 °C) (Locarnini et al., 2010), even during interglacials. During interglacial periods, summer SST (Fig. 2d) were on average 1 to 2 °C colder than at present and, during glacials, they were 2 to 4 °C colder. Nevertheless, during cooling episodes, summer SST dropped 6 °C below Holocene levels (18 °C, Bard et al., 2000) and those of previous interglacial, MIS 3, (17–18 °C, de Abreu et al., 2003; Vautravers and Shackleton, 2006). Winter SST (Fig. 2c) remained, on average, less than 1 °C lower than at present during all interglacials and during glacials MIS 20 and MIS 14, and were higher than today during most of MIS 19, in the warmest periods of MIS 21 and 15, and even in some very short spells during glacial stages MIS 18, MIS 16 and MIS 14. Only during MIS 18 winter SST were considerably lower (2.5 °C in average) than at present. The warmest period of the studied interval was MIS 19 and the coldest one was MIS 18. Isotope stages 17 and 13 were the coldest interglacial periods, with summer SST between 1 and 2 °C colder than at present and closer to the values recorded during glacial periods, and winter SST generally below modern values.

SST oscillations were, in general, less frequent and less pronounced during interglacials (less than 7 °C drop or rise) than during glacials (up to 11 °C oscillation), except for MIS 21f, that shows one of the steepest sea surface temperature oscillations (7.3 °C) of the whole studied interval.

ANN-reconstructed seasonality (Fig. 2e) during middle Pleistocene is lower than today and, in general, it shows small amplitude variability along the whole interval. Most of the deep oscillations in seasonality correspond to outstanding SST fluctuations. Increases in seasonality coincide with drops in winter SST and vice-versa. The highest seasonality values occurred in MIS 16b (6.2 °C), MIS 15e (6 °C) and 15b (5.9 °C). Since MIS 15a seasonality values were lower and show a slow increasing trend until the end of MIS 13, encompassing the cooling trend recorded by SST. During isotope stages 16 and 15 the amplitude of seasonality oscillations was between 1 and 2 °C higher than during the rest of the interval.

5. Discussion

5.1. Sea surface cooling on the Portuguese margin at deglaciations during middle Pleistocene

The planktonic foraminifer assemblages, SST and oxygen isotope data studied at Site U1385 indicate that during this period, and superimposed on the glacial-interglacial variations, suborbital millennial-scale climatic variability off Iberia reflects the influence of millennial changes in surface circulation in the NE Atlantic.

In order to identify millennial-scale climate events that may not be resolved with the resolution of our SST record we compare our data with the Ca/Ti record (Hodell et al., 2015), which provides an estimated resolution of 0.1 ka. Previous studies along the Portuguese margin reported that Ca/Ti reflects millennial-scale climate changes as well as sea level variations (Hodell et al., 2013a). Higher Ca/Ti ratios are linked to higher productivity of calcareous plankton during warmer periods and lower siliciclastic input from the continent (Hodell et al., 2013a).

Summer SST at the Portuguese margin remained relatively warm from MIS 21 to MIS 13, although lower than present-day summer SST, oscillating between 15 and 18 °C irrespective of the glacial or interglacial periods (Fig. 2d). This relatively warm temperature was, however, punctuated by abrupt SST cooling events, recorded throughout the record by pronounced peaks in abundance of Nps and sharp increases of *G. bulloides* $\delta^{18}O$ values, as well as very low values of the Ca/Ti ratio (Fig. 2, 3).

A close comparison of SST with the benthic $\delta^{18}O$ record for U1385 and the global benthic oxygen isotope stack (LR04) shows that all these cooling events were coetaneous with drops in the benthic $\delta^{18}O$. Longer and more pronounced cooling episodes in the Portuguese margin occurred at Terminations (Fig. 2a–c), particularly during Termination IX and VIII, but also at the transitions from glacial-interglacial substages MIS 21b to 21a, MIS 18e to 18d, and, especially, MIS 15b to 15a.

5.1.1. MIS 21–20

During the ninth climatic cycle (MIS 21–MIS 20) four main cooling events (6 to 8 °C drop) were recorded, all of them at transitions from higher to lower $\delta^{18}O$ values in the benthic oxygen isotope record. The amplitude and duration of these cooling episodes are related to the amplitude of the benthic isotope change (Fig. 2a–c). The most pronounced cooling occurred at Termination IX corresponding with a high amplitude change in the isotopes undoubtedly related to a major sea level rise and deglaciation. Another major cooling (6.4 °C) occurred at the transition MIS21b/a, also related to an important deglaciation and sea level rise. The first two cooling events recorded in this period also occurred at glacial/interglacial transitions, MIS 21f/e and MIS 21d/c. All these events of cool surface temperatures are also registered by heavier planktonic $\delta^{18}O$ and lower Ca/Ti values (Fig. 3b–d).

Based on the benthic $\delta^{18}O$ record climatic cycle MIS 21–20 encompasses two glacial, obliquity-driven cycles, the two more pronounced cooling events reflecting the culmination of these two glacial cycles. These cooling events were followed by remarkably warm intervals, showing the characteristic millennial-scale, stadial-interstadial climate oscillations (Fig. 3a,d,g). In particular, the four cool-warm oscillations recorded in MIS 21 have also been recorded in various sites of the North Atlantic (Flower et al., 2000; Kleiven et al., 2003; Hodell et al., 2008; Ferretti et al., 2010; Hernandez-Almeida et al., 2012) during the stage of progressive extension of the northern Hemisphere ice sheets during MIS 21. The cooling events off Iberia were marked by high percentages of the polar species Nps (Fig. 3e) but they were not linked to high IRD as has been reported for the same events at sites 984, 980 (Wright and Flower, 2002; hereafter, W&F02) and U1314 (Hernández-Almeida et al., 2013) in the North Atlantic.

5.1.2. MIS 19–18

During this cycle, sea surface waters along the Portuguese margin experienced a pronounced cooling during three episodes (Fig. 3d), being the greatest in amplitude (7.2 °C) and the coldest (6.2 °C, winter SST), the one recorded at Termination VIII. The other two cooling events were also linked to global drops in benthic $\delta^{18}O$ at the transitions MIS 18e/d and MIS 18b/c (Fig. 3a,d). Like in the previous climate cycle the amplitude of the cooling events is related to the amplitude of the deglaciations, being the cooling event associated to MIS 18b/c of lesser amplitude. Low Ca/Ti ratios, high planktonic $\delta^{18}O$ and high percentages of Nps also registered these cooling events that, with the exception of Termination VIII when SST increased gradually, were followed by abrupt warming (Fig. 3b–e).

Similar cooling episodes have been recorded in the subpolar North Atlantic at sites 980 (W&F02), U1314 (Alonso-Garcia et al., 2011a) (Fig. 4b) and U1302 (Channell et al., 2012), as well as at site U1308

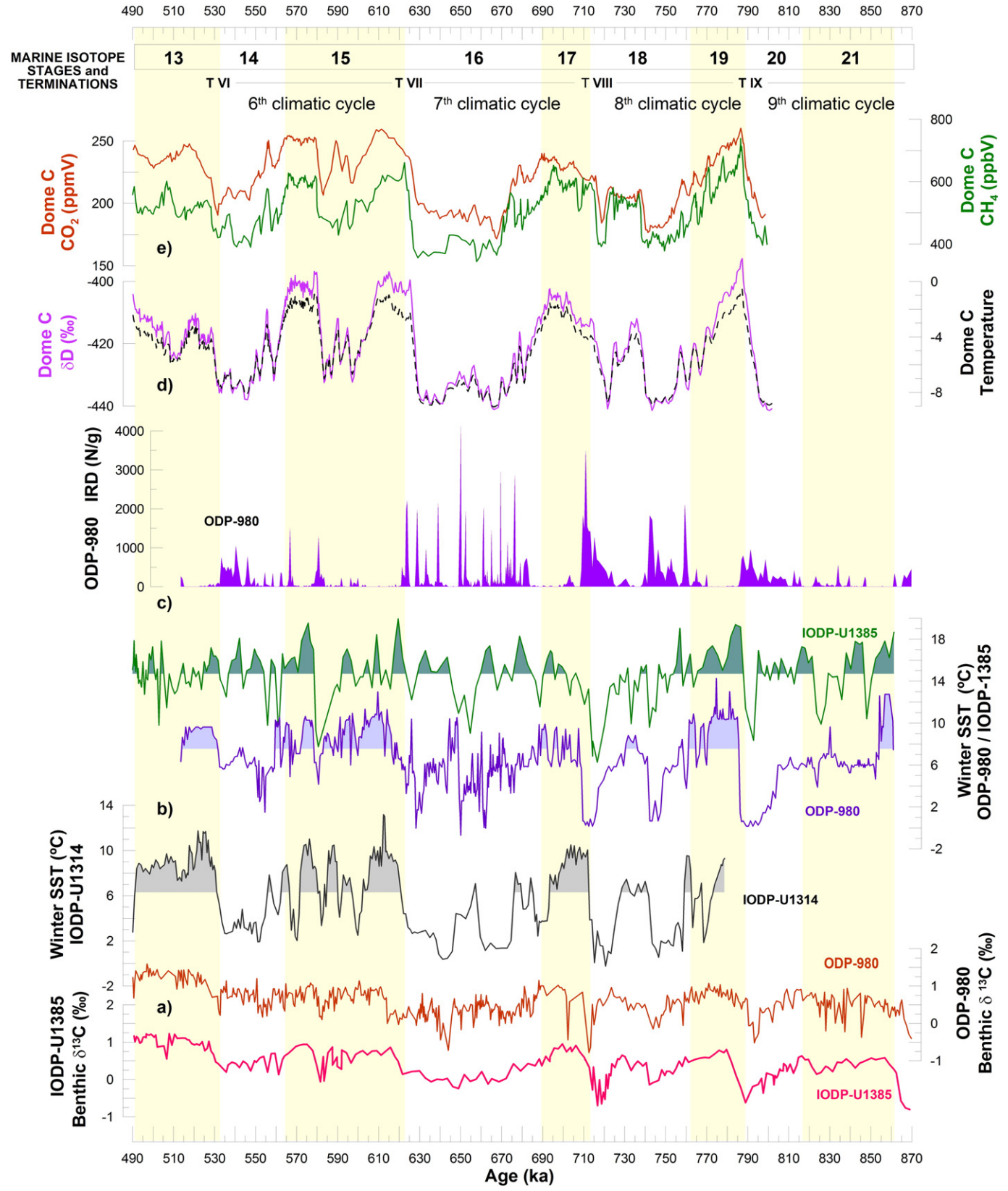

Fig. 4. Comparison between SST record from site IODP-U1385 (this work) and other climatic records from ninth to fifth climatic cycles. (a) Benthic $\delta^{13}C$ profile from U1385 (pink) and ODP-980 (W&F02) (brown). (b) Winter SST records from 58° N site U1314 (this work, gray), from 55°N site 980 (W&F02) (blue) and from site U1385 (green). SST above average for the interval are shaded in all the plots. (c) IRD content (in number of particles per gram of sediment) from site 980 (W&F02). The age model for site 980 has been recalculated according to LR04. (d) Antarctic Dome C δD record (purple) and reconstructed temperature (black dashed line) (Jouzel et al., 2007) (e) Content of greenhouse gases CH_4 (green) and CO_2 (red) in the Antarctic ice (Loulergue et al., 2008 and Lüthi et al., 2008, respectively).

(Hodell et al., 2008), but in that region they were associated to ice-rafting events (Fig.4c).

5.1.3. MIS 17–16

Based on the global benthic Stack (LR04) MIS 16 was the longest and the most prominent glacial of the middle Pleistocene. Ice sheets grew continuously from 695 to 630 ka, with a lower rate of growth or retreat between 660 and 650 ka. It is at this time when surface waters in the Portuguese margin experienced a prominent drop (8 °C) in temperature (Fig. 3d). The beginning of this prominent cooling (659 ka) was synchronous with a low-amplitude warming phase recorded in Antarctic ice cores (Fig. 4b,d) and occurred nearly in phase with maximum obliquity of Earth's axis (Fig. 3d,g).

Unlike other Terminations, a weak cooling event (12.2 °C winter SST) was recorded at Termination VII, although this is one of the largest amplitude deglaciations. An also low amplitude drop in Ca/Ti reflects the small magnitude of this event (Fig.3c). Nevertheless, it coincided with IRD accumulation in site 980 (Fig. 4c) and was contemporaneous with Heinrich event 16.1 recorded at sites U1308 and U1302/03 (Hodell et al., 2008; Channell et al., 2012).

5.1.4. MIS 15–13

In the upper part of our record, again SST experienced prominent cooling events at deglaciation between MIS 15b/a (7.7 °C winter SST) and at transition MIS 13b/a (11.4 winter SST). Two more short cooling events (9 and 9.7 °C winter SST) occurred at 561.35 and 555.87 ka, similar to those recorded in the subpolar cores 980 and U1314 (Fig. 4b).

A less pronounced cooling (5 °C drop) occurred at Termination VI that is also marked by a decrease in Ca/Ti (Fig. 3c-d).

5.2. Important reorganizations of North Atlantic circulation at the onset of northern hemisphere ice sheet retreats

While in other North Atlantic sites, especially those that are at higher latitude, SST remained relatively low during glacial times, the Portuguese margin was under the influence of relatively warm temperate waters during most glacial periods (Fig. 4b). The occurrence of temperate-warm surface waters at site U1385 during long time periods reflects the persistent influence of the North Atlantic Current (NAC) and its continuous advection of temperate-warm waters to the eastern margin of the subtropical North Atlantic gyre. The stadial-interstadial oscillations observed in this study were the result of enhanced/reduced advection of heat to the Southern Iberian Margin through the NAC. However, during most deglaciations a major reorganization of surface circulation in the North Atlantic reduced the northward flow of the NAC, promoting the southward expansion of cold subpolar waters along the western European margin.

The severe cooling episodes associated to most deglaciations were followed by a prominent warming event that marks the onset of a climate optimum interstadial event usually present in the first stage of interglacial periods. This climate optimum event was the warmest interstadial of each interglacial. Good examples of these high amplitude changes in temperature can be seen at Termination IX, when SST rose from 8.3 to 19 °C, and at transitions MIS 21f/e, MIS 21b/a, MIS 15b/a, etc. (Figs. 2c-d, 3d).

In parallel to the pronounced surface cooling events, the record of the Portuguese margin shows that deep-water circulation was also severely affected. A remarkable decrease in the benthic $\delta^{13}C$ is observed at deglaciations (Fig. 4a), especially in Terminations IX and VIII, but also at other glacial-interglacial transitions. These drops in benthic $\delta^{13}C$ have been recognized in other sites from the North Atlantic (W&F02; Hodell et al., 2008; Alonso-Garcia et al., 2011b; Ferretti et al., 2015). Drops in the benthic $\delta^{13}C$ have traditionally been attributed to slowdown of NADW formation triggered by lower sea surface salinities in the north Atlantic. In more recent climate cycles lower benthic $\delta^{13}C$ have been observed during Heinrich events that were triggered by freshwater discharge at times of ice sheet collapse (Shackleton et al., 2000; Skinner and Elderfield, 2007; Martrat et al., 2007). Pulses of repeated freshwater release to the North Atlantic originate the millennial-scale, stadial-interstadial oscillations of late Pleistocene caused by reduced/enhanced Atlantic meridional overturning circulation (AMOC) alternations. Events of reduced AMOC led to lower rates of heat transfer to the North Atlantic that resulted in decreased SST (e.g: Broecker et al., 1989; Stocker, 1999; McManus et al., 2004; Pisias et al., 2010). Although these millennial-scale climate oscillations are recorded at site U1385, the highest amplitude cooling/warming oscillations on the Portuguese margin coincided with deglaciations, both Terminations and the transitions from glacial to interglacial substages, and were marked by significant changes in the planktonic foraminifer assemblage from high percentages of Nps to increased relative abundance of subtropical species (Fig. 3e–f).

We interpret that the pronounced cooling events observed along the Iberian margin were triggered by freshwater released to the Atlantic at the onset of northern Hemisphere ice sheet retreats. The mechanism is similar to what happened during Heinrich stadials recorded at the end of the last two glacial periods (e.g. Rühlemann et al., 1999; Böhm et al., 2014), when the extension of the polar water and icebergs have been reported to reach the latitude of Southern Iberia (e.g., Skinner et al., 2003; Skinner and Shackleton, 2006). Although IRD were not recorded at site U1385 the advection of polar waters to the Portuguese margin only at deglaciations suggests that only freshwater perturbations of a certain magnitude, such as those related to ice-sheet retreats, had a profound effect on the SW Iberian margin.

The remarkable warming episodes that immediately followed deglaciations (Figs. 2a–c, 3a,d) were triggered by the resumption of NADW formation after the end of freshwater perturbations originated during ice sheet collapse. An increase in the strength of the AMOC led to invigoration of the NAC and the transport of warm surface waters to the Portuguese margin, which is recorded by a significant increase in the subtropical species in the planktonic foraminifer assemblage (Fig. 3f).

Ice sheets during Middle Pleistocene tended to collapse at times of high northern Hemisphere summer insolation that resulted from the combination of high obliquity and minimum precession (Imbrie et al., 1993; Huybers and Wunsch, 2003; Huybers, 2011). While obliquity mainly governed the time between deglaciations, precession determined the precise timing of deglaciations (Huybers, 2011) and ice discharge to the Ocean. This, in turn, triggered the major reorganizations of surface circulation in the North Atlantic and the advection of polar water to the Iberian margin. The coincidence in timing between these pronounced cooling events in Portugal with increasing northern Hemisphere summer insolation (Fig. 3d,g), strongly suggests a causal effect with ice sheet collapse events and deglaciations. Most of these events occurred at times of obliquity maxima when obliquity governs insolation at high latitudes. However there are two notable exceptions, the cooling episodes recorded at 650 and 710 ka when obliquity was relatively low or decreasing (Fig. 3g). Instead, these two cooling events occurred at times of increasing summer insolation driven by precession when the perihelion was aligned with northern Hemisphere summer solstice.

Recently it has been proposed that the energy received during summer (called integrated summer insolation, with summer defined as the period when insolation intensity exceeds the ~275 W/m^2 threshold) is the parameter that better reflects the amount of ice sheet melting (Huybers, 2006). The summer energy at 65°N (using the 275 W/m^2 threshold) shows high values during all terminations and transitions from glacial to interglacial substages (Fig. 3g), and may be advocated as the trigger for the major reorganizations in North Atlantic circulation observed in our Iberian margin record, in response to deglaciations.

5.3. North Atlantic SST gradient during ice sheet growth

One of the most characteristic features of the SST record in the Portuguese margin is that both the early phase of ice sheet growth, as

recorded by the rapid increase in the benthic and planktonic $\delta^{18}O$, and glacial maxima, were coeval with warm SST at Site U1385 (Figs. 2a-c, 3a,b,d). In fact, off the Iberian margin none of the ice volume maxima corresponded to the lowest SST. When comparing SST records of this study with those from northern sites 980 and U1314 (Fig. 4b) an increasing N–S latitudinal SST gradient can be observed. After the pronounced warming recorded at the beginning of interglacials, millennial-scale climate changes are recorded both at high and at middle latitudes, but southern waters remained relatively warm, while the northern ones cooled as a result of the progressive extension of the northern Hemisphere ice sheets and associated southward advance of the AF (WF02; Alonso-Garcia et al., 2011a). This pattern is particularly noticeable at transitions MIS 19/18, MIS17/16 and MIS15/14. During the early phase of glacials, areas at latitudes of 37°N were influenced by the warm subtropical waters of the Azores current, as indicated by the presence of the subtropical assemblage in our Site (Fig. 3f). SST were similar during glacials, especially MIS 20, and interglacials, especially during MIS 20. A similar situation was observed in site U1313 during MIS 16, when warm and stratified surface waters coexisted with the presence of IRD layers produced by Heinrich-like Events (Naafs et al., 2011).

This lack of correspondence between SST and ice volume maxima was also recorded in the mid-latitude North Atlantic in more recent isotope stages, like MIS 6 (Martrat et al., 2007) and the Last Glacial Maximum, when surface water temperature was almost as high as today, according to SST reconstructions from the Portuguese margin (Cayre et al., 1999; de Abreu et al., 2003) and the North Atlantic at the same latitude (Chapman and Shackleton, 1998).

This mismatch between increasing global ice volume, cool SST in the northern latitudes and warm surface waters off Iberia supports the instrumental role that warm surface waters of mid-latitude North Atlantic had in building northern hemisphere ice sheets, providing an important source of water vapor to promote ice growth (Ruddiman and McIntyre, 1981; Sánchez Goñi et al., 2013).

6. Conclusions

Our study of the variation of planktonic foraminifers assemblages and SST, from the Shackleton site during the middle Pleistocene, as well as the comparison of our results with both benthic and planktonic $\delta^{18}O$ records and Ca/Ti data from the same Site (Hodell et al., 2015), allows the characterization of climatic conditions in the North Atlantic back to the ninth climatic cycle (867 ka). SST was generally colder during the middle Pleistocene than today off the southwestern Iberian margin, especially summer temperature, which was higher than today only during very short periods in some interglacials. During this period and superimposed on the glacial-interglacial variations, millennial-scale climatic variability was recorded.

All deglaciations on the Portuguese margin, both Terminations (particularly T IX and VIII) and the transitions from glacial to interglacial substages (MIS 21b/a, MIS 18e/d and especially MIS 15b/a), show a prominent (up to 10 °C in amplitude) cold-warm climate oscillation. This high amplitude variation in temperature during deglaciations is recorded by a remarkable change in the planktonic foraminifer assemblages from high relative abundance of the polar species Nps to high relative abundance of the subtropical association (Fig. 3e–f).

These high amplitude oscillations in temperature were the result of major reorganizations of Sea surface and deep water circulation in the North Atlantic triggered by freshwater releases to the Ocean when Ice sheets in the northern Hemisphere started to retreat. Reduced salinities at surface shutdown NADW formation and reduced the northward advection of heat and the transport of warm waters to the eastern margin of the subtropical gyre, causing the advection of subpolar waters to the SW Iberian margin. This scenario rapidly changed when the freshwater perturbation stopped. The reinitiating of NADW formation enhanced the strength of the AMOC leading to an intensification of the NAC and the flux of warm waters to the Iberian margin.

The comparison with SST records from higher latitudes of the North Atlantic reveals the development of a steeper latitudinal SST gradient between the sub-tropical and the sub-polar North Atlantic as ice sheets were growing in the northern Hemisphere, providing a source of water vapor that could promote the growth of ice sheets.

Acknowledgments

We want to acknowledge the Integrated Ocean Drilling Program (IODP) for providing the sediment samples. Funding from Spanish projects GRACCIE (Consolider Ingenio 2011 CSD2007-00067, CGL2011-26493 and CTM2012-38248) is greatly acknowledged, as well as Castilla and Leon funding to "Grupo GR37" and project number SA263U14. MAG acknowledges the funding from the FCT fellowship SFRH/BPD/96960/2013. This research was also supported by the Natural Environmental Research Council Grant NE/K005804/1 and NE/J017922/1 to DAH. We also thank the kind help and useful comments from Dr. A. Voelker

Appendix A. Planktonic foraminifer species and morphotypes identified

Beella digitata
Candenia nitida
Globigerina bulloides
Globigerina falconensis
Globigerinella calida
Globigerinella siphonifera (*aequilateralis*)
Globigerinita glutinata
Globigerinita uvula
Globigerinoides conglobatus
Globigerinoides ruber (pink)
Globigerinoides ruber (white)
Globigerinoides sacculifer (with sac)
Globigerinoides sacculifer (without sac)
Globorotalia crassaformis (dextral)
Globorotalia crassaformis (sinistral)
Globorotalia hirsuta
Globorotalia inflata
Globorotalia scitula (dextral)
Globorotalia scitula (sinistral)
Globorotalia truncatulinoides (dextral)
Globorotalia truncatulinoides (sinistral)
Globorotaloides hexagonus
Globoturborotalita rubescens
Globoturborrotalita tenella
Neogloboquadrina dutertrei
Neogloboquadrina pachyderma (dextral)
Neogloboquadrina pachyderma (sinistral)
Orbulina universa
Pulleniatina obliquiloculata
Sphaeroidinella dehiscens
Tenuitella munda
Turborotalita humilis
Turborotalia quinqueloba

References

de Abreu, L., Agrantes, F., Shackleton, N.J., Tzedakis, P.C., McManus, J.F., Oppo, D.W., Hall, M.A., 2005. Ocean climate variability in the eastern North Atlantic during interglacial marine isotope stage 11: a partial analogue to the Holocene? Paleoceanography 20. http://dx.doi.org/10.1029/2004PA001091.

de Abreu, L., Shackleton, N.J., Schönfeld, J., Hall, M.A., Chapman, M., 2003. Millennial-scale oceanic climate variability off the western Iberian margin during the last two glacial periods. Mar. Geol. 196, 1–20.

Allen, J.R.M., Brandt, U., Brauer, A., Hubberten, H.W., Huntley, B., Keller, J., Kraml, M., Mackensen, A., Mingram, J., Negendank, J.F.W., Nowaczyk, N.R., Oberhansli, H.,

Watts, W.A., Wulf, S., Zolitschka, B., 1999. Rapid environmental changes in southern Europe during the last glacial period. Nature 400, 740–742.
Alonso-Garcia, M., Sierro, F.J., Flores, J.A., 2011a. Arctic front shifts in the subpolar north Atlantic during the Mid-Pleistocene (800–400 ka) and their implications for ocean circulation. Palaeogeogr. Palaeoclimatol. Palaeoecol. 311, 268–280.
Alonso-Garcia, M., Sierro, F.J., Kucera, M., Flores, J.A., Cacho, I., Andersen, N., 2011b. Ocean circulation, ice sheet growth and interhemispheric coupling of millennial climate variability during the mid-Pleistocene (ca 800–400 ka). Quat. Sci. Rev. 30, 3234–3247.
Bard, E., Rostek, F., Turon, J.L., Gendreau, S., 2000. Hydrological impact of Heinrich events in the Subtropical Northeast Atlantic. Science 289, 1321–1324. http://dx.doi.org/10.1126/science289.5483,1321.
Bauch, D., Carstens, J., Wefer, G., 1997. Oxygen isotope composition of living *Neogloboquadrina pachyderma* (sin) in the Arctic Ocean. Earth Planet. Sci. Lett. 146, 47–58.
Bé, A.W.H., Tolderlund, D.S., 1971. Distribution and ecology of living planktonic foraminifera in surface waters of the Atlantic and Indian Oceans. In: Funnell, B., Riedel, W.R. (Eds.), The Micropaleontology of the Oceans. Cambridge Univ. Press, London, pp. 105–149.
Böhm, E., Lippold, J., Gutjahr, M., Frank, M., Blaser, P., Antz, B., Fohlmeister, J., Frank, N., Andersen, M.B., Deininger, M., 2014. Strong and Deep Atlantic Meridional Overturning Circulation During the Last Glacial Cycle. http://dx.doi.org/10.1038/nature14059.
Bond, G., Heinrich, H., Broecker, W., Labeyrie, L., McManus, J., Andrews, J., Huon, S., Jantschik, R., Clasen, S., Simet, C., Tedesco, K., Klas, M., Bonani, G., Ivy, S., 1992. Evidence for massive discharges of icebergs into the North Atlantic ocean during the last glacial period. Nature 360, 245–249. http://dx.doi.org/10.1038/360245a0.
Broecker, W.S., Kennett, J.P., Flower, B.P., Teller, J.T., Trumbore, S., Bonani, G., Wolfli, W., 1989. Routing of meltwater from the Laurentide ice sheet during the younger Dryas cold episode. Nature 341, 318–321.
Cayre, O., Lancelot, Y., Vincent, E., 1999. Paleoceaanographic reconstructions from planktonic foraminifera off the Iberian margin: temperature, salinity and Heinrich events. Paleoceanography 14 (3), 384–396.
Channell, J.E.T., Hodell, D.A., Romero, O., Hillaire-Marcel, C., de Vernal, A., Stoner, J.S., Mazaud, A., Röhl, U., 2012. A 750-kyr detrital-layer stratigraphy for the north Atlantic (IODP sites U1302–U1303, Orphan Knoll, Labrador Sea). Earth Planet. Sci. Lett. 317–318, 218–230.
Chapman, M.R., Shackleton, N.J., 1998. Millennial-scale fluctuations in North Atlantic heat flux during the last 150,000 years. Earth Planet. Sci. Lett. 159, 57–70.
Clark, P.U., Archer, D., Pollard, D., Blum, J.D., Rial, J.A., Brovkin, V., Mix, A.C., Pisias, N.G., Roy, M., 2006. The middle Pleistocene transition: characteristics, mechanisms, and implications for long-term changes in atmospheric pCO2. Quat. Sci. Rev. 25, 3150–3184.
Eynaud, F., de Abreu, L., Voelker, A., Schönfeld, J., Salgueiro, E., Turon, J.L., Penaud, A., Toucanne, S., Naughton, F., Sanchez-Goñi, M.F., Malaizé, B., Cacho, I., 2009. Position of the Polar Front along the western Iberian Margin during key cold episodes of the last 45 ka. Geochem. Geophys. Geosyst. 10, Q07U05. http://dx.doi.org/10.1029/2009GC002398.
Ferretti, P., Crowhurst, S.J., Hall, M.A., Cacho, I., 2010. North Atlantic millennial scale climate variability 910,000 to 790,000 years and the role of the equatorial insolation forcing. Earth Planet. Sci. Lett. 293, 28–41. http://dx.doi.org/10.1016/j.epsl.2010.02.016.
Ferretti, P., Crowhurst, S.J., Naafs, B.D.A., Barbante, C., 2015. The marine isotope stage 19 in the mid-latitude North Atlantic ocean: astronomical signature and intra-interglacial variability. Quat. Sci. Rev. 108. http://dx.doi.org/10.1016/j.quascirev.2014.10.024.
Fiúza, A.F.G., Hamann, M., Ambar, I., Díaz del Río, G., González, N., Cabanas, J.M., 1998. Water masses and their circulation off western Iberia during May 1993. Deep-Sea Res. 45, 1127–1160.
Flower, B.P., Oppo, D.W., McManus, J.F., Venz, K.A., Hodell, D.A., Cullen, J.L., 2000. North Atlantic intermediate to deep water circulation and chemical stratification during the past 1 Myr. Paleoceanography 15, 388–403.
Hernandez-Almeida, I., Sierro, F.J., Cacho, I., Flores, J.A., 2012. Impact of suborbital climate changes in the North Atlantic on ice sheet dynamics at the Mid-Pleistocene transition. Paleoceanography 27, PA3214.
Hernández-Almeida, I., Sierro, F.J., Flores, J.A., Cacho, I., Filippelli, G.M., 2013. Palaeoceanographic changes in the North Atlantic during the Mid-Pleistocene transition (MIS 31–19) as inferred from planktonic foraminiferal and calcium carbonate records. Boreas 41, 140–159.
Hodell, D.A., Channell, J.E.T., Curtis, J.H., Romero, O.E., Röhl, U., 2008. Onset of "Hudson Strait" Heinrich events in the eastern North Atlantic at the end of the middle Pleistocene transition (~640 ka)? Paleoceanography 23. http://dx.doi.org/10.1029/2008PA001591.
Hodell, D., Crowhurst, S., Skinner, L., Tzedakis, P.C., Margari, V., Channell, J.E.T., Kamenov, G., Maclachlan, S., Rothwell, G., 2013b. Response of Iberian margin sediments to orbital and suborbital forcing over the past 420 ka. Paleoceanography 28 (1), 185–199. http://dx.doi.org/10.1002/palo.20017.
Hodell, D., Lourens, L., Crowhurst, S., Konijnendijk, T., Tjallingii, R., Jiménez-Espejo, F., Skinner, L., Tzedakis, P.C., the Shackleton Site Project Members, 2015. A reference time scale for site U1385 (Shackleton site) on the SW Iberian Margin. Glob. Planet. Chang. 133, 49–64.
Hodell, D.A., Lourens, L., Stow, D.A.V., Hernández-Molina, J., Alvarez Zarikian, C.A., the Shackleton Site Project Members, 2013a. The "Shackleton site" (IODP site U1385) on the Iberian Margin. Sci. Drill. 16, 13–19.
Huybers, P., 2006. Early Pleistocene glacial cycles and the integrated summer insolation forcing. Science 313, 5786. http://dx.doi.org/10.1126/science.1125249 (708-511).
Huybers, P., 2011. Combined obliquity and precession pacing of late Pleistocene deglaciations. Nature 480, 229–232.
Huybers, P., Wunsch, C., 2003. Rectification and precession-period signals in the climate system. Geophys. Res. Lett. 30. http://dx.doi.org/10.1029/2003GL017875.
Imbrie, J., Berger, A., Boyle, E.A., Clemens, S.C., Duffy, A., Howard, W.R., Kukla, G., Kutzbach, J., Martinson, D.G., McIntyre, A., Mix, A.C., Molfino, B., Morley, J.J., Peterson, L.C., Pisias, N.G., Prell, W.L., Raymo, M.E., Shackleton, N.J., Toggweiler, J.R., 1993. On the structure and origin of major glaciation cycles: 2. The 100,000-year cycle. Paleoceanography 8, 699–735. http://dx.doi.org/10.1029/93PA02751.
Johannessen, T., Jansen, E., Flatoy, A., Ravelo, A.C., 1994. The relationship between surface water masses, oceanographic fronts and paleoclimatic proxies in surface sediments of the Greenland, Iceland, Norwegian seas. In: Zahn, R., et al. (Eds.), NATO ASI Series 117. Springer-Verlag, New York, pp. 61–85.
Jouzel, J., Masson-Delmotte, V., Cattani, O., Dreyfus, G., Falourd, S., Hoffmann, G., Minster, B., Nouet, J., Barnola, J.M., Chappellaz, J., Fischer, H., Gallet, J.C., Johnsen, S., Leuenberger, M., Loulergue, L., Luethi, D., Oerter, H., Parrenin, F., Raisbeck, G., Raynaud, D., Schilt, A., Schwander, J., Selmo, E., Souchez, R., Spahni, R., Stauffer, B., Steffensen, J.P., Stenni, B., Stocker, T.F., Tison, J.L., Wener, M., Wolff, E.W., 2007. Orbital and millennial Antarctic climate variability over the past 800,000 years. Science 317, 793–796. http://dx.doi.org/10.1126/science,1141038.
Kennett, J.P., Srinivasan, M.S., 1983. Neogene Planktonic Foraminifera. A Phylogenetic Atlas. Hutchinson Ross Publishing Company, New York.
Kleiven, H.F., Jansen, E., Curry, W.B., Hodell, D.A., Venz, K.A., 2003. Atlantic Ocean thermohaline circulation changes on orbital to suborbital timescales during the mid-Pleistocene. Paleoceanography 18, 1008.
Kucera, M., Weinelt, M., Kiefer, T., Pflaumann, U., Hayes, A., Weinelt, M., Chen, M., Mix, A.C., Barrows, T.T., Cortijo, E., Duprat, J., Juggins, S., Waelbroeck, C., 2005. Reconstruction of sea-surface temperatures from assemblages of planktonic foraminifera: multi-technique approach based on geographically constrained calibration data sets and its application to glacial Atlantic and Pacific Oceans. Quat. Sci. Rev. 24, 951–998. http://dx.doi.org/10.1016/j.quascirev.2004.07.014.
Laskar, J., Robutel, P., Joutel, F., Gastineau, M., Correia, A.C.M., Levrard, B., 2004. A long-term numerical solution for the insolation quantities of the Earth. Astron. Astrophys. 428, 1. http://dx.doi.org/10.1051/0004-6361:20041335.
Lebreiro, S.M., Moreno, J.C., Abrantes, F., Pflaumann, U., 1997. Productivity and paleoceanographic implications on the Tore Seamount (Iberian Margin) during the last 225 kyr: foraminiferal evidence. Paleoceanography 12 (5), 718–727.
Lebreiro, S.M., Moreno, J.C., McCave, I.N., Weaver, P.P.E., 1996. Evidence for Heinrich layers off Portugal (Tore Seamount: 39°N, 12°W). Mar. Geol. 131, 47–56. http://dx.doi.org/10.1016/0025-3227(95)00142-5.
Lisiecki, L.E., Raymo, M.E., 2005. A Pliocene–Pleistocene stack of 57 globally distributed benthic $d^{18}O$ records. Paleoceanography 20, PA1003. http://dx.doi.org/10.1029/2004PA001071.
Locarnini, R.A., Mishonov, A.V., Antonov, J.I., Boyer, T.P., Garcia, H.E., Baranova, O.K., Zweng, M.M., Johnson, D.R., 2010. World Ocean Atlas 2009, Volume 1: Temperature. In: Levitus, S. (Ed.), NOAA Atlas NESDIS 68. U.S. Government Printing Office, Washington, D.C. (184 pp.).
Loulergue, L., Schilt, A., Spahni, R., Masson-Delmotte, V., Blunier, T., Lemieux, B., Barnola, J.M., Raynaud, D., Stocker, T.F., Chappellaz, J., 2008. Orbital and millennial-scale features of atmospheric CH_4 over the past 800,000 years. Nature 453, 383. http://dx.doi.org/10.1038/nature06950.
Lüthi, D., Le Floch, M., Bereiter, B., Blunier, T., Barnola, J.M., Siegenthaler, U., Raynaud, D., Jouzel, J., Fischer, H., Kawamura, K., Stocker, T.F., 2008. High-resolution carbon dioxide concentration record 650,000–800,000 years before present. Nature 453, 379. http://dx.doi.org/10.1038/nature06949.
Malmgren, B.A., Kucera, M., Nyberg, J., Waelbroeck, C., 2001. Comparison of statistical and artificial neural network techniques for estimating past sea surface temperatures from planktonic foraminifer census data. Paleoceanography 16, 520–530.
Martrat, B., Grimalt, J.O., Shackleton, N.J., de Abreu, L., Hutterli, M.A., Stocker, T.F., 2007. Four climate cycles of recurring deep and surface water destabilizations on the Iberian Margin. Science 317 (5837), 502–507. http://dx.doi.org/10.1126/science.1101706.
McManus, J.F., Francois, R., Gherardi, J.M., Keigwin, L.D., Brown-Leger, S., 2004. Collapse and rapid resumption of Atlantic meridional circulation linked to deglacial climate changes. Nature 428 (6985), 834–837. http://dx.doi.org/10.1038/nature02494.
McManus, J.F., Oppo, D.W., Cullen, J.L., 1999. A 0.5-million year record of millennial. Scale climate variability in the North Atlantic. Science 283 (5404), 971–975. http://dx.doi.org/10.1126/science.283.5404.971.
Miao, Q., Thunell, R.C., Anderson, D.M., 1994. Glacial-Holocene carbonate dissolution and sea surface temperatures in the South China and Sulu Seas. Paleoceanography 9, 269–290.
Naafs, B.D.A., Hefter, J., Ferretti, P., Stein, R., Haug, G.H., 2011. Sea surface temperatures did not control the first occurrence of Hudson strait Heinrich events during MIS 16. Paleoceanography 26. http://dx.doi.org/10.1029/2011PA002135.
Ottens, J.J., 1991. Planktic foraminifera as North Atlantic watermass indicators. Oceanol. Acta 14, 123–140.
Peliz, A., Dubert, J., Santos, A.M.P., Oliveira, P.B., Le Cann, B., 2005. Winter upper ocean circulation in the Western Iberian basin — fronts, eddies and poleward flows: an overview. Deep-Sea Res. I Oceanogr. Res. Pap. 52, 621–646. http://dx.doi.org/10.1016/j.dsr.2004.11.005.
Pflaumann, U., Sarnthein, M., Chapman, M., d'Abreu, L., Funnell, B., Huels, M., Kiefer, T., Maslin, M., Schulz, H., Swallow, J., van Kreveld, S., Vautravers, M., Vogelsang, E., Weinelt, M., 2003. Glacial North Atlantic: sea-surface conditions reconstructed by GLAMAP 2000. Paleoceanography 18, 1065. http://dx.doi.org/10.1029/2002PA000774.
Pisias, N.G., Clark, P.U., Brook, E.J., 2010. Modes of global climate variability during marine isotope stage 3 (60–26 ka). J. Clim. 23 (6), 1581–1588. http://dx.doi.org/10.1175/2009JCLI3416,1.
Prell, W.L., 1985. The Stability of low-Latitude sea-Surface Temperatures: An Evaluation of the CLIMAP Reconstruction with Emphasis on the Positive SST Anomalies. Brown Univ., Providence, RI (USA). Dept. of Geological Sciences.

Railsback, L.B., Gibbard, P.L., Head, M.J., Voarintsoa, N.R.G., Toucanne, S., 2015. An optimized scheme of lettered marine isotope substages for the last 1.0 million years, and the climatostratigraphic nature of isotope stages and substages. Quat. Sci. Rev. 111, 94–106.

Rodrigues, T., Voelker, A.H.L., Grimalt, J.O., Abrantes, F., Naughton, F., 2011. Iberian Margin sea surface temperature during MIS15 to 9 (580–300 ka): glacial suborbital variability versus interglacial stability. Paleoceanography 26, 1–16. http://dx.doi.org/10.1029/2010PA001927.

Roucoux, K.H., de Abreu, L., Shackleton, N.J., Tzedakis, P.C., 2005. The response of NW Iberian vegetation to North Atlantic climate oscillations during the last 65 kyr. Quat. Sci. Rev. 24, 1637–1653. http://dx.doi.org/10.1016/j.quascirev.2004.08.022.

Ruddiman, W.F., McIntyre, A., 1981. Oceanic mechanisms for amplification of the 23,000-year cycle. Science 212, 617–627.

Rühlemann, C., Mulitza, S., Müller, P.J., Wefer, G., Zahn, R., 1999. Warming of the tropical Atlantic Ocean and slowdown of thermohaline circulation during the last deglaciation. Nature 402, 511–514. http://dx.doi.org/10.1038/990069.

Sánchez Goñi, M.F., Bard, E., Landais, A., Rossignol, L., d'Errico, F., 2013. Air–sea temperature decoupling in western Europe during the last interglacial–glacial transition. Nat. Geosci. http://dx.doi.org/10.1038/NGEO1924.

Sánchez Goñi, M.F., Landais, A., Fletcher, W.J., Desprat, S., Duprat, J., 2008. Contrasting impacts of Dansgaard-Oeschger events over a latitudinal transect modulated by orbital parameters. Quat. Sci. Rev. 27, 1136–1151. http://dx.doi.org/10.1016/j.quascirev.2008.03.003.

Serra, N., Ambar, I., Boutov, D., 2010. Surface expression of Mediterranean water dipoles and their contribution to the shelf/slope-open ocean exchange. Ocean Sci. 6, 191–209.

Shackleton, N.J., Hall, M.A., Vincent, E., 2000. Phase relationships between millennial-scale events 64000–24000 years ago. Paleoceanography 15-6, 565–569. http://dx.doi.org/10.1029/2000PA000513.

Skinner, L.C., Elderfield, H., 2007. Rapid fluctuations in the deep North Atlantic heat budget during the last glacial period. Paleoceanography 22, PA1205. http://dx.doi.org/10.1029/2006PA001338.

Skinner, L.C., Shackleton, N.J., 2006. Deconstructing termination I and II: revisiting the glaciowustatic paradigm base don deep-water temperatura estimates. Quat. Sci. Rev. 25, 3312–3321.

Skinner, L.C., Shackleton, N.J., Elderfield, H., 2003. Millennial-scale variability of deep-water termperature and δ18Odw indicating deep-water source variations in the Northeast Atlantic, 0–34 cal. ka BP. Geochem. Geophys. Geosyst. 4, 1098. http://dx.doi.org/10.1029/2003GC000585.

Stocker, T.F., 1999. Past and future reorganisations in the climate system. Quat. Sci. Rev. 19, 301–319.

Stow, D.A.V., Hernández-Molina, F.J., Alvarez-Zarikian, C.A., Expedition 339 Scientists, 2012. Mediterranean outflow: environmental significance of the Mediterranean outflow water and its global implications. IODP Preliminary Report 339. http://dx.doi.org/10.2204/iodp.pr.339.2012.

Swift, J., 1986. The Arctic waters. In: Hurdle, B.G. (Ed.), The Nordic Seas. Springer, New York, pp. 129–151.

Thunell, R.C., 1976. Optimum indices of calcium carbonate dissolution in deep-sea sediments. Geology 4, 525–528.

Tolderlund, D.S., Bé, A.W.H., 1971. Seasonal distribution of planktonic foraminifera in the western North Atlantic. Micropaleontology 17, 297–329.

Vautravers, M.J., Shackleton, N.J., 2006. Centennial-scale surface hydrology off Portugal during marine isotope stage 3: insights from planktonic foraminiferal fauna variability. Paleoceanography 21, PA3004. http://dx.doi.org/10.1029/2005PA001144.

Wright, A.K., Flower, B.P., 2002. Surface and deep ocean circulation in the subpolar North Atlantic during the mid-Pleistocene revolution. Paleoceanography 17, 1068. http://dx.doi.org/10.1029/2002PA000782.

Zahn, R., Schönfeld, J., Kudrass, H.R., Park, M.H., Erlenkeuser, H., Grootes, P., 1997. Thermohaline instability in the North Atlantic during meltwater events: stable isotope and ice-rafted detritus records from core SO75-26KL, Portuguese margin. Paleoceanography 12, 696–710.

Global and Planetary Change 133 (2015) 176–187

Contents lists available at ScienceDirect

Global and Planetary Change

journal homepage: www.elsevier.com/locate/gloplacha

Response of macrobenthic and foraminifer communities to changes in deep-sea environmental conditions from Marine Isotope Stage (MIS) 12 to 11 at the "Shackleton Site"

Francisco J. Rodríguez-Tovar [a,*], Javier Dorador [a], Gloria M. Martin-Garcia [b], Francisco J. Sierro [b], José A. Flores [b], David A. Hodell [c]

[a] Departamento de Estratigrafía y Paleontología, Universidad de Granada, 18002 Granada, Spain
[b] Department of Geology, University of Salamanca, Spain
[c] Godwin Laboratory, University of Cambridge, Department of Earth Sciences, United Kingdom

ARTICLE INFO

Article history:
Received 11 March 2015
Received in revised form 14 August 2015
Accepted 18 August 2015
Available online 22 August 2015

Keywords:
Integrated Ocean Drilling Program
Expedition 339
Site U1385
Marine Isotope Stages 12 and 11
Trace fossils
Planktonic and benthic foraminifers

ABSTRACT

Integrative research including facies characterization, ichnological composition and foraminifer analysis has been conducted on cores from Site U1385 of the IODP Expedition 339 to evaluate the incidence of Marine Isotope Stage (MIS) 12 and MIS 11 on deep-sea environmental changes. Four color facies groups have been differentiated, showing variable transitions between them (bioturbated, gradual and sharp contacts). Trace fossil assemblage, assigned to the *Zoophycos* ichnofacies, consists of light and dark filled structures, with *Alcyonidiopsis*, *Chondrites*, *Nereites*, *Planolites*, *Spirophyton*, *Thalassinoides*, *Thalassinoides*-like structures, and *Zoophycos*. A deep-sea multi-tiered trace fossil community is interpreted, revealing predominance of well-oxygenated bottom and pore-waters, as well as abundance of food in the sediment for macrobenthic tracemaker community. Changes in environmental parameters are interpreted to be associated with significant variations in trace fossil distribution according to the differentiated intervals (A to M). Benthic foraminifer concentration in the sediments and variations of the planktonic foraminifer assemblages suggest significant changes in surface productivity and food supply to the sea floor since the ending of MIS 13 to the end of MIS 11 that could be correlated with the registered changes in facies and trace fossil assemblages. At the end of MIS 13 values of annual export productivity were very low, that together with the presence of light-color sediments and the continuous presence of light *Planolites* and *Thalassinoides*, reveal lower organic carbon flux to the bottom and high oxygen conditions (interval A). Afterwards the organic matter supply increased rapidly and remained very high until Termination V, determining an eutrophic environment, expressed by high benthic foraminifer accumulation rates, and reduced availability of oxygen, that correlate with the record of *Spirophyton* and *Zoophycos*, and the presence of *Chondrites*, observed in intervals B and D. Lower benthic foraminifer accumulation rates during MIS 11 suggest an oligotrophic environment at the bottom consistent with lower inputs of organic carbon, associated with high oxygen content of bottom waters that agrees with the lighter color of the sediments as well as by the continuous presence of light *Planolites* and *Thalassinoides* in the differentiated interval M. The evolution of the macrobenthic tracemaker community during MIS 12 and MIS 11 responds to major changes in bottom water ventilation probably linked to variations in deep water (North Atlantic) thermohaline circulation, determining variations in oxygen and food availability.

1. Introduction

Glacial/interglacial climatic cycles occurring during the Quaternary have been extensively studied due to their incidence on variations in the atmosphere/ocean dynamics and on the involved biota, including hominids. From several glacial/interglacial episodes, some of them are of special interest, as occurs with those corresponding with the Marine Isotope Stage (MIS) 12 and 11 (MIS 12 and MIS 11). The time interval involving MIS 12 and MIS 11 is considered one of the most extreme glacial and interglacial periods of the middle Pleistocene. The glacial MIS 12 is characterized by strong cold conditions, and the interglacial MIS 11 is one exceptionally long interglacial warm period. The Mid-Brunhes Event (MBE), close to the MIS 12/MIS 11 transition, at around 450 ka BP, a climatic transition between MIS 13 and MIS 11, separates 2 significantly different climatic modes, with interglacials characterized

* Corresponding author.
E-mail addresses: fjrtovar@ugr.es (F.J. Rodríguez-Tovar), javidr@ugr.es (J. Dorador), gm.martin@usal.es (G.M. Martin-Garcia), sierro@usal.es (F.J. Sierro), flores@usal.es (J.A. Flores), dah73@cam.ac.uk (D.A. Hodell).

http://dx.doi.org/10.1016/j.gloplacha.2015.08.012
0921-8181/

by only moderate warmth previous to this event (early Middle Pleistocene interglacials; 780–450 ka), and interglacial characterized by greater warmth after this event (Middle and Late Pleistocene interglacials; after 450 ka) (i.e., Candy et al., 2010). The transition MIS 12/11, corresponding with Termination V, is the longest glacial Termination of the past 450 ka, having major incidence for the biogeography and human occupation (Candy et al., 2014).

MIS 11 is considered as one of the appropriate climate analogs for the Holocene, being of special interest even for the analysis of future climate variations, which is reflected by the amount of information obtained on this episode (see two consecutive reviews by Droxler et al., 2003; Candy et al., 2014). All this information allows a detailed characterization of MIS 11, the warm climatic features, and the induced changes in the atmosphere/ocean dynamics. Thus, according to the last revision by Candy et al. (2014), and references therein, several features of MIS 11 are the following: a) the warm episode MIS 11 consists of an interglacial (MIS 11c) and several interstadial and stadial events (i.e., MIS 11a and MIS 11b), with differences in the number and magnitude according to the studied records, b) MIS 11c is a long warm climate period that lasted for about 25–30 ka, c) temperature data reveals that MIS 11 was an interglacial of relatively moderate warmth, similar to, or slightly cooler than the Holocene, and d) most of the evidences suggest that MIS 11c is characterized by sea levels significantly above those from the Holocene, even turnovers in fauna are consistent with prolonged period of lower sea levels at the beginning and middle part of MIS 11c.

Detailed analyses of MIS 11 and MIS 12 have been conducted in a number of studies on marine, ice core, lacustrine and terrestrial sequences, involving numerous biotic (i.e., pollen and foraminiferal assemblages) and abiotic (i.e., stable isotope and elemental chemistry) proxies, allowing interpretation of environmental parameters such as the global ice volume or sea surface temperatures. In this sense, as pointed out by Candy et al. (2014) for the identification of MIS 11 in British terrestrial record, terrestrial deposits contain numerous proxies allowing interpretation of different environmental parameters, whereas ice and marine core records contain, frequently, a single proxy. In marine cores the usually applied biotic proxies are foraminiferal (benthic and planktonic) assemblages. In this sense, little attention has been focused on the ichnological record; being very scarce, near absent, the approaches are based on the study of the trace fossil assemblage (see Löwemark et al., 2006, 2012, on trace fossil assemblage studies including MIS 11 in the eastern Mediterranean Sea and Artic Ocean, respectively). Here we present a detailed ichnological analysis of MIS 11 and MIS 12 on cores from IODP Expedition 339 Site U1385, in order to interpret changes in deep-sea environmental conditions, affecting the macrobenthic environment. Integration with information from benthic and planktonic foraminifers, allows integrative interpretations. Moreover, paleoceanographic implications will be assessed.

2. Site U1385 at IODP Expedition 339

IODP Site U1385 is located off the west Iberian Margin (37°34.285′N, 10°7.562′W; Fig. 1), on a spur, the Promontorio dos Principes de Avis, along the continental slope of the southwestern Iberian margin, at a water depth of 2578 m b.s.l. (Hodell et al., 2013a). This Site U1385, was drilled near the position of core MD01-2444 (Vautravers and Shackleton, 2006; Martrat et al., 2007; Skinner and Elderfield, 2007; Margari et al., 2010; Expedition 339 Scientists, 2013a; Hodell et al., 2013b), one of the cores retrieved from the SW Iberian Margin by the R/V Marion Dufresne in 1995, 1999 and 2011, including Core MD95-2042 (the "Shackleton Site") used as a key archive to approach millennial-scale climate variability over the last glacial cycle (Shackleton et al., 2000, 2004). Site U1385 was drilled to create a marine reference section of sub-Milankovitch (millennial-scale) climate variability and changes in surface and deep-water circulation occurring during the Pleistocene (Expedition 339 Scientists, 2013a,b).

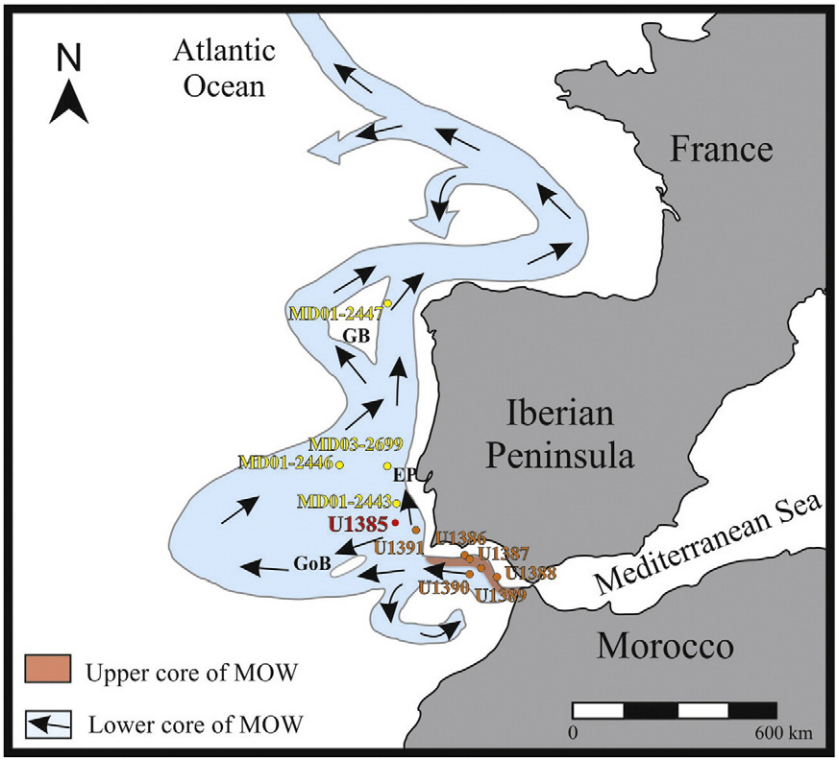

Fig. 1. General circulation pattern of the Mediterranean Outflow Water (MOW) (Expedition 339 Scientists, 2013b), with location of IODP Expedition 339 drill sites (red point for Site U1385 and orange points for the rest of sites), together with sites MD01-2447 (Desprat et al., 2005) in the North, MD01-2446 and MD03-2699 (Voelker et al., 2010) in the central, and MD01-2443 (de Abreu et al., 2005) in the South of the West Iberian Margin (blue points). Note: GB, Galicia Bank; EP, Extremadura Promontory; GoB, Gorringe Bank.

At Site U1385 five Holes were cored, recovering a total of around 622 m of a uniform lithologic unit dominated by bioturbated calcareous muds and calcareous clays (Expedition 339 Scientists, 2013a,b), with no notable gaps or disturbed intervals to 166.5 mcd (Expedition 339 Scientists, 2013a; Hodell et al., 2013a). Recently a very low sedimentation rate, a condensed section in which the complete interval from 415 to 431 ka is compressed into 4 cm, has been recognized at the early MIS 11 (Hodell et al., 2015-in this issue; Sánchez-Goñi et al., submitted for publication). The site contains a complete record from the Holocene to 1.43 Ma (MIS 46), allowing a fine-tuning by correlation of millennial events to ice core and speleothem records for the last 800 ka (Hodell et al., 2013a, 2015-in this issue). High-resolution sampling at 1 cm intervals enables resolving millennial climate events, as well as glacial–interglacial cycles, including their corresponding Terminations.

Site U1385 is close to site MD01-2443 (Fig. 1; de Abreu et al., 2005) in the South of the West Iberian Margin, that yielded significant records of MIS 11 for the interpretation of the involved climatic changes. On this base, Site U1385 is of major interest to study MIS 11 and MIS 12.

3. Material and methods

The research has been conducted on Cores 7H-4 to 7H-1 from Hole U1385D ("Shackleton Site"). Facies characterization has been integrated with the analysis of trace fossils, and benthic/planktonic foraminifers.

Facies analysis is based on the study of lithological composition, type of contacts, and primary sedimentary structures, with special attention to stratigraphic variations. Digital image treatment allows recognition of variations in color, difficult to recognize based, exclusively, on visual observations (Dorador and Rodríguez-Tovar, submitted for publication). Ichnological analysis focused on trace fossil assemblages, including trace fossil composition, infilling material, cross-cutting relationships, tiering structure, and relative abundances. Ichnotaxonomical classification was conducted as the ichnogenus level, as usual for core analysis. Ichnological analysis consists of detailed observations of half-cut sections of the core in the IODP core repository at Bremen (Germany), together with the study of high-resolution images. Several techniques of digital image treatment to improve the trace fossil visibility were applied for ichnological characterization (Dorador and Rodríguez-Tovar, 2014; Dorador et al., 2014a,b; Rodríguez-Tovar and Dorador, 2014, in press).

Sampling for export productivity (Pexp) reconstruction and isotope studies was performed every 20 cm providing an estimated average 2 ka resolution record, and for counts on both benthic and planktonic foraminifers sampling was performed at an average 4.6 cm separation, providing an estimated average 0.79 ka resolution. Samples (1 cm-thick) were freeze-dried, weighed and washed over a 63 μm mesh sieve. The >63 μm residue was dried, weighed and sieved again to separate and weigh the >150 μm fraction. Counts on planktonic and benthic foraminifer taxa were conducted on this sediment fraction, which was successively split until a minimum of 300 specimens were obtained. Planktonic species were used to reconstruct Pexp with the modern analog technique (MAT) (Hutson, 1980) and the modern analog database compiled by Salgueiro et al. (2010). Stable isotopes were measured on the planktonic foraminifer *Globigerina bulloides* picked from the 250 to 355 μm size fraction and the benthic foraminifer *Cibicidoides wuellerstorfi* from the >212 μm fraction (see Hodell et al., 2015-in this issue). Isotopic measurements were performed at the Godwin Laboratory (University of Cambridge, Cambridge, United Kingdom) on a VG SIRA mass spectrometer with automatic carbonate preparation system and calibrated to the Vienna Peedee Belemnite (VPB) standard, allowing an analytical precision better than 0.08‰.

The age model of the studied section is based on the correlation of the benthic oxygen isotope record to the global benthic LR04 isotope stack (Lisiecki and Raymo, 2005; see Hodell et al., 2015-in this issue).

4. Results

4.1. Facies characterization

As in general for the entire Site U1385, the studied interval consists of bioturbated calcareous muds and calcareous clays (Expedition 339 Scientists, 2013a,b). Primary sedimentary structures (i.e., lamination) are near absent; occasionally horizontal lamination into the darker/black intervals is observed (Expedition 339 Scientists, 2013a,b). Moreover, no significant changes in grain size are observed. In this general, homogenized, pattern, clear differentiations can be recognized, mainly related to variations in color, probably associated with the organic matter content, usually linked to changes in the trace fossil assemblage (see below). These variations in color can be observed directly on cores, but are even more evident when digital image treatment is applied (Dorador and Rodríguez-Tovar, submitted for publication). Thus, mainly according to variations in color, upper and lower contacts, and ichnological composition, several intervals have been differentiated (A to M); see Table 1 and Fig. 2 for a detailed characterization of the intervals. These intervals can be grouped into four color groups, from light tone gray/greenish, middle dark tone gray/greenish, very dark tone gray/greenish and dark/black, showing variable transitions between them (bioturbated, gradual and sharp contacts). From here we will refer to gray tone in substitution for gray/greenish.

As a general picture, light tone gray sediments are dominant, mainly registered and thicker in the lower/middle part of Core U1385D-7H-4 (interval A), and in the upper part of U1385D-7H-2 and the entire U1385D-7H-1 (interval M). Another thinner light interval is registered at the base of Core U1385D-7H-3 (interval E). In general these intervals show a relatively scarce trace fossils filled with light material.

At the opposite, dark/black intervals are scarce and thin, being located exclusively in the middle and upper parts of Core U1385D-7H-4 (intervals B and D). These intervals are characterized by dark trace fossils, which occasionally are also observed downward into the upper parts of the lighter intervals below (intervals A and C).

Middle and dark gray tone intervals are dominant in Cores U1385D-7H-2 and 3 (intervals F, G, H, I, J, K, and L), and are also registered in the upper part of Core U1385D-7H-4 (interval C). Middle gray tone intervals (intervals C, G, I, and lower K) mainly consist of a well developed light trace fossil assemblage on a mottled background. In the very dark tone gray intervals (intervals F, H, J and upper K) light and dark trace fossils are observed on a light/dark mottled background. Two intervals (intervals J and L) into the dark gray intervals show slight differences in color, with the presence of grayish/blue/pink sediments.

4.2. Ichnological analysis

Digital image treatment allows a clear differentiation between biodeformational structures and trace fossils (Dorador and Rodríguez-Tovar, 2014; Dorador et al., 2014a,b; Rodríguez-Tovar and Dorador, 2014, in press). Biodeformational structures, showing undifferentiated outlines and the absence of a defined geometry, which impede an ichnotaxonomical classification (see Uchman and Wetzel, 2011; Wetzel and Uchman, 2012), are registered as a mottled background, with color mixture and predominance of lighter or darker sediments related to the recognized intervals. Trace fossils show a variable degree of diffusiveness, from diffuse to discrete structures, as well as variable infilling material, from light to dark, being clearly distinguished from the host sediment based on their characteristic shape, although, sometimes, this differentiation is difficult.

4.2.1. Trace fossil assemblage

In general, a relatively diverse trace fossil assemblage was recognized, including structures filled with light and dark sediments (light and dark filled structures), consisting of *Alcyonidiopsis*, *Chondrites*, *Nereites*, *Planolites*, *Spirophyton*, *Thalassinoides*, *Thalassinoides*-like structures, and

Table 1
Differentiated intervals with lithological and ichnological features.

Interval (thickness/location)	Facies color	Contacts	Background	Light traces	Dark traces	Cross-cutting relationships
A (75 cm): from 150 to around 75 cm of U1385 7H4	Light tone gray	Bioturbated upper contact	Mottled background	Diffuse *Thalassinoides* (l*Th*) & *Planolites* (l*Pl*)	*Chondrites* (d*Ch*) from 89 to 75 cm	d*Ch* crosscutting l*Th* & l*Pl*
B (14 cm): from 75 to 61 cm of U1385 7H4	Dark/black	Gradual upper contacts	Mottled background	*Thalassinoides* from 67 to 61 cm	Dominant *Chondrites* (d*Ch*). *Planolites* (d*Pl*) & *Thalassinoides* (d*Th*) at the base	*dCh* crosscutting d*Th* & d*Pl*
C (43 cm): from 61 to 18 cm of U1385 7H4	Middle dark tone gray	Bioturbated upper contact	Mottled background	Diffuse *Thalassinoides* (l*Th*) and *Planolites* (l*Pl*)	Dominant *Chondrites* (d*Ch*), *Planolites* (d*Pl*), *Thalassinoides* (d*Th*), *Spirophyton* (d*Sp*) & *Zoophycos* (d*Zo*)	Dark traces crosscutting light traces & d*Ch* crosscutting d*Pl*, d*Tha* & d*Sp*
D (13 cm): from 18 to 5 cm of U1385 7H4	Dark/black	More or less shap upper contact			Dominant *Chondrites* (d*Ch*) & *Zoophycos* (d*Zo*). *Thalassinoides* (d*Th*) at the base	*dCh* crosscutting d*Th*
E (35 cm): from 5 cm of U1385D 7H4 to 119 cm of U1385 7H3	Light tone gray	Sharp upper contact, channel morphology	Mottled background, especially on top	Discrete, dominant *Thalassinoides* (l*Th*), and few *Planolites* (l*Pl*)		
F (58 cm): from 119 to 61 cm of U1385 7H3	Very dark tone gray, with increasing darker upward	Sharp upper contact	Mottled background	*Planolites* (l*Pl*), on top	*Planolites* (d*Pl*) &*Thalassinoides* (d*Th*), then *Zoophycos* (d*Zo*). Probable *Thalassinoides*-like (d*Th*-l)	d*Zo* cross-cutting d*Th* on top
G (74 cm): from 61 of U1385 7H3 to 137 cm of U1385 7H2	Middle dark tone gray, with a thick (56 cm) darker horizon at the middle part	Bioturbated upper contact	Mottled background at the lighter parts	*Thalassinoides* (l*Th*) and *Planolites* (l*Pl*) as exclusive in the lighter part, and also in the upper part of the darker horizon	Diffuse, abundant *Zoophycos* (d*Zo*), but also *Thalassinoides* (d*Th*-l), and probable *Planolites* (*dPl*) in the darker horizon *Alcyonidiopsis* (d*Al*), *Chondrites* (d*Ch*), *Planolites* (d*Pl*), *Thalassinoides* (d*Th*) & *Zoophycos* (d*Zo*) in the upper light interval, coming from the next dark interval	d*Zo* cross-cutting d*Th* *dCh* cross-cutting the rest of traces
H (33 cm): from 137 to 104 cm of U1385 7H2	Very dark tone gray	Bioturbated upper contact	Mottled background	Probable *Thalassinoides* (l*Th*) on top	Dominant, near exclusive, *Zoophycos* (d*Zo*)	
I (12 cm): from 104 to 92 cm of U1385 7H2	Middle dark tone gray	Sharp/bioturbated upper contact? Minor erosion?	Mottled background	*Planolites* (l*Pl*) & probable *Thalassinoides* (l*Th*)	*Planolites* (d*Pl*), *Thalassinoides* (d*Th*) & dominant, diffuse, *Zoophycos* (d*Zo*)	d*Zo* cross-cutting d*Pl* and d*Th*
J (18 cm): from 92 to 74 cm of U1385 7H2	Very dark grayish/blue/pink	Mixture of sediments Sharp/bioturbated upper contact?	Mottled background	*Thalassinoides* (l*Th*) & *Planolites* (l*Pl*)	Diffuse *Planolites* (d*Pl*) *Thalassinoides*,(d*Th*) and *Zoophycos* (d*Zo*)	d*Zo* cross-cutting d*Th*
K (47 cm): from 74 to 27 cm of U1385 7H2	Middle to very dark tone gray/pink	Darker color upward. Sharp upper contact?	Mottled background	Diffuse *Planolites* (l*Pl*) & *Thalassinoides* (l*Th*)	Diffuse *Zoophycos* (d*Zo*)	
L (12 cm): from 27 to 15 cm of U1385 7H2	Very dark grayish/blue/pink	Gradual contact to lighter color & decreasing bioturbation	Mottled background	*Thalassinoides* (l*Th*) & *Planolites* (l*Pl*), sinuous traces	*Planolites* (d*Pl*), sinuous, bifurcate traces	
M (165 cm); from 15 cm of U1385D 7H2 to 0 of U1385D 7H1	Light tone gray with darker intercalation	Gradual alternations in color	Mottled background	Diffuse *Planolites* (l*Pl*), *Thalassinoides* (l*Th*) & local *Nereites* (l*Ne*)	Diffuse *Planolites* (d*Pl*) and *Thalassinoides* (d*Th*), probably *Zoophycos* (d*Zo*),	

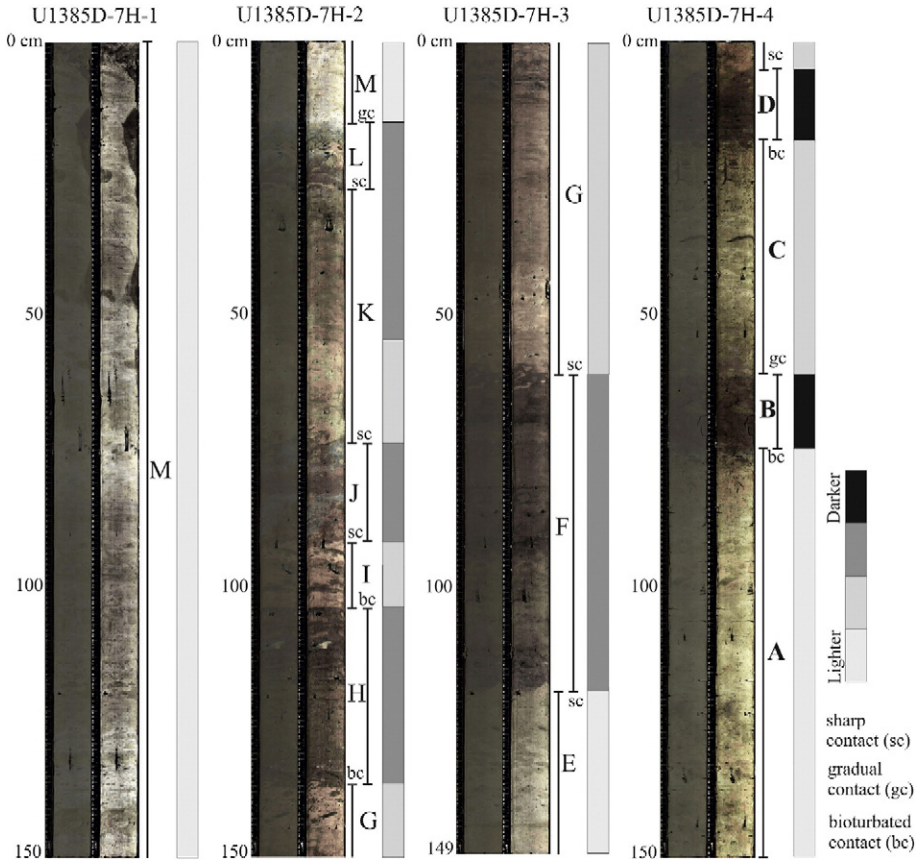

Fig. 2. Studied cores from Hole U1385D-7H-1 to U1385D-7H-4, showing the recognized intervals A to M, contacts, and color differentiation. Left and right parts of the cores before and after digital image treatment.

Zoophycos (Figs. 3, 4). Moreover, undifferentiated sinuous traces have been observed in interval L. Light infilling traces refer to those light traces slightly darker than the light host sediment. Light infilling *Planolites* and *Thalassinoides* are the dominant, near exclusive, ichnotaxa, whereas light *Nereites* are locally observed (Fig. 3). Dark infilling traces can be produced into the middle and very dark tone gray intervals or into the dark/black sediments. In the dark trace fossil assemblage *Zoophycos* is dominant, *Planolites* and *Thalassinoides* are frequent, while *Alcyonidiopsis*, *Chondrites*, *Spirophyton*, and *Thalassinoides*-like structures are rare (Fig. 4).

The trace fossil assemblage can be assigned to the *Zoophycos* ichnofacies, typical for deep-sea environments, as was previously proposed for Site U1385 (Rodríguez-Tovar and Dorador, 2014). As a general rule, dark trace fossils are registered as cross-cutting light ones. Into the dark trace fossil assemblage, usually *Chondrites* and *Zoophycos* are observed cross-cutting the rest of traces, such as *Planolites*, *Spirophyton* and *Thalassinoides*. A brief description of the differentiated ichnotaxa is as follows:

Alcyonidiopsis corresponds to a single elongate cylinder, slightly oblique, dark filled, 30 mm long and 6 mm wide, showing a pelloidal-like outline (see Uchman, 1999; Rodríguez-Tovar and Uchman, 2010 for interpretation).

Chondrites is generally observed as dense clusters of circular to elliptical spots, and short tubes, filled with dark sediment; occasionally branching. Mainly small forms (<1.5 mm wide) are observed that could correspond to *Chondrites intricatus* (Brongniart, 1823).

Nereites consists of small-medium size (2–5 mm diameter) circular to elliptical forms, with a dark-filled internal zone surrounded by a light filled envelope, observed as closed (paired) structures in horizontal planes.

Planolites occurs as unlined, unbranched, and mainly as circular to subcircular cylindrical tubular forms (4–7 mm in diameter, 5–2.5 mm in length). It is largely registered as horizontal or slightly oblique, filled with light or dark sediment, with a variable grade of diffusiveness. Fill is structureless, with different lithologies from the host rock.

Spirophyton is registered as a single trace consisting of a central, axial, J-shaped shaft (around 8 cm high), with alternating horizontal structures (around 2–3 mm wide and 20 mm long) extending from the axial shaft. Spreite has not been observed. Similar to *Zoophycos*, it differs by the small size and shape of horizontal structures.

Thalassinoides is observed as large, oval spots, circular to subcircular (6–12 mm wide), together with straight or slightly winding, horizontal to oblique smooth cylinders (20–43 mm long), showing a variable grade of diffusiveness. Structures are filled with light or dark sediment. Occasionally, mainly light filled *Thalassinoides*, are observed in clusters of circular to elliptical spots, corresponding to variable cross-sections of branching burrow systems.

Thalassinoides-like structures occur locally as circular to subcircular sections, 6–12 mm wide, filled with dark sediment. The shape is similar to *Thalassinoides*, but showing a variably developed irregular wall, resembling *Ophiomorpha*.

Zoophycos, is registered as repeated, more or less horizontal, spreiten structures (2–8 mm wide), consisting of alternating dark and light material. A variable degree of diffusiveness is observed, determining a more or less clear differentiation of the lamellae into the lamina. Frequently several horizontal traces (up to 6), probably belonging to a unique structure, are observed, evidencing a depth of penetration at least of 16 cm.

4.2.2. Distribution

The trace fossil assemblage shows clear variations along the differentiated intervals that can be related to the features (color) of the host sediment (Fig. 5). Light trace fossil assemblage, consisting of *Planolites*

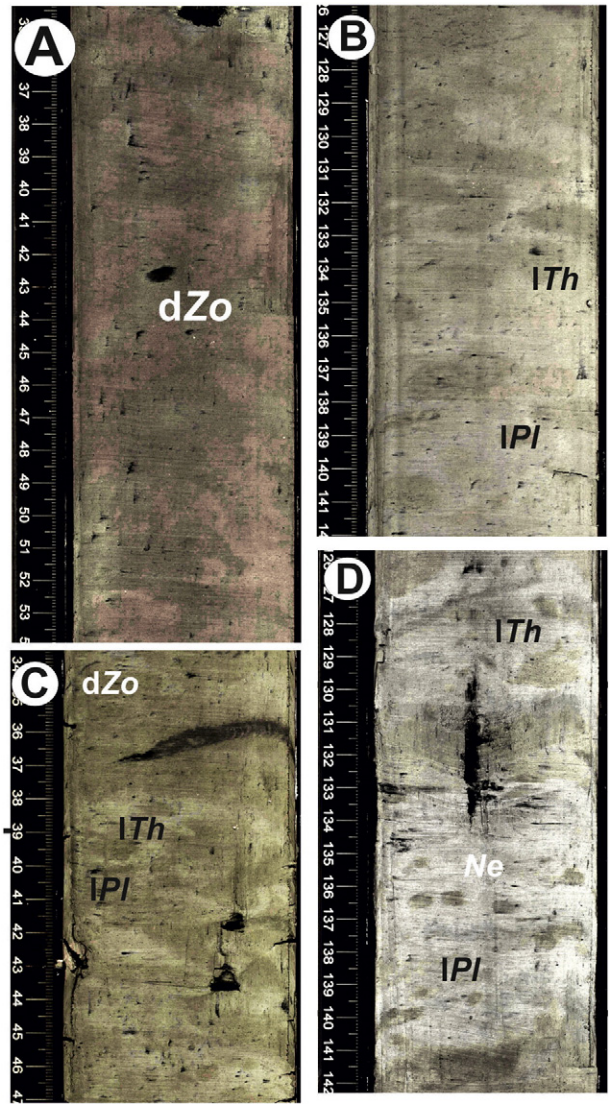

Fig. 3. Light trace fossils and local dark *Zoophycos* from gray (light, middle and dark tones) intervals. (A) Diffuse dark *Zooophycos* (d*Zo*) from dark tone gray interval K (U1385D-7H-2) on a well-developed mottled background. (B) Light *Thalassinoides* (l*Th*) and *Planolites* (l*Pl*) from light tone gray interval E (U1385D-7H-3). (C) Light *Thalassinoides* (l*Th*) and *Planolites* (l*Pl*), and dark *Zoophycos* (d*Zo*) from middle tone gray interval C (U1385D-7H-4). (D) Light *Thalassinoides* (l*Th*) and *Planolites* (l*Pl*), and *Nereites* (*Ne*) from light tone gray interval E (U1385D-7H-1).

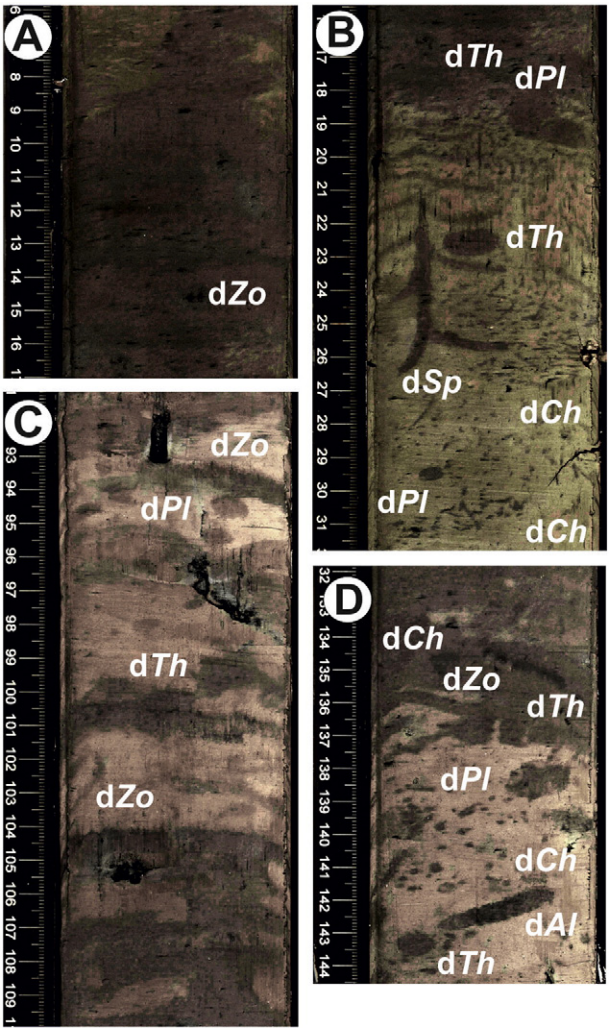

Fig. 4. Dark trace fossils from gray (middle and dark tone) and dark/black intervals. (A) Dark *Zoophycos* (d*Zo*) from the dark/black interval D (U1385-7H-4). (B) Dark *Chondrites* (d*Ch*), *Planolites* (d*Pl*), *Spirophyton* (d*Sp*) and *Thalassinoides* (*dTh*) from the upper part of the middle gray tone interval C transition to dark/black interval D (U1385-7H-4). (C) Dark *Thalassinoides* (*dTh*) and dark *Zoophycos* (d*Zo*) from the upper part of dark gray tone interval H to middle gray tone interval I (U1385-7H-2) (D) Dark *Alcyonidiopsis* (d*Al*), *Chondrites* (d*Ch*), *Planolites* (d*Pl*), *Thalassinoides* (*dTh*) and *Zoophycos* (d*Zo*) from the upper part of the middle gray tone interval G transition to dark gray tone interval H (U1385-7H-2).

and dominant *Thalassinoides*, is registered in most of the intervals, except, in the dark/black interval D, being dominated by light and middle gray tone intervals (A, C, E, G, I and M). However, in the light tone intervals (A and M), this light trace fossil assemblage is comparatively scarce, and the mottled background is less developed. The light trace fossil assemblage represents the bioturbation of tracemakers during deposition of the lighter host sediment. The dark trace fossil assemblage consists of frequent *Planolites* and *Thalassinoides*, associated with middle and very dark gray tone intervals, reflecting the mixture of phases of sedimentation corresponding to different colors; bioturbation by shallowest and shallow tier organisms produces the observed mixture of colored sediment. These trace dark *Planolites* and *Thalassinoides* are also observed in intervals showing a more or less developed alternation, not mixture, of colored sediments, such as in interval M. Occasionally, this assemblage is also registered at the base of black/dark color sediment (intervals B and D), probably reflecting a progressive, gradual, change. *Zoophycos* is the dominant dark trace fossil, observed in middle and very dark gray intervals, as well as in the black/dark ones. This trace originated during deposition of darker sediments, probably revealing latter phases of bioturbation by the dark trace fossil community, after *Planolites* and *Thalassinoides* producer. *Chondrites* and *Spirophyton* are mainly related to the dark/black intervals (B and D), are even located downward in the lighter intervals below, and associated with the particular environmental conditions of these dark (black) sediments.

4.3. Micropaleontological analysis

Benthic oxygen-isotope values have been used to identify MIS 13 to MIS 11 in the sediment cores. Based on the benthic oxygen isotope record glacial Termination V was recorded in IODP Site U1385 at around 55.70 crmcd. The previously described intervals A to M correspond to the final stages of MIS 13 (intervals A, B and half of the C), MIS 12 (half of interval C, intervals D–L and the first 20 cm of interval M), and early MIS 11 (the rest of interval M) (Fig. 6).

Analysis of the planktonic/benthic foraminifer ratio (Fig. 6d) reveals that planktonic microfauna is more abundant, in general, during interglacial conditions. However, during early glacial substage MIS 12b (and coinciding with interval G) elevated percentages of planktonic

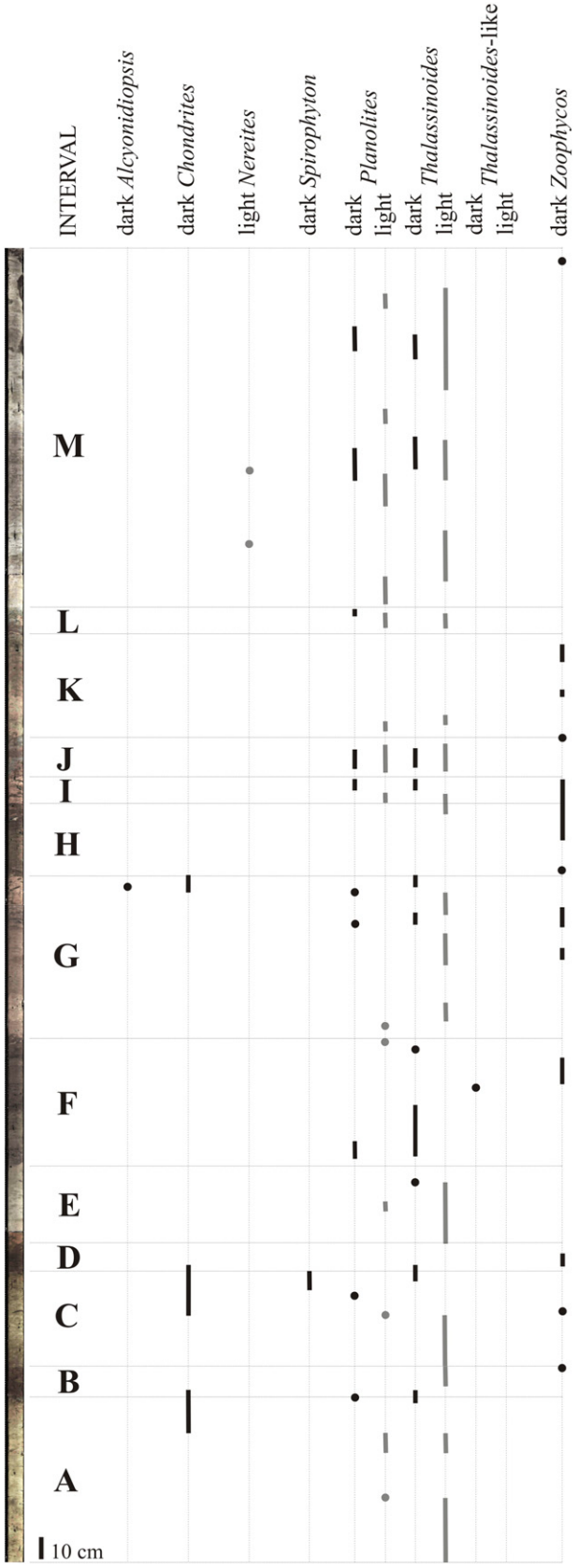

Fig. 5. Distribution of light and dark trace fossils in the studied cores from Hole 1385D-7H-4 (bottom) to U1385D-7H-1 (top), according to the differentiated intervals A to M.

foraminifers were also recorded. These high planktonic/benthic values are mainly due to low benthic production, expressed both by concentration (Fig. 6e) and accumulation rate (Fig. 6f). Benthic accumulation rate (measured in number of tests per cm^2 and ka) is higher during the glacial stage, especially at the beginning and end of the stage. The extraordinarily high number of benthic foraminifers per mass of sediment (Fig. 6e) during the glacial maximum MIS 12a, is probably due to low accumulation of other sedimentary components at this time (Fig. 6). Export productivity (Pexp) is low during MIS 11 and much higher in MIS 12, especially in the early part of this stage, as well as during the last part of MIS 13. In consequence, during the interglacial periods MIS 11 and MIS 13 low Pexp at the surface corresponds to low concentration of benthic foraminifers at the sea floor (Fig. 6e, h). By contrast, high Pexp in MIS 12 is linked, in general, to higher benthic foraminifer production.

5. Interpretation and discussion

5.1. Facies distribution and trace fossil composition

Major factors determining ichnological features (i.e., abundance, composition and diversity of trace fossil assemblages) in a deep-sea setting are food availability, bottom and pore-water oxygenation, substrate consistency, and rate of sedimentation (Wetzel, 1991; Uchman et al., 2008, 2013a,b; Rodríguez-Tovar et al., 2009a,b; Rodríguez-Tovar and Uchman, 2010; Uchman and Wetzel, 2011; Wetzel and Uchman, 2012; Rodríguez-Tovar and Reolid, 2013; Rodríguez-Tovar and Dorador, 2014). In the case study, the generalized mottled background, together with the observed trace fossil assemblage, reveals a deep-sea multi-tiered trace fossil community, interpreted as revealing predominance of well-oxygenated bottom and pore-waters, as well as abundance of food in the sediment for macrobenthic tracemaker community, as previously interpreted for Site U1385 (Rodríguez-Tovar and Dorador, 2014). In the generalized context of relatively good environmental conditions for the macrobenthic habitat, several changes can be interpreted, determining variations in facies and ichnological features.

Lighter sediments, as those represented by intervals A, E and M, are characterized by a relatively poorly developed mottled background together with light *Thalassinoides* and *Planolites*. *Thalassinoides* and *Planolites*, as facies-crossing forms, are found in a great variety of marine environments, usually associated with oxygenated sediments. *Thalassinoides* is related to soft but cohesive sediments (see Fürsich, 1973; Ekdale et al., 1984; Ekdale, 1992; Schlirf, 2000), and *Planolites*, an actively filled burrow, is interpreted as a pascichnion in shallow tiers (see Pemberton and Frey, 1982; Keighley and Pickerill, 1995 for discussion). Thus, good environmental conditions (mainly bottom and pore-water oxygenation, and food availability) can be interpreted, at least in the upper centimeters of the substrate, where shallowest and shallow tier communities are developed. Variations in the relative abundance of light *Planolites* and *Thalassinoides*, as well as in the diffusiveness can correspond with the rate of deposition and the firmness. The presence of dark *Planolites* and *Thalassinoides*, together with the local record of *Nereites* at interval M could reveal fluctuations in the organic matter content probably associated with variations in the detrital input and in the surface export productivity as revealed by planktonic foraminifer-reconstructed Pexp (Fig. 6h); the latter is interpreted as a shallow tier, pascichnia structure, in deep-marine, low energetic, oxygenated, environments (Uchman, 1995; Mángano et al., 2002; Wetzel, 2002; Löwemark et al., 2012), associated with increase food flux, feeding on microbes that occur in high concentrations (Wetzel, 2002; Löwemark et al., 2012).

Dark/black sediments, as represented by intervals B and D, reveal significant changes in the environmental conditions. The presence of dark *Planolites* and *Thalassinoides* at the base of the intervals, and then *Zoophycos* and dominant *Chondrites* could be interpreted as a gradual deterioration of the environmental conditions, probably related to increase in the organic matter content and decreasing oxygenation

more favorable for *Zoophycos* and *Chondrites* tracemakers. Both, *Zoophycos* and *Chondrites* are deep tier feeding structures. In general, *Zoophycos* producer has been related to variations in energy, sedimentation rate, food content, or bottom-water oxygenation; its relative independence of substrate features would allow for colonization of sediments with comparative low oxygenation, or even to collect food particles from the sea floor (e.g., Löwemark and Schäfer, 2003; Rodríguez-Tovar and Uchman, 2006, 2008). Several ethological models have been proposed of *Zoophycos* tracemaker (see Löwemark and Werner, 2001; Bromley and Hanken, 2003; Löwemark and Schäfer, 2003; Löwemark et al., 2004; Löwemark, 2015). *Chondrites* tracemaker is associated with poorly oxygenated bottom or pore waters, able to live in dysaerobic conditions, at the aerobic–anoxic interface, as a chemosymbiotic organism (Seilacher, 1990; Fu, 1991). Upwards in the dark/black intervals, a progressive return improvement can be envisaged by the presence of light structures (i.e., light *Thalassinoides*) in the upper part. The presence in the interval D of a well-developed dark trace fossil assemblage consisting of discrete structures, could be associated with a decrease in the sedimentation rate, increase in firmness and higher time of bioturbation, together with local concentration of food. This agrees with the record of delicate, complex, structures of *Spirophyton* and *Zoophycos*. *Spirophyton* has been interpreted, mainly for marine-margin deposits, as revealing an opportunistic strategy; formed rapidly after sudden influxes of organic material (Miller and Johnson, 1981; Miller, 1991, 2003; Bromley, 1996; Gaillard et al., 1999). The *Zoophycos* tracemaker is interpreted as bioturbating firmer, organic rich substrates with oxygen depleted pore waters (e.g., Rodríguez-Tovar and Uchman, 2004a,b; Rodríguez-Tovar and Dorador, 2014, and references therein). Distribution of *Zoophycos* has been related to Milankovicth orbital scale climatic changes, determining variations in the organic matter content and flux (Rodríguez-Tovar et al., 2011).

Middle and dark gray tone sediments, corresponding to intervals C, F, G, H, I, J, K, and L, reveal, in general, variable intermediate cases between dark/black sediments and the lighter ones. Both types of sediments consist of a well-developed mottled background in the first case with dominance of light color sediments while in the second a mixture between light and dark sediments is observed. In both cases *Planolites* and *Thalassinoides* are the most abundant traces, being light structures dominant in the first case while in dark gray tone sediments dark *Planolites* and *Thalassinoides* are also observed. Dark *Zoophycos* are also registered, especially in the dark gray tone intervals, but dark *Chondrites* are not observed. Middle and dark gray tone sediments could reflect a generalized good bottom and pore-water oxygen conditions and higher abundance in the organic matter content at the surface but also in the first centimeters of the sediment, allowing bioturbation by shallowest, shallow and middle tiers tracemakers. When input of organic matter content (as indicated by Pexp) is maintained during a comparatively long time (Intervals F, or H to K), deep tier traces, i.e., *Zoophycos*, can be developed, probably reflecting a comparatively higher organic matter content and a slight decrease in oxygenation probably related to the presence of the poorly ventilated and benthic $\delta^{13}C$-deplected Antarctic bottom water AABW (Adkins et al., 2005; Hoogakker et al., 2006) (Fig. 6b).

5.2. Environmental conditions during MIS 13–MIS 11 and the macrobenthic and foraminifer record

The benthic foraminifer concentration in the sediments and variations of the planktonic foraminifer assemblages suggest significant changes in surface water productivity and food supply to the sea floor occurring in the Portuguese margin during MIS 12 and MIS 11 that could be correlated with the registered changes in facies and trace fossil

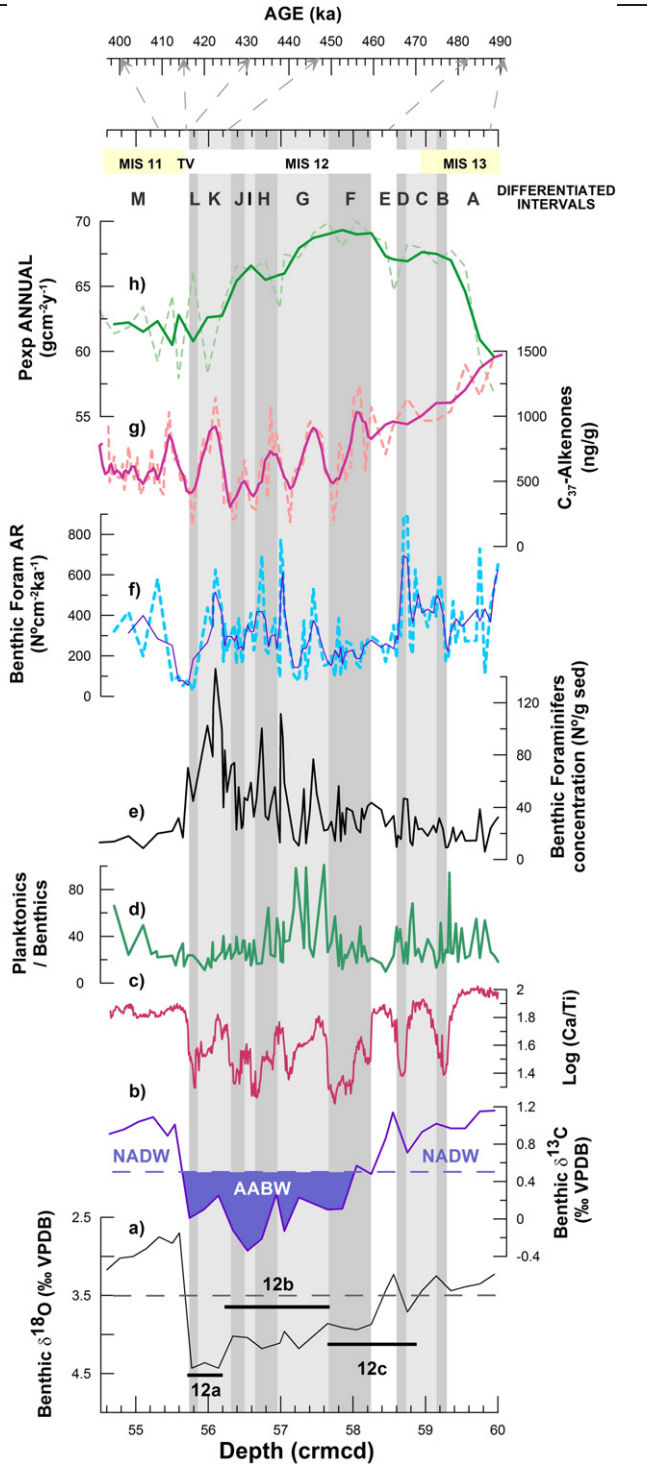

Fig. 6. Stratigraphic and temporal distribution of intervals A to M, differentiated according to color and trace fossil assemblage, and comparison with foraminifer records and other data from IODP-U1385. a) Benthic $\delta^{18}O$ (‰ VPDB) (Hodell et al., 2015-in this issue); substages are named according to Railsback et al. (2015); horizontal dashed line shows the ice volume threshold separating stable and unstable climatic conditions (McManus et al., 1999). b) Benthic $\delta^{13}C$ record (‰ VPDB); filling indicates typical values for Antarctic Botom Water (AABW) according to Adkins et al. (2005). c) Log Ca/Ti record (Hodell et al., 2015-in this issue). d) Planktonic/benthic foraminifer ratio. e) Benthic foraminifer concentration in number of tests per gram of dry sediment. f) Benthic foraminifer accumulation rate in number of tests per cm^2 and ka (dashed line) and 3-point running mean (solid). g) Total alkenone concentration (ng/g) of 37 carbon atoms (Maiorano et al., 2015-in this issue; courtesy of T. Rodrigues) reflects the coccolithophore productivity (dashed line) and 5-point running mean (solid). h) Export productivity (dashed line) and 3-point running mean (solid). Glacial and interglacial stages are highlighted by horizontal bands. Vertical bands correspond to the differentiated intervals with lithological and ichnological features, with its facies color highlighted: light gray (in white)–middle dark gray–very dark/black. Control points linking depth (crmcd) to LR04-reconstructed age (Hodell et al., 2015-in this issue) are represented by arrows.

assemblages (Fig. 6). Similar changes occurred across the more recent Terminations IV, II and I (Grunert et al., 2015-in this issue; Rodríguez-Tovar et al., 2015-in this issue).

Benthic communities living at the sea floor are limited by the flux of organic carbon reaching the sea floor that, in turn, are a function of Pexp and oxygen content along the water column and interstitial waters within the sediments. Higher densities of benthic foraminifers in bottom sediments have been related to higher rates of organic carbon supply to the sea floor, both in the same Site U1385 (Grunert et al., 2015-in this issue; Rodríguez-Tovar et al., 2015-in this issue) and in other locations (Schmiedl et al., 1997; Wollenburg et al., 2004; Mojtahid et al., 2009).

A trend of increased productivity both primary, according to coccolithophores (NAR) and alkenone data (Maiorano et al., 2015-in this issue), and secondary, according to planktonic foraminifer-reconstructed Pexp (Fig. 6g–h), occurred during the final stage of MIS 13 coinciding with warm SST inferred from the Ca/Ti record in our site (Hodell et al., 2015-in this issue). Low abundance of the coccolithophore *Florisphaera profunda* (Maiorano et al., 2015-in this issue), suggests a less stratified upper water column. During MIS 11 Pexp was very low and both intervals coincided with the presence of light-color sediments as well as with the continuous presence of light *Planolites* and *Thalassinoides* in the differentiated intervals A and M (Fig. 6). By contrast, during MIS 12 Pexp is higher, especially in the early part, but decreases towards the end of the stage. Benthic foraminifer accumulation rates do not follow this trend. This decoupling between Pexp, and benthic accumulation rates can be the result of the changing conditions of water column oxidation that are mainly reflected by the benthic $\delta^{13}C$ record. The high benthic $\delta^{13}C$ during MIS 11 and MIS 13 reflects the high bottom water oxygenation during these interglacial periods. Higher bottom water ventilation tends to decrease the accumulation of organic matter in the sediments and therefore reduce food availability for the macrobenthic and microbenthic communities.

Microbenthic fauna proliferated during the glacial stage as reflected by the higher benthic foraminifer accumulation rates, which can reach values over 800 individuals/cm^{2}ka. Similar enhanced fluxes of organic matter occurred also in the South Atlantic upwelling region during this glacial period (Scmiedl and Mackensen, 1997). This high organic carbon flux to the bottom, due to high Pexp and/or poor bottom water ventilation, allowed an eutrophic environment expressed by high benthic foraminifer accumulation rates. Nevertheless, high amounts of organic matter reaching the bottom could reduce the availability of oxygen and produce a subsequent impoverishment of the benthic habitat when bottom water ventilation is low (Grunert et al., 2015-in this issue; Rodríguez-Tovar et al., 2015-in this issue). These conditions happened during short intervals along MIS 12 and in Termination V when the Site was under the influence of less oxygenated bottom water (AABW), and are registered by the micro-benthos, as a decrease in benthic foraminifer accumulation rate coupled with increase in both Pexp and total alkenone production (Fig. 6). Macrobenthos also reveals the punctual pulse (increasing) in organic matter reaching the bottom, by the record of *Spirophyton* and *Zoophycos*, and the associated decrease in oxygen availability mainly revealed by the presence of *Chondrites*, observed in intervals B and D (Fig. 6). Differentiation of several intervals (A to L) during the ending of MIS 13 and the whole MIS 12, based on the trace fossil record agrees with the idea that tracemakers are more sensitive than foraminifers to depth variations in the redox boundary in near-surface sediments leading to the movement of trace-fossil tiers, as indicated by Baas et al. (1998) and also recently demonstrated by Rodríguez-Tovar et al. (2015-in this issue). Termination V, similarly to more recent Terminations II and IV and in opposition to Termination I (Rodríguez-Tovar et al., 2015-in this issue), was characterized by increasing Pexp and accumulation of organic matter without depletion of oxygenation, as increasing $\delta^{13}C$ coinciding with the lighter color interval M suggests (Fig. 6).

By contrast with MIS 12, lower benthic foraminifer accumulation rates during MIS 11 indicate an oligotrophic environment at the bottom and are consistent with lower inputs of organic carbon inferred from total alkenone accumulation (Maiorano et al., 2015-in this issue) and planktonic foraminifer Pexp, as well as with low NAR (Maiorano et al., 2015-in this issue). This oligotrophic environment is characteristic of peak interglacial periods in this region, as studies on sediments ranging from MIS 6 to the Holocene show (Pailler and Bard, 2002). Oxygen consumption in deep sea waters during MIS 11 due to the weak organic carbon supply was low which, together with the presence of the more ventilated North Atlantic Deep Water (NADW) as can be inferred from the high values of benthic $\delta^{13}C$ (Fig. 6b), resulted in higher oxygen content of bottom waters. This agrees with the lighter color of the sediments in the differentiated interval M, as well as by the continuous presence of light *Planolites* and *Thalassinoides*. This higher bottom-water oxygen concentration during the interglacial compared to the previous glacial maximum occurred on the Portuguese margin also during the last two climatic cycles (Hoogakker et al., 2015), and can be related to increased ventilation linked to a reorganization of ocean circulation after deglaciations (McManus et al., 2004). Oscillations in Pexp during these interglacial produced fluctuations of the organic matter content in the bottom, which is registered in the macrobenthos by the presence of dark *Planolites* and *Thalassinoides*, and the local record of *Nereites*. North Atlantic coccolithophore analyses allow for envisaging a relationship between lighter color sediments and high coccolith content in MIS 11 (Amore et al., 2012; Marino et al., 2014; Maiorano et al., 2015-in this issue).

The low availability of organic matter for benthic macro- and microfauna along MIS 11 could evidence a possible stratification of the superficial water masses in the area, as indicated by higher percentage of the coccolithophore *F. profunda* compared with the previous interglacial (Maiorano et al., 2015-in this issue), or be related to a reduced input of land-derived nutrients during the sea level highstand (Rodrigues et al., 2011). Such possibility should be explored with the study of planktonic fauna and the evolution of the sea surface conditions for the same period in the same site.

In a few cases, trace fossil assemblage in sediments corresponding to MIS 12 and MIS 11 has been characterized. At the eastern Mediterranean Sea, and in relation with the ichnological response to late Quaternary sapropel formation, a detailed trace fossil analysis was conducted on two cores from the last 400 ka, involving the base part of MIS 11 (Löwemark et al., 2006). As a general pattern, the sediment in the two cores is characterized by mottled burrows, with few trace fossils of *Scolicia*, *Thalassinoides*, *Chondrites*, and *Trichichnus*, attributed to well-oxygenated and warm bottom waters in an oligotrophic environment typical for non-sapropel times (Löwemark et al., 2006). Recently, variability in trace fossil abundance and diversity associated with glacial–interglacial cycles, including MIS 11, was recognized in Late Quaternary sediment cores from the Artic Ocean; during interglacial periods the increase food flux, rather than changes in deep water circulation, is responsible for higher abundance and diversity (i.e., *Scolicia*, *Planolites* or *Nereites*), while in glacial interval characterized by extremely low food flux consist of impoverished ichnofauna dominated by *Trichichnus* and *Chondrites* (Löwemark et al., 2012).

Obtained results allow addressing interpretations on local (?) paleoceanographic dynamics. Although higher resolution climatic records need to be carried out in this time period, benthic $\delta^{13}C$ data prove that the evolution of macrobenthic tracemaker community during MIS 12 and MIS 11 responded to major changes in bottom water ventilation probably linked to variations in deep water thermohaline circulation, determining variations in oxygen and food availability.

During glacial MIS 12 a higher planktonic foraminifer-reconstructed Pexp from surface waters, together with reduced deep water formation in the North Atlantic probably resulted in higher accumulation rates of organic matter in the sea floor, favoring the development of macrobenthic communities typically living in these environments, characterized by comparatively high food, and low oxygen availability. This was probably more intense at some particular time periods such as intervals B and D that may be linked to times of extremely poor

bottom-water ventilation associated with cooling events at the surface. In particular, dark intervals during MIS 12 show low Ca/Ti ratios (Fig. 6c) that are usually associated with cool stadials in the Portuguese margin (Hodell et al., 2013b, 2015-in this issue). The low benthic $\delta^{13}C$ values during MIS 12, especially in the dark intervals, indicate low bottom water ventilation probably due to a higher influence of AABW during this time period. Low bottom water oxygenation favored the preservation of organic matter, increasing food availability for the benthic macrofauna, even though the flux of organic matter from the surface was low.

By contrast, intense North Atlantic deep water formation during MIS 11 (interval M) (Poirier and Billups, 2014), and probably late MIS 13 (interval A), together with lower export production at the surface led to more oxygenated bottom waters in the Portuguese margin, determining a well-developed deep-sea tiered assemblage.

Near Termination V an extremely low sedimentation rate has been recognized based on the chronology elaborated for this site (Hodell et al., 2015-in this issue). The lowermost 40 cm at the base of MIS 11 (bottom of interval M) represent a condensed interval of 30 ka, with a more extreme condensation recorded in the first 5 cm at the base of this interval.

6. Conclusions

The present study including facies characterization, ichnological composition and foraminifer analysis, allowed interpretation of deep-sea paleoenvironmental conditions during the transition MIS 13/MIS 12, MIS 12 and MIS 11.

A generalized context of well-oxygenated bottom and pore-waters, as well as abundance of food in the sediment for macrobenthic tracemaker community can be interpreted, with marked changes in these paleoenviromental factors as revealed by variations in composition and distribution of trace fossils according to the differentiated intervals A to M.

Benthic foraminifer concentration in the sediments and variations of the planktonic foraminifer assemblages suggest significant changes in surface productivity and food supply to the sea floor during MIS 12 and MIS 11 that could be correlated with the registered changes in facies and ichnology.

The end of MIS 13 is characterized by low values of annual export productivity, that together with the presence of light-color sediments and the continuous presence of light *Planolites* and *Thalassinoides* at interval A, reveals relatively low organic carbon flux to the bottom and high oxygen conditions. These initial conditions were changed during development of MIS 12, showing the rapid increase in the organic matter supply and then remaining very high until Termination V, determining a eutrophic environment, as is revealed by high benthic foraminifer accumulation rates. This change and the associated reduced availability of oxygen, correlate with the record of *Spirophyton* and *Zoophycos*, and the presence of *Chondrites*, observed in intervals B and D. During MIS 11 lower benthic foraminifer accumulation rates are registered suggesting an oligotrophic environment at the bottom, associated with lower inputs of organic carbon, and high oxygen content of bottom waters, in agreement with the lighter color of the sediments as well as the continuous presence of light *Planolites* and *Thalassinoides* at interval M.

In conclusion, the evolution of macrobenthic tracemaker community during MIS 12 and MIS 11 responded to major changes in bottom water ventilation probably linked to variations in deep water (North Atlantic) thermohaline circulation.

Acknowledgments

This paper benefited from comments and suggestions by Drs Voelker (Instituto Portugues do Mar e da Atmosfera), and Löwemark (National Taiwan University). This research used samples and/or data provided by the Integrated Ocean Drilling Program (IODP). Funding for the research by R-T & D was provided by Project CGL2012-33281 (Secretaría de Estado de I + D + I, Spain), and Research Group RNM-178 (Junta de Andalucía). We want to thank Dr. Teresa Rodrigues who courteously provided her alkenone data used in Fig. 6.

Appendix A. Planktic foraminifer species and morphotypes used to reconstruct export productivity

Beella digitata

Globigerina bulloides
Globigerina falconensis
Globigerinella calida
Globigerinella siphonifera (aequilateralis)
Globigerinita glutinata
Globigerinoides ruber (pink)
Globigerinoides ruber (white)
Globigerinoides sacculifer
Globigerinoides trilobus
Globorotalia hirsuta
Globorotalia inflata
Globorotalia scitula
Globorotalia truncatulinoides
Globoturborotalita rubescens
Globoturborrotalita tenella
Neogloboquadrina dutertrei
Neogloboq. pachyderma (dextral)
Neogloboq. pachyderma (sinistral)
Orbulina
Pulleniatina obliquiloculata
Turborotalita humilis
Turborotalia quinqueloba

References

Adkins, J.F., Ingersoll, A.P., Pasquero, C., 2005. Rapid climate change and conditional instability of the glacial deep ocean from the thermobaric effect and geothermal heating. Quat. Sci. Rev. 24, 581–594.
Amore, F.O., Flores, J.A., Voelker, A.H.L., Lebreiro, S.M., Palumbo, E., Sierro, F.J., 2012. A Middle Pleistocene Northeast Atlantic coccolithophore record: paleoclimatology and paleoproductivity aspects. Mar. Micropaleontol. 90–91, 44–59.
Baas, J., Schönfeld, J., Zahn, R., 1998. Mid-depth oxygen drawdown during Heinrich events: evidence from benthic foraminiferal community structure, trace-fossil tiering, and benthic $\delta^{13}C$ at the Portuguese Margin. Mar. Geol. 152 (1), 25–55.
Bromley, R.G., 1996. Trace Fossils. Biology, Taphonomy and Applications Second edition. Chapman & Hall, London.
Bromley, R.G., Hanken, N.M., 2003. Structure and function of large, lobed *Zoophycos*, Pliocene of Rhodes, Greece. Palaeogeogr. Palaeoclimatol. Palaeoecol. 192, 79–100.
Brongniart, A.T., 1823. Observations sur les Fucoïdes. Mém. Soc. Hist. Nat. Paris 1, 301–320.
Candy, I., Coope, G.R., Lee, J.R., Parfi tt, S.A., Preece, R.C., Rose, J., Schreve, D.C., 2010. Pronounced warmth during early middle Pleistocene interglacials: investigating the Mid-Brunhes Event in the British terrestrial sequence. Earth Sci. Rev. 103, 183–196.
Candy, I., Schreve, D.C., Sherriff, J., Tye, G.J., 2014. Marine Isotope Stage 11: palaeoclimates, palaeoenvironments and its role as an analogue for the current interglacial. Earth Sci. Rev. 128, 18–51.
de Abreu, L., Abrantes, F.F., Shackleton, N.J., Tzedakis, P.C., McManus, J.F., Oppo, D.W., Hall, M.A., 2005. Ocean climate variability in the eastern North Atlantic during interglacial marine isotope stage 11: a partial analogue for the Holocene? Paleoceanography 20, PA3009. http://dx.doi.org/10.1029/2004PA001091.
Desprat, S., Sanchez-Goni, M.F., Turon, J.L., McManus, J.F., Loutre, M.F., Duprat, J., Malaize, B., Peyron, O., Peypouquet, J.P., 2005. Is vegetation responsible for glacial inception during periods of muted insolation changes? Quat. Sci. Rev. 24, 1361–1374.
Dorador, J., Rodríguez-Tovar, F.J., 2014. A novel application of quantitative pixels analysis to trace fossil research in marine cores. Palaios 29, 533–538.
Dorador, J., Rodríguez-Tovar, F.J., 2015. Color analysis on cores from IODP Expedition 339: new advances, sedimentological application and ichnological influence. Stratigraphic variation in ichnofabric Marine Geology (submitted for publication).
Dorador, J., Rodríguez-Tovar, F.J., IODP Expedition 339 Scientists, 2014a. Quantitative estimation of bioturbation based on digital image analysis. Mar. Geol. 349, 55–60.
Dorador, J., Rodríguez-Tovar, F.J., IODP Expedition 339 Scientists, 2014b. Digital image treatment applied to ichnological analysis of marine core sediments. Facies 60 (1), 39–44.

Droxler, A.W., Poore, R.Z., Burckle, L.H., 2003. Earth's Climate and Orbital Eccentricity: The Marine Isotope Stage 11 Question. In: Droxler, A.W., Poore, R.Z., Burckle, L.H. (Eds.), GeophyMonograph Series 137. AGU, Washington, D.C. (240 pp.).
Ekdale, A., 1992. Muckraking and mudslinging: the joys of deposit-feeding. In: Maples, C.G., West, R.R. (Eds.), Trace FossilsShort Courses in Paleontology. Paleontological Society, pp. 145–171.
Ekdale, A.A., Bromley, R.G., Pemberton, S.G., 1984. Ichnology: the use of trace fossils in sedimentology and stratigraphy. Short Course 15. Society of Economics Paleontologists and Mineralogists (316 pp.).
Expedition 339 Scientists, 2013a. Site U1385. In: Stow, D.A.V., Hernández-Molina, F.J., Alvarez-Zarikian, C.A., Expedition 339 Scientists (Eds.), Proceedings of the Integrated Ocean Drilling Program. Integrated Ocean Drilling Program Management International, Inc., Tokyo http://dx.doi.org/10.2204/iodp.proc.339.103.2013.
Expedition 339 Scientists, 2013b. Expedition 339 summary. In: Stow, D.A.V., Hernández-Molina, F.J., Alvarez-Zarikian, C.A., Expedition 339 Scientists (Eds.), Proceedings of the Integrated Ocean Drilling Program. Integrated Ocean Drilling Program Management International, Inc., Tokyo http://dx.doi.org/10.2204/iodp.proc.339.101.2013.
Fu, S., 1991. Funktion, Verhalten und Einteilung fucoider und lophoctenoider Lebensspuren. Cour. Forschungsinstitut Senckenberg 135, 1–79.
Fürsich, F., 1973. A revision of the trace fossils *Spongeliomorpha*, *Ophiomorpha* and *Thalassinoides*. Neues Jb. Geol. Paläontol. Monat. 12, 719–735.
Gaillard, C., Hennebert, M., Olivero, D., 1999. Lower Carboniferous *Zoophycos* from the Tournai area (Belgium): environmental and ethologic significance. Geobios 32, 513–524.
Grunert, P., Skinner, L., Hodell, D., Piller, W.E., 2015. A micropalaeontological perspective on export productivity, oxygenation and temperature in NE Atlantic deep-waters across Terminations I and II. Glob. Planet. Chang. 131, 174–191.
Hodell, D.A., Lourens, L., Stow, D.A.V., Hernández-Molina, J., Alvarez Zarikian, C.A., Shackleton Site Project Members, 2013a. The "Shackleton Site" (IODP Site U1385) on the Iberian Margin. Sci. Drill. 16, 13–19.
Hodell, D.A., Crowhurst, S., Skinner, L., Tzedakis, P.C., Margari, V., Channell, J.E.T., Kamenov, G., Maclachlan, S., Rothwell, G., 2013b. Response of Iberian Margin sediments to orbital and suborbital forcing over the past 420 ka. Paleoceanography 28, 1–15.
Hodell, D., Lourens, L., Crowhurst, S., Konijnendijk, T., Tjallingii, R., Jimenez-Espejo, F., Skinner, L., Tzedakis, P.C., Shackleton Site Project Members, 2015. A reference time scale for Site U1385 (Shackleton Site) on the SW Iberian Margin. Glob. Planet. Chang. 133, 49–64 (in this issue).
Hoogakker, B.A., Rohling, E.J., Palmer, M.R., Tyrrell, T., Rothwell, R.G., 2006. Earth Planet. Sci. Lett. 248, 15–29. http://dx.doi.org/10.1016/j.epsl.2006.05.007.
Hoogakker, B.A., Elderfield, H., Schmiedl, G., McCave, I.N., Rickaby, R.E., 2015. Glacial–interglacial changes in bottom-water oxygen content on the Portuguese margin. Nat. Geosci. 8, 40–43. http://dx.doi.org/10.1038/ngeo2317.
Hutson, W.H., 1980. The Agulhas current during the late Pleistocene: analysis of modern faunal analogs. Science 207, 64–66.
Keighley, G., Pickerill, R.K., 1995. The ichnotaxa *Palaeophycus* and *Planolites*: historical perspectives and recommendations. Ichnos Int. J. Plant Anim. Traces 3 (4), 301–309.
Lisiecki, L.E., Raymo, M.E., 2005. A Pliocene-Pleistocene stack of 57 globally distributed benthic $\delta^{18}O$ records. Paleoceanography 20, PA1003. http://dx.doi.org/10.1029/2004PA001071.
Löwemark, L., 2015. Testing ethological hypotheses of the trace fossil *Zoophycos* based on Quaternary material from the Greenland and Norwegian Seas. Palaeogeogr. Palaeoclimatol. Palaeoecol. 425, 1–13.
Löwemark, L., Schäfer, P., 2003. Ethological implications from a detailed X-ray radiograph and ^{14}C-study of the modern deep-sea *Zoophycos*. Palaeogeogr. Palaeoclimatol. Palaeoecol. 192, 101–121.
Löwemark, L., Werner, F., 2001. Dating errors in high-resolution stratigraphy: a detailed X-ray radiograph and AMS-^{14}C study of *Zoophycos* burrows. Mar. Geol. 177, 191–198.
Löwemark, L., Lin, I.-T., Wang, C.-H., Huh, C.-A., Wei, K.-Y., Chen, C.-W., 2004. Ethology of the *Zoophycos*-producer: arguments against the gardening model from $\delta^{13}C$org evidences of the spreiten material. TAO 15, 713–725.
Löwemark, L., Lin, Y., Chen, H.-F., Yang, T.-N., Beier, C., Werner, F., Lee, C.-Y., Song, S.-R., Kao, S.-J., 2006. Sapropel burn-down and ichnological response to late Quaternary sapropel formation in two ~400 ky records from the eastern Mediterranean Sea. Palaeogeogr. Palaeoclimatol. Palaeoecol. 239, 406–425.
Löwemark, L., O'Regan, M., Hanebuth, T., Jakobsson, M., 2012. Late Quaternary spatial and temporal variability in Arctic deep-sea bioturbation and its relation to Mn cycles. Palaeogeogr. Palaeoclimatol. Palaeoecol. 365, 192–208.
Maiorano, P., Marino, M., Balestra, B., Flores, J.A., Hodell, D.A., Rodrigues, T., 2015. Coccolithophore variability from the Shackleton Site (IODP Site U1385) through MIS 16–10. Glob. Planet. Chang. 133, 35–48 (in this issue).
Mángano, M.G., Buatois, L., West, R.R., Maples, C.G., 2002. Ichnology of a Pennsylvanian equatorial tidal flat — the Stull Shale Member at Waverly, eastern Kansas. Kans. Geol. Surv. Bull. 245, 1–133.
Margari, V., Skinner, L.C., Tzedakis, P.C., Ganopolski, A., Vautravers, M., Shackleton, N.J., 2010. The nature of millennial-scale climate variability during the past two glacial periods. Nat. Geosci. 3, 127–131.
Marino, M., Maiorano, P., Tarantino, F., Voelker, A., Capotondi, L., Girone, A., Lirer, F., Flores, J.-A., Naafs, B.D.A., 2014. Coccolithophores as proxy of sea-water changes at orbital-to-millennial scale during middle Pleistocene Marine Isotope Stages 14–9 in North Atlantic core MD01-2446. Paleoceanography 29. http://dx.doi.org/10.1002/2013PA002574 (2013PA002574).
Martrat, B., Grimalt, J.O., Shackleton, N.J., de Abreu, L., Hutterli, M.A., Stocker, T.F., 2007. Four climate cycles of recurring deep and surface water destabilizations on the Iberian margin. Science 317 (5837), 502–507.
McManus, J.F., Oppo, D.W., Cullen, J.L., 1999. A 0.5-million.year record of millennial.scale climate variability in the North Atlantic. Science 283 (5404), 971–975.
McManus, J.F., Francois, R., Gherardi, J.M., Keigwin, L.D., Brown-Leger, S., 2004. Collapse and rapid resumption of Atlantic meridional circulation linked to deglacial climate changes. Nature 428, 834–837. http://dx.doi.org/10.1038/nature02494.
Miller, M.F., 1991. Morphology and palaeoenvironmental distribution of Paleozoic *Spirophyton* and *Zoophycos*: implications for the *Zoophycos* ichnofacies. Palaios 6, 410–425.
Miller, M.F., 2003. Styles of behavioral complexity recorded by selected trace fossils. Palaeogeogr. Palaeoclimatol. Palaeoecol. 192, 33–43.
Miller, M.F., Johnson, K.G., 1981. *Spirophyton* in alluvial-tidal facies of the Castkill deltaic complex: possible biological control of ichnofossil distribution. J. Paleontol. 55, 1016–1027.
Mojtahid, M., Jorissen, F., Lansard, B., Fontanier, C., Bombled, B., Rabouille, C., 2009. Spatial distribution of live benthic foraminifera in the Rhone prodelta: faunal response to a continental – marine organic matter gradient. Mar. Micropaleontol. 70, 177–200.
Pailler, D., Bard, E., 2002. High frequency palaeoceanographic changes during the past 140 000 yr recorded by the organic matter in sediments of the Iberian Margin. Palaeogeogr. Palaeoclimatol. Palaeoecol. 181, 431–452.
Pemberton, S.G., Frey, R.W., 1982. Trace fossil nomenclature and the *Planolites*–*Palaeophycus* dilemma. J. Paleontol. 56 (4), 843–881.
Poirier, R.K., Billups, K., 2014. The intensification of northern component deep water formation during the mid-Pleistocene climate transition. Paleoceanography http://dx.doi.org/10.1002/2014PA002661.
Railsback, L.B., Gibbard, P.L., Head, M.J., Voarintsoa, N.R.G., Toucanne, S., 2015. An optimized scheme of lettered marine isotope substages for the last 1.0 million years, and the climatostratigraphic nature of isotope stages and substages. Quat. Sci. Rev. 111, 94–106.
Rodríguez-Tovar, F.J., Dorador, J., 2014. Ichnological analysis of Pleistocene sediments from the IODP Site U1385 "Shackleton Site" on the Iberian Margin: approaching palaeoenvironmental conditions. Palaeogeogr. Palaeoclimatol. Palaeoecol. 409, 24–32.
Rodríguez-Tovar, F.J., Dorador, J., 2015. Ichnofabric characterization in cores: a method of digital image treatment. Ann. Soc. Geol. Pol. (in press).
Rodríguez-Tovar, F.J., Reolid, M., 2013. Environmental conditions during the Toarcian Oceanic Anoxic Event (T-OEA) in the westernmost Tethys: influence of the regional context on a global phenomenon. Bull. Geosci. 88, 697–712.
Rodríguez-Tovar, F.J., Uchman, A., 2004a. Trace fossils after the K–T boundary event from the Agost section, SE Spain. Geol. Mag. 141, 429–440.
Rodríguez-Tovar, F.J., Uchman, A., 2004b. Ichnotaxonomic analysis of the Cretaceous/Palaeogene boundary interval in the Agost section, south-east Spain. Cretac. Res. 25, 635–647.
Rodríguez-Tovar, F.J., Uchman, A., 2006. Ichnological analysis of the Cretaceous–Palaeogene boundary interval at the Caravaca section, SE Spain. Palaeogeogr. Palaeoclimatol. Palaeoecol. 242, 313–325.
Rodríguez-Tovar, F.J., Uchman, A., 2008. Bioturbational disturbance of the Cretaceous–Palaeogene (K–Pg) boundary layer: implications for the interpretation of the K–Pg boundary impact event. Geobios 41, 661–667.
Rodríguez-Tovar, F.J., Uchman, A., 2010. Ichnofabric evidence for the lack of bottom anoxia during the Lower Toarcian Oceanic Anoxic event in the Fuente de la Vidriera section, Betic Cordillera, Spain. Palaios 25, 576–587.
Rodríguez-Tovar, F.J., Uchman, A., Martín-Algarra, A., 2009a. Oceanic anoxic event at the Cenomanian–Turonian boundary interval (OAE-2): ichnological approach from the Betic Cordillera, southern Spain. Lethaia 42, 407–417.
Rodríguez-Tovar, F.J., Uchman, A., Martín-Algarra, A., O'Dogherty, L., 2009b. Nutrient spatial variation during intrabasinal upwelling at the Cenomanian–Turonian oceanic anoxic event in the westernmost Tethys: an ichnological and facies approach. Sediment. Geol. 215, 83–93.
Rodríguez-Tovar, F.J., Löwemark, L., Pardo-Igúzquiza, E., 2011. *Zoophycos* cyclicity during the last 425 ka in the northeastern South China Sea: Evidence for monsoon fluctuation at the Milankovitch scale. Palaeogeography, Palaeoclimatology, Palaeoecology 305, 256–263.
Rodríguez-Tovar, F.J., Dorador, J., Grunert, P., Hodell, D., 2015. Deep-sea trace fossil and benthic foraminiferal assemblages across glacial Terminations 1, 2 and 4 at the "Shackleton Site" (IODP Expedition 339, Site U1385). Glob. Planet. Chang. 133, 359–370 (in this issue).
Salgueiro, E., Voelker, A.H.L., de Abreu, L., Abrantes, F., Meggers, H., Wefer, G., 2010. Temperature and productivity changes off the western Iberian margin during the last 150 ky. Quat. Sci. Rev. 29, 680–695.
Sánchez-Goñi, M.F., Llave, E., Oliveira, D., Naughton, F., Desprat, S., Ducassou, E., Hodell, D.A., 2015. Climate changes in south western Iberia and Mediterranean Outflow variations during two contrasting cycles of the last 1 Myrs: MIS 31–MIS 30 and MIS 12–MIS 11. Glob. Planet. Chang. (submitted for publication).
Schlirf, M., 2000. Upper Jurassic trace fossils from the Boulonnais (northern France). Geol. Palaeontol. 34, 145–213.
Schmiedl, G., Mackensen, A., Muller, P.J., 1997. Recent benthic foraminifera from the eastern South Atlantic Ocean: dependence on food supply and water masses. Mar. Micropaleontol. 32, 249–287.
Scmiedl, G., Mackensen, A., 1997. Late Quaternary paleoproductivity and deep water circulation in the eastern South Atlantic Ocean: evidence from benthic foraminifera. Palaeogeogr. Palaeoclimatol. Palaeoecol. 130, 43–80.
Seilacher, A., 1990. Aberrations in bivalve evolution related to photo-and chemosymbiosis. Hist. Biol. 3 (4), 289–311.
Shackleton, N.J., Hall, M.A., Vincent, E., 2000. Phase relationships between millennial-scale events 64,000–24,000 years ago. Paleoceanography 15 (6), 565–569.

Shackleton, N., Fairbanks, R., Chiu, T.-c., Parrenin, F., 2004. Absolute calibration of the Greenland time scale: implications for Antarctic time scales and for $\delta^{14}C$. Quat. Sci. Rev. 23 (14), 1513–1522.

Skinner, L., Elderfield, H., 2007. Rapid fluctuations in the deep North Atlantic heat budget during the last glacial period. Paleoceanography 22 (1), PA1205. http://dx.doi.org/10.1029/2006PA001338.

Uchman, A., 1995. Taxonomy and palaeoecology of flysch trace fossils: the Marnoso-arenacea Formation and associated facies (Miocene, Northern Appenines, Italy). Beringeria 15, 1–114.

Uchman, A., 1999. Ichnology of the Rhenodanubian Flysch (Lower Cretaceous–Eocene) in Austria and Germany. Beringeria 25, 67–173.

Uchman, A., Wetzel, A., 2011. Deep-sea ichnology: the relationships between depositional environment and endobenthic organisms. In: Hüneke, H., Mulder, T. (Eds.), Deep-Sea SedimentsDevelopments in Sedimentology 63. Elsevier, Amsterdam, pp. 517–555.

Uchman, A., Bak, A., Rodríguez-Tovar, F.J., 2008. Ichnological record of deep-sea palaeoenvironmental changes around the Oceanic Anoxic Event 2 (Cenomanian–Turonian boundary): an example from the Barnasiówka section, Polish Outer Carpathians. Palaeogeogr. Palaeoclimatol. Palaeoecol. 262, 61–71.

Uchman, A., Rodríguez-Tovar, F.J., Machaniec, E., Kędzierski, M., 2013a. Ichnological characteristics of Late Cretaceous hemipelagic and pelagic sediments in a submarine high around the OAE-2 event: a case from the Rybie section, Polish Carpathians. Palaeogeogr. Palaeoclimatol. Palaeoecol. 370, 222–231.

Uchman, A., Rodríguez-Tovar, F.J., Oszczypko, N., 2013b. Exceptionally favourable life conditions for macrobenthos during the Late Cenomanian OAE-2 event: ichnological record from the Bonarelli Level in the Grajcarek Unit, Polish Carpathians. Cretac. Res. 46, 1–10.

Vautravers, M.J., Shackleton, N.J., 2006. Centennial-scale surface hydrology off Portugal during marine isotope stage 3: insights from planktonic foraminiferal fauna variability. Paleoceanography 21 (3), PA3004. http://dx.doi.org/10.1029/2005PA001144.

Voelker, A.H.L., Rodrigues, T., Billups, K., Oppo, D., McManus, J., Stein, R., Hefter, J., Grimalt, J.O., 2010. Variations in mid-latitude North Atlantic surface water properties during the mid-Brunhes (MIS 9–14) and their implications for the thermohaline circulation. Clim. Past 6, 531–552.

Wetzel, A., 1991. Ecologic interpretation of deep-sea trace fossil communities. Palaeogeogr. Palaeoclimatol. Palaeoecol. 85 (1–2), 47–69.

Wetzel, A., 2002. Modern *Nereites* in the South China Sea—ecological association with redox conditions in the sediment. Palaios 17 (5), 507–515.

Wetzel, A., Uchman, A., 2012. Hemipelagic and pelagic basin plains. In: Bromley, R.G., Knaust, D. (Eds.), Trace Fossils as Indicators of Sedimentary EnvironmentsDevelopments in Sedimentology 64. Elsevier, Amsterdam, pp. 673–701.

Wollenburg, J.E., Knies, J., Mackensen, A., 2004. High-resolution paleoproductivity fluctuations during the past 24 kyr as indicated by benthic foraminifera in the marginal Arctic Ocean. Palaeogeogr. Palaeoclimatol. Palaeoecol. 204, 209–238.

AGRADECIMIENTOS

En primer lugar, quiero agradecer la ayuda y el apoyo de los Profesores Francisco Javier Sierro y José Abel Flores, que aceptaron dirigir esta tesis aún a sabiendas de que yo no podría dedicarle todo el tiempo que a todos nos hubiera gustado.

Quiero agradecerles también, al igual que al Profesor Jorge Civis y al resto de mis profesores de Paleontología Maruja Valle, José Ángel González, Mª Ángeles Bárcena y Guillermo Francés, sus clases y, sobre todo, los fantásticos campamentos en los que tanto aprendí y que me permitieron desarrollar y dar respaldo científico a mi afición natural.

Así mismo debo reconocer la labor de todos los profesores que tuve durante mis estudios de Geología. Sus enseñanzas me proporcionaron otra visión del mundo, otra escala y perspectiva de pensamiento.

No puedo olvidarme de los compañeros del Grupo de Geociencias Oceánicas, Gatsby, Montse, Mariem, Iván, Aleix, Eloy, Miguel Ángel, Margarita, Marta, Blanca, Marlies, Bas, Diana, Ana y, muy especialmente Rocío y José Ignacio. Todos ellos, la mayoría ya doctores y situados en otros puestos, me han tratado con simpatía y me han ayudado en todo lo que han podido. Quiero agradecer especialmente a la Montse y Rubén su acogida durante mi estancia en Portugal. A Rocío y José Ignacio les debo, no sólo que me hayan ayudado siempre aunque tuvieran que aumentar su carga de trabajo, sino su alegría y entusiasmo contagioso por el trabajo bien hecho. Gracias a todos por ser como sois, espero que no cambiéis nunca.

I thank Dr. Fatima Abrantes, in the *Instituto Português do Mar e da Atmosfera*, her helpful disposition and valuable suggestions, as well as her kindness, while my staying in the IPMA. Thank you for making paperwork problems much easier and for the good talks we shared. I want also thank the other components of the group at the IPMA, especially Drs. Antje Voelker, Teresa Rodrigues and Emilia Salgueiro for their help.

Finalmente, pero no en último lugar, a mi familia quiero agradeceros vuestro permanente ánimo y apoyo, vuestra ayuda constante y, especialmente, el comprender y compartir mis inquietudes e intereses. Sin vosotros no sería lo que soy ni habría terminado esta tesis.

ÍNDICE / *INDEX*

INTRODUCCIÓN

El estudio de las variaciones climáticas y ambientales a lo largo de la historia geológica responde al interés por conocer el funcionamiento de los sistemas naturales y sus efectos. Una cuestión clave para su comprensión reside en el conocimiento de la forma concreta en que cada sistema terrestre responde a los cambios ambientales y la escala temporal a la que lo hace. En el caso del océano, la respuesta dinámica a las influencias climáticas tiene como consecuencia la reorganización de la circulación superficial global y el reajuste de la circulación termohalina ("*conveyor belt model*"). Como consecuencia, el registro de las variaciones climáticas pasadas y los procesos paleoceanográficos asociados a ellas ha venido centrando el interés de la comunidad científica en los últimos años. La comprensión de los mecanismos y procesos que han actuado a lo largo de la historia geológica reciente permitirá interpretar los procesos ambientales que están ocurriendo en la actualidad, así como predecir el comportamiento y evolución del sistema climático en un futuro próximo.

Para resolver tales cuestiones es clave la utilización de registros sedimentarios marinos cuya localización geográfica y alta resolución temporal permitan estudiar los distintos procesos que integran el sistema climático terrestre. El margen occidental de la península Ibérica es una de estas áreas estratégicas. Se ha demostrado que su registro sedimentario puede compararse directamente con los registros de hielo antártico y de Groenlandia, ofreciendo datos fiables para el estudio de variaciones climáticas a escala milenaria tanto del hemisferio norte como del sur. Esto es especialmente interesante para reconstruir el sistema climático de épocas para las que no se dispone de registros de hielo.

El margen occidental ibérico está en el área de influencia del giro subtropical del Atlántico Norte y recibe aguas tanto de la corriente de las Azores, como de la corriente de Portugal, rama descendente de la Corriente del Atlántico Norte. Esta especial localización, en el límite entre distintas masas de agua, hace de esta un área muy sensible a cambios de intensidad en el flujo de dichas corrientes y, por lo tanto, clave para el estudio de variaciones paleoceanográficas en el Atlántico Norte. De hecho,

diversos estudios han relacionado las variaciones climáticas milenarias registradas en esta región durante el Cuaternario con cambios en los frentes oceánicos y en la distribución de las corrientes.

Sin embargo ningún estudio realizado en el margen ibérico alcanzaba más allá de los 580 ka, puesto que no existían registros sedimentarios anteriores. La campaña de IODP 339, con su sondeo U1385, ha permitido extender el registro sedimentario disponible hasta el millón de años. Para la elaboración de esta tesis doctoral he estudiado las asociaciones de foraminíferos planctónicos y los datos isotópicos obtenidos de los sedimentos de este sondeo para reconstruir la historia climática y oceanográfica de esta región a escala milenaria entre los estadios isotópicos MIS 21 y MIS 11, así como su correlación con eventos oceanográficos en el Atlántico Norte y climáticos a escala global.

Los principales objetivos de esta tesis podrían resumirse en:

- Elaboración de un registro de las variaciones en las asociaciones de foraminíferos planctónicos durante el período estudiado
- Reconstrucción de paleotemperaturas mediante distintas funciones de transferencia, basadas en asociaciones de foraminíferos planctónicos
- Reconstrucción de la paleoproductividad exportada mediante funciones de transferencia, basadas en asociaciones de foraminíferos planctónicos
- Estudiar las oscilaciones climáticas a escala milenaria durante los estadios isotópicos 21 al 11
- Identificar las causas de dichas variaciones climáticas y el agente responsable (orbital, oceanográfico…)
- Estudiar el comportamiento de las corrientes oceánicas superficiales del Atlántico Norte que afectan al área de estudio durante los estadios glaciales del MIS 20 al MIS 14
- Estudiar variaciones ambientales tanto superficiales como profundas, que afectan a la distribución de comunidades bentónicas durante los estadios isotópicos MIS 13 al MIS 11
- Comparar los registros obtenidos con datos publicados procedentes de otras regiones para poder establecer variaciones ambientales a nivel global

MÉTODOS

Preparación del sedimento y estudio de foraminíferos

Las muestras de sedimento se liofilizan, se pesan y se tamizan bajo el chorro de agua con un tamiz de 63 μm. La fracción obtenida se seca en estufa y se vuelve a pesar. Posteriormente se tamiza para separar la fracción >150 μm, que es la que se utilizará. Esta fracción se cuartea hasta obtener una alícuota que contenga entre 300 y 500 ejemplares, que se identifican utilizando un microscopio estereoscópico. Se calculan las abundancias relativas de las especies y morfotipos identificados.

Reconstrucción de la paleotemperatura oceánica

Los valores de temperatura oceánica superficial se reconstruyen utilizando un sistema de redes neuronales (ANN). Este sistema consiste en la comparación de cada muestra fósil con una base de datos de asociaciones faunísticas modernas en que, para cada localización, se han medido valores reales de temperatura de agua de mar.

Para comprobar el grado de similaridad de las reconstrucciones obtenidas, se calcula un índice de similaridad mediante el método de análogos modernos.

Reconstrucción de la paleoproductividad exportada

La productividad exportada de cada muestra fósil se reconstruye mediante el método de análogos modernos, utilizando una base de datos actual desarrollada para la misma área en que se realiza este estudio.

RESUMEN

En esta tesis se reconstruyen las condiciones paleoceanográficas superficiales en el margen occidental ibérico mediante el análisis de las asociaciones de foraminíferos planctónicos de sedimentos procedentes del testigo IODP-U1385 (37º34.285´N, 10º7.562´W; 2585 m de profundidad). Los datos proporcionan un registro climático continuo y de alta resolución para los estadios isotópicos marinos (MIS) 21 a 11, ampliando el registro existente del margen ibérico hasta el noveno ciclo climático (867 ka).

Se identifican oscilaciones en la temperatura del agua superficial a escala milenaria tanto durante los períodos interglaciales como los glaciales, pero las oscilaciones de mayor amplitud (>5 º C) suceden en los inicios y terminaciones glaciales. En todas las desglaciaciones del Pleistoceno medio se registraron eventos de extremando enfriamiento marcados por máximos en el porcentaje de *Neogloboquadrina pachyderma* sinistral, con valores altos de $\delta^{18}O$ medido en foraminíferos planctónicos y mínimos en la relación Ca/Ti. Estos eventos de prominente enfriamiento de las aguas superficiales a lo largo del margen ibérico son el resultado de importantes reorganizaciones de la circulación en el Atlántico Norte, tanto a nivel de superficie como de aguas profundas, que tuvieron lugar como consecuencia del aporte de grandes cantidades de agua dulce al Atlántico Norte al inicio de las deglaciaciones. De hecho, la mayor parte de estos eventos fríos ocurrieron cuando la insolación de verano del hemisferio norte estaba próxima a sus valores máximos. La disminución de la formación de agua profunda en el Atlántico Norte redujo el aporte de aguas cálidas hacia el norte, que tiene lugar mediante el giro subtropical del Atlántico Norte. Esta disminución de aporte cálido fue registrada en el margen ibérico por el incremento en el aporte de aguas subpolares frías. Después de cada episodio de enfriamiento profundo asociado a las deglaciaciones, el agua superficial experimentó un rápido calentamiento que marcaba el inicio del óptimo climático durante la fase temprana de los interglaciales. Los calentamientos bruscos quedaron registrados por un aumento repentino de la asociación subtropical, lo que

indica incremento en el transporte del calor hacia latitudes altas a través de la corriente del Atlántico Norte. En el inicio de las glaciaciones, la temperatura de superficie en el margen portugués se mantuvo relativamente cálida, mientras que las aguas superficiales del Atlántico Norte se enfriaban, generando un alto gradiente latitudinal de temperatura superficial oceánica.

Se ha demostrado que el margen Ibérico suroeste es muy sensible a cambios en la distribución de corrientes oceánicas y masas de agua superficiales del Atlántico norte, así como a variaciones en la posición de los frentes ártico y subtropical. Durante los estadios glaciales del final del Calabriense y el Pleistoceno medio, tuvo lugar una importante reorganización en la circulación del Atlántico Norte que afectó a la distribución superficial de las distintas masas de agua y el trazado de las corrientes oceánicas. Este cambio tuvo lugar principalmente durante el estadio isotópico MIS 16, asociado al cambio de posición del frente ártico y a la intensificación en la formación de agua profunda Nord-atlántica, fenómenos ambos que tuvieron lugar durante este estadio glacial y el interglacial previo. Durante los períodos glaciales anteriores al MIS 16 el frente ártico estaba localizado en latitudes medias, lo que unido a los continuos flujos de hielo que al fundirse producían grandes cantidades de agua de muy baja salinidad, y por tanto muy baja densidad, dificultaba en gran medida la formación de aguas profundas Nord-atlánticas. La drástica reducción de la circulación profunda debilitó la circulación superficial, afectando a la corriente Nord-atlántica y facilitando la dispersión de aguas polares por latitudes medias del Atlántico Norte. La corriente del Atlántico Norte quedaba desviada al sur, adquiriendo una trayectoria casi oeste-este, y las aguas cálidas subtropicales llegaban al margen de Portugal circulando superficialmente sobre las aguas polares que llegaban desde el norte. Desde el MIS 16 el frente ártico adquiere una posición más al norte, lo que unido al incremento en la formación de aguas profundas reactivó la NAC y facilitó el aporte de aguas templadas altas latitudes. La corriente de Portugal incrementó su intensidad a lo largo del margen oeste ibérico, impidiendo que las aguas subtropicales aportadas por la corriente de las Azores llegaran cerca de la costa, como quedó registrado en el sondeo U1385 por la reducida abundancia relativa de la asociación cálida superficial.

Parte del trabajo de esta tesis consiste en el estudio integrado de las condiciones oceánicas superficiales y las profundas durante los estadios isotópicos 13 al 11. Este estudio revela el predominio de aguas bien oxigenadas en el fondo, así como abundancia de disponibilidad de alimento para las comunidades bentónicas. La concentración de foraminíferos bentónicos en los sedimentos y las variaciones de las asociaciones de foraminíferos planctónicos sugieren cambios significativos en la productividad superficial y el aporte de nutrientes hacia el fondo marino desde el final del MIS 13 hasta el final del MIS 11. Hacia el final del MIS 13 la productividad exportada fue muy baja. Este hecho, junto a la presencia de sedimentos claros indica bajo aporte de carbono orgánico al fondo y altos niveles de oxigenación. Posteriormente, el aporte de materia orgánica se incrementó considerablemente y mantuvo altos valores hasta la Terminación V, permitiendo condiciones eutróficas, indicadas por valores altos de la tasa de acumulación de foraminíferos bentónicos. Durante el MIS 11 se registraron valores más bajos en la tasa de acumulación de foraminíferos bentónicos, lo que sugiere condiciones oligotróficas en el fondo y menor aporte de carbono orgánico. Esta variación de las condiciones ambientales bentónicas responde a cambios importantes en la ventilación del agua, probablemente ligados a variaciones en la circulación termohalina profunda del Atlántico Norte que, en último término determina el contenido de oxígeno y la disponibilidad de alimento en los sedimentos.

CONCLUSIONES

El estudio de las asociaciones de foraminíferos planctónicos procedentes del sondeo U1385 en el margen atlántico ibérico, así como la comparación de los resultados obtenidos con datos de $\delta^{18}O$, tanto bentónicos como planctónicos, y el registro de Ca/Ti del mismo sitio (Hodell et al., 2015), permite la caracterización climática y paleoceanográfica del Atlántico Norte de los estadios isotópicos (MIS) 21 al 11. A continuación se presentan las principales conclusiones obtenidas para este intervalo.

Todas las desglaciaciones registradas en el margen portugués, tanto las Terminaciones (particularmente T IX y VIII) como las transiciones glacial/interglacial entre subestadios (MIS 21b/a, MIS 18e/d y especialmente MIS 15b/a), muestran una prominente oscilación climática que puede alcanzar los 10 ºC de variación. Esta importante oscilación térmica durante las desglaciaciones coincide con un cambio notable en las asociaciones de foraminíferos planctónicos, pasando rápidamente de una alta abundancia relativa de la especie polar Nps a una alta abundancia relativa de la Asociación subtropical. Estas oscilaciones térmicas de alta amplitud se produjeron como consecuencia de importantes reorganizaciones de la circulación superficial y profunda en el Atlántico Norte provocadas, a su vez, por aportes de agua dulce al océano cuando las masas de hielo del hemisferio norte comenzaron a retirarse. La reducción de salinidad superficial paralizó la formación de aguas profundas en el Atlántico Norte y, como consecuencia, el aporte de calor hacia latitudes altas y la llegada de aguas cálidas al margen oriental del giro subtropical, lo que provocó el aporte de aguas subpolares al margen occidental ibérico. Esta situación cambió rápidamente tras cesar la perturbación del agua dulce. La reiniciación de la formación de NADW reactivó la circulación profunda y condujo a una intensificación de la NAC y la llegada de aguas cálidas al margen ibérico.

La comparación con registros de temperatura oceánica superficial a latitudes altas del Atlántico Norte revela el desarrollo de un acusado gradiente térmico latitudinal entre el Atlántico Norte subtropical y el polar a medida que las masas de hielo del

hemisferio norte se van formando. Este acusado gradiente proporciona una fuente de vapor de agua que podría favorecer el crecimiento de las masas de hielo.

Durante el intervalo MIS 13-11, la temperatura oceánica superficial del margen SW ibérico era, en general, más fría que en la actualidad, en especial durante los meses más cálidos. La temperatura oceánica superó los valores actuales sólo durante cortos intervalos de los óptimos interglaciales. Los enfriamientos registrados en el U1385 durante el intervalo MIS 13-11 fueron menos pronunciados que los registrados durante MIS 20 ó MIS 15.

Durante MIS 12 el agua superficial en latitudes medias era, en general, más fría que durante los interglaciales, con baja estacionalidad y menor amplitud de oscilación térmica, especialmente durante los meses cálidos. Las oscilaciones climáticas eran mayores durante la expansión de las masas de hielo y se cree que la disminución de la variación climática antes del máximo glacial condujo a una de las glaciaciones más pronunciadas del último millón de años.

El MIS 11c se caracterizó por estabilidad climática, inviernos templados y muy baja estacionalidad, como corresponde a una baja excentricidad y precesión reducida. Tales condiciones climáticas provocaron la estratificación del agua superficial y el debilitamiento del sistema de upwelling regional en la zona de estudio.

Las variaciones climáticas desde el MIS 13 al MIS 11 muestran la existencia de siete secuencias climáticas formadas por episodios progresivamente más fríos y que culminaban con un enfriamiento importante que era seguido por un repentino y drástico calentamiento. Dichas secuencias son similares a los ciclos Bond descritos en el Pleistoceno superior y la mayor parte de los episodios finales de enfriamiento registrados en el U1385 coincidieron con eventos tipo Heinrich registrados en altas latitudes del océano Atlántico. Estas secuencias climáticas se corresponden con períodos de incremento gradual en el registro de $\delta^{18}O$ que se interrumpe, o disminuye, hacia el final de cada secuencia; también se corresponden con secuencias similares en del registro sintético de temperatura sobre Groenlandia (GLTsyn of Barker et al., 2011). Los principales enfriamientos coincidieron con la abrupta disminución y/o valores bajos de la AMOC, estadiales sobre Groenlandia y, salvo excepciones, también con alta temperatura sobre Antártica. Esto sugiere que el modelo en dientes de sierra, que

explica las oscilaciones climáticas del último ciclo glacial, funcionó también durante el quinto ciclo climático.

Durante el MIS 13 y el inicio de la siguiente glaciación se registró un claro desfase entre las variaciones de SST y el volumen del hielo, según el $\delta^{18}O$ bentónico. Los valores más altos de SST durante MIS 13a se alcanzaron ~4.5 ky después del mínimo volumen de hielo, y la SST empezó a descender de nuevo ~3 ky después del inicio de la nueva fase del crecimiento del hielo. Durante este inicio glacial se formó un gradiente térmico superficial muy acusado entre el Atlántico NW y latitudes medias, en respuesta al avance del AF en dirección este o el sureste.

Las variaciones de las asociaciones de foraminíferos planctónicos del U1385 indican una fuerte conexión entre la presencia del agua cálida superficial en el margen Ibérico y la migración del AF. El avance del frente ártico en latitudes altas produciría el desplazamiento hacia el sur del giro subtropical, mientras que los episodios del retroceso del AF permitirían la migración hacia el norte de dicho giro y la llegada de masas superficiales cálidas a latitudes más altas. Durante la transición MIS 12b/a el aumento en volumen del hielo no se acompañó de la migración hacia el sur del giro subtropical, lo que indica que la circulación superficial de Atlántico Norte se mantuvo sin grandes alteraciones en el margen del este, probablemente debido a que el AF tenía una orientación sudoeste-noreste y el lugar de hundimiento de aguas no resultó afectado durante este período. Esta interpretación se respalda por valores del $\delta^{13}C$, que son ~0.5‰ más altos que durante otros intervalos del MIS 12, lo que sugiere la existencia de una AMOC reducida, pero aún activa comparada con otros intervalos del mismo período glacial.

El margen suroeste ibérico es muy sensible a los cambios en la distribución de las corrientes del Atlántico Norte y las masas de agua, así como a los cambios en la posición de los frentes ártico y subtropical. Las variaciones en la abundancia de las asociaciones de microfauna asociadas a las diversas corrientes del Atlántico Norte indican un cambio en la circulación general de esta parte del océano durante el estadio MIS 16. Antes del MIS 16, cuando la posición del frente Ártico (AF) era más meridional, tanto durante los glaciales como los interglacials, la circulación del Atlántico Norte estaba condicionada por la migración del AF hacia el sur conforme avanzaba las

condiciones glaciales. Durante los máximos glaciales de MIS 20 y MIS 18, coincidiendo con la posición más meridional del AF, la corriente del Atlántico Norte (NAC) quedó desviada hacia el sur y adquirió una posición casi puramente oeste-este, lo que produjo un menor transporte de calor a latitudes altas. Durante estos dos estadios glaciales, especialmente durante MIS 20, la corriente subtropical de las Azores aportaba aguas subtropicales cálidas a lo largo del margen ibérico, fluyendo superficialmente sobre las aguas más frías que llegaban procedentes de latitudes subpolares en dirección sur.

En el margen ibérico el cambio de posición del AF quedó registrado en torno a los 655 ka mediante el descenso en porcentaje de la especie polar *Neogloboquadrina pachyderma* (sinistral) y el incremento de la especie subpolar, *Turborotalita quinqueloba*.

Desde el MIS 16 la circulación general del Atlántico Norte estaba menos condicionada por las diferentes posiciones del AF que en estadios anteriores. Durante MIS 14 la NAC llegaba con mayor intensidad a latitudes altas, coincidiendo con el avance de la glaciación. Desde el MIS 16, la microfauna característica de la NAC dominó la asociación registrada en el margen oriental subtropical, indicando una reactivación importante de la corriente de Portugal, rama descendente de la NAC, a lo largo del margen Ibérico. Esta corriente produciría el desvío del agua cálida superficial hacia mar abierto y, en consecuencia, la disminución en el porcentaje de especies cálida en el U1385.

La evolución de las comunidades bentónicas durante el intervalo MIS 13 al 11 responde a importantes cambios en la ventilación del fondo, probablemente ligada a variaciones en la circulación termohalina profunda del Atlántico Norte.

Las condiciones ambientales del fondo para el intervalo de tiempo MIS 13 - 11 se pueden interpretar como de buena oxigenación, tanto del fondo como del agua intersticial del sedimento, así como de abundancia de nutrientes para las comunidades bentónicas.

La concentración de foraminíferos bentónicos y las variaciones en las asociaciones de planctónicos, sugieren cambios significativos en la productividad superficial y el

aporte de nutrientes al fondo oceánico durante MIS 13-11 que pueden correlacionarse con los cambios registrados de icnofacies.

El final del MIS 13 se caracteriza por valores muy bajos de la productividad anual exportada, lo que conjuntamente con la presencia de sedimentos claros indica un flujo relativamente bajo de carbono orgánico hacia el fondo, así como buena oxigenación. Estas condiciones iniciales cambiaron durante el MIS 12, con un rápido incremento del aporte de materia orgánica, que mantuvo altos valores hasta la Terminación V. Durante este tiempo las condiciones eran eutróficas, como indica la elevada tasa de acumulación de foraminíferos bentónicos. Durante MIS 11 se registró una menor tasa de acumulación de foraminíferos bentónicos, lo que sugiere un ambiente oligotrófico en el fondo asociado a menores aportes de carbono orgánico y alto contenido de oxígeno en el fondo, lo que produjo sedimentos de color más claro.